ESA Climate Change Initiative

Aerosol_cci+

PRODUCT VALIDATION AND INTERCOMPARISON REPORT

Version 3.1

Document reference: Aerosol_cci+_PVIR_v3.1.doc

DOCUMENT STATUS SHEET

	FUNCTION	NAME	DATE	SIGNATURE
contributing authors	Editors	T. Popp	10.03.2020 30.03.2021 06.05.2022 18.07.2022	
Evalaution team	Contributing authors	L. Sogacheva T. Popp	15.07.2020 30.03.2021 29.04.2022	
reviewed by	Science leader	T. Popp	28.07.2020 28.08.2020 30.03.2021 06.05.2022 18.07.2022	
approved by	Technical officer (ESA)	S. Pinnock M. Eisinger		
issued by	Project manager	T. Popp		

EXECUTIVE SUMMARY

This document evaluates the three versions of test datasets within the ESA Climate Change Initiative extensions project Aerosol_cci+. The test datasets have been developed and processed by Swansea university (SU) with their mature algorithm and Rayference (RF) with their new CISAR algorithm and cover all four sensors from the dual view sensor line (SU) / the SLSTR instrument onboard Sentinel-3A (RF): ATSR-2 (1998), AATSR (2008), SLSTR onboard Sentinel3-A and Sentinel3-B (2019). For each sensor the contractual coverage of the initial dataset is for four months in all seasons (March, June, September, December; SU) / 4 months at the end of 2019 (September, October, November, December; RF). In the last versions of all datasets full 12 months per year have been processed and analysed.

The evaluations are first done with level2 10x10km orbit projection datasets for the main variable Aerosol Optical Depth (AOD) and the Fine Mode AOD (FM-AOD). Reference data-sets are from the AERONET sun photometer network which measure AOD with a typical uncertainty of 0.01 (Eck, et al., 1999). Secondly, inter-comparisons to other satellite aerosol datasets are made (MODIS, MISR, POLDER) which constitute the "state of the art" for satellite retrievals, but are not the independent truth since those other satellite retrievals do also have their own uncertainties.

For the first versions of the SU algorithm (ATSR 4.32, SLSTR Ver.1.12) assessed in this report, differences for AOD to AERONET show good agreement for ATSR-2 and AATSR but larger noise and a significant positive bias for both SLSTR. More detailed analysis for different stations / regions and differentiating between low (<0.2) and high (>0.2) AOD ranges reveal detailed issues which should be targeted by further algorithm improvements. For Fine Mode AOD an additional positive bias for all sensors can be observed, with similar geographical patterns as for AOD. For the second SU algorithm versions (ATSR Ver4.33, SLSTR Ver1.14) a reduction in AOD bias by ~30%, especially for regions with bright surfaces can be shown. The final SU algorithm version (ATSR Ver 4.35) shows some reduction of biases for AOD and their uncertainties as well. For the first RF algorithm version, which works without an external cloud mask, a significant positive AOD over-estimation for low to medium AOD is identified, which points at possible remaining cloud contamination at low optical depth conditions, where the algorithm may have difficulties to correctly differentiate the probabilities of thin clouds and aerosols. The second version of the RF algorithm shows a significant improvement of AOD and FM-AOD bias and a clearly better representation of true error distributions by the predicted uncertainties (also highly consistent between North and South hemispheres and between land and ocean).

For the first SU versions the comparisons to other satellites reveal that in year 2008 the AOD difference between AATSR and GRASP over land, ocean and globally, is within the accepted difference (estimated by the total uncertainty based on uncorrelated GCOS accuracy requirements for both datasets). AATSR AOD is higher than MISR AOD over land and lower than MODIS AOD over ocean; both differences are slightly above the accepted difference. Differences between AATSR and MISR over ocean and AATSR and MODIS over land are within

the accepted difference. Regional analysis shows a considerable difference between the products.

Positive offsets between S3 (S3A and S3B) and MODIS/MISR AOD products are observed in 2019 over land. Over ocean, the difference between S3 and MODIS and MISR is, with only few exceptions, within the accepted difference. Globally, differences between S3A and MODIS and MISR are within the accepted difference. The difference between S3B and MODIS is within the accepted difference, while the difference with MISR is slightly higher. Regional analysis shows a considerable difference between the products also in year 2019. Differences between S3A and S3B AOD are within the accepted value, with one exception in March for the Atlantic region influenced by the Saharan dust transport.

For the second SU versions, monthly AOD inter-comparisons show significantly increased global coverage for ATSR-2, mostly over ocean and no coverage change for other sensors (AATSR, SLSTR). For ATSR-2 high AOD over land decreased in Ver.4.33. Comparisons to other ATSR-2 products, ADV, show that ATSR-2 SU AOD is higher over land and lower over ocean than the ADV AOD. There are no clear differences between versions v4.32 And v4.33 for AATSR. The main results from the evaluation of SU v4.33 monthly AOD product with MODIS, MISR and POLDER have not changed much, as compared with evaluation results of SU v4.32 monthly AOD product evaluation. There are no considerable changes for regional differences of AATSR to other sensors (MODIS, MISR, POLDER).

Compared with SU v1.11, difference between S3A and S3B AOD has not changed much globally, over land and ocean. However, reginal differences have changed considerably in March, when relative difference between S3A and S3B in SU v1.14 AOD product in Europe, North Asia and eastern part of the North America became negative and 2-4 time higher than the absolute difference. Over AfN, S3A AOD is higher than S3B AOD with the RD almost twice higher than AD. In June, September and December, regional differences between S3A and S3B products are withing the AD for most of the regions. In general, S3A and S3B SU AOD products show similar regional differences with MODIS and MISR.

Over land, relative difference between S3 SU and MODIS is within the accepted difference for all months except December. However, significant regional differences exist. Differencea between S3 SU and MISR AOD products is within the accepted difference in Europe (except for June), Australia and Northern Africa. Positive offsets between S3 are MISR are observed over other land regions, which resulted in positive relative difference above accepted difference over the whole land region. Over ocean, the difference between S3 and MODIS and MISR is, with only few exceptions, within the AD. Globally, differences between S3 and MODIS and MISR are within the AD for all months and regions, except for S3B-MISR in June and September.

Inter-comparisons of monthly maps for S3A RF AOD to SLSTR SU and other sensors show that this product clearly differs from the other AOD products with unrealistically high AOD e.g., over Eurasia in September and over potentially clean areas over ocean. One of the reasons for high AOD values in S3A RF AOD product can be cloud contamination, which may be a consequence from the absence of a cloud masking module in the aerosol retrieval in the RF (CISAR) algorithm.

In addition to the validation of AOD and FM-AOD, this report also does a thorough validation of the pixel-level uncertainties provided for AOD within the product files. This is done by comparing them statistically to estimates of the true error represented by the differences of retrieved AOD to AERONET AOD. This means that such an assessment can only cover the conditions contained in the AERONET measurements, i.e. cloud-filtered observations measured at land, shore and few island stations with significant gaps in some remote regions and the Southern hemisphere.

In the final iteration of this validation and inter-comparison report, also ship cruise reference data over oceans from the MAN database and from selected clean background sites were analysed. This analysis showed small biases to the ship cruise datasets of 0.02 (SU SLSTR algorithm) and 0.04 (RF SLSTR algorithm) and even lower bias for SU SLSTR of 0.01 and RF SLSTR of -0.01 for clean background sites, while for AATSR there is a bias of 0.05 for the clean background sites.

This report starts with definitions (sec. 1), a brief overview of the reference data (sec. 2) and the test data to be evaluated (sec. 3) before summarizing results of the level2 validation (sec. 4), the prognostic uncertainty validation (sec. 5) and the inter-comparisons to other satellite AOD data (sec. 6). It concludes with a summary of findings (sec. 7), references (sec. 8) and detailed listings of station statistics (Annex). The evaluation sections 4 -6 contain different sub sections for each dataset version assessed (for new versions only where significant changes were identified).

Document change record

Issue	Date	Modified Items / Reason for Change
0.9	10.03.2020	issue of the template
1.0	15.07.2020	Contributions by evaluation partners
1.1	28.07.2020	Review by science lead, final layout and editing
1.2	28.08.2020	Correction of minor RIDs raised by ESA Further elaboration of quantitative agreement between different satellite datasets in section 6
2.0	30.03.2021	Add 2nd evaluation results: SU v2 algorithm / RF v1 algorithm
3.0	25.04.2022	Third and final evaluation results: SU v3 algorithm / RF v2 algorithm Updates of: Executive Summary, Summary, figure 2.1, table 3.1 New (same analysis for new dataset version or new year): figures 3.8 – 3.11, sections 4.1.3, 4.1.5, 4.2.3, 4.2.5, 5.1.3, 5.1.5, 6.4, 6.5 New (completely new analysis): sections 4.3, 5.3
3.1	18.07.2022	Minor revisions due to ESA review Update of section 4.3

LIST OF TABLES

LIST OF FIGURES

TABLE OF CONTENTS

1 DEFINITIONS AND ABBREVIATIONS

This section summarizes the major definitions relevant for the validation report.

AAOD (Absorption Aerosol Optical Depth) is the vertically normalized atmospheric column integrated aerosol absorption at a certain wavelength (usually at 550 nm, the reference wavelength in global modelling) [note, AAOD = AOD*(1-SSA)]

AERONET represents a federated network of globally distributed ground-based CIMEL sun-/sky-photometers, which is maintained (calibration facility, data processing and aerosol and water vapor products access) by NASA (National Aeronautics and Space Administration) and PHOTONS (PHOtométrie pour le Traitement Opérationnel de Normalisation Satellitaire)

ANG (Ångström exponent), a parameter which describes the logarithmic wavelength dependence of AOD. It can be interpreted as a measure of the aerosol particle size for mono-modal aerosol size distributions (AND~0 means large; ANG~2 means small particles)

AOD (Aerosol Optical Depth) is the vertically normalized atmospheric column integrated aerosol extinction at a certain wavelength or waveband (usually at 550nm, the reference wavelength in modelling). AOD is also often referred to as Aerosol Optical Thickness (AOT).

AODdu (Dust Aerosol Optical Depth) is the component of total AOD due to dust particles.

AODf of **FM-AOD** (Fine Mode Aerosol Optical Depth) is the component of total AOD due to fine particles (usually with radius < 0.5 µm).

AODc (Coarse Mode Aerosol Optical Depth) is the component of total AOD due to coarse particles (usually with radius < 0.5 µm).

ATSR (Along Track Scanning Radiometer) was a multi-channel imaging radiometer (with dual view capabilities in the visible and near-IR solar spectrum). Two versions are used for aerosol retrieval: ATSR-2 on board of the European Space Agency's ERS-2 satellite (1995-2002) and the advanced ATSR (AATSR) on ESA's ENVISAT satellite (2002-2012).

ECV (Essential Climate Variables) are geo-physical quantities of the Earth-Atmosphere-System that are technically and economically feasible for systematic (climate) observations.

ENVISAT ("Environmental Satellite") is a now inoperative ESA polar-orbiting (ca 10am local overpass) satellite, which supplied between 2002 and 2012 atmospheric data, including for aerosol remote sensing relevant AATSR, MERIS and GOMOS sensor data.

FCDR (Fundamental Climate Data Records or simply **CDR**) represent long-term records of measurements or retrieved physical quantities from remote sensing. FCDRs require consistency across multiple platforms with respect to (1) calibration, (2) algorithms, (3) spatial and temporal resolution, (4) quantification of errors and biases (5) data format and (6) applied ancillary data.

FMF (Fine Mode Fraction) is the fraction of the total AOD which is contributed by aerosol particles smaller than 1μm in diameter. Due to their smaller size these aerosol particles are referred to as fine-mode aerosol, in contrast to larger or coarse model aerosol particles.

GCOS (Global Climate Observing System), located at WMO in Geneve, is intended to be a long-term, user-driven operational system capable of providing the comprehensive observations required for (1) monitoring the climate system, (2) detecting and attributing climate change, (3) assessing impacts of, and supporting adaptation to, climate variability and change, (4) application to national economic development and (5) research to improve understanding, modelling and prediction of the climate.

MAN (Marine Aerosol Network) is the ocean branch of the AERONET network, based on handheld solar attenuation measurements with calibrated MICROTOPS-II sun-photometers.

MISR (Multi-angle Imaging Spectro-Radiometer) is a multi-spectral sensor on NASA's EOS Terra platform with (9) multi-directional view capabilities.

MODIS (Moderate Resolution Imaging Spectro-Radiometer) is a multi-spectral sensor on NASA's EOS Terra and Aqua platforms.

POLDER (POLarization and Directionality of the Earth's Reflectances) is a passive optical imaging radiometer and polarimeter for studies on radiative and microphysical properties of clouds and aerosols on the French CNES PARASOL (Polarization and Anisotropy of Reflectances for Atmospheric Sciences coupled with Observations from a Lidar).

SDA (Spectral De-Convolution Algorithm), exploits AOD at several wavelengths to estiamte the fraction of fine and Coarse Mode AOD; the algorithm divides aerosols into fine and coarse mode fractions in an optical sense (O'Neill, et al., 2003). This parameter differs moderately from a sub-micron fraction which is defined according to a simple microphysical (radius) cutoff.

The **Sentinel** constellation of satellites provides Earth Observations from space as part of the joint ESA and EU Copernicus program, formerly GMES (Global Monitoring for Environment and Security)

SLSTR The SLSTR instrument on Sentinel-3 maintains the continuity with the (A)ATSR series of instruments. The design supports the basic functionality of AATSR, with the addition of a wider swath, new channels dedicated to fire and cirrus cloud detection.

SSA (Single Scattering Albedo) quantifies the likelihood of scattering during an attenuation (or 'extinction') event by an atmospheric particle of given size and shape at a certain wavelength (most important at 550 nm, the reference wavelength in global modeling). The remaining fraction, 1-SSA referred to co-single scattering albedo, quantifies the likelihood of absorption during an attenuation (or extinction) event.

2 REFERENCE DATA

AERONET/MAN offers high quality data on aerosol column properties via measurements of solar radiation at cloud-free conditions. Direct solar attenuation data provide highly accurate data of AOD at different solar wavelengths so that even a mid-visible (550nm) AOD split into super-micron size (coarse-mode) aerosol as by mineral dust and sea-salt and to sub-micron size (fine-mode) aerosol (FM-AOD) as by pollution and wildfires can be assigned. Particular informative are complementary sky-radiance samples (at more than 400 AERONET continental of island sites worldwide) which in combination with direct attenuation data provide detailed information on aerosol size (22 bin size-distributions) and on aerosol composition (refractive indices and thus SSA). While most AERONET sites have good data coverage over all seasons, the site distribution over land is highly uneven and often missing in important regions. This means that not all major global / seasonal aerosol plumes are well covered in the global validation statistics (especially for ATSR-2 / 1998 with much less stations) as can be seen in Fig. 2.1. Furthermore, it is obvious that the statistics are dominated by stations in the US and Europe and by stations with low mean AOD values (<0.2; darker blue in fig. 2.1). To address oceanic references, the MAN dataset will be added which offers data of about 200 research voyages over the last decade.

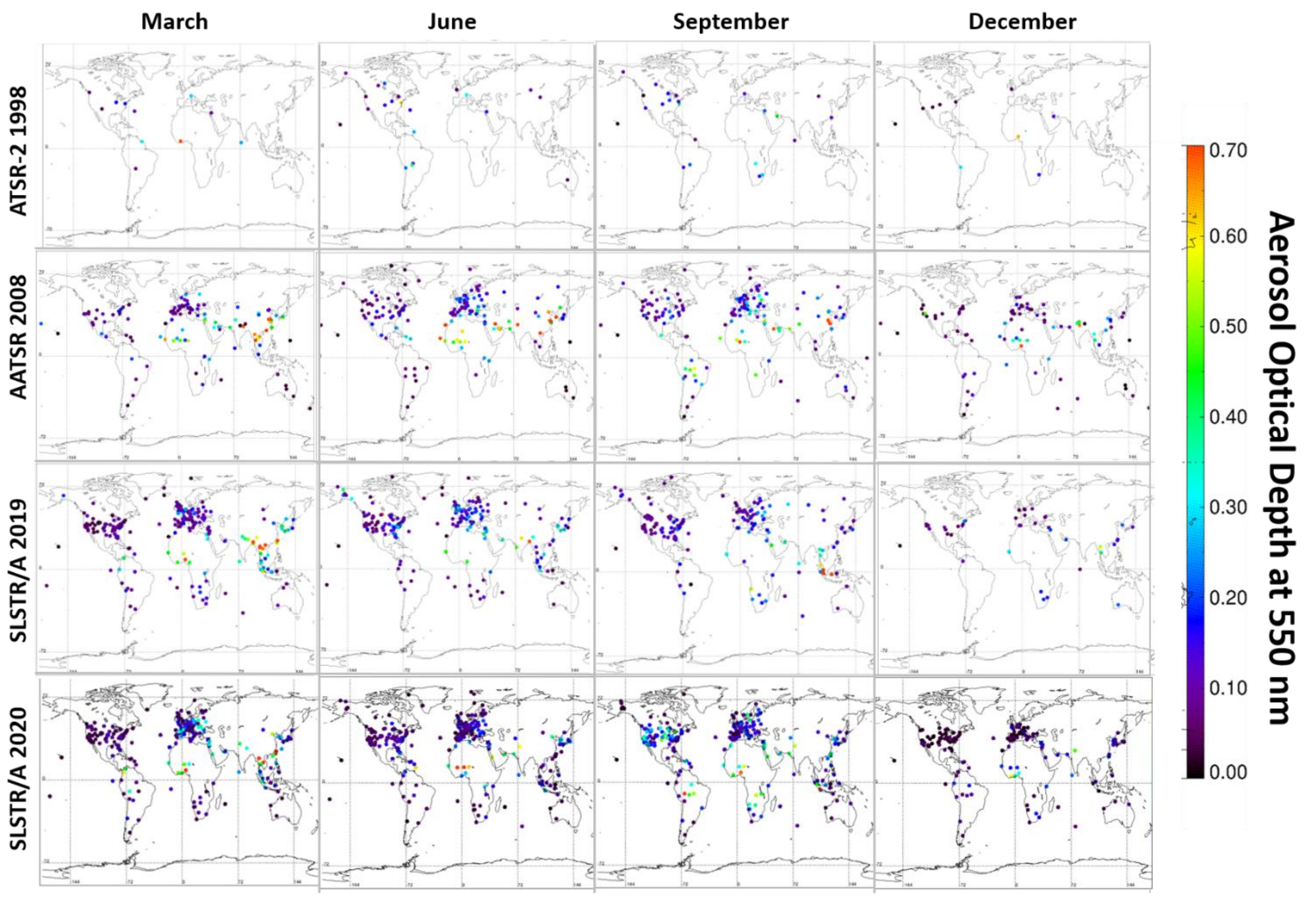

Figure 2.1 *Monthly AOD550 mean maps from AERONET matched to the 4 sensors and 4 years*

MODIS is the most widely used satellite-sensor based aerosol product data-set (e.g. AOD, fire counts), (1) as global coverage (with at least two daytime overpasses) is among the best (an important element in data assimilations), (2) the retrieval (improved over two decades) has reached a higher level of maturity and (3) its retrieval data can be accessed relatively easy. As retrieval over brighter (land) surfaces remain difficult, there appears (despite of pulling information from two different [deep blue and dark target] approaches) a tendency to overestimate AOD over continents. In this study, MODIS aerosol data of the most recent collection 6.1 (combined DR&DB) processing are applied. As data for AODf in that processing are (officially) only offered over oceans, AODf estimates for MODIS over land were added based on a method by P. Ginoux were added, which also provides AODdu estimates over continents. AODc is simply defined by the difference: AOD minus AODf. Monthly (March, June, September and December) MODIS maps for years 2008 and 2019 mid-visible total AOD are presented in Figure 6.1, fine-mode AOD (AODf), coarse-mode AOD (AODc) and dust AOD (AODdu) will be analyzed in the next version of the report.

MISR offers advanced aerosol retrievals with its multi-spectral and multi-viewing capabilities. In past retrieval comparisons, the older MISR v22 AOD retrieval was a top performer over continents but displayed a strong AOD high bias over oceans. In the new MISR v32 retrieval not only pixel resolution was improved but also the ocean bias was largely removed. Still, MISR has limited spatial daily coverage and its monthly statistics (even at 1x1 degree spatial resolution) is poor compared to polar orbiting satellite sensors with a wider swath. Thus, only larger differences that are consistent over larger regions should be discussed in more detail. AODf is here represented by MISR assigned AOD to small aerosol sizes, AODc represents the MISR assigned AOD to mid and larger aerosol sizes and AODdu refers to MISR assigned AOD to non-spherical aerosol. Monthly (March, June, September and December) MISR maps for years 2008 and 2019 mid-visible total AOD are presented in Figure 6.1, fine-mode AOD (AODf), coarse-mode AOD (AODc) and dust AOD (AODdu) will be analyzed in the next version of the report.

POLDER The POLarization and Directionality of the Earth's Reflectances) is a key sensor dedicated to cloud and aerosol aboard the Parasol satellite, which flies in formation with the A-train formation including Aqua and CALIOP (afternoon daytime overpass). POLDER provides global coverage every one to two days. The retrieved aerosol products are primarily AOD and ANG over oceans. Moreover, polarization capabilities allow estimates of dust AOD over oceans and FM-AOD over continents. This instrument was operated 2005 – 2013 and can thus only be used for comparison with AATSR, not with SLSTR. Monthly (March, June, September and December) POLDER/GRASP maps for years 2008 and 2019 mid-visible total AOD are presented in Figure 6.1.

For year 1998, AOD products from other satellites which can be used for the evaluation of the ATSR-2 SU AOD product are not available. For ATSR-2 SU AOD product evaluation we use **ATSR-2 ADV v2.31 AOD** product (https://climate.esa.int/sites/default/files/Aerosol_cci2_PVIR_v3.41.pdf), as a reference.

3 OVERVIEW OF TEST DATA FOR EVALUATION

The SU v1 test data include 4 months global observations with 10km horizontal resolution for each of the four sensors concerned as shown in Table 3.1. Figures 3.1 – 3.3 show monthly mean maps of SU v1 AOD at 550 nm, the uncertainty of AOD at 550 nm and the FM-AOD at 550 nm of the four months in each year which will be analysed. The images show similar dominant seasonal patterns (e.g. summer Atlantic desert outbreaks, autumn biomass burning events in the Southern hemisphere, Eastern Asian pollution) and some inter-annual differences. They also reveal the limitations of coverage due to low sun and underlying snow / ice (respective hemisphere winters). Particularly good agreement between the 2 SLSTR maps of the same year (last 2 rows) can be seen as well as the weaker coverage of the earliest sensor ATSR-2 (first lines). Fine-Mode AOD suppresses the large dust outbreaks well but not completely. It appears slightly larger for the 2 SLSTR datasets than for the 2 ATSR datasets. Pixel-level uncertainties show distinctly larger values for SLSTR than for ATSR-2 and AATSR in the Northern hemisphere (except the Sahara) and smaller values in the Southern hemisphere.

Figures 3.4 – 3.6 show monthly mean maps of SU v2 AOD at 550 nm, the uncertainty of AOD at 550 nm and the FM-AOD at 550 nm of the four months in each year which will be analysed. The major patterns for the ATSR instruments agree mostly for v1 and v2 datasets, while there is better coverage with v4.33 for ATSR-2. For both SLSTR instruments there are reduced AOD values in areas of bright surfaces (Middle-East, higher latitudes, South America) and some AOD increase over India and in the Southern Sahara from v1.11 to v1.14; also AOD uncertainties in Northern mid-latitudes are slightly reduced.

Figure 3.7 shows monthly AOD maps of the second algorithm (Rayference / CISAR) covering only 2/3 of the globe (excluding the Americas so far) and for different months (September – December). These monthly averages have been produced by the provider, selecting only pixels with Quality Index > 0. While there is some similarity with the SU maps of AOD peak regions in the common months September and December, there are major differences: CISAR AOD is overall much higher (in particular near plume areas over ocean, but also in the background levels in remote regions).

***Table 3.1** analysed dataset list*

label	***retrieval version***	***provider***	***period***
CRDP-1: SU v1 datasets			
ATSR2 SU v4.32	ATSR-2, SU, v4.32 (corrected)	Swansea	1998: 3, 6, 9, 12
AATSR SU v4.32	AATSR, SU, v4.32	Swansea	2008: 3, 6, 9, 12
SLSTRA SU v1.11	SLSTR/S3A, SU, v1.11	Swansea	2019: 3, 6, 9, 12
SLSTRB SU v1.11	SLSTR/S3B, SU, v1.11	Swansea	2019: 3, 6, 9, 12
CRDP-2: SU v2 datasets			
ATSR2 SU v4.33	ATSR-2, SU, v4.33	Swansea	1998: 3, 6, 9, 12
AATSR SU v4.33	AATSR, SU, v4.33	Swansea	2008: 3, 6, 9, 12
SLSTRA SU v1.14	SLSTR/S3A, SU, v1.14	Swansea	2019: 3, 6, 9, 12
SLSTRB SU v1.14	SLSTR/S3B, SU, v1.14	Swansea	2019: 3, 6, 9, 12
CRDP-2: RF v1 dataset			
SLSTRA RF v2.0.0	SLSTR/S3A, RF, v2.0.0	Rayference	2019: 9 - 12
CRDP-3: SU v3 datasets			
ATSR2 SU v4.35	ATSR-2, SU, v4.33	Swansea	1998: 1-12
AATSR SU v4.35	AATSR, SU, v4.33	Swansea	2008: 1 - 12
SLSTRA SU v1.14	SLSTR/S3A, SU, v1.14	Swansea	2020: 1 - 12
SLSTRB SU v1.14	SLSTR/S3B, SU, v1.14	Swansea	2020: 1 - 12
CRDP-3: RF v2 dataset			
SLSTRA RF V2.2.1	SLSTR/S3A, RF, V2.2.1	Rayference	2020: 1 - 12

Note that in the SLSTR SU v1.11 products two variables have been swapped (AAOD and FM-AOD). We rectified this by reading the variable "AAOD" for evaluating FM-AOD.

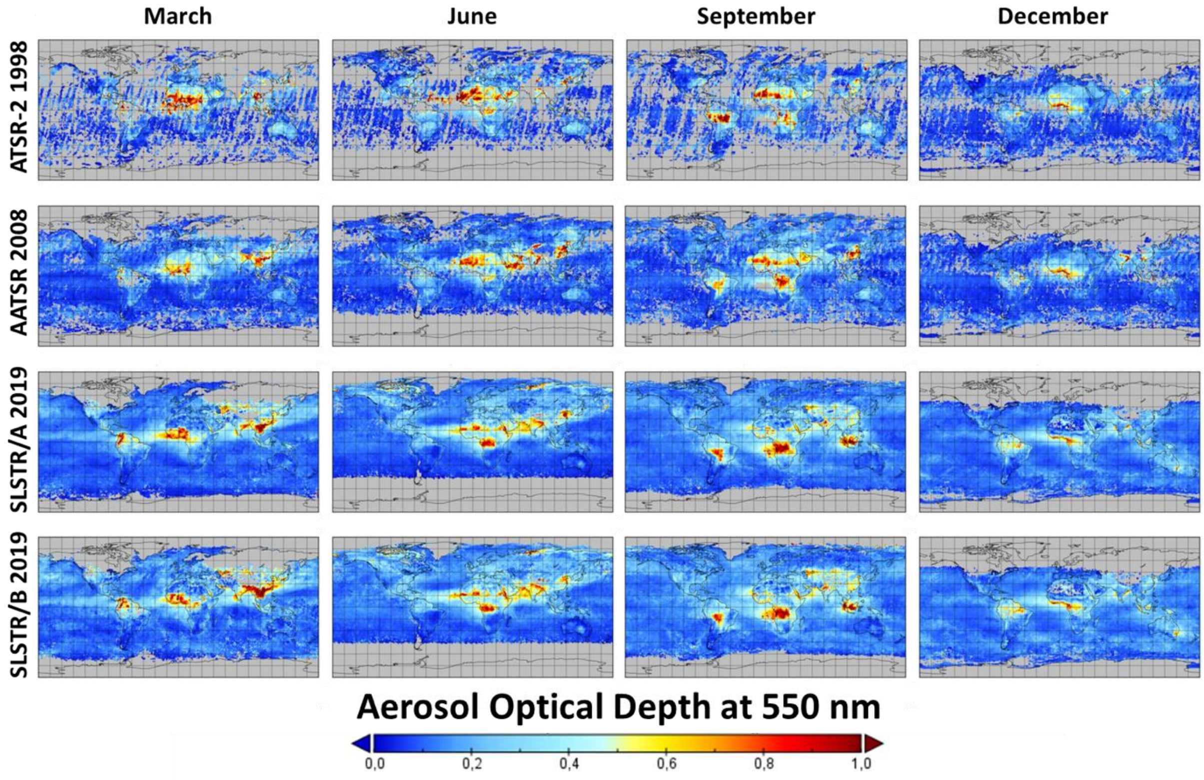

***Figure 3.1** Monthly SU v1 AOD550 mean maps of the 4 sensor datasets*

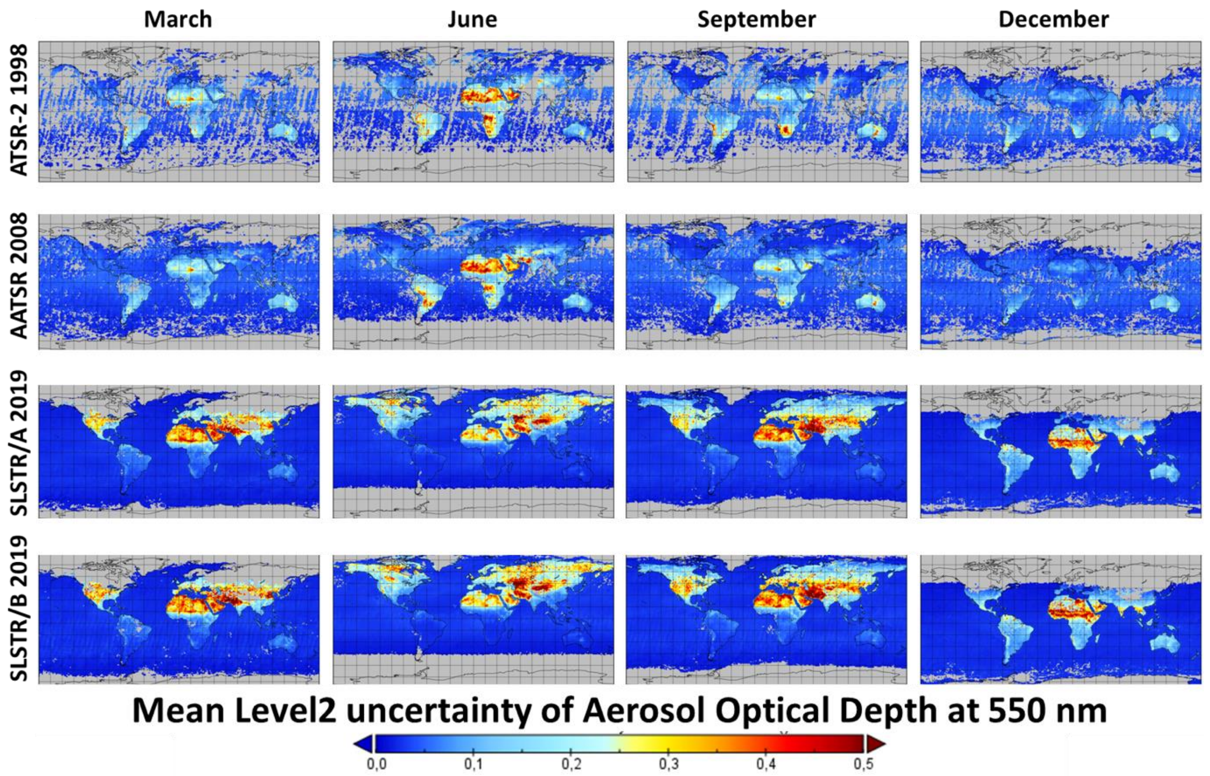

Figure 3.2 *Monthly SU v1 AOD550 uncertainty mean maps of the 4 sensor datasets (L2 uncertainty mean)*

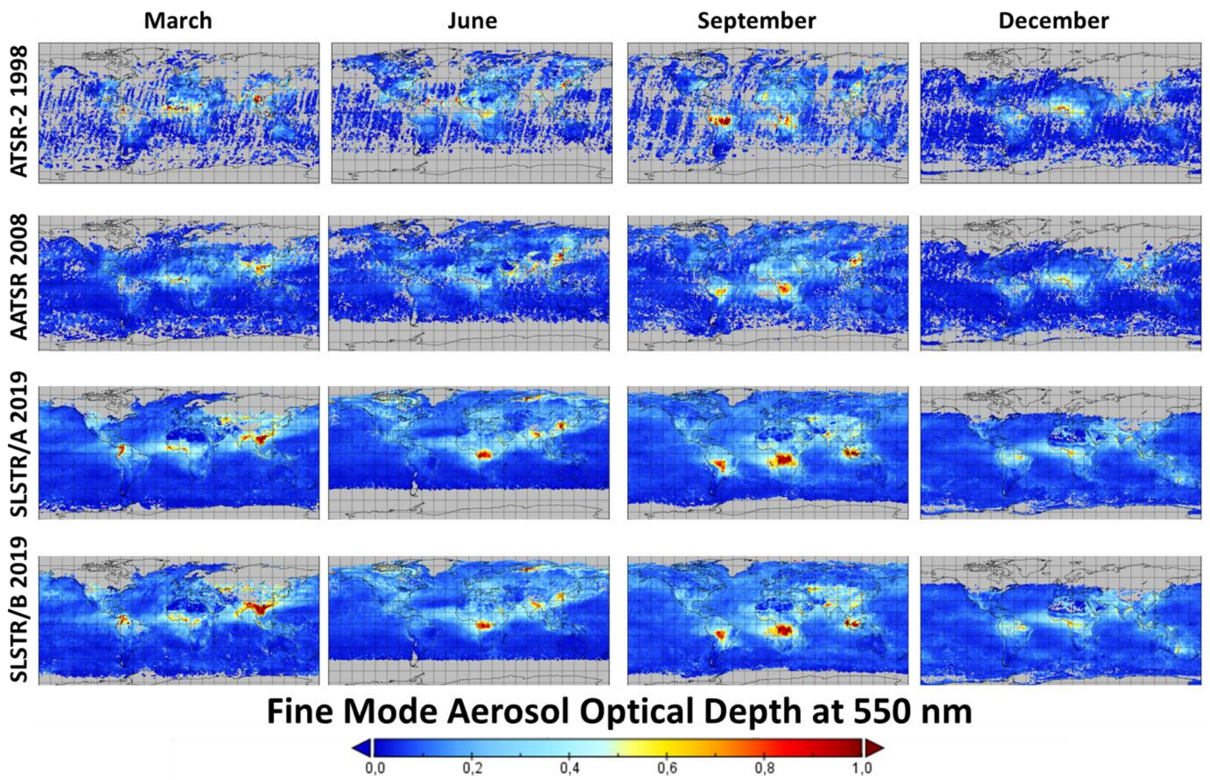

Figure 3.3 *Monthly SU v1 FM-AOD550 mean maps of the 4 sensor datasets*

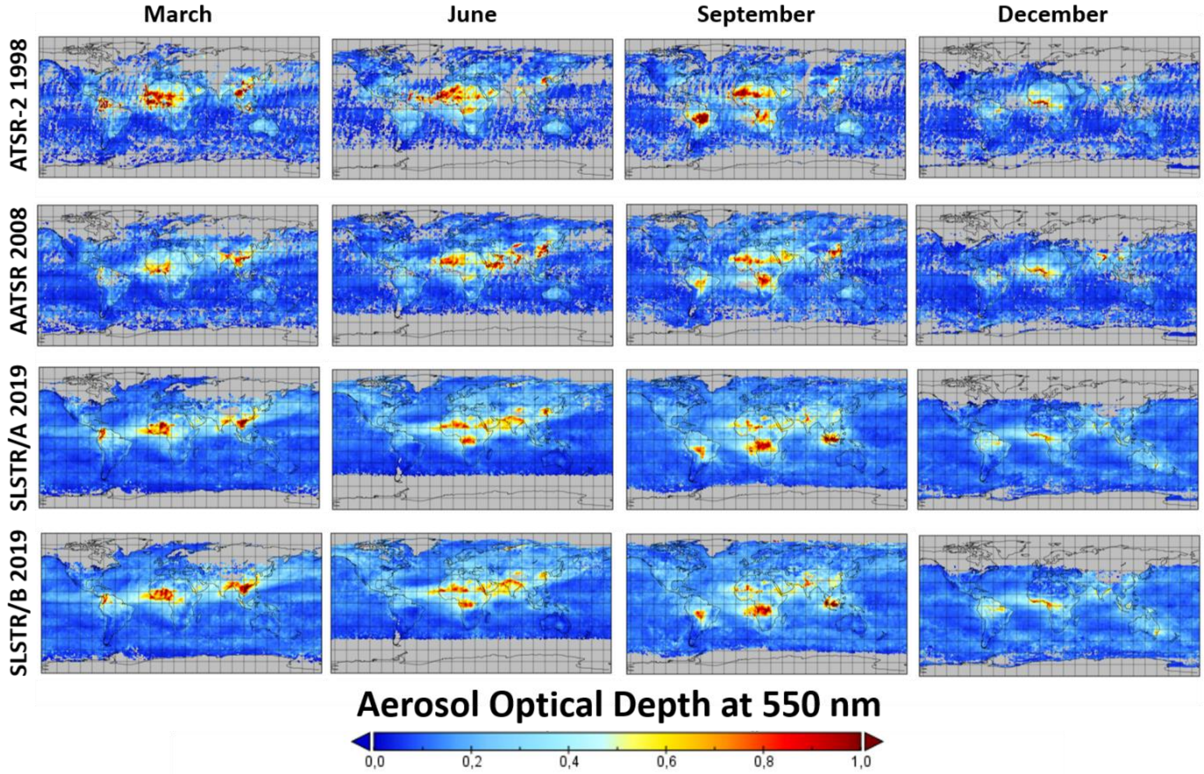

Figure 3.4 *Monthly SU v2 AOD550 mean maps of the 4 sensor datasets*

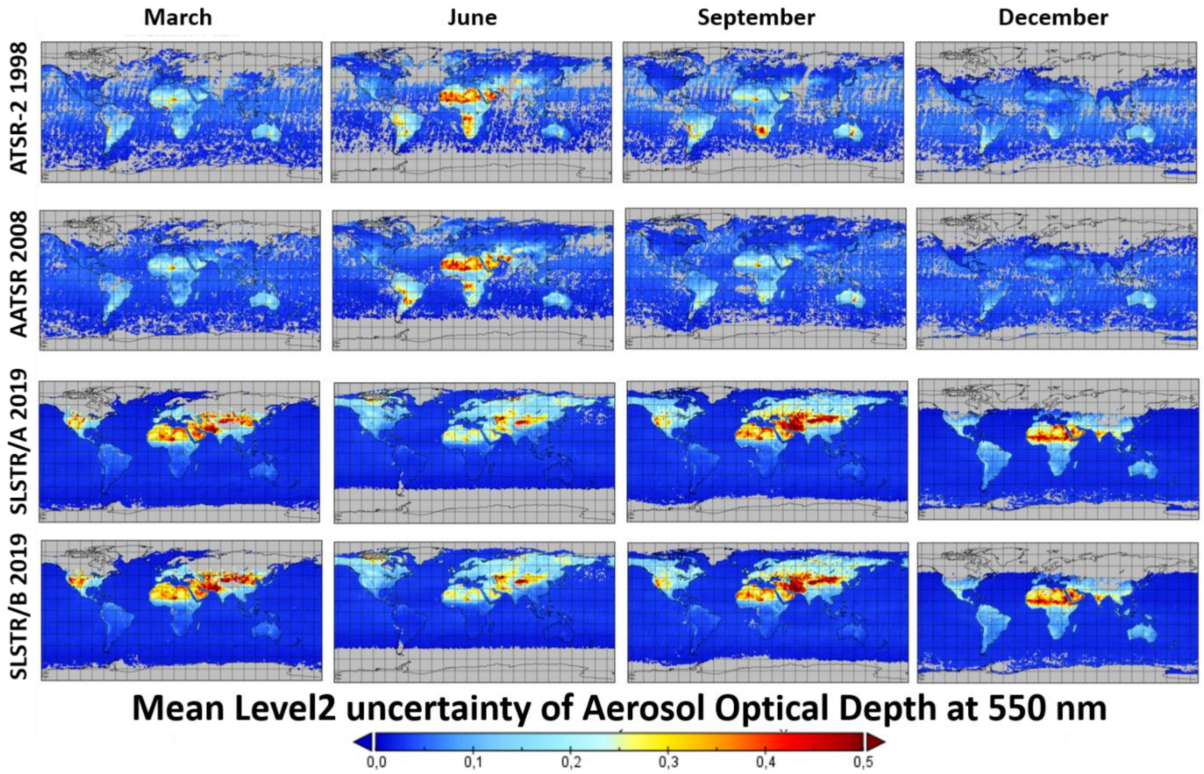

Figure 3.5 *Monthly SU v2 AOD550 uncertainty L2 mean maps of the 4 sensor datasets*

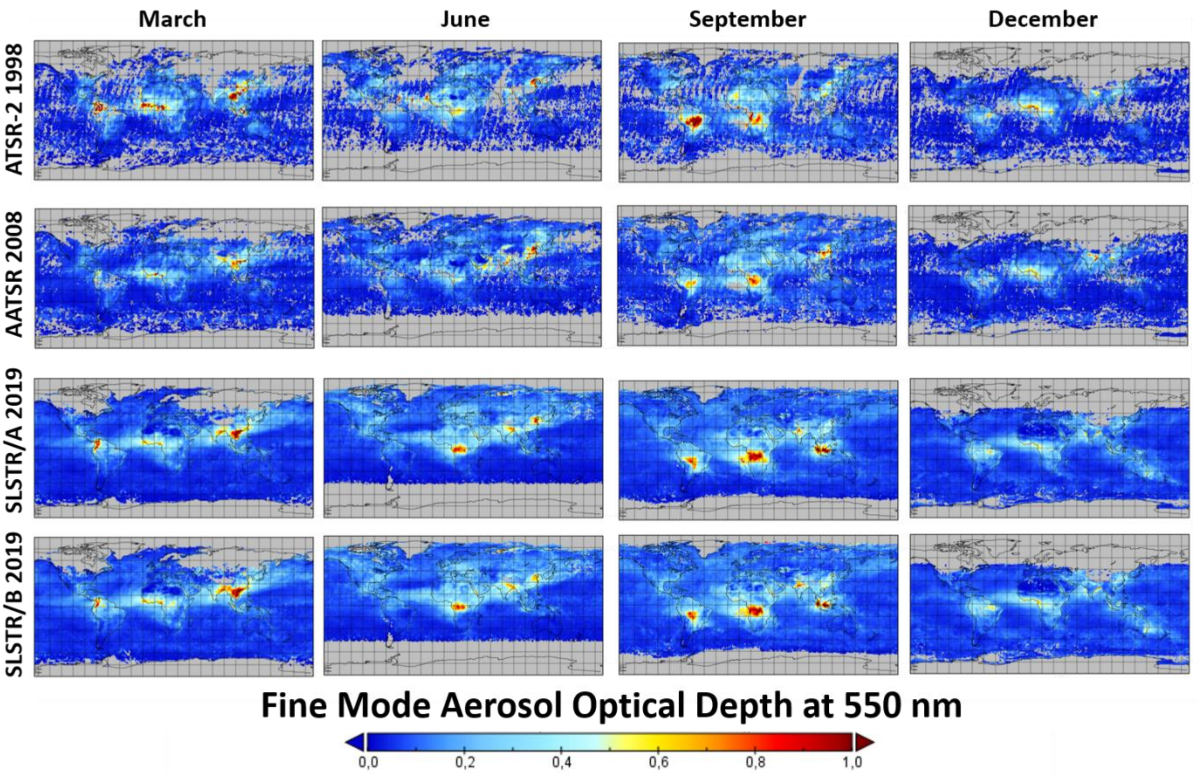

Figure 3.6 *Monthly SU v2 FM-AOD550 mean maps of the 4 sensor datasets*

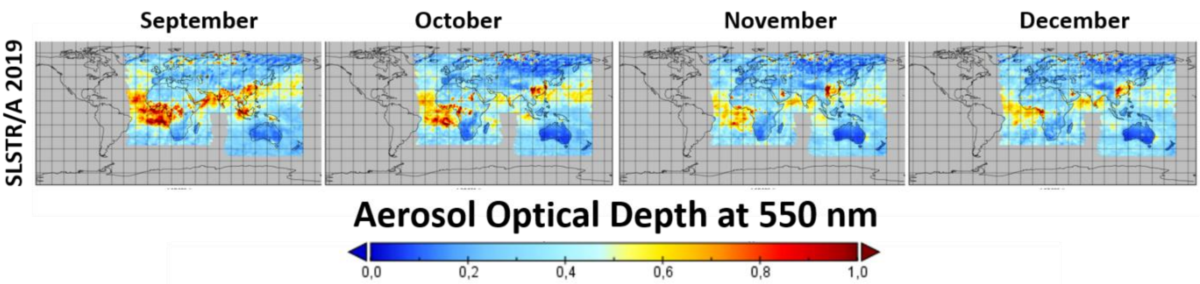

Figure 3.7 *Monthly RF v1 AOD550 mean maps of SLSTR/3A*

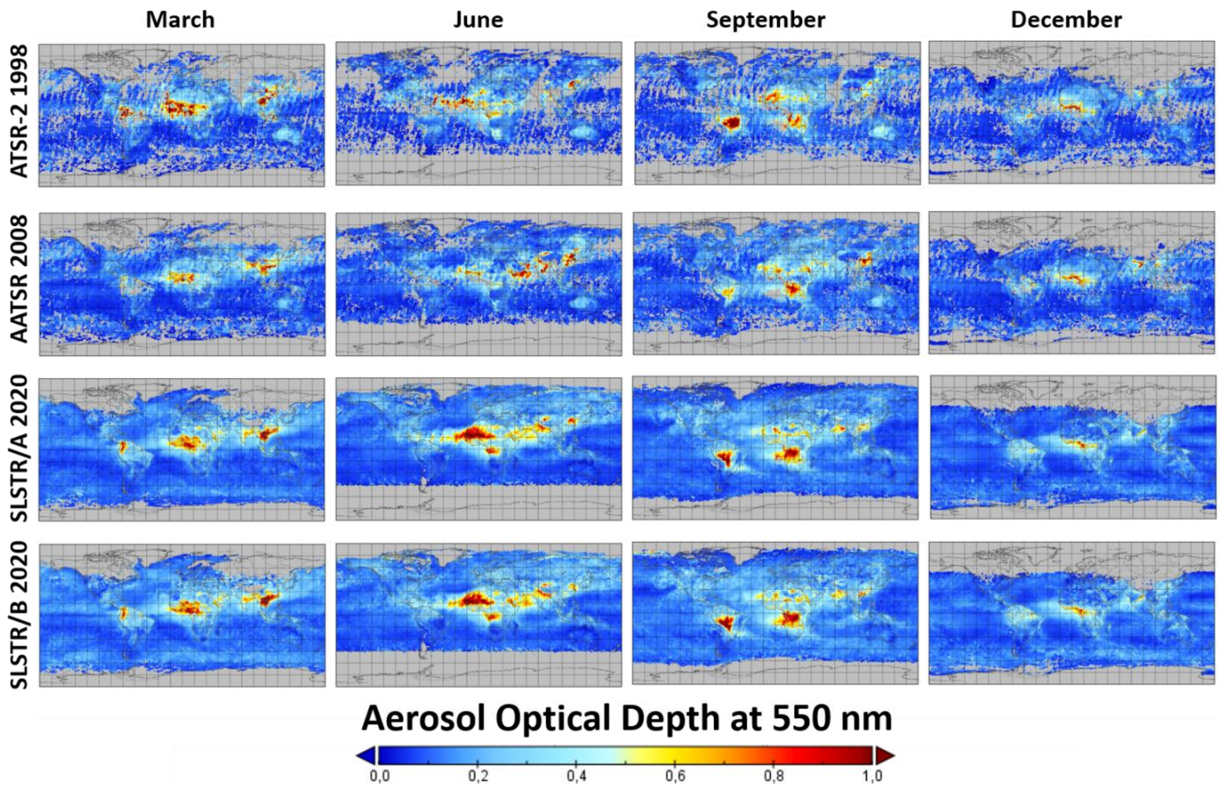

Figure 3.8 *Monthly SU v3 AOD550 mean maps of the 4 sensor datasets*

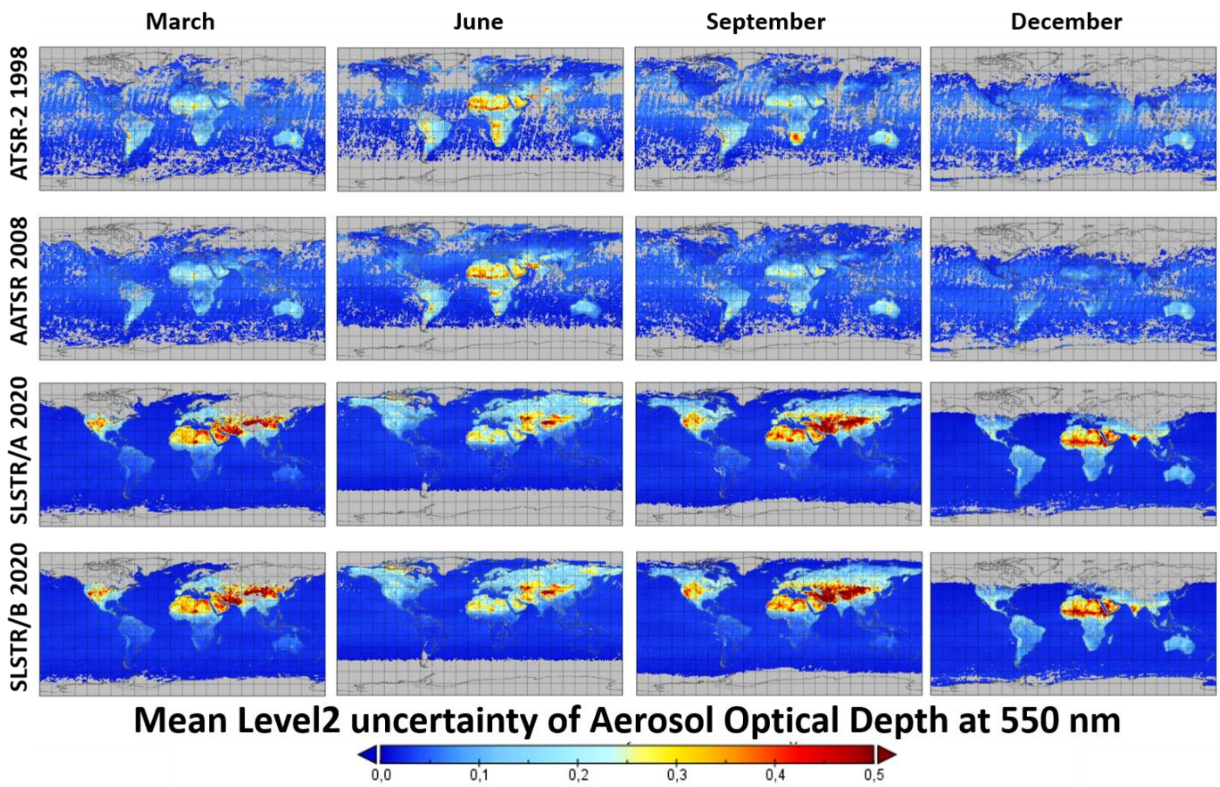

Figure 3.9 *Monthly SU v3 AOD550 uncertainty L2 mean maps of the 4 sensor datasets*

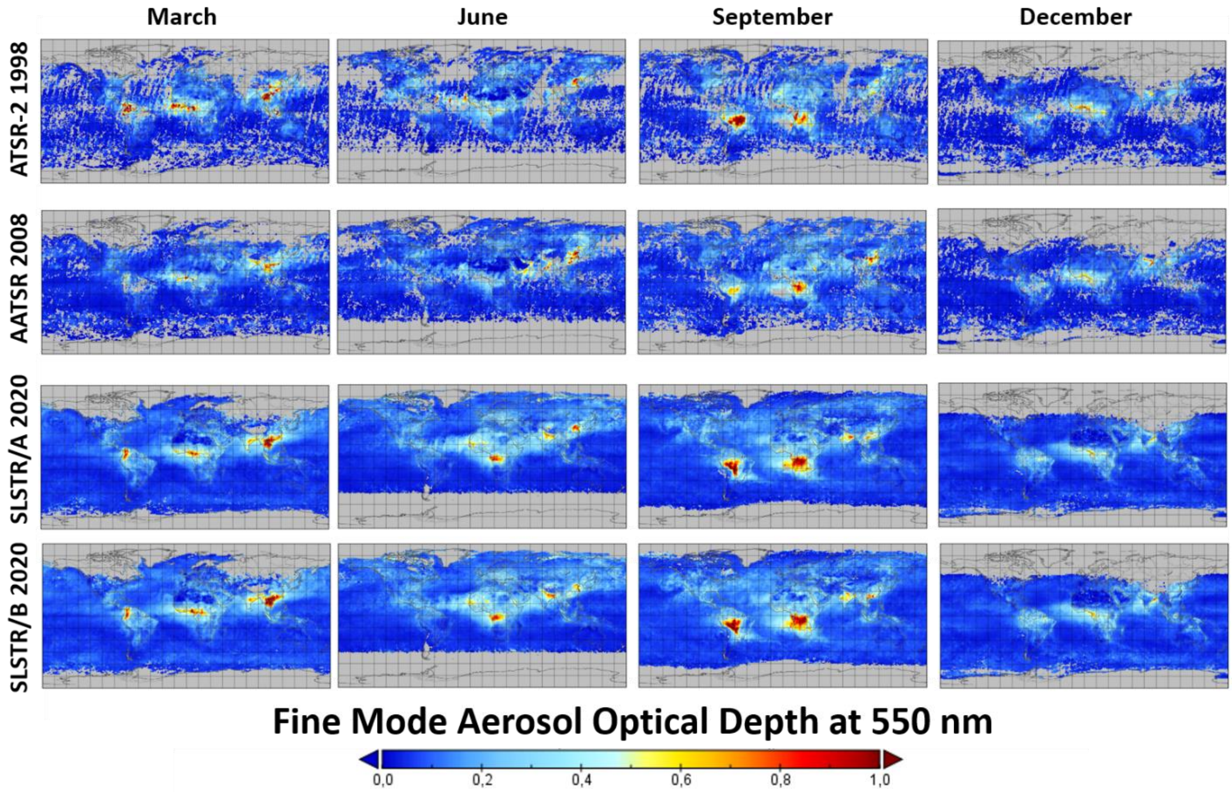

Figure 3.10 *Monthly SU v3 FM-AOD550 mean maps of the 4 sensor datasets*

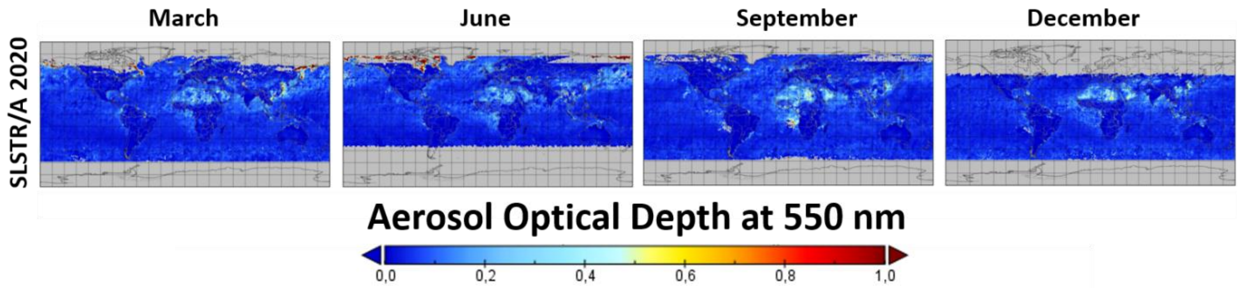

Figure 3.11 *Monthly RF v2 AOD550 mean maps of SLSTR/3A*

4 LEVEL2 EVALUATION AGAINST AERONET

4.1 Validation of AOD550

According to the standard procedure established in the community, the validation is done for the level2 datasets with 10x10 km^2 resolution in orbit projection, which are closest to the retrieval and therefore are able to provide direct insight into their quality. For each dataset version per algorithm and sensor, matching to AERONET (and future MAN) reference measurements is made within ±30 minutes and ±50km. We keep individual satellite pixels (no spatial averaging; in particular to avoid averaging the prognostic uncertainties) which are counted as "Number of sat pixel" in Table 4.1. This means that several satellite pixels may match with the same Aeronet station observation (which we count as "Number1 of stat obs"). We use the newest AERONET version 3 data with better coverage of high AOD cases. In the matching all available AERONET measurements within the time window for one day / location are averaged, while individual satellite pixels are kept to avoid changes due to averaging of the level2 values. We calculate then statistical quantities (**bias, rmse, stdv, Pearson correlation, fraction of pixels within GCOS requirement envelope**) for AOD per station and on global average for all land stations and all coastal / ocean stations. The accuracy requirement for AOD provided by GCOS is represented as a combination of absolute and relative accuracy due to the log-normal AOD distribution with many low values as **max (0.03 or 10%)**. We calculate the fraction of pixels which fall into this envelope ("**GCOS fraction**") which should be **68%** for a normal distribution of errors. We also calculate a "Bias corrected GCOS fraction" where we subtract the mean bias from all satellite observations for testing the GCOS envelope. Furthermore, we try to iteratively fit the smallest possible envelope which contains 68% of the errors of all pixels (in steps of 0.01 and 3.3% rounded), which we name "Adapted GCOS envelope".

4.1.1 CRDP-1 SU v1 validation results

All statistical quantities are presented per sensor / year separately over land and ocean in Table 4.1. Those values are furthermore presented separately per sensor / year for each station in Table A.1 in the Annex (section 9). It should be noted that the statistics for ATSR-2 (with much less stations operating in the early days of AERONET and less coverage of ATSR-2) and for some stations are of low significance when the number of matching pairs is low (all statistics) or when only low AOD values occur (correlation is of less meaning). The tables in the Annex contain the relevant station information (latitude, longitude, elevation, land / water assignment) and further statistical values (number of matching pairs, mean AOD of AERONET and Satellite, split of bias for all / low / high AOD.

Table 4.1 shows low bias for ATSR-2 and AATSR (0.01 to 0.02) over land, somewhat larger bias for ATSR-2 and AATSR over ocean (0.03 to 0.04), but consistently larger bias for both SLSTR over land and ocean (0.05 to 0.06). Standard deviations (except ATSR-2 with less matching pairs) range from 0.07 or 0.08 over ocean for all sensors to 0.11 over land for AATSR and 0.15 over land for both SLSTR. Correlation coefficients over ocean are similar for all sensors (better than 0.8) and over land range from 0.6 (ATSR-2) to 0.9 (AATSR). GCOS fractions are near 50% for ATSR-2 and AATSR (and after bias-correction only slightly larger) and below 40% for SLSTR (after bias-correction over ocean increased to about 55%). Adapted GCOS envelopes (not bias-corrected!) range from [0.03 or 29%] for AATSR over ocean to [0.04 or 29%] for AATSR over land and [0.06 or 29%] for SLSTR over ocean and [0.09 or 23%] for SLSTR over land – altogether showing larger noise for large AOD values. In summary, both SLSTR datasets have high bias and stdv (in particular over land) with lower GCOS fractions and wider adapted GCOS envelopes.

Table 4.1 Global validation statistics for SU v1 AOD at 550nm

year	sensor	alg_version	area	Number of sat pixel	number1 of stat obs	bias	rmse	stdv	Pearson corr	GCOS fraction	Corrected GCOS fraction	Adapted GCOS envelope
CRDP-1 SU v1 datasets												
1998	ATSR2	SU_v4.32	land	6597	119	0.01	0.20	0.19	0.59	48.8	49.3	max(0.05 or 29%)
1998	ATSR2	SU_v4.32	ocean	1283	42	0.04	0.08	0.07	0.78	45.6	47.5	max(0.07 or 3%)
2008	AATSR	SU_v4.32	land	65636	1302	0.02	0.11	0.11	0.89	52.3	51.0	max(0.04 or 29%)
2008	AATSR	SU_v4.32	ocean	9314	296	0.03	0.12	0.11	0.84	57.0	59.7	max(0.03 or 29%)
2019	SLSTRA	SU_v1.11	land	112397	2925	0.05	0.16	0.15	0.73	35.2	34.6	max(0.09 or 23%)
2019	SLSTRA	SU_v1.11	ocean	55781	1085	0.05	0.10	0.08	0.86	40.3	55.6	max(0.06 or 29%)
2019	SLSTRB	SU_v1.11	land	92417	2300	0.05	0.15	0.15	0.68	34.3	33.7	max(0.09 or 33%)
2019	SLSTRB	SU_v1.11	ocean	44100	850	0.06	0.10	0.08	0.86	33.6	54.4	max(0.07 or 26%)

Suitable for the log-normal AOD distributions we do not calculate linear fits but show as validation summaries for each sensor / year separated over land and ocean box-whisker plots (fig. 4.1 and 4.2) and density scatter plots (Fig. 4.3 and 4.4). Both plot types show the retrieved AOD values against the AERONET reference AOD values. In Fig. 4.1. and 4.2 AOD statistical values are averaged for a suitable number of bins with approximately equal numbers (30 except for ATSR-2 with 15). For each bin the mean and the standard deviation of the AERONET and retrieval AOD values and the 5% / 95% range of the retrievals are shown as asterix, box and vertical line, respectively. With this visualisation AOD bias and spread can be seen as function of the reference AOD value. As additional information those plots also show the GCOS envelope (dashed) and an

AOD frequency distribution (to see which range of AOD values will dominate the overall statistics). Furthermore, those plots also show in green boxes the uncertainty values (AERONET set to 0.01 and retrieval averaged from the pixel level uncertainty values in the data files). The plots are rather noisy for ATSR-2 and show for ATSR-2 and AATSR good agreement with some tendency to over-estimate high AOD values and to over-estimate the lowest AOD bin. Averaged uncertainties for AATSR remain smaller than the standard deviation of AOD values while for ATSR-2 they are a bit larger. For SLSTR the plots show a significant overall bias for low AOD over land (decreasing for larger AOD) and for the whole AOD range over ocean. Averaged uncertainties are smaller than the standard deviations over ocean but clearly larger than the stdv over land and also larger than for AATSR. The density scatter plots (Fig. 4.3 and 4.4) show similar information with SLSTR bias generally higher (in particular over ocean) and also SLSTR scatter larger; for ATSR-2 the statistics are generally weak due to low numbers.
Furthermore, difference histograms over land and ocean are calculated and split for low (<0.2) and high (>0.2) AOD550 ranges per sensor / year (Fig. 4.5 and Fig. 4.6). For AATSR the stdv of high AOD values is larger than for low AOD values while the bias is equally small for all of them (ATSR-2 histograms are noisy but show similar tendencies). For SLSTR over land also stdv is larger for high AOD, but the mean bias is clearly smaller than for low AOD; over ocean a similar tendency can be seen for stdv, but the bias is equal over the whole AOD range.

The maps of mean bias and stdv per station (fig. 4.7 and fig. 4.8) show for the ATSR instruments low bias and stdv (with slightly larger values in Northern tropical latitudes for AATSR), but again a significant positive bias for both SLSTR (a bit lower in the Southern hemisphere, but with less stations) and larger stdv values in the Northern hemisphere over land / mid-latitudes. These findings point to a dependency of retrieval errors to the observing geometry which differs between ATSR and SLSTR instruments with most favourable conditions over the Northern hemisphere for ATSR and the Southern hemisphere for SLSTR.

We also investigated monthly regional bias for each sensor. Those maps are not shown, but we report here a few clear observations of exceptional behaviour (in many other cases there are only one or two stations with exceptional bias or scattered biases between neighbour stations which we do not regard sufficient). For ATSR-2 / 1998 there are too few stations to analyse seasonal and regional behaviour with 4 monhts of data. For AATSR /2008 in March and June the Sahel region has large positive bias, whereas East Asia and Middle East in March and the Atlantic off Africa and South America in June have negative bias. For both SLSTR instruments in 2019 there is a general positive bias in the Northern hemisphere and even larger positive bias in Central North America in Marhc, while negative bias occurs in South Asia and Arabia in March and in Europe in September.

We finally split the validation over the two hemispheres as we are aware of different scattering angle distributions between them. Tab. 4.2 shows the major validation statistics and indicates (but not in all metrics) that for the ATSR instruments AOD retrieval perform less accurately in the South than in the North, while the SLSTR instruments behave in the opposite direction.

Table 4.2 *Validation statistics for SU v1 AOD at 550nm for Northern / Southern hemispheres*

year	sensor	Algorithm / version	area	Number of sat pixel	Number1 of stat obs	bias	stdv	Pearson corr	GCOS fraction
1998	ATSR2	SU_v4.32	land	6597 4956 1641	119 90 28	0.01 0.00 0.05	0.19 0.21 0.12	0.59 0.59 0.63	48.8 53.9 33.3
1998	ATSR2	SU_v4.32	ocean	1283 2182	42 41	0.04 0.04 -	0.07 0.07 -	0.78 0.78 -	45.6 45.6 -
2008	AATSR	SU_v4.32	land	65636 56962 8674	1302 1119 182	0.02 0.01 0.06	0.11 0.11 0.10	0.89 0.89 0.83	52.3 55.0 34.9
2008	AATSR	SU_v4.32	ocean	9314 8621 693	296 273 22	0.03 0.03 0.02	0.11 0.12 0.03	0.84 0.84 0.73	57.0 56.2 66.7
2019	SLSTRA	SU_v1.11	land	112397 94804 17593	2925 2614 310	0.05 0.05 0.04	0.15 0.14 0.20	0.73 0.77 0.59	35.2 31.3 56.0
2019	SLSTRA	SU_v1.11	ocean	55781 52525 3256	1085 1020 64	0.05 0.05 0.03	0.08 0.09 0.04	0.86 0.86 0.78	40.3 38.5 69.6
2019	SLSTRB	SU_v1.11	land	92417 78279 14138	2300 2059 240	0.05 0.06 0.04	0.15 0.14 0.19	0.68 0.71 0.60	34.3 30.8 53.5
2019	SLSTRB	SU_v1.11	ocean	44100 41478 2622	850 797 52	0.06 0.06 0.03	0.08 0.08 0.04	0.86 0.86 0.62	33.6 31.7 65.0

All North South "South validation is worse" "South validation is better"

Summary for the validation of total AOD

- High positive bias and larger scatter for SLSTR
- decreasing for bias for SLSTR with increasing AOD over land
- constant bias for SLSTR over the whole AOD range over ocean
- SLSTR uncertainties over land significantly larger
- Indication of hemispheric differences in data quality (with less stations in the South), swapped for ATSR and SLSTR

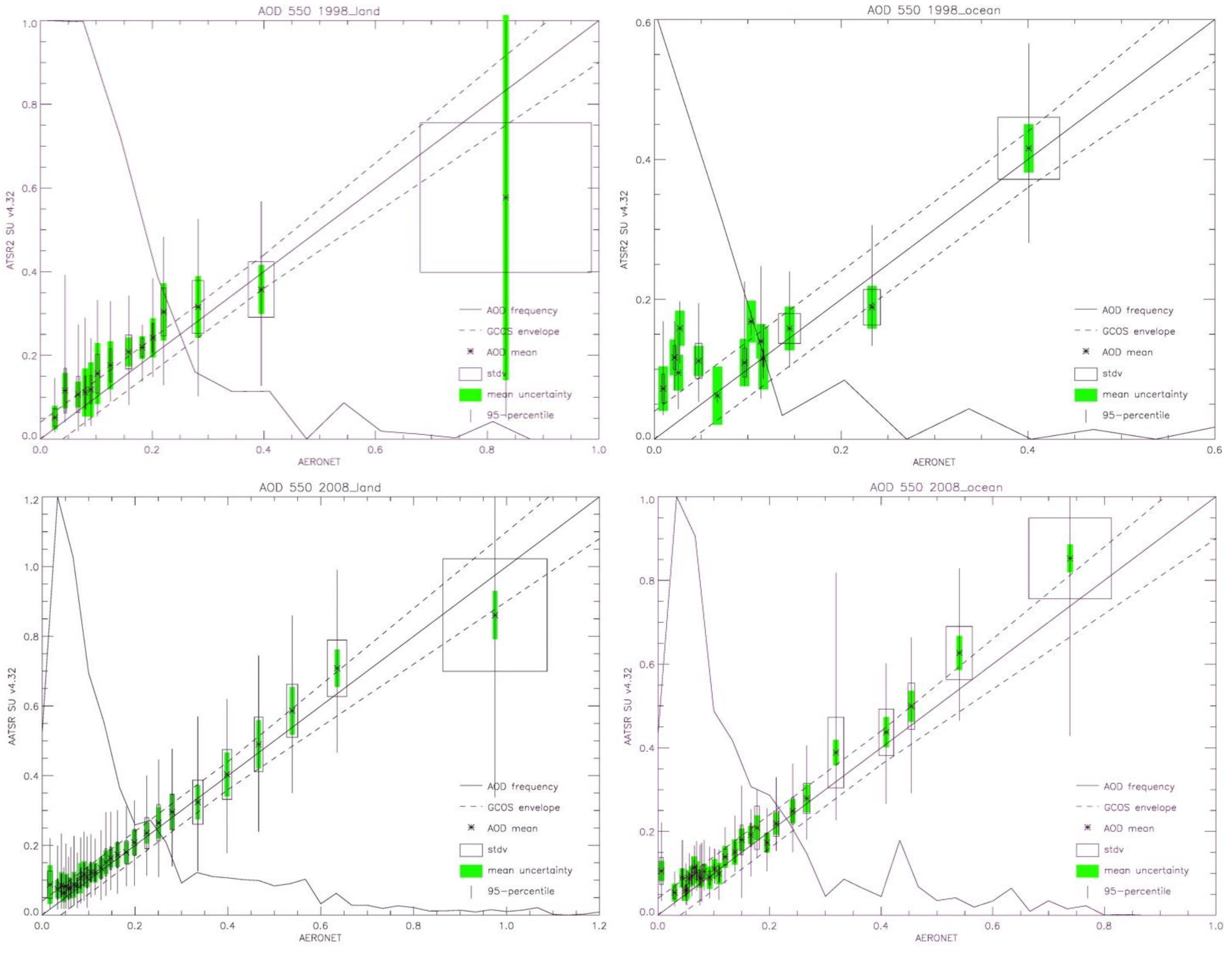

Figure 4.1 *Validation summary plots for ATSR-2 (top) and AATSR (bottom) over land (left) and ocean (right).*

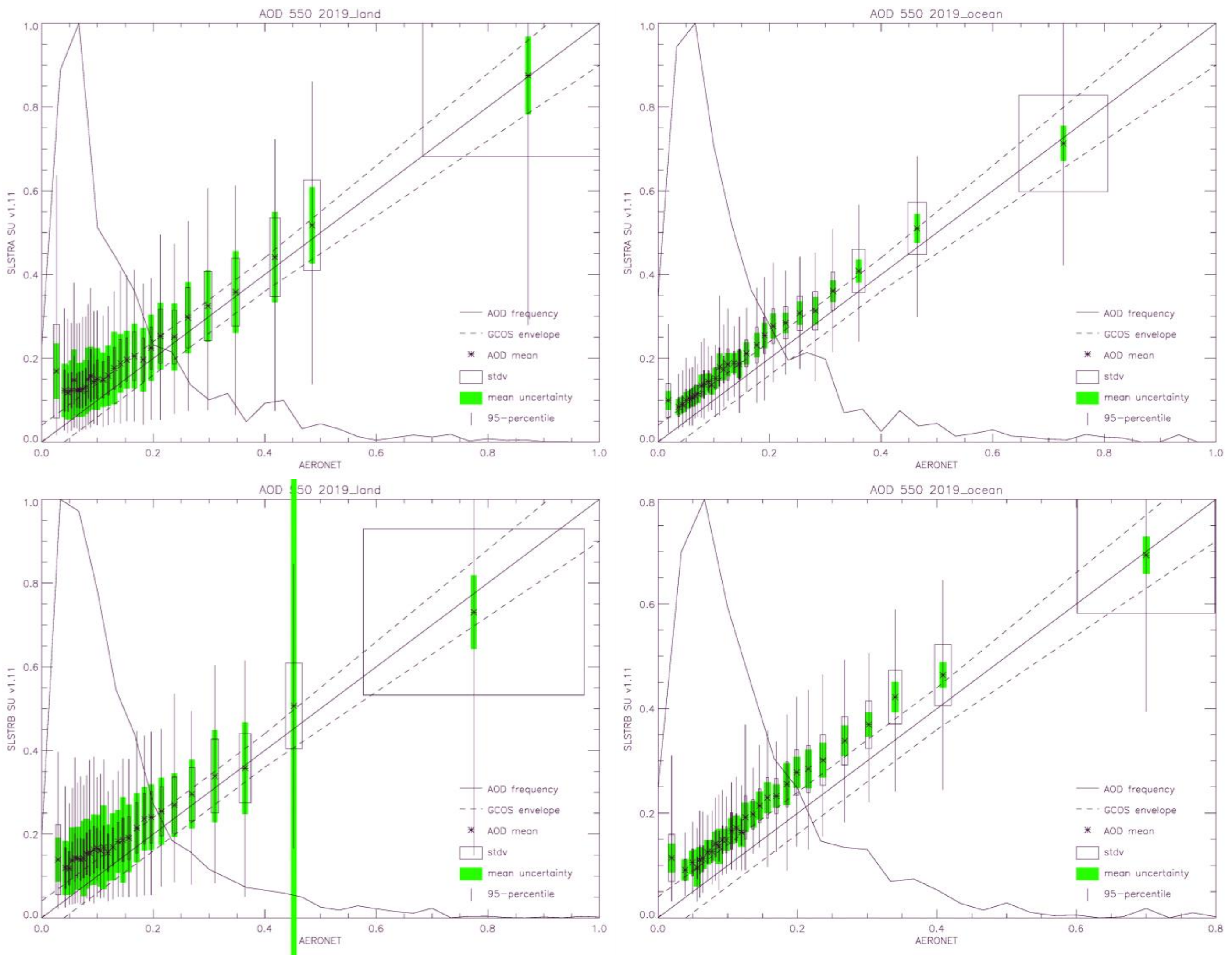

***Figure 4.2** Validation summary plots for SLSTR/3A (top) and SLSTR/3B (bottom) over land (left) and ocean (right).*

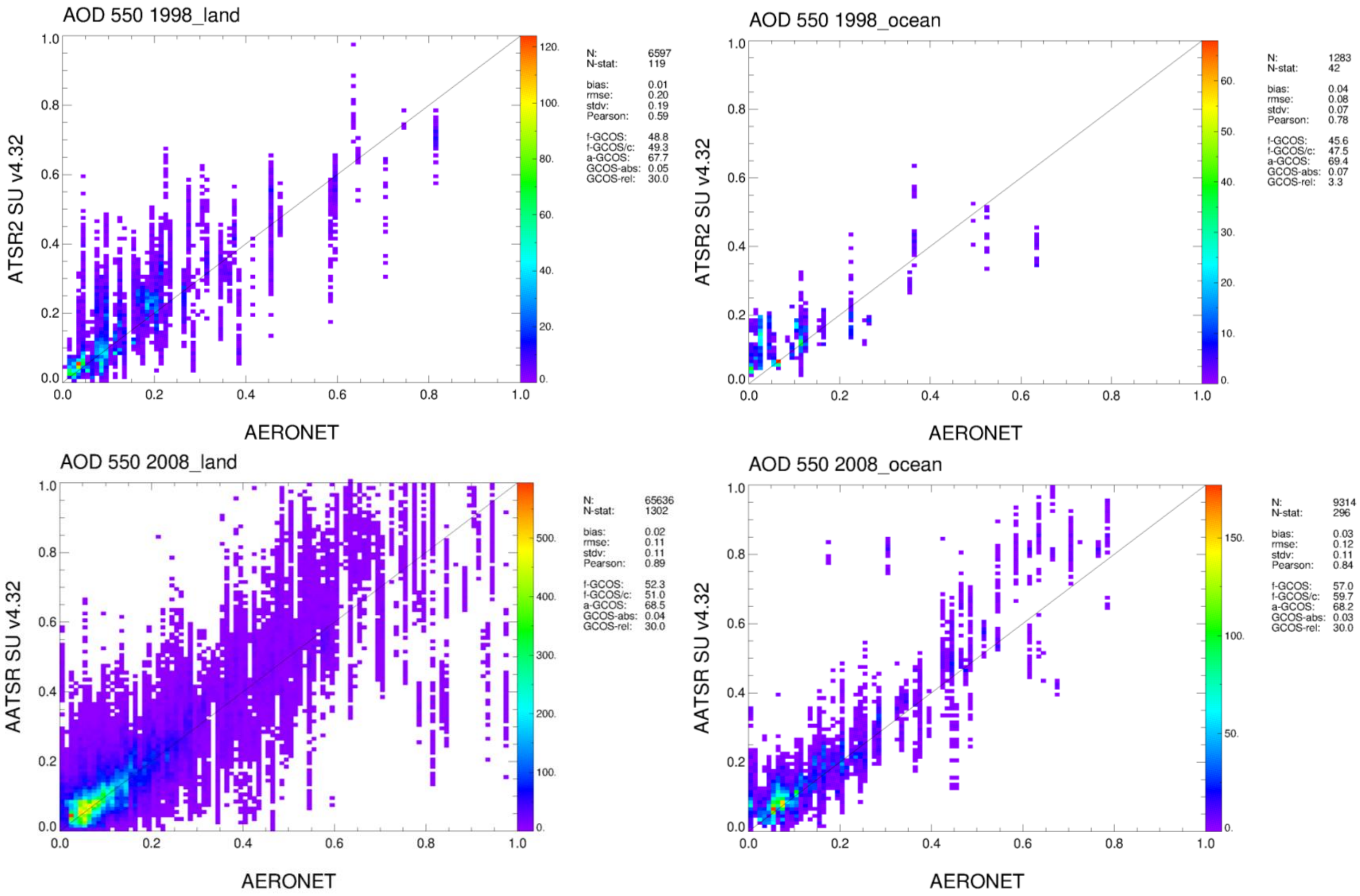

***Figure 4.3** Density scatter plots for ATSR-2 (top) and AATSR (bottom) over land (left) and ocean (right).*

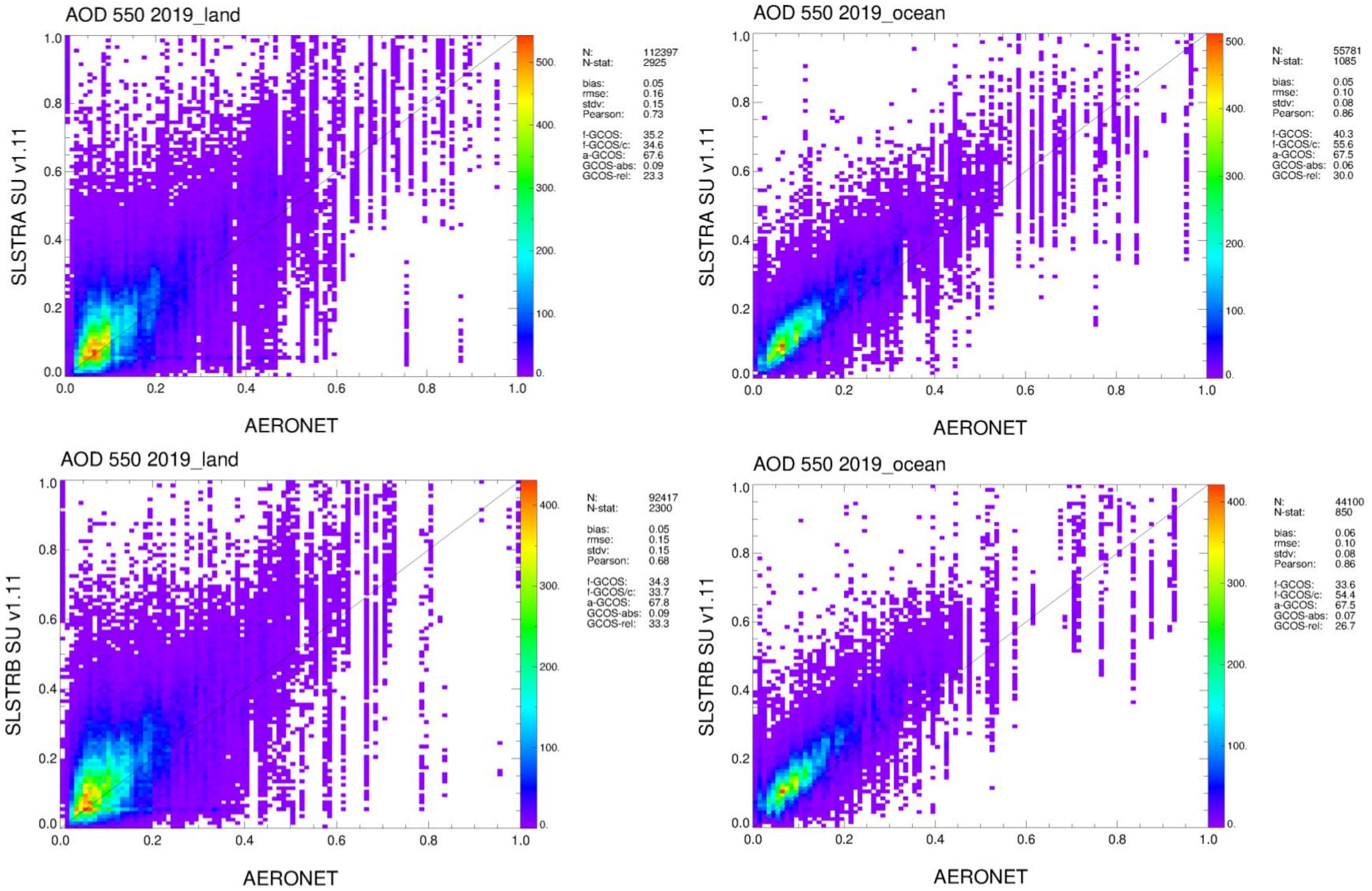

***Figure 4.4** Density scatter plots for SLSTR/3A (top) and SLSTR/3B (bottom) over land (left) and ocean (right).*

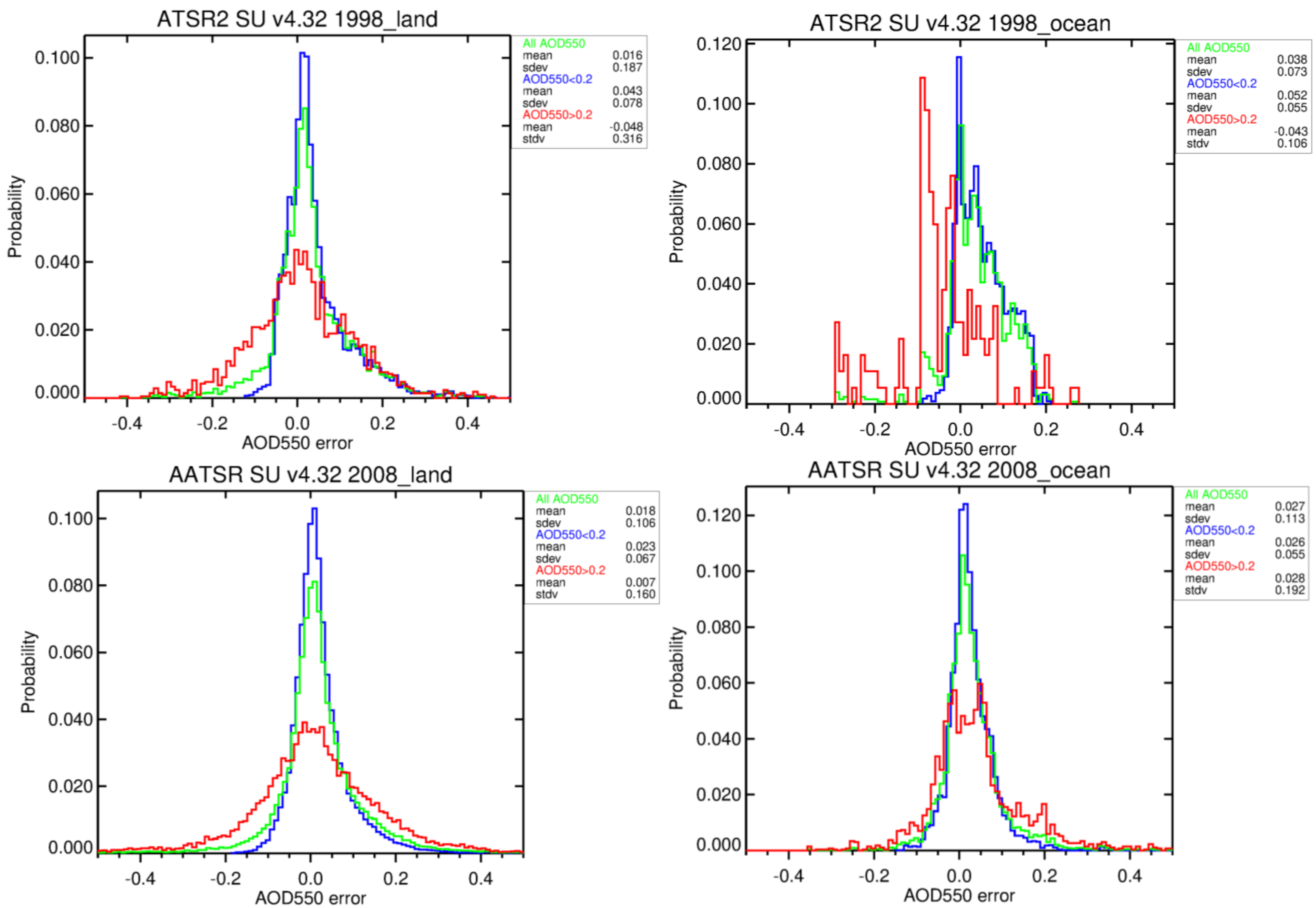

***Figure 4.5** Difference histograms for ATSR-2 (top) and AATSR (bottom) over land (left) and ocean (right).*

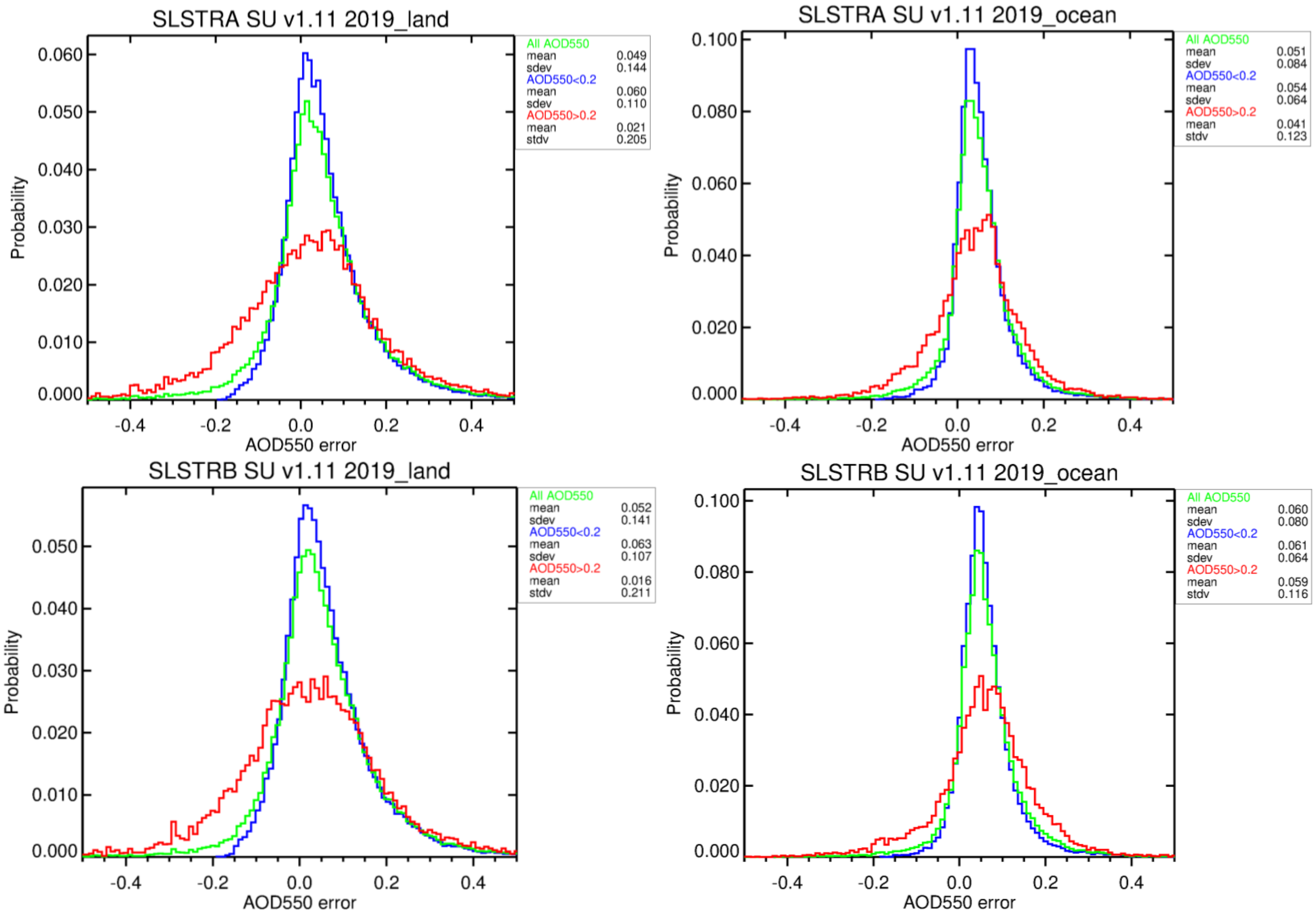

***Figure 4.6** Difference histograms for SLSTR/3A (top) and SLSTR/3B (bottom) over land (left) and ocean (right).*

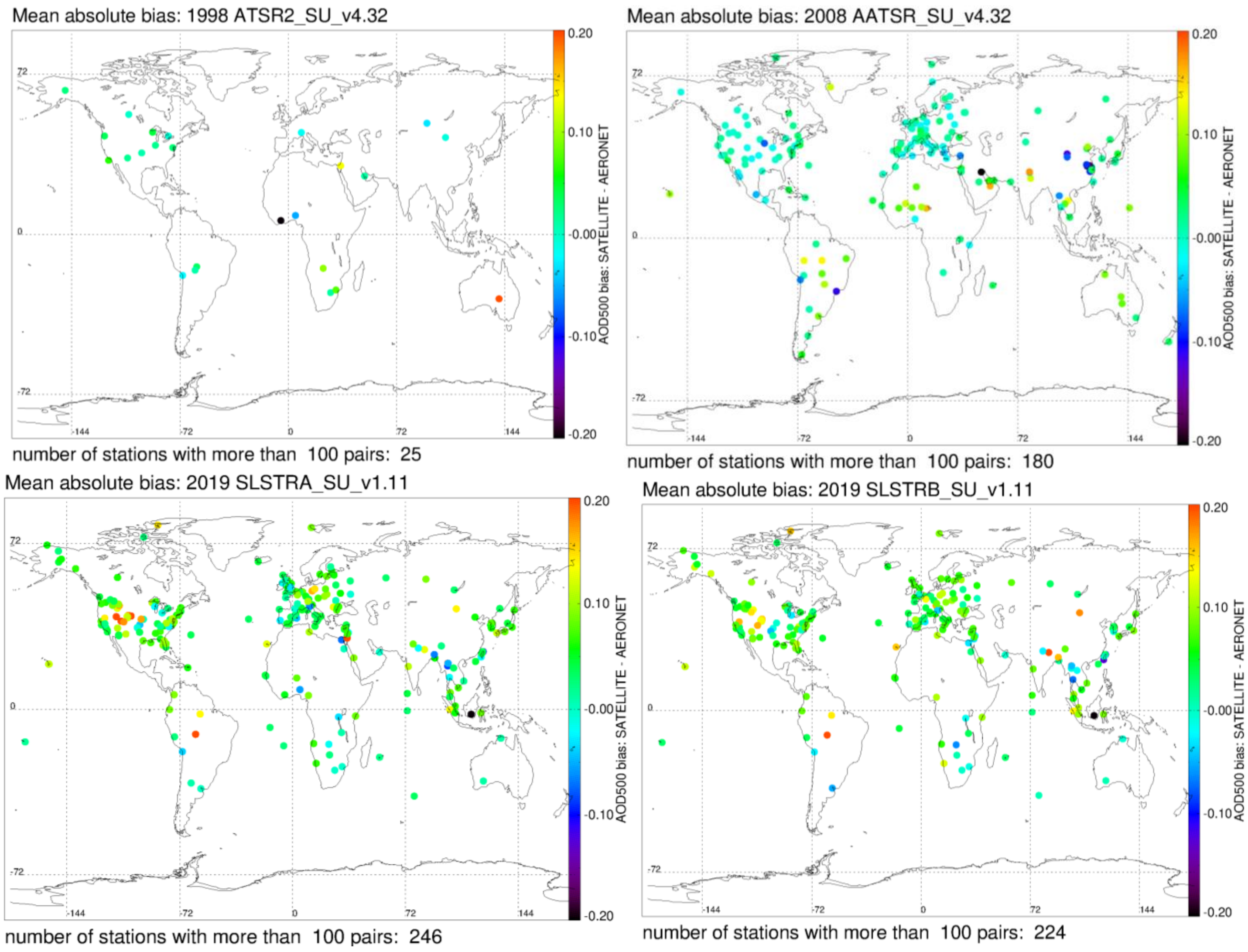

***Figure 4.7** Maps of significant station mean AOD bias (Satellite – AERONET) for all 4 sensors.*

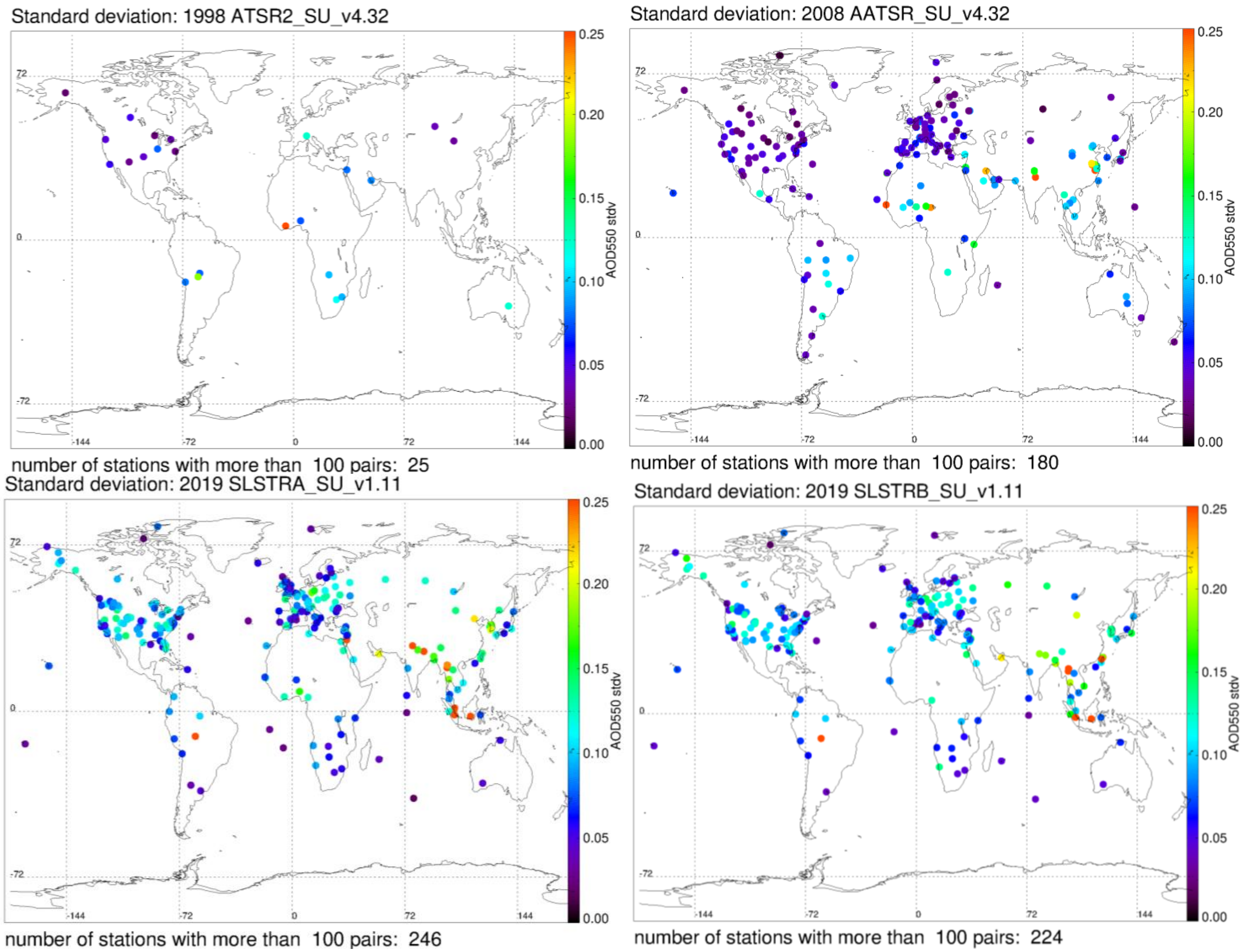

***Figure 4.8** Maps of significant station AOD stdv of Satellite and AERONET for all 4 sensors.*

4.1.2 CRDP-2 SU v2 validation results

The statistical analysis of the SU v2 datasets in comparison to AERONET station measurements is presented in Table 4.3 (like Tab. 4.1 for SU v1) and Figures 4.9 – 4.16 (like Fig. 4.1 – 4.8 for SU v1). This analysis confirms the visual impressions in section 3 with reduced bias and stdv and slightly increased correlation and GCOS fractions for both SLSTR instruments with the new v1.14 while there is little difference for the ATSR instruments. The bias maps show the reduction of the AOD over-estimation in Central Asian regions with slightly more blueish colours. Despite of using the same AERONET dataset, the number of matching pairs for both SLSTR instruments has also increased.

Table 4.3 Global validation statistics for SU v2 AOD at 550nm

year	sensor	alg_version	area	Number of sat pixel	number1 of stat obs	bias	rmse	stdv	Pearson corr	GCOS fraction	Corrected GCOS fraction	Adapted GCOS envelope
CRDP-2 SU v2 datasets												
1998	ATSR2	SU_v4.33	land	6597	119	0.01	0.20	0.19	0.59	48.8	49.3	max(0.05 or 29%)
1998	ATSR2	SU_v4.33	ocean	1283	42	0.04	0.08	0.07	0.78	45.6	47.5	max(0.07 or 3%)
2008	AATSR	SU_v4.33	land	65654	1302	0.02	0.11	0.11	0.89	52.3	51.0	max(0.04 or 29%)
2008	AATSR	SU_v4.33	ocean	9315	296	0.03	0.12	0.11	0.84	57.0	59.6	max(0.03 or 29%)
2019	SLSTRA	SU_v1.14	land	128117	2890	0.04	0.14	0.13	0.76	40.5	40.3	max(0.07 or 33%)
2019	SLSTRA	SU_v1.14	ocean	57727	1089	0.04	0.09	0.08	0.87	48.0	56.7	max(0.05 or 26%)
2019	SLSTRB	SU_v1.14	land	121772	2712	0.04	0.14	0.13	0.77	39.8	39.5	max(0.08 or 3%)
2019	SLSTRB	SU_v1.14	ocean	54579	1034	0.05	0.09	0.08	0.87	44.4	55.7	max(0.06 or 13%)

Summary for the validation of SU v2 total AOD

- Better coverage for ATSR-2
- High positive bias and larger scatter for SLSTR is reduced in some regions
- Otherwise most features are similar to SU v1 datasets

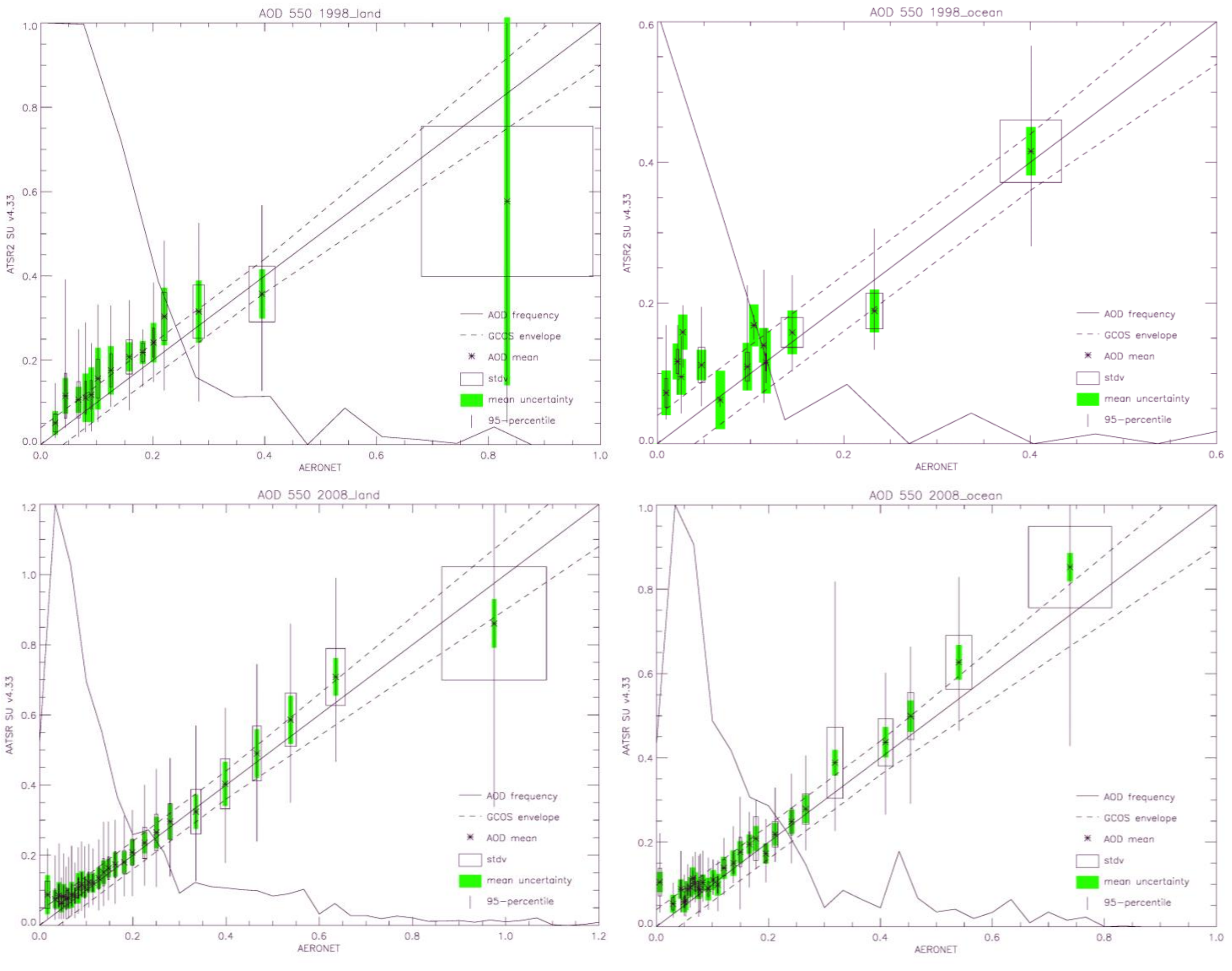

Figure 4.9 *Validation summary plots for ATSR-2 (top) and AATSR (bottom) over land (left) and ocean (right).*

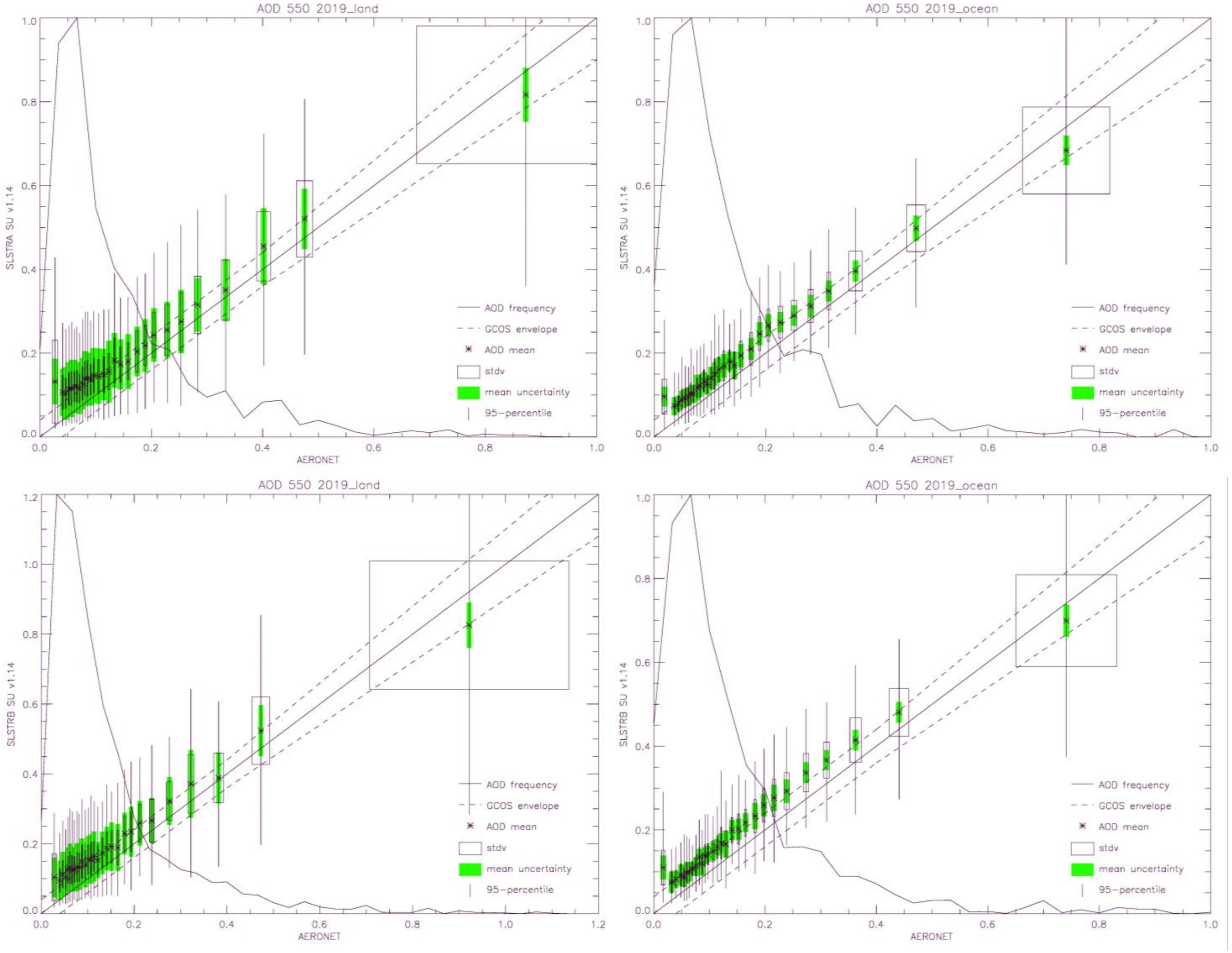

Figure 4.10 *Validation summary plots for SLSTR/3A (top) and SLSTR/3B (bottom) over land (left) and ocean (right).*

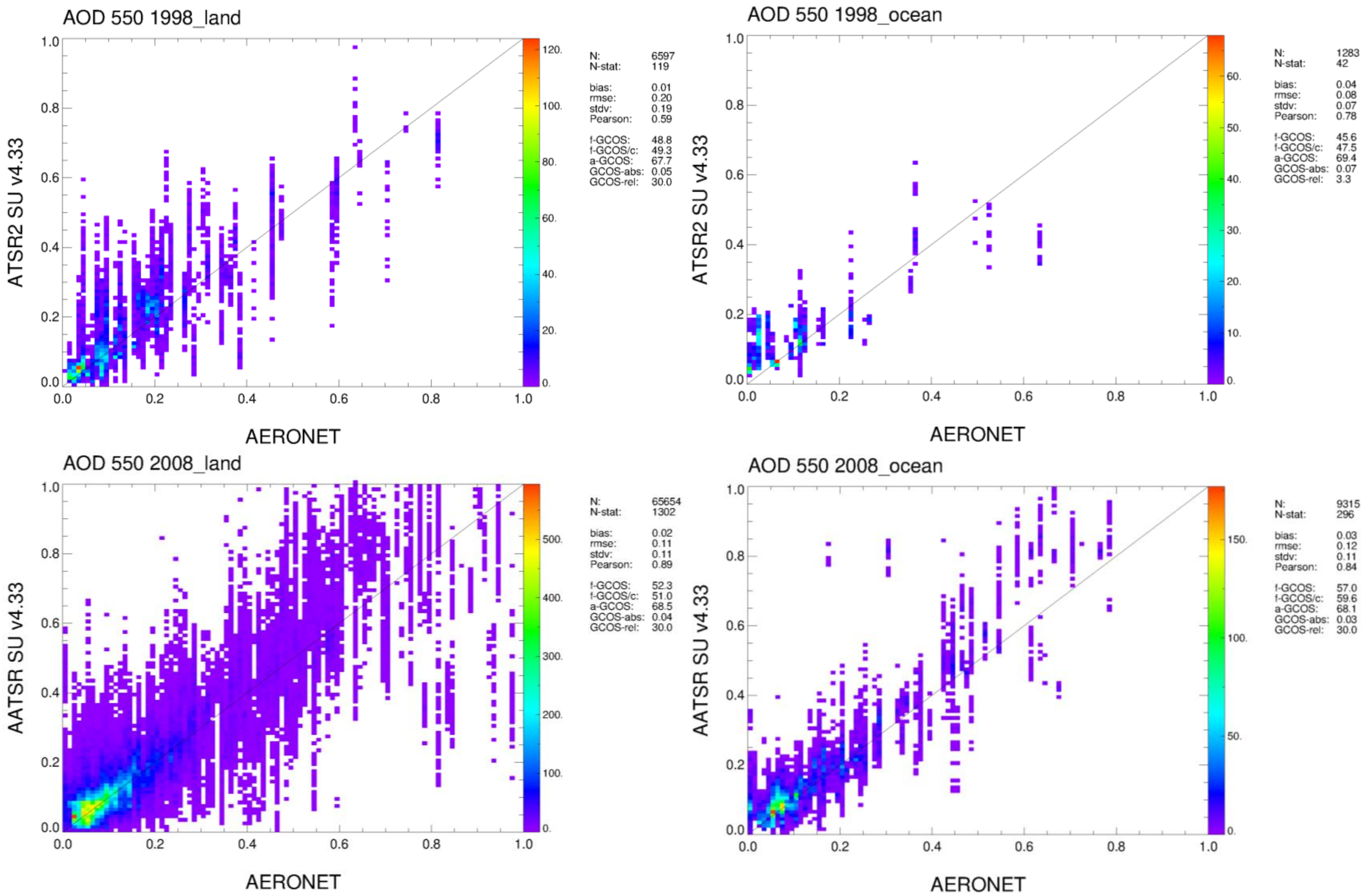

***Figure 4.11** Density scatter plots for ATSR-2 (top) and AATSR (bottom) over land (left) and ocean (right).*

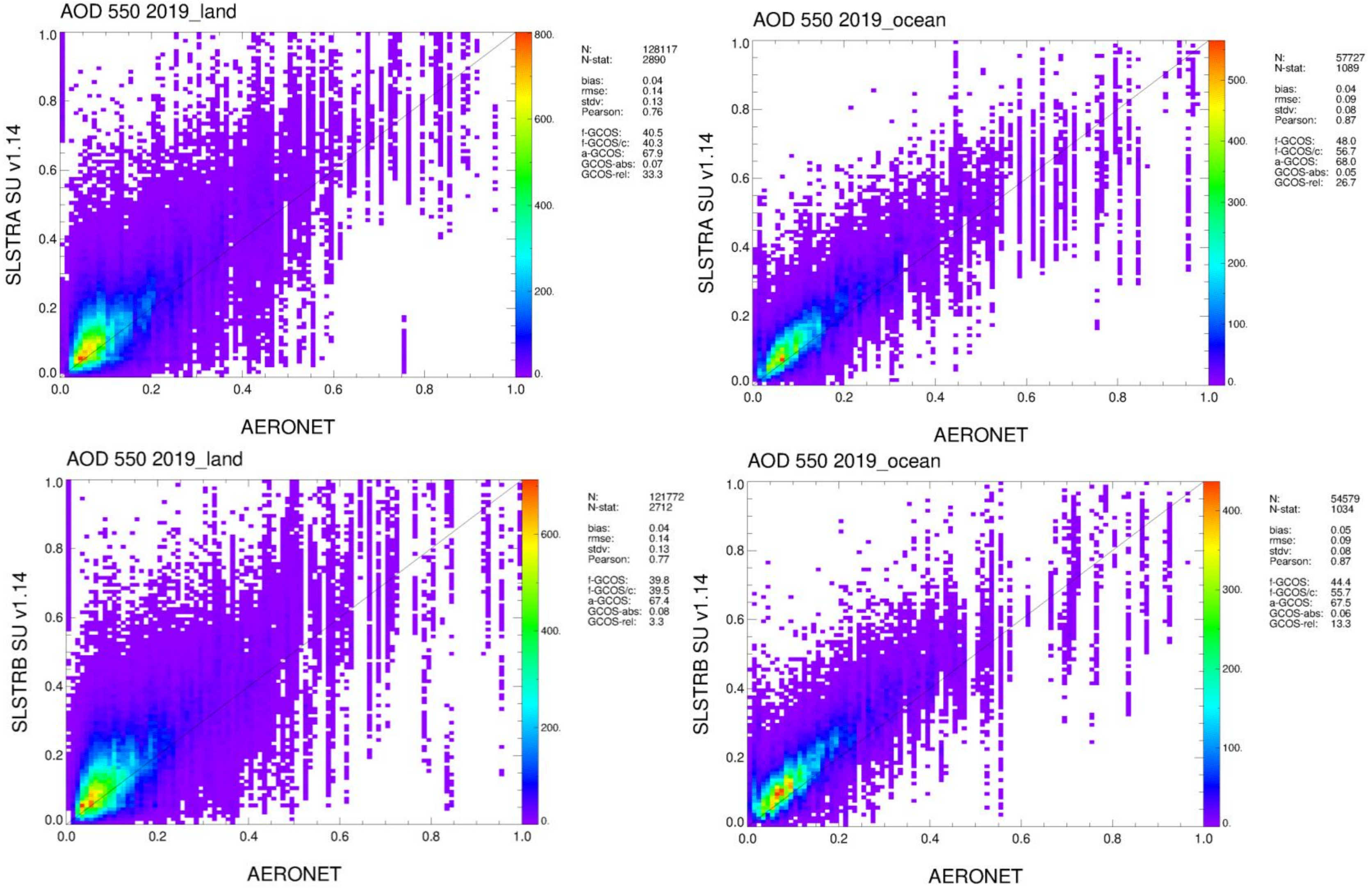

Figure 4.12 *Density scatter plots for SLSTR/3A (top) and SLSTR/3B (bottom) over land (left) and ocean (right).*

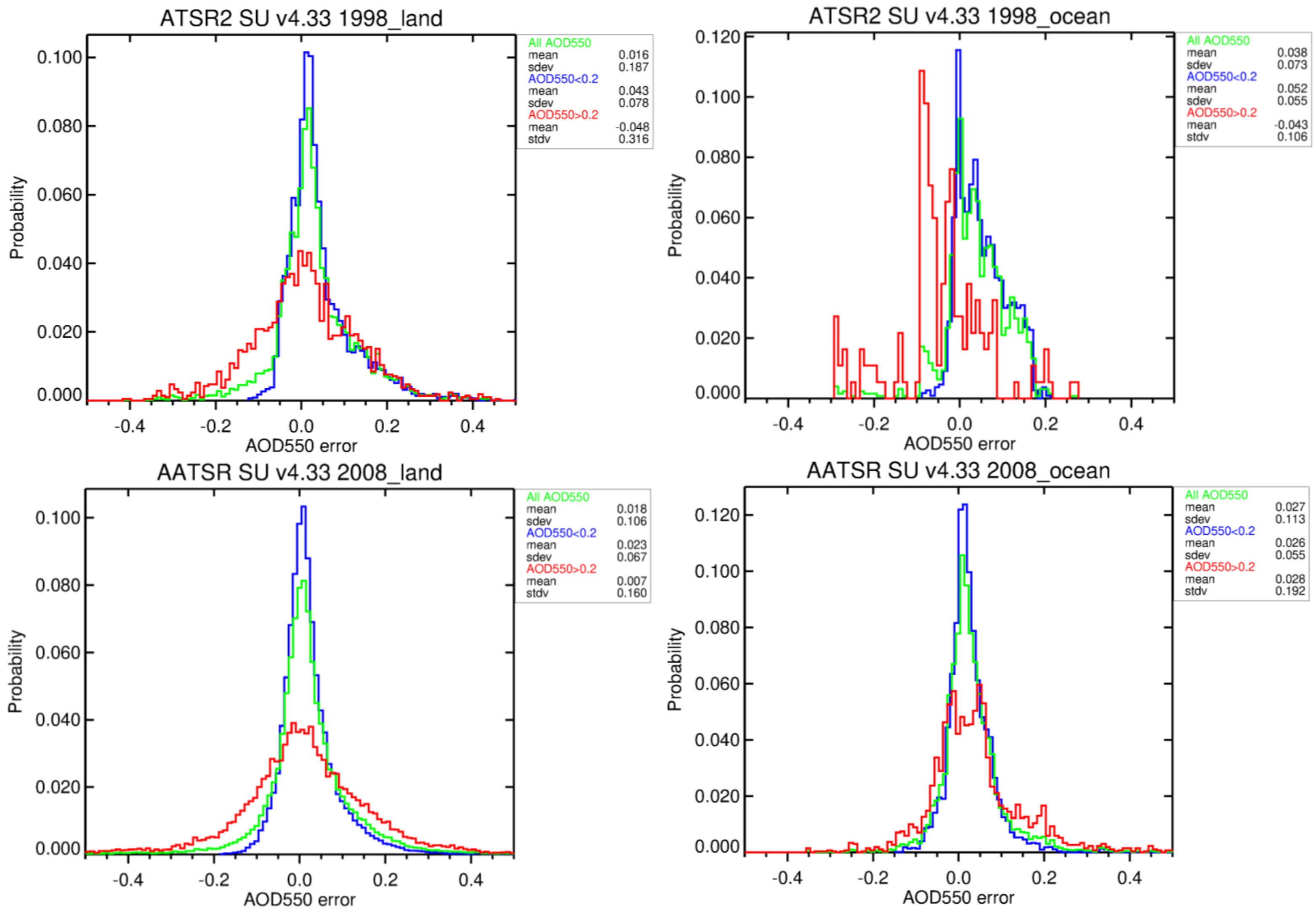

Figure 4.13 *Difference histograms for ATSR-2 (top) and AATSR (bottom) over land (left) and ocean (right).*

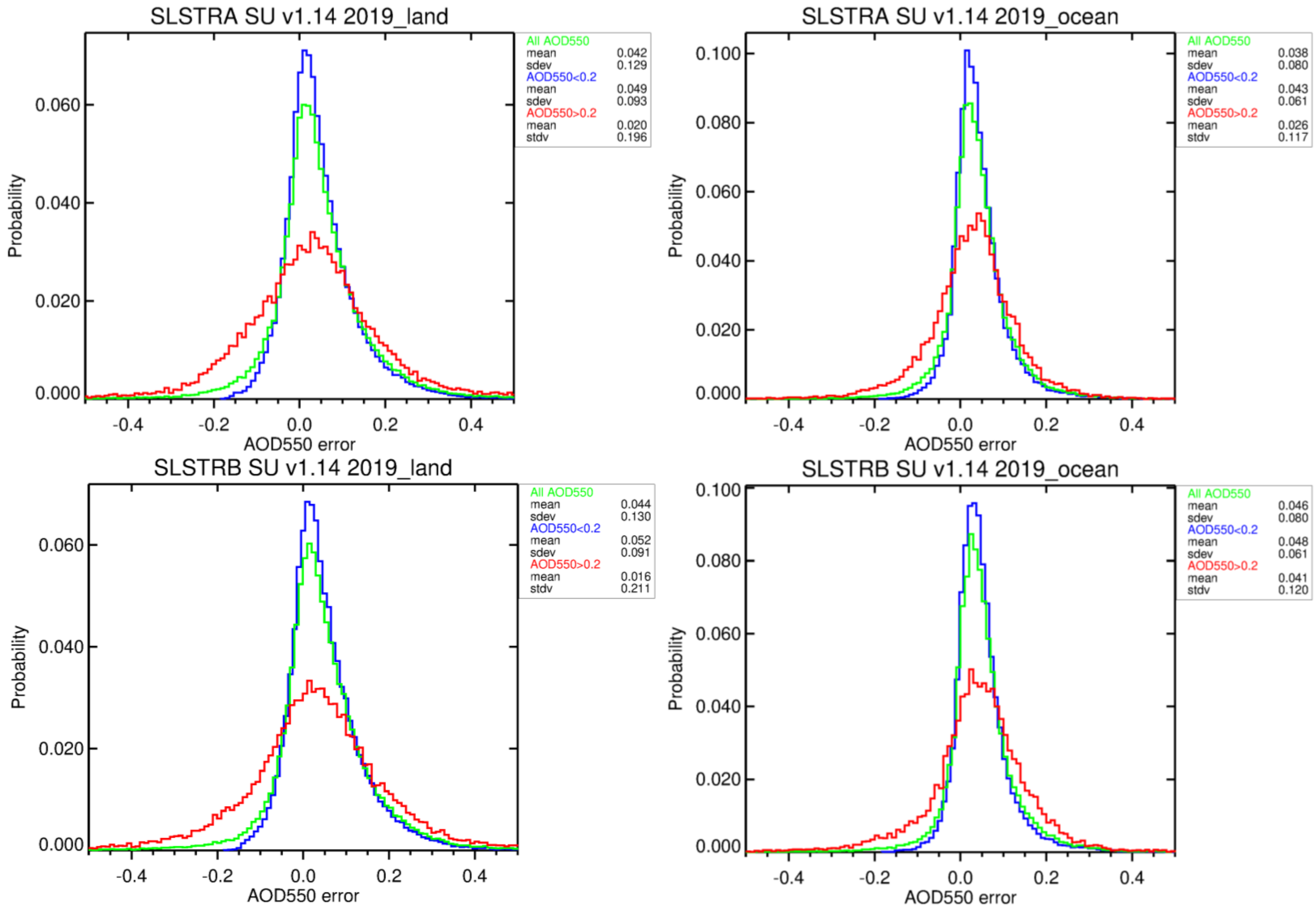

Figure 4.14 *Difference histograms for SLSTR/3A (top) and SLSTR/3B (bottom) over land (left) and ocean (right).*

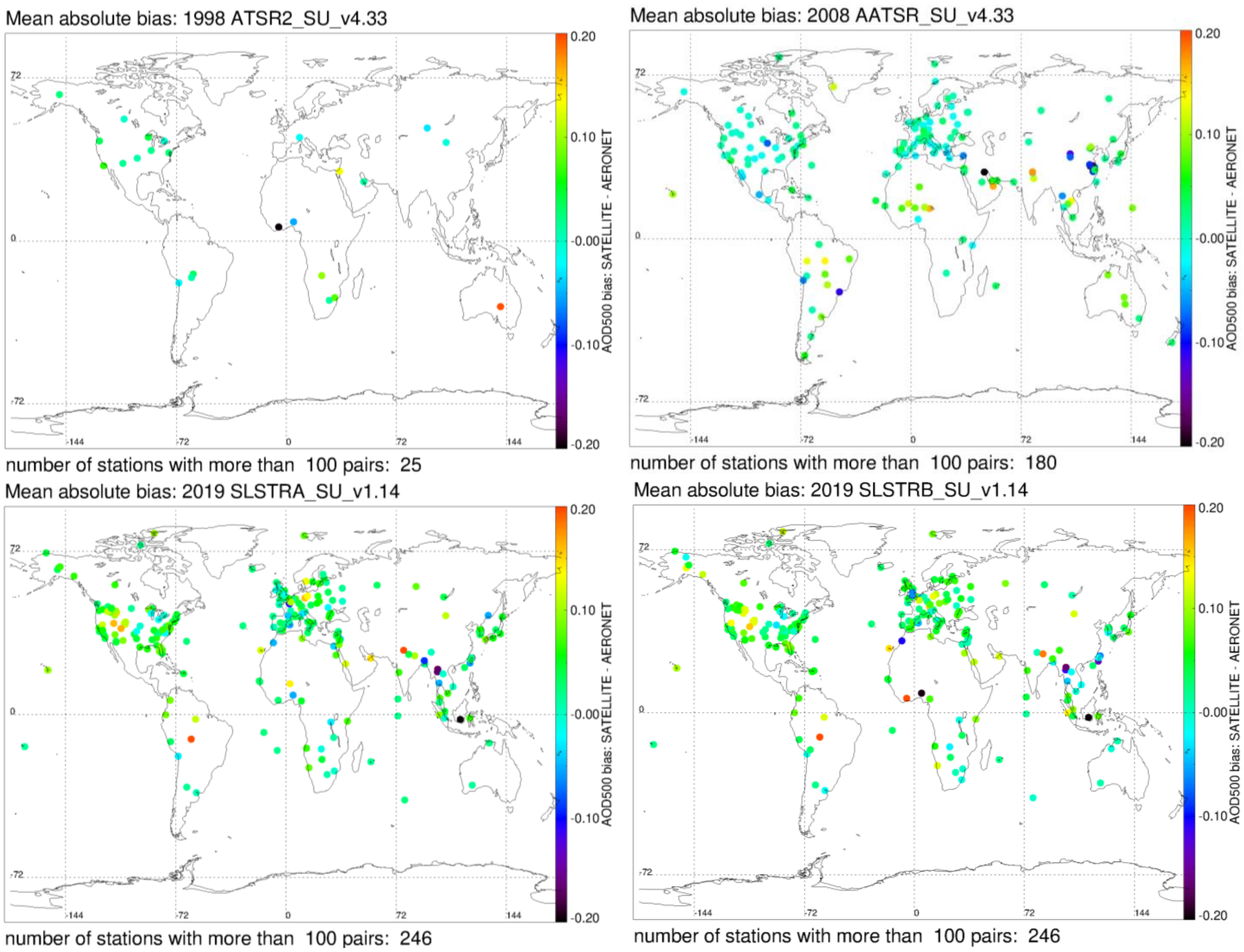

Figure 4.15 *Maps of significant station mean AOD bias (Satellite – AERONET) for all 4 sensors.*

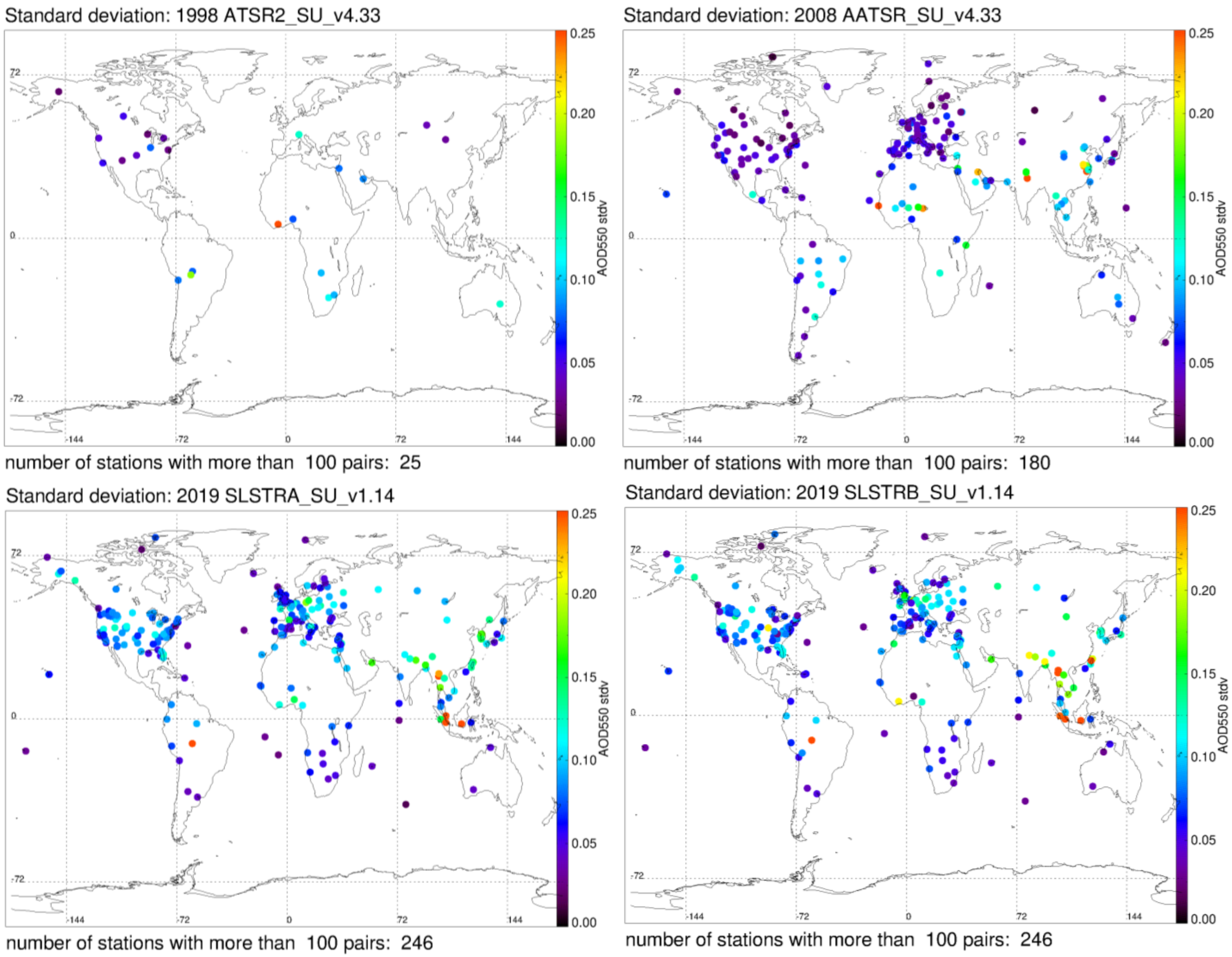

Figure 4.16 *Maps of significant station AOD stdv of Satellite and AERONET for all 4 sensors.*

4.1.3 CRDP-3 SU v3 validation results

The statistical analysis of the SU v3 datasets in comparison to AERONET station measurements is presented in Table 4.4 (like Tab. 4.1 for SU v1) and Table 4.5 in comparison to v2 as well as in Figures 4.17 – 4.22 (like Fig. 4.1 – 4.8 for SU v1). This analysis confirms improvements with reduced bias and stdv and slightly increased correlation and GCOS fractions for both SLSTR instruments with the final v1.14 as compared to the initial v1.11 and also for the ATSR instruments with the final v4.35 as compared to the earlier v4.33.

It should be noted that the final validation covered a full data year while the earlier versions only included 4 months in each year representing the 4 seasons (March, June, September, December). For the SLSTR instruments no new version was ready but a new data year was processed (2020 vs. 2019 for v2); we therefore compare to the initial version v1.11 at the start of the project in table 4.5. For the ATSR instruments a new version v4.35 was available and evaluated for the same data years (1998 and 2008); here we compare to the earlier version v4.33.

As can be seen also in monthly mean maps (fig. 3.8 – 3.10) as compared to maps of earlier versions (fig. 3.1 – 3.6), there are no drastic changes in fig. 4.17 - 4.22 in comparison to fig 4.1 – 4.8, but overall there is a clear reduction of bias and noise.

Table 4.4 Global validation statistics for SU v3 AOD at 550nm

year	sensor	alg_version	area	Number of sat pixel	number1 of stat obs	bias	rmse	stdv	Pearson corr	GCOS fraction	Corrected GCOS fraction	Adapted GCOS envelope
CRDP-3 SU v3 datasets												
1998	ATSR2	SU_v4.35	land	14974	299	0.02	0.14	0.14	0.83	47.3	47.0	max(0.05, 33%)
1998	ATSR2	SU_v4.35	ocean	2012	70	0.02	0.09	0.08	0.76	54.6	56.9	max(0.05, 29%)
2008	AATSR	SU_v4.35	land	162865	3307	0.01	0.11	0.11	0.87	54.0	54.0	max(0.04, 26%)
2008	AATSR	SU_v4.35	ocean	24905	782	0.02	0.08	0.07	0.89	58.9	61.3	max(0.03, 26%)
2020	SLSTRA	SU_v1.14	land	564004	13076	0.03	0.12	0.12	0.80	42.7	44.9	max(0.07, 10%)
2020	SLSTRA	SU_v1.14	ocean	250841	4901	0.04	0.08	0.08	0.83	52.4	60.0	max(0.05, 3%)
2020	SLSTRB	SU_v1.14	land	589684	13531	0.04	0.12	0.12	0.78	41.3	43.3	max(0.07, 26%)
2020	SLSTRB	SU_v1.14	ocean	258965	5028	0.04	0.09	0.08	0.82	47.8	57.1	max(0.05, 33%

Table 4.5 Global validation statistics for SU v3 AOD at 550nm: AATSR comparison to v2, SLSTR comparison to v1

year	sensor	alg_version	area	Number of sat pixel	number1 of stat obs	bias	rmse	stdv	Pearson corr	GCOS fraction
2008	AATSR	SU_v4.33	Land / Northern hemisphere	56978	1119	0.01	0.11	0.11	0.89	55.0
2008	AATSR	SU_v4.35	Land / Northern hemisphere	144957	2897	0.00	0.11	0.11	0.87	55.7
2008	AATSR	SU_v4.33	Land / Southern hemisphere	8676	182	0.06	0.12	0.10	0.83	34.9
2008	AATSR	SU_v4.35	Land / Southern hemisphere	17908	409	0.04	0.10	0.09	0.79	40.1
2008	AATSR	SU_v4.33	Ocean / Northern hemisphere	8622	273	0.03	0.12	0.12	0.84	56.2
2008	AATSR	SU_v4.35	Ocean / Northern hemisphere	22603	716	0.02	0.08	0.08	0.88	56.6

2008	AATSR	SU_v4.33	Ocean / Southern hemisphere	693	22	0.02	0.04	0.03	0.73	66.7
2008	AATSR	SU_v4.35	Ocean / Southern hemisphere	2302	65	0.02	0.04	0.03	0.66	81.2
2019	SLSTRA	SU_v1.11	land	112397	2925	0.05	0.16	0.15	0.73	35.2
2020	SLSTRA	SU_v1.14	land	564004	13076	0.03	0.12	0.12	0.80	42.7
2019	SLSTRA	SU_v1.11	ocean	55781	1085	0.05	0.10	0.08	0.86	40.3
2020	SLSTRA	SU_v1.14	ocean	250841	4901	0.04	0.08	0.08	0.83	52.4
2019	SLSTRB	SU_v1.11	land	92417	2300	0.05	0.15	0.15	0.68	34.3
2020	SLSTRB	SU_v1.14	land	589684	13531	0.04	0.12	0.12	0.78	41.3
2019	SLSTRB	SU_v1.11	ocean	44100	850	0.06	0.10	0.08	0.86	33.6
2020	SLSTRB	SU_v1.14	ocean	258965	5028	0.04	0.09	0.08	0.82	47.8

Summary for the validation of SU v3 total AOD

- Reduced bias for AATSR compared to v2
- No major changes for SLSTR between v3 (2020) and v2(1019), but clear improvement against v1 (2019)

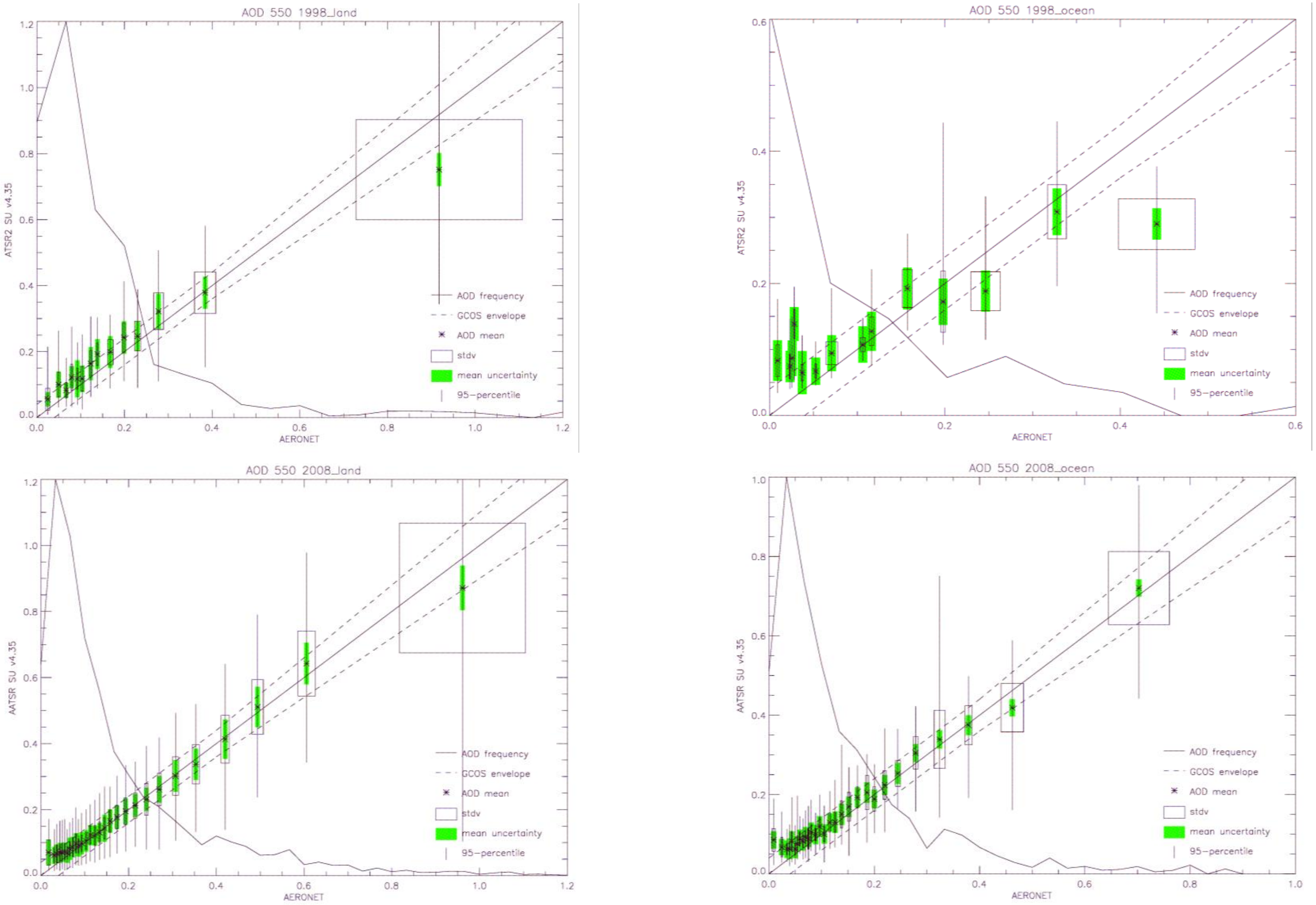

Figure 4.17 *Validation summary plots for ATSR-2 (top) and AATSR (bottom) over land (left) and ocean (right).*

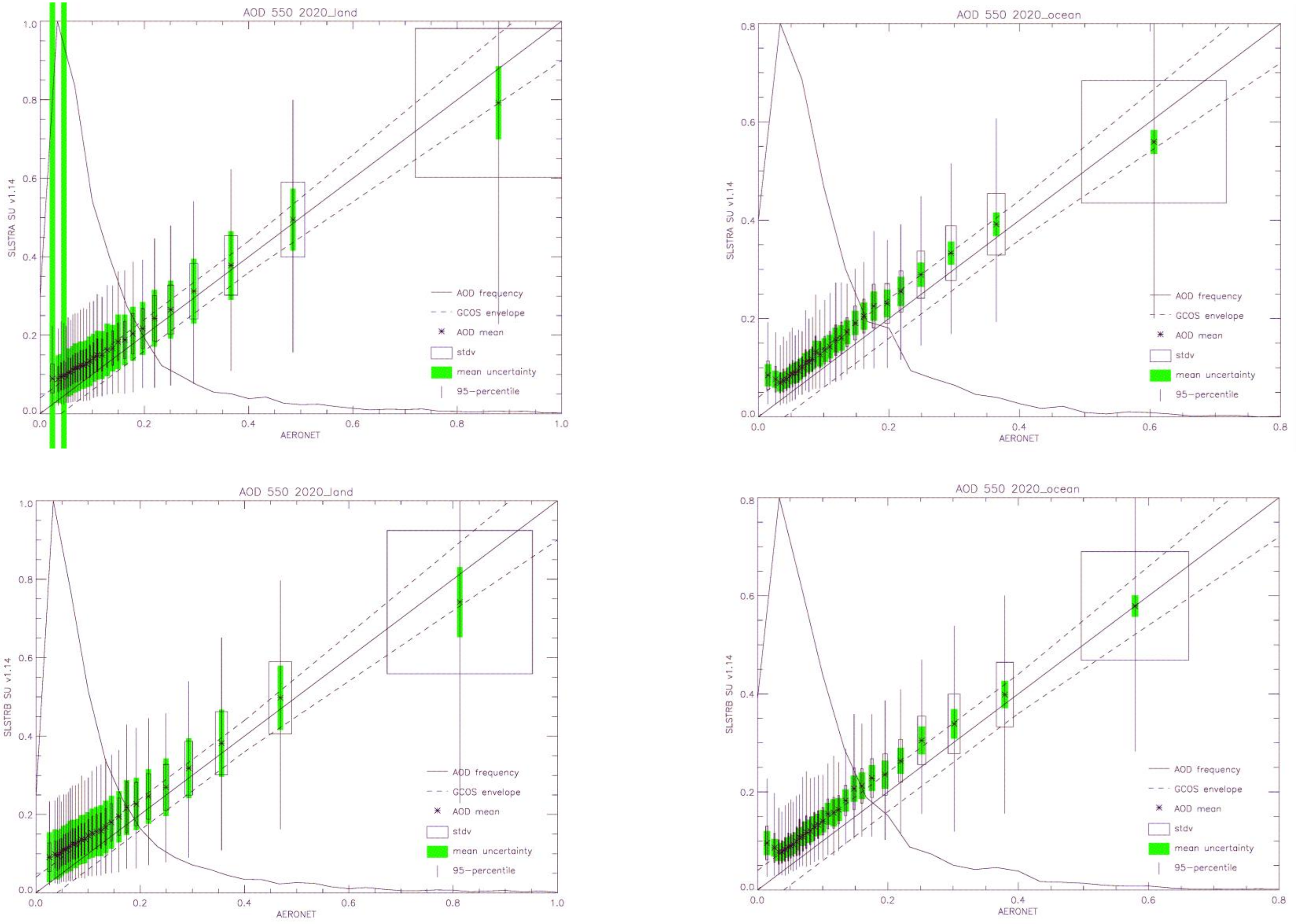

Figure 4.18 *Validation summary plots for SLSTR/3A (top) and SLSTR/3B (bottom) over land (left) and ocean (right).*

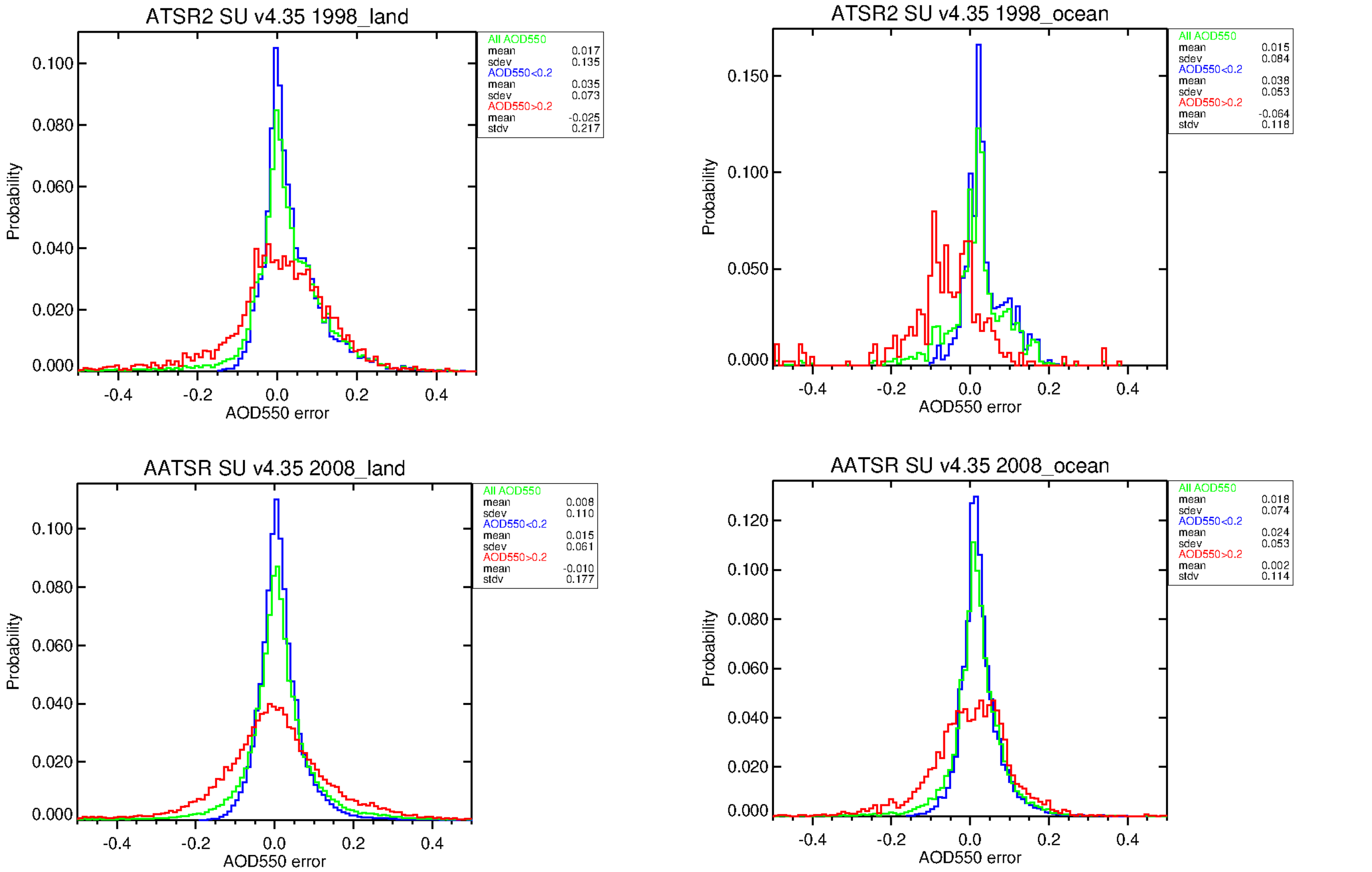

Figure 4.19 *Difference histograms for ATSR-2 (top) and AATSR (bottom) over land (left) and ocean (right).*

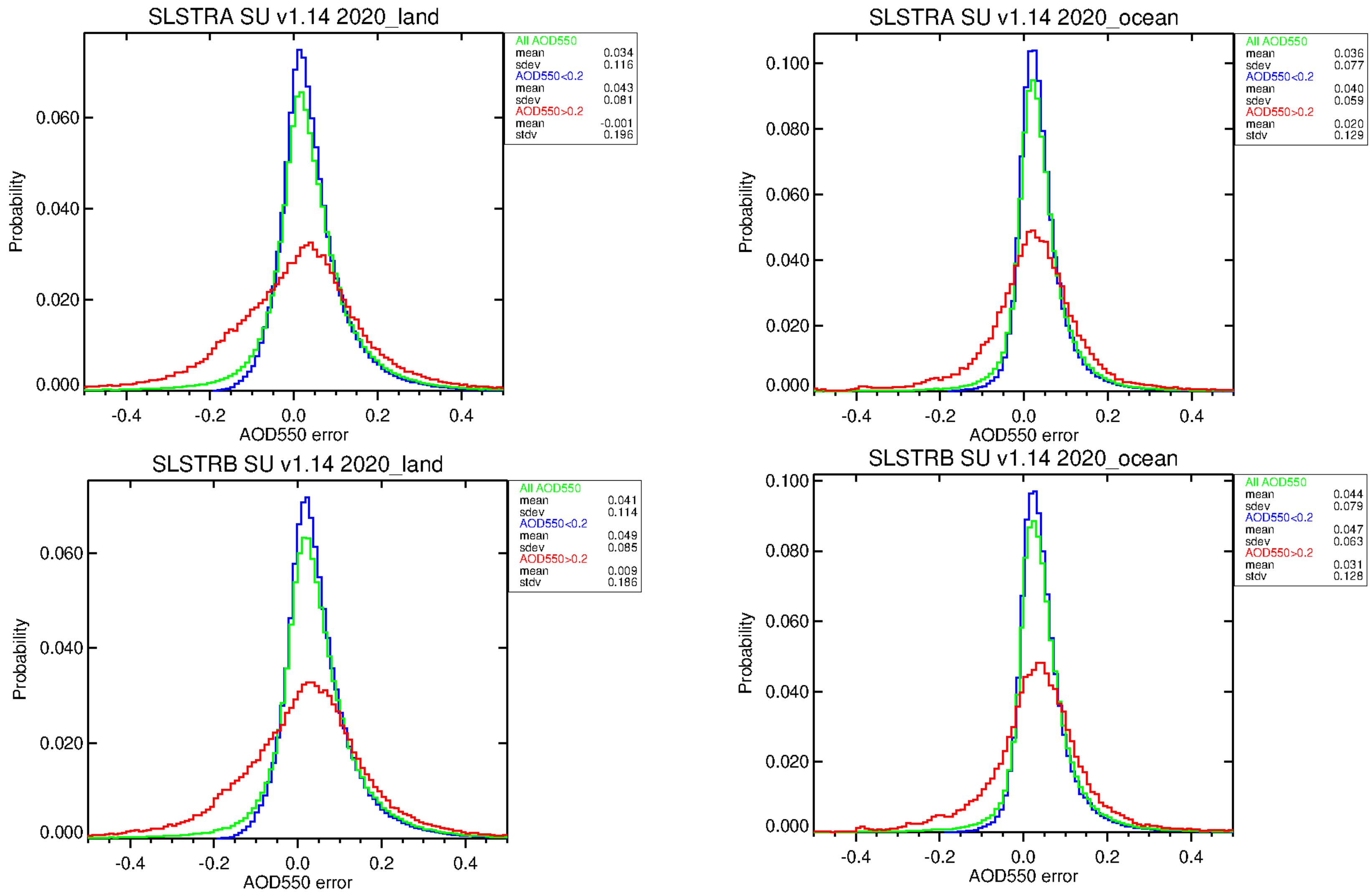

Figure 4.20 *Difference histograms for SLSTR/3A (top) and SLSTR/3B (bottom) over land (left) and ocean (right).*

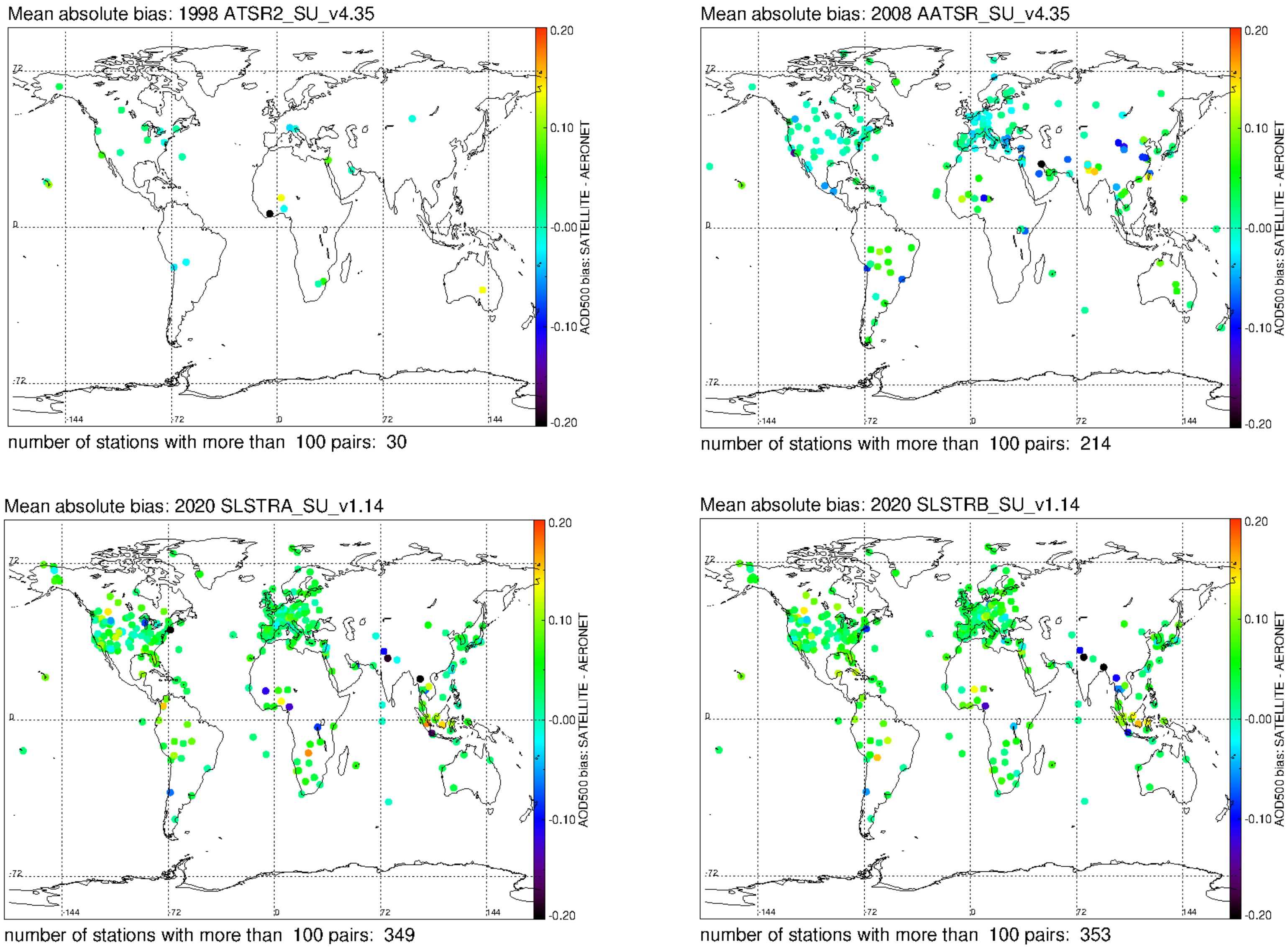

Figure 4.21 *Maps of significant station mean AOD bias (Satellite – AERONET) for all 4 sensors.*

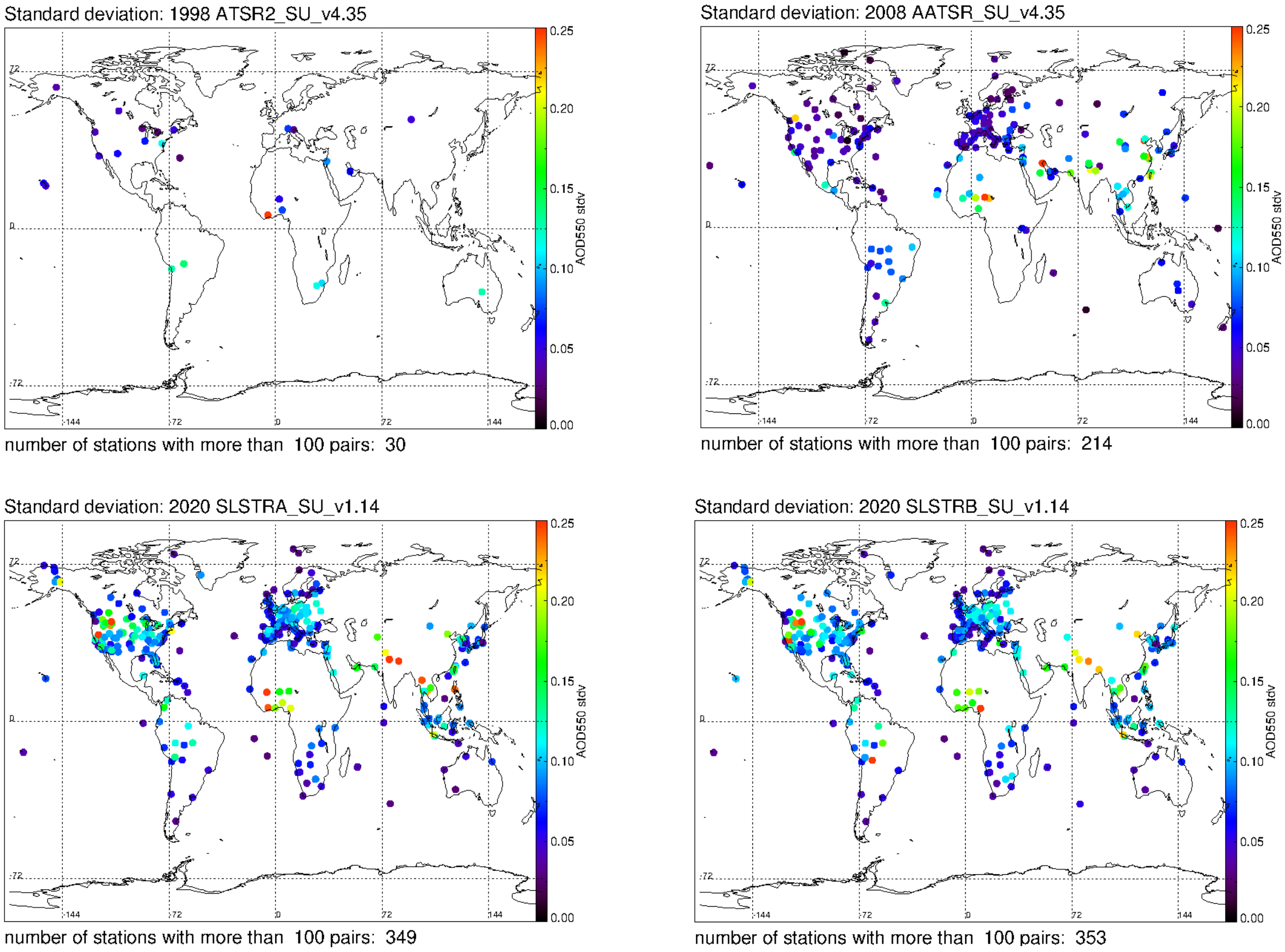

Figure 4.22 *Maps of significant station AOD stdv of Satellite and AERONET for all 4 sensors.*

4.1.4 CRDP-2 RF v1 validation results

The statistical analysis of the RF v1 datasets in comparison to AERONET station measurements is presented in Table 4.4 (like Tab. 4.1 for SU v1) and Figures 4.17 – 4.20 (like Fig. 4.1 – 4.8 for SU v1). As defined by the provider, inter-comparisons to AERONET are only made for pixels with Quality Index > 0. In comparison to the SU dataset validation for SLSTR/3A, CISAR statistics show larger numbers of matching pairs (reflecting the 5km resolution) but smaller number of Aeronet stations involved (due to missing 1/3 of the global coverage so far).

The analysis confirms the visual impressions in section 3 with large bias and stdv with lower correlations and GCOS fractions for the RF dataset. The box-whisker plots (Fig. 4.17) show that on average the AOD over-estimation is largest for low AOD (below 0.2 over land and below 0.4 over ocean). The bias map (Fig. 4.20) shows lower average bias per station over land (green colours) than for coastal stations (ref colours). It must be notes that AERONET data are automatically cloud-screened (by temporal stability) and therefore cannot be used to assess AOD quality near clouds. This means that the unique feature of the CISAR algorithm to avoid an external cloud mask cannot be assessed with AERONET. However, for cloud-free conditions, AERONET is well suited to assess satellite retrievals. Also here, (e.g. in and clean background areas) the CISAR AOD shows a significant positive bias against AERONET.

Table 4.6 Global validation statistics for RF v1 AOD at 550nm

year	sensor	alg_version	area	Number of sat pixel	number1 of stat obs	bias	rmse	stdv	Pearson corr	GCOS fraction	Corrected GCOS fraction	Adapted GCOS envelope
CRDP-2 RF v1 datasets												
2019	SLSTRA	RF_v2.0.0	land	199550	1284	0.08	0.41	0.41	0.17	23.0	17.4	max(0.11 or 36%)
2019	SLSTRA	RF_v2.0.0	ocean	95565	527	0.14	0.37	0.35	0.28	19.0	17.3	max(0.11 or 36%)

Summary for the validation of RF v1 total AOD

- High positive bias and larger scatter for SLSTR / 3A
- Positive bias is mostly over ocean (for AOD < 0.4) but also over land (for AOD < 0.2)

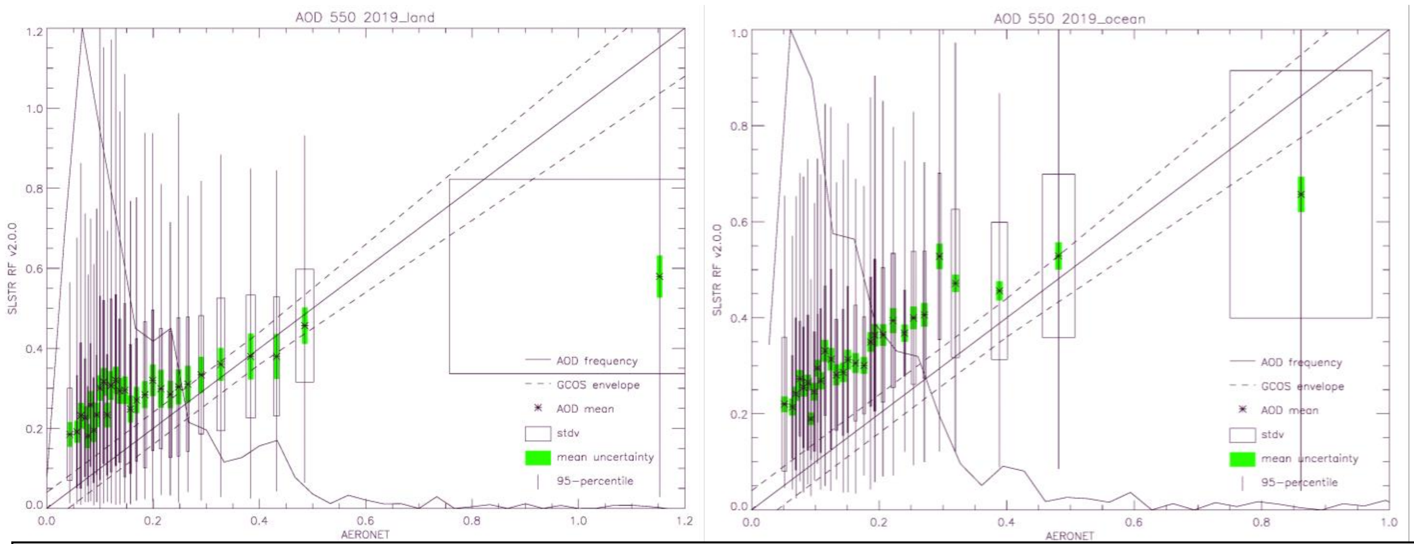

Figure 4.23 *Validation summary plots for SLSTR/3A over land (left) and ocean (right).*

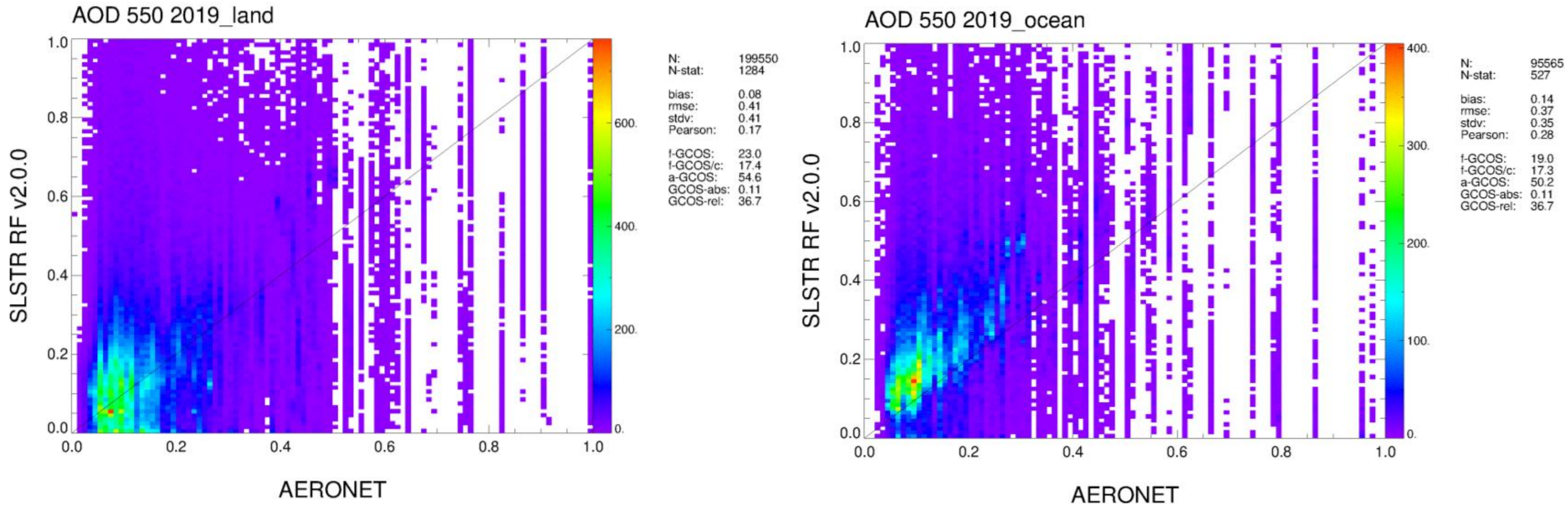

Figure 4.24 *Density scatter plots for SLSTR/3A over land (left) and ocean (right).*

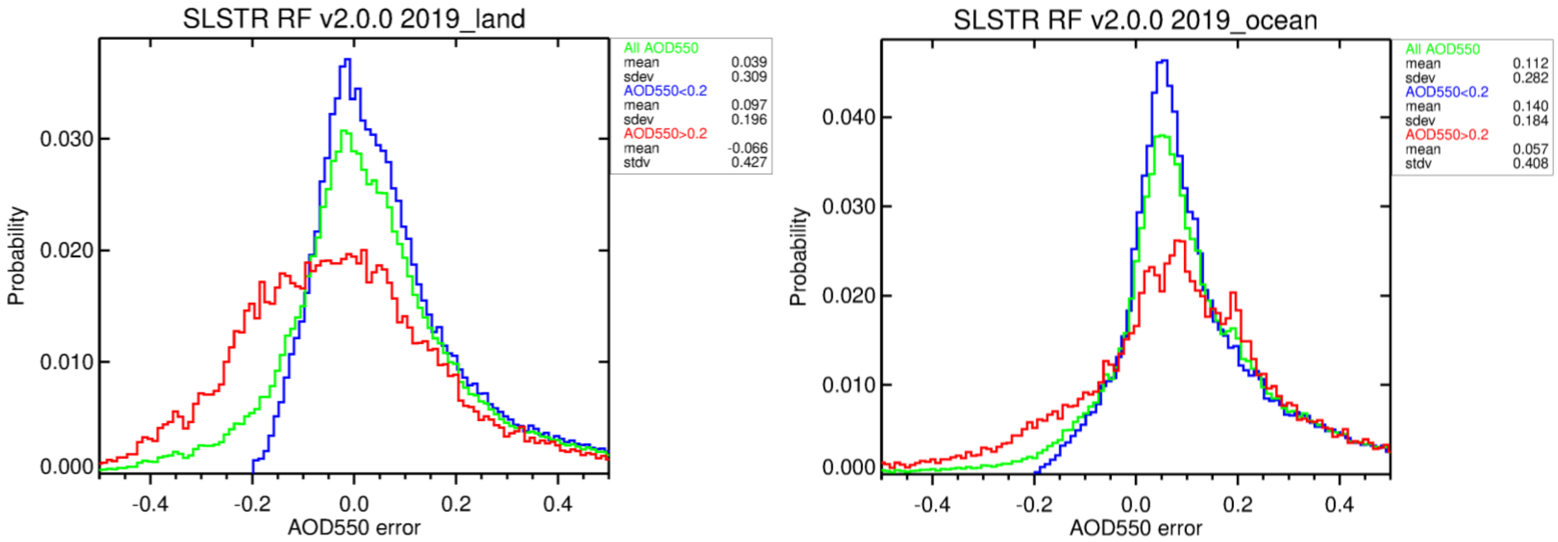

Figure 4.25 *Difference histograms for SLSTR/3A over land (left) and ocean (right).*

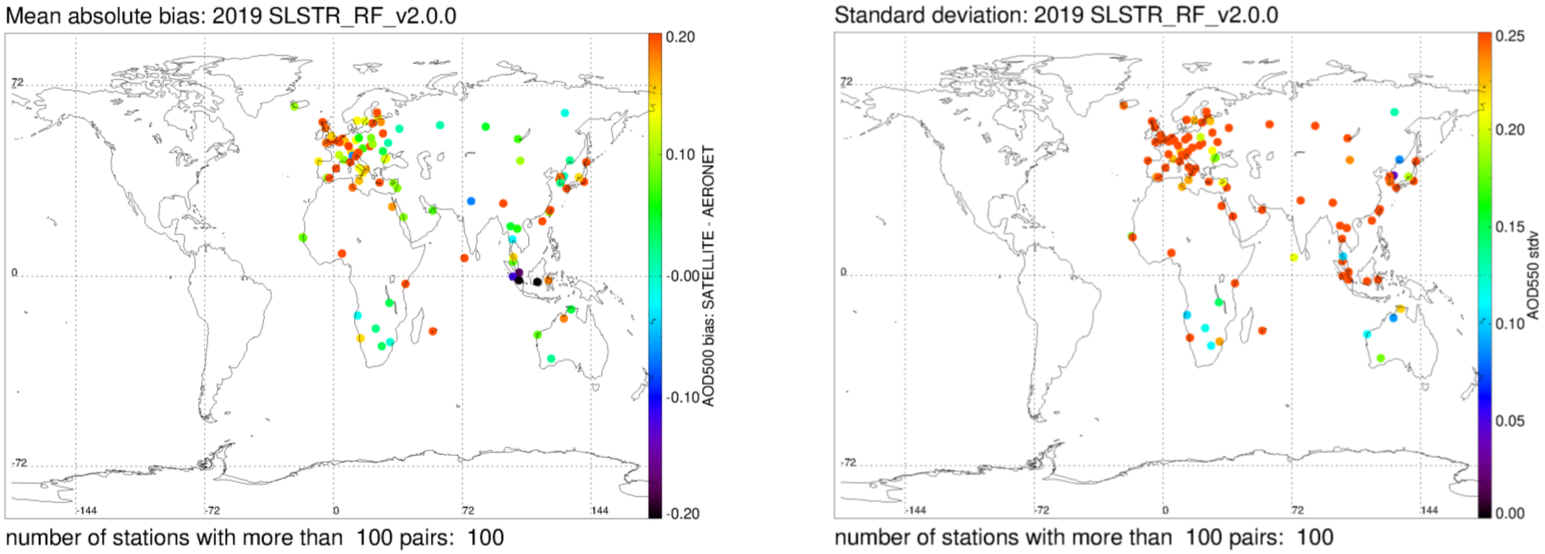

Figure 4.26 *Maps of significant station mean AOD bias and stdv (Satellite – AERONET) for SLSTR/3A.*

4.1.5 CRDP-3 RF v2 validation results

The statistical analysis of the RF v2 datasets in comparison to AERONET station measurements is presented in Table 4.7 (like Tab. 4.1 for SU v1) and Figures 4.27 – 4.29 (like Fig. 4.1 – 4.8 for SU v1). As defined by the provider, inter-comparisons to AERONET are only made for pixels with Quality Index > 0. In comparison to the CISAR / RF v1 evaluation (which had only covered 2/3 of the globe), now a full global analysis was made.

The analysis of fig. 4.27 – 4.29 confirms a significant improvement of the overall validation statistics (significantly reduced high bias and noise), but at the cost of a new under-estimation of high AOD (>0.2) over land, which leads to the loss of the major global patterns in monthly mean maps (fig. 3.11). For low AOD there remains a smaller over-estimation.

It must be noted that AERONET data are automatically cloud-screened (by temporal stability) and therefore cannot be used to assess AOD quality near clouds. This means that the unique feature of the CISAR algorithm to avoid an external cloud mask cannot be assessed with AERONET. However, for cloud-free conditions, AERONET is well suited to assess satellite retrievals.

Table 4.7 Global validation statistics for RF v2 AOD at 550nm

year	sensor	alg_version	area	Number of sat pixel	number1 of stat obs	bias	rmse	stdv	Pearson corr	GCOS fraction	Corrected GCOS fraction	Adapted GCOS envelope
CRDP-2 RF v2 datasets												
2020	SLSTRA	RF_V2.2.1	land	827289	19865	0.00	0.14	0.14	0.45	38.6	38.7	max(0.08 or 3%)
2020	SLSTRA	RF_V2.2.1	ocean	160227	4841	0.05	0.12	0.11	0.59	38.7	43.3	max(0.08 or 3%)

Summary for the validation of RF v2 total AOD

- Significant (but not complete) reduction of bias and noise for SLSTR / 3A CISAR / RF algorithm v2, especially for low AOD (<0.2)
- New under-estimation of higher AOD (>0.2) over land

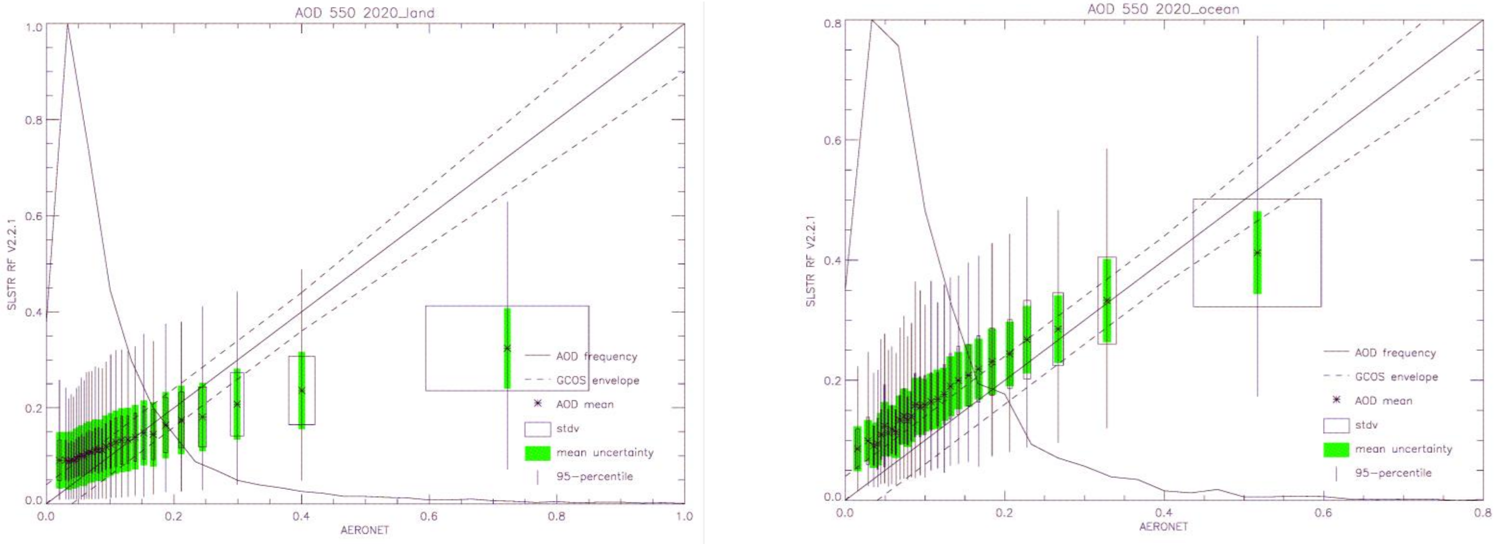

Figure 4.27 *Validation summary plots for SLSTR/3A over land (left) and ocean (right).*

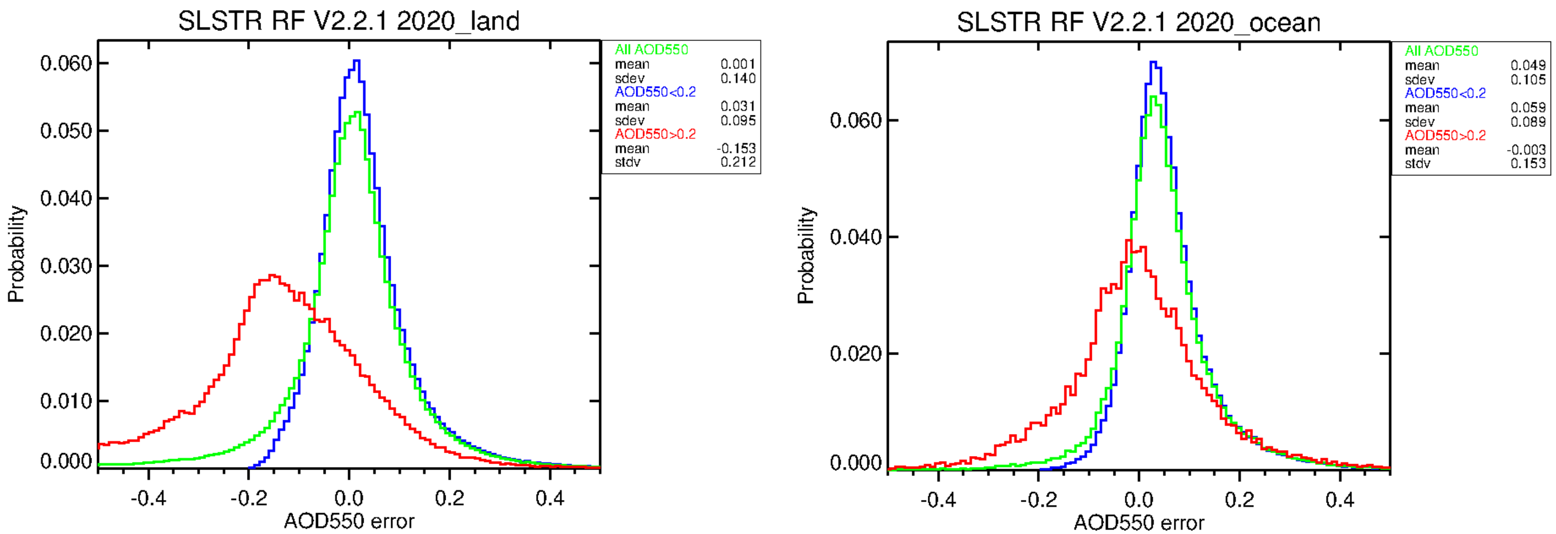

Figure 4.28 *Difference histograms for SLSTR/3A over land (left) and ocean (right).*

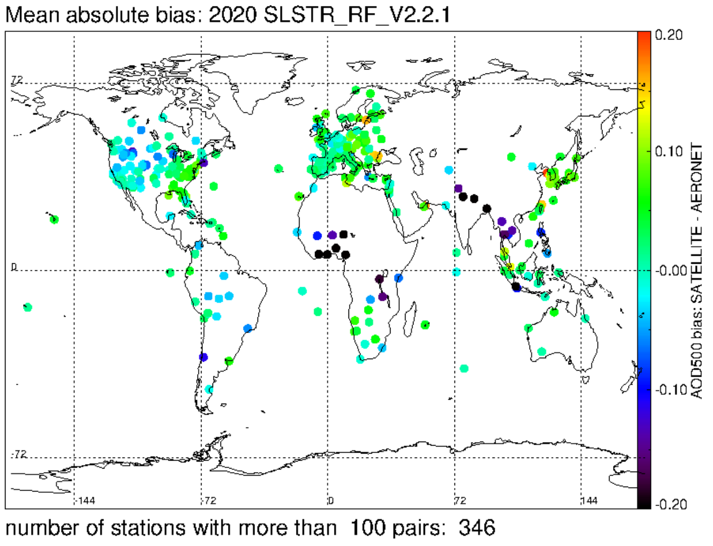

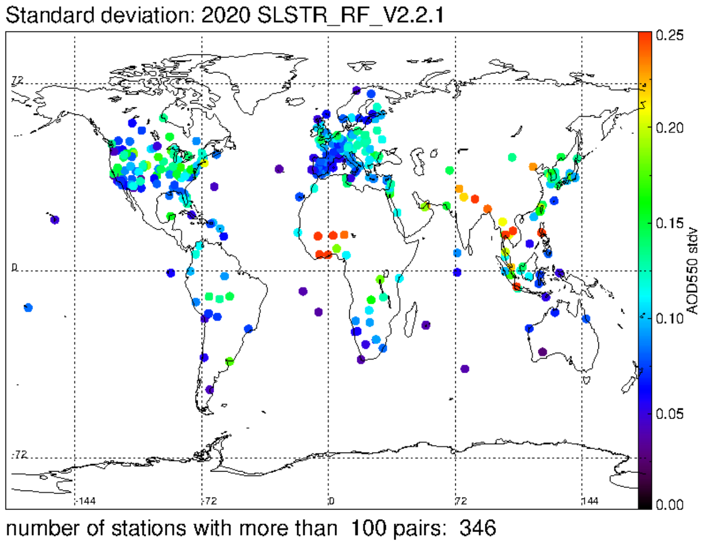

Figure 4.29 *Maps of significant station mean AOD bias and stdv (Satellite – AERONET) for SLSTR/3A.*

4.2 Validation of FM-AOD550

The valdiation of FM_AOD at 550 nm is conducted similarly to the valdiation of total AOD. As one exception no GCOS fractions are calculated since there is no such envelope defined by GCOS for FM-AOD. Also no pixel-level uncertainties are provided. It is noteworthy that the uncertainty of FM-AOD from AERONET calculated with the SDA algorithm must also be considered larger than the one for AOD, especially for low AOD values.

4.2.1 CRDP-1 SU v1 validation results

The analysis shown for FM-AOD contains again an overview Table (Tab 4.5), box-whisker plots (fig. 4.21 and fig. 4.22, but without uncertainties), density scatterplots (fig. 4.23 and fig. 4.24) and maps of mean bias and stdv per station (fig. 4.25 and fig. 4.26).

Table 4.8 Validation statistics for SU v1 FM-AOD at 550nm

year	sensor	alg_version	area	Number of sat pixel	number1 of stat obs	bias	rmse	stdv	Pearson corr
CRDP-1 SU v1 datasets									
1998	ATSR2	SU_v4.32	land	5514	94	0.06	0.11	0.09	0.77
1998	ATSR2	SU_v4.32	ocean	1044	33	0.04	0.06	0.04	0.82
2008	AATSR	SU_v4.32	land	49679	993	0.03	0.09	0.08	0.88
2008	AATSR	SU_v4.32	ocean	7117	232	0.05	0.11	0.10	0.58
2019	SLSTRA	SU_v1.11	land	102805	2670	0.07	0.15	0.13	0.77
2019	SLSTRA	SU_v1.11	ocean	46384	932	0.07	0.12	0.09	0.79
2019	SLSTRB	SU_v1.11	land	83991	2080	0.08	0.15	0.13	0.67
2019	SLSTRB	SU_v1.11	ocean	36817	737	0.08	0.12	0.09	0.77

Overall, there is a positive bias of FM-AOD for all sensors over land and ocean (larger for SLSTR with ~0.075 than for the ATSR instruments with ~0.045), while stdv values over land are again larger for SLSTR (0.13) than for the ATSR instruments ~0.085); over ocean stdv values are similar (~0.095) except for the statistically weak ATSR analysis (0.04). Correlations range from 0.7 (SLSTR/3A) to 0.9 (AATSR) over land and are ~0.8 over ocean (except for AATSR with 0.6). Over ocean the FM-AOD bias appears to increase with increasing AOD for SLSTR. The geographical patterns follow largely those of the AOD errors (e.g. large positive bias for AATSR over the Atlantic off Africa in June and in South America, large negative bias over East and South Asia in March, September and December; for SLSTR over-estimations in Central North America in March and September, and under-estimations in March over South Asia, and in September over Eastern Asia and East Europe).

Summary for the validation of FM-AOD

- Overall positive bias for all sensors over land and ocean
- Bias and stdv over land larger for SLSTR than for the ATSR instruments with ~0.045)
- Over ocean bias appears to increase with increasing AOD for SLSTR
- Geographical patterns follow largely those of the AOD errors

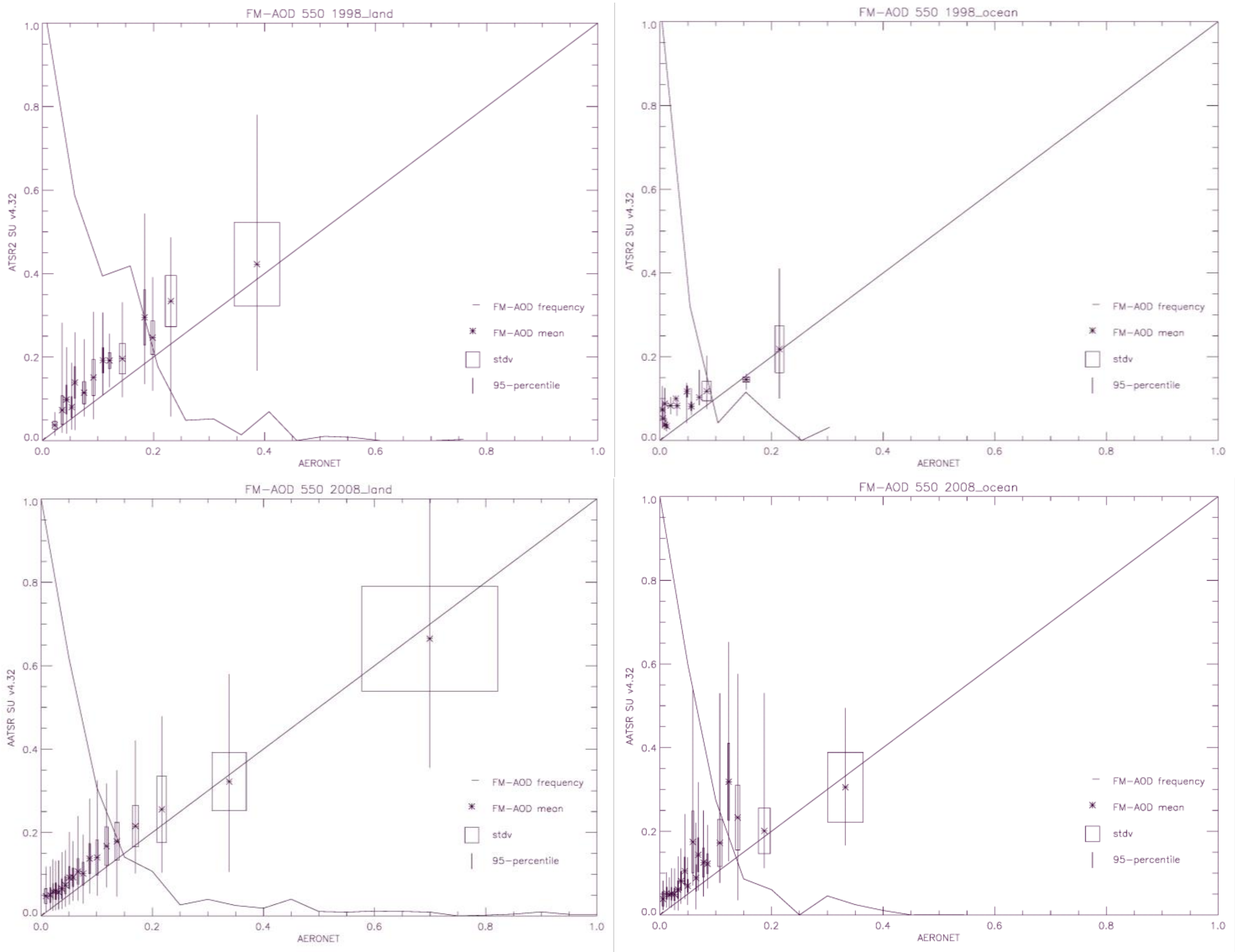

***Figure 4.30** Validation summary plots for FM-AOD of ATSR-2 (top) and AATSR (bottom) over land (left) and ocean (right).*

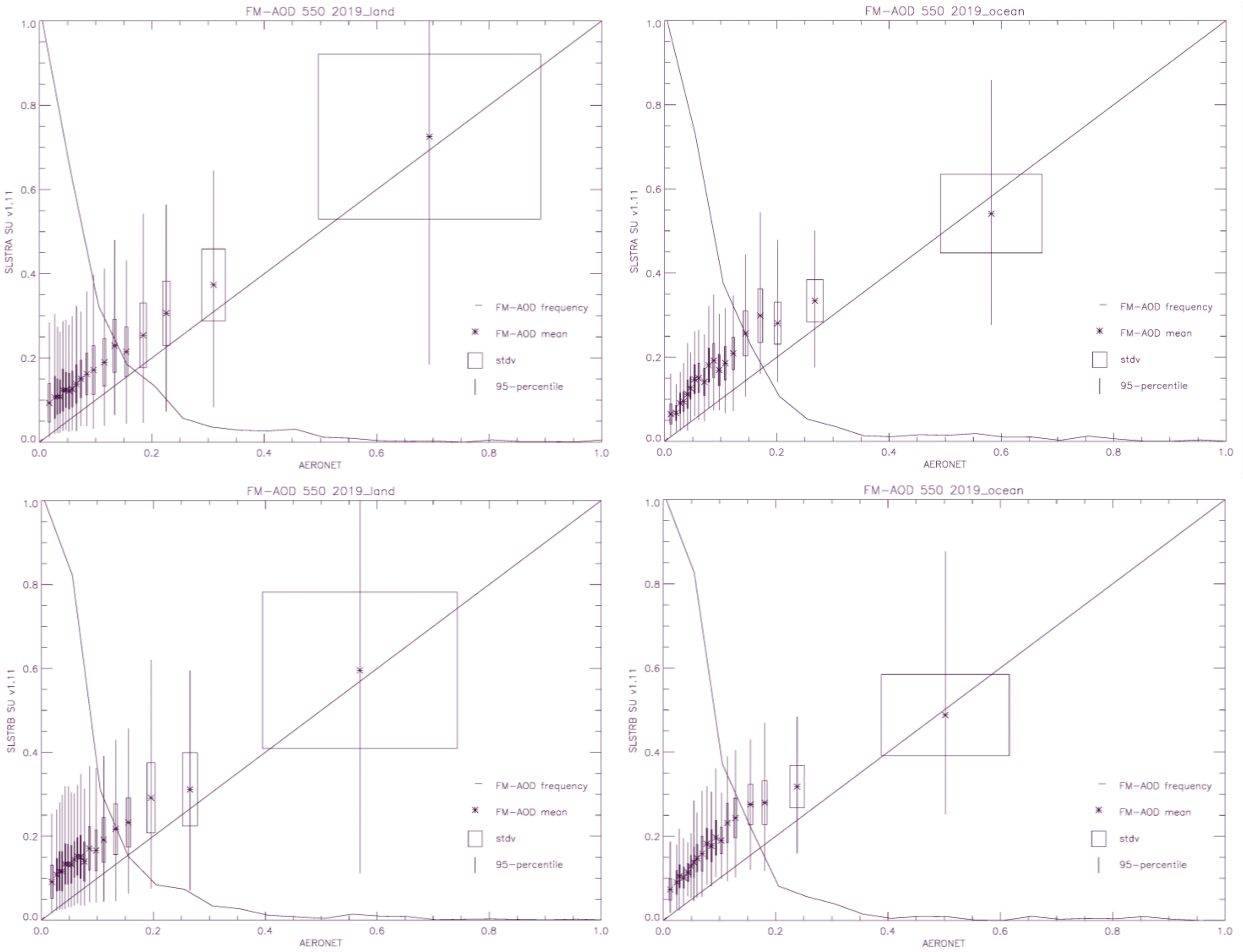

Figure 4.31 *Validation summary plots for FM-AOD of SLSTR/3A (top) and SLSTR/3B (bottom) over land (left) and ocean (right).*

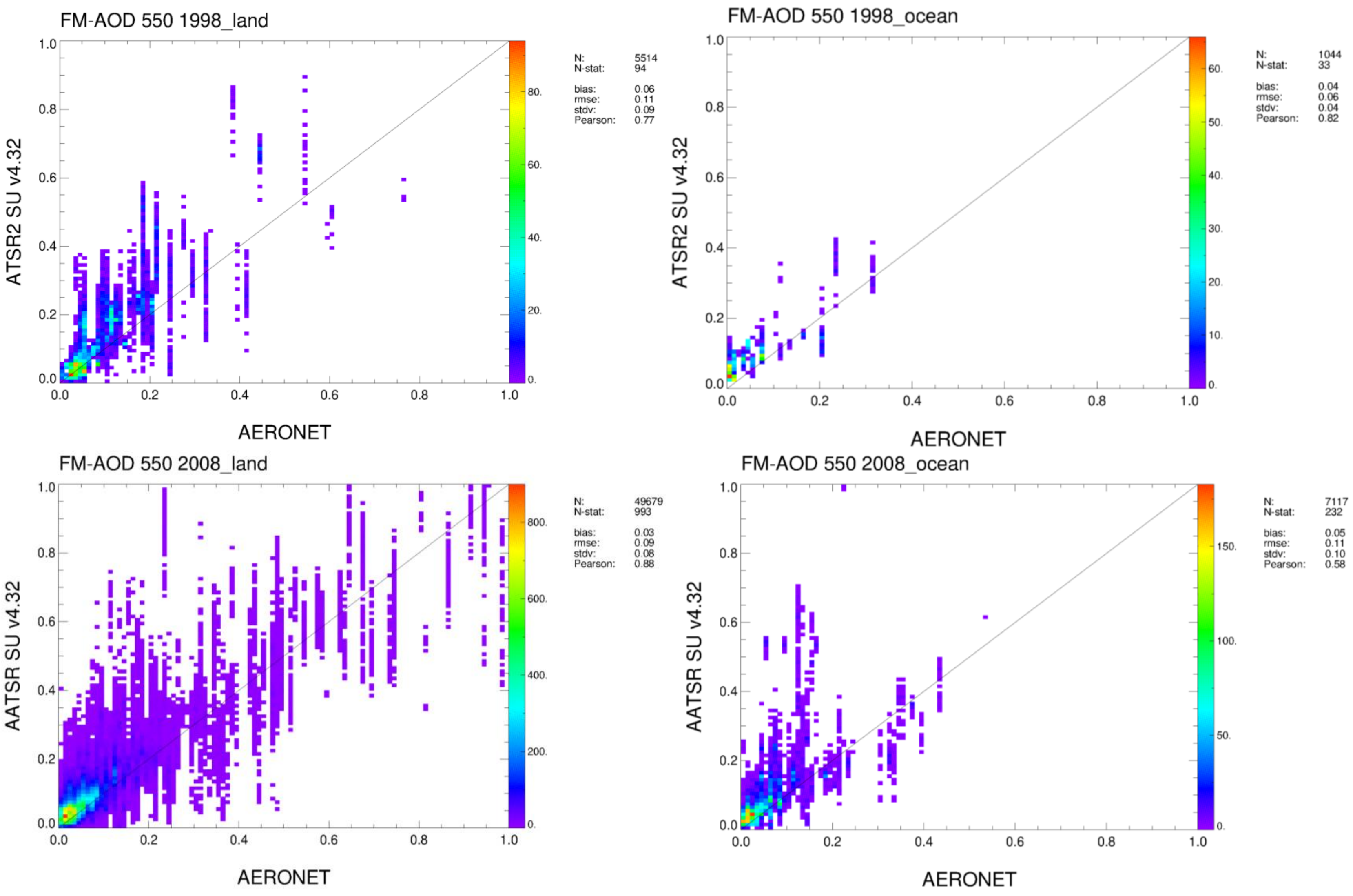

Figure 4.32 *Density scatter plots for FM-AOD of ATSR-2 (top) and AATSR (bottom) over land (left) and ocean (right).*

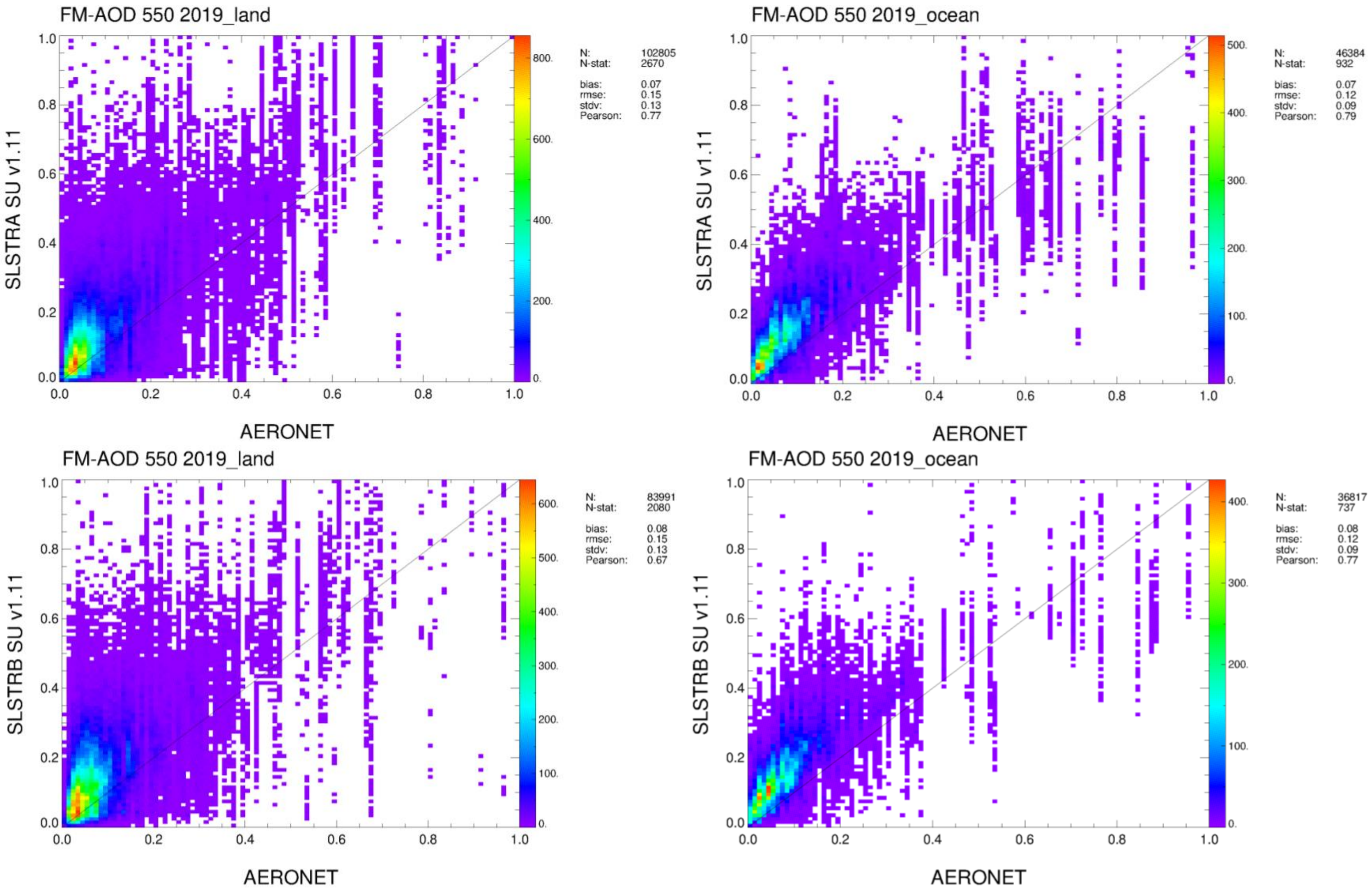

Figure 4.33 *Density scatter plots for FM-AOD of SLSTR/3A (top) and SLSTR/3B (bottom) over land (left) and ocean (right).*

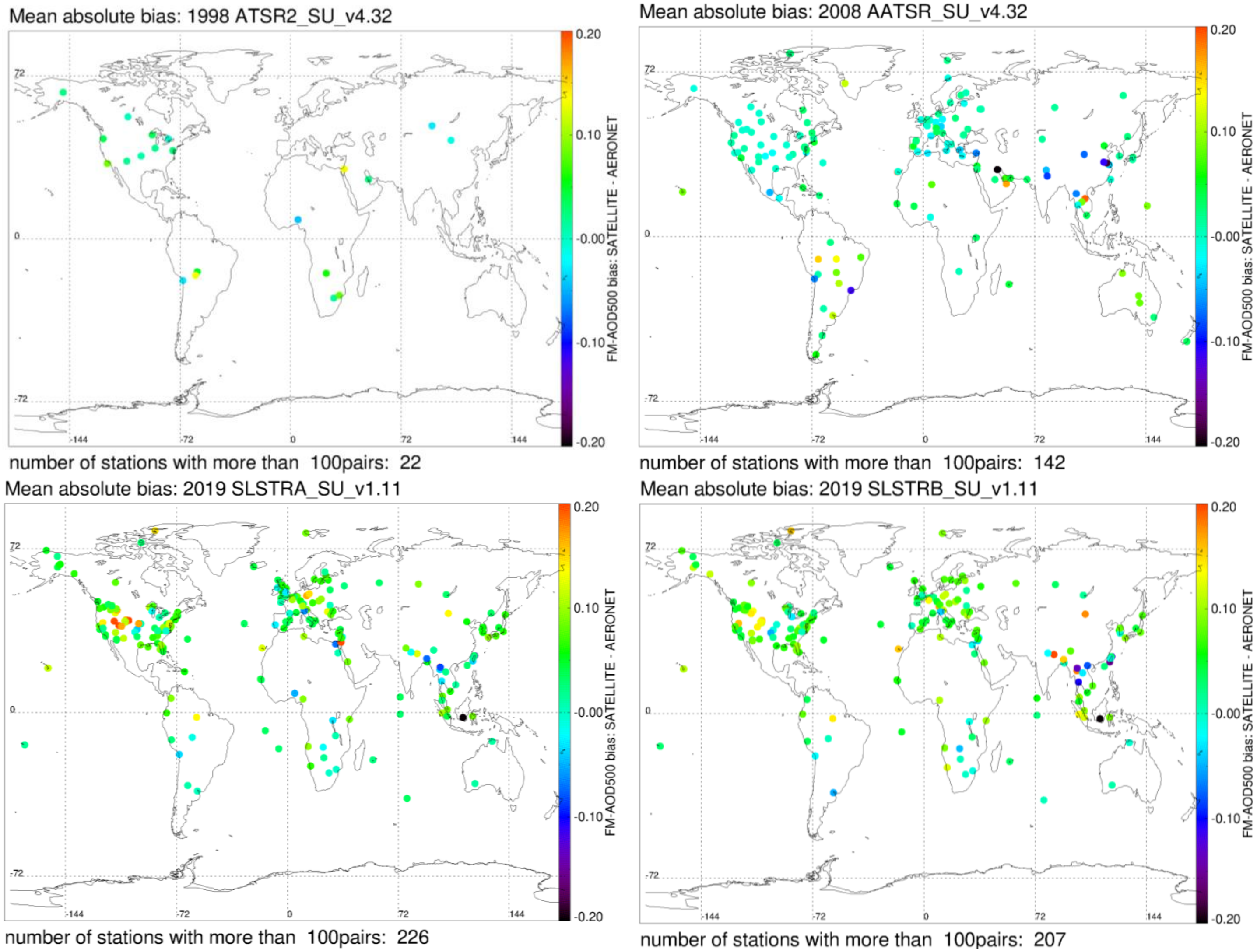

Figure 4.34 *Maps of significant station mean FM-AOD bias (Satellite – AERONET) for all 4 sensors.*

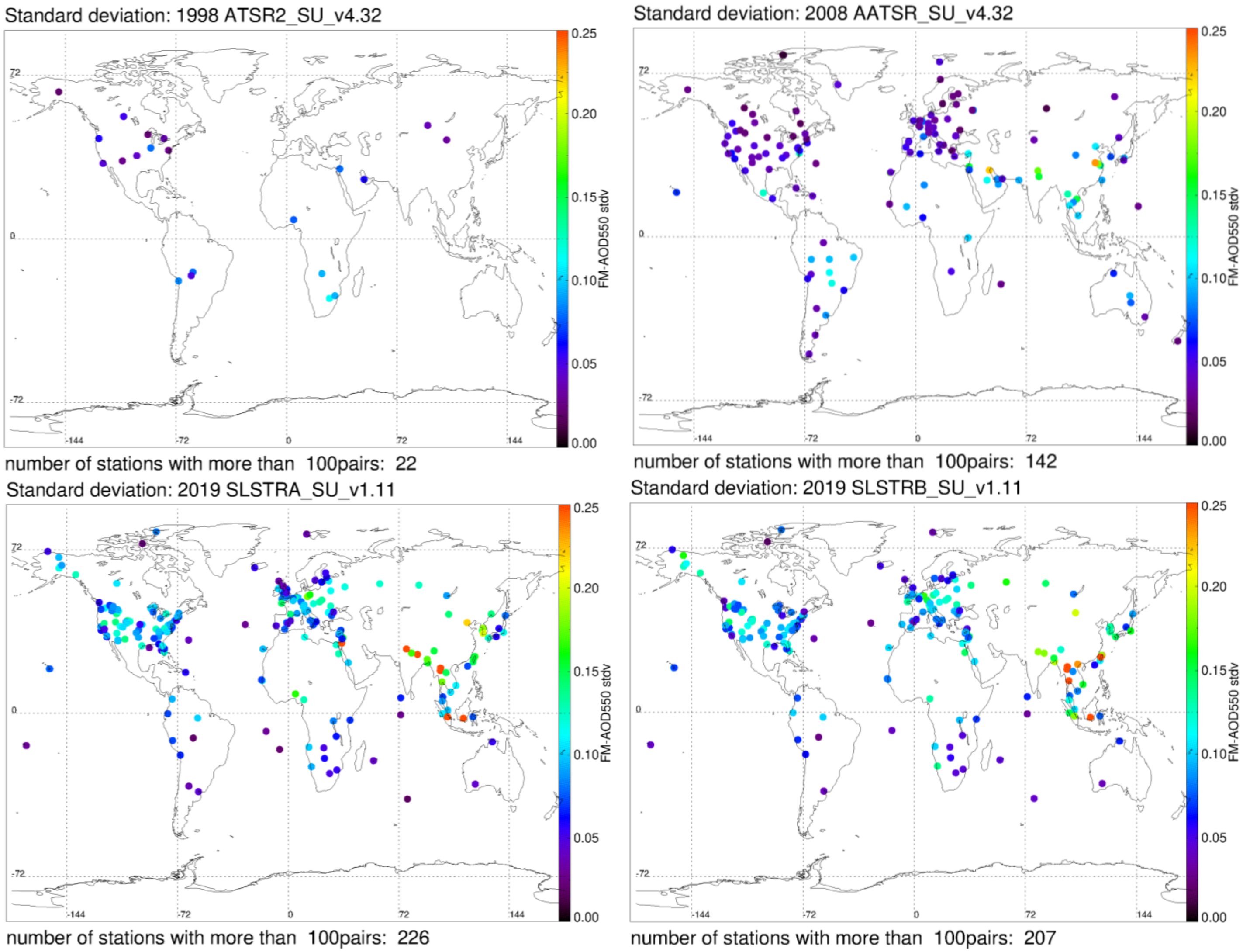

Figure 4.35 *Maps of significant station FM-AOD stdv of Satellite and AERONET for all 4 sensors.*

4.2.2 CRDP-2 SU v2 validation results

Table 4.6 (like Tab. 4.5 for SU v1) and Figures 4.27 – 4.32 (like Fig. 4.30 – 4.35 for SU v1) show the analysis of FM-AOD from SU v2 datasets against AERONET SDA station measurements. Overall, the FM-AOD charactersistics are mainly determined by the total AOD characteristics.

Table 4.9 *Validation statistics for SU v2 FM-AOD* ***at 550nm***

year	sensor	alg_version	area	Number of sat pixel	number1 of stat obs	bias	rmse	stdv	Pearson corr
CRDP-2 SU v2 datasets									
1998	ATSR2	SU_v4.33	land	5514	94	0.06	0.11	0.09	0.77
1998	ATSR2	SU_v4.33	ocean	1044	33	0.04	0.06	0.04	0.82
2008	AATSR	SU_v4.33	land	49689	993	0.03	0.09	0.08	0.88
2008	AATSR	SU_v4.33	ocean	7118	232	0.05	0.11	0.10	0.58
2019	SLSTRA	SU_v1.14	land	117195	2634	0.06	0.13	0.12	0.79
2019	SLSTRA	SU_v1.14	ocean	47920	936	0.06	0.11	0.09	0.79
2019	SLSTRB	SU_v1.14	land	110797	2449	0.06	0.14	0.13	0.76
2019	SLSTRB	SU_v1.14	ocean	46042	904	0.07	0.11	0.09	0.79

Summary for the validation of SU v2 FM-AOD

- Overall positive bias for all sensors over land and ocean remains
- Geographical patterns follow largely those of the AOD errors

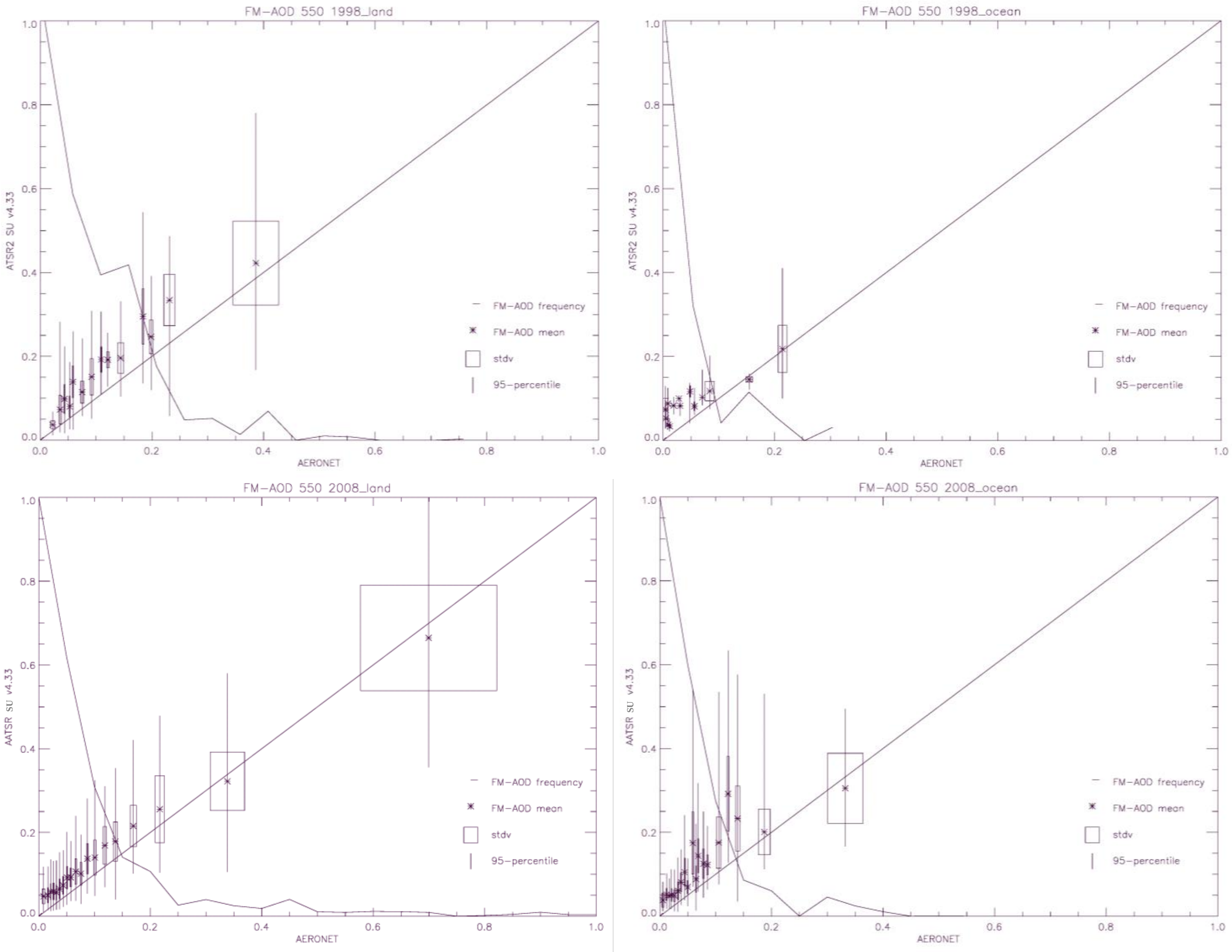

Figure 4.36 *Validation summary plots for FM-AOD of ATSR-2 (top) and AATSR (bottom) over land (left) and ocean (right).*

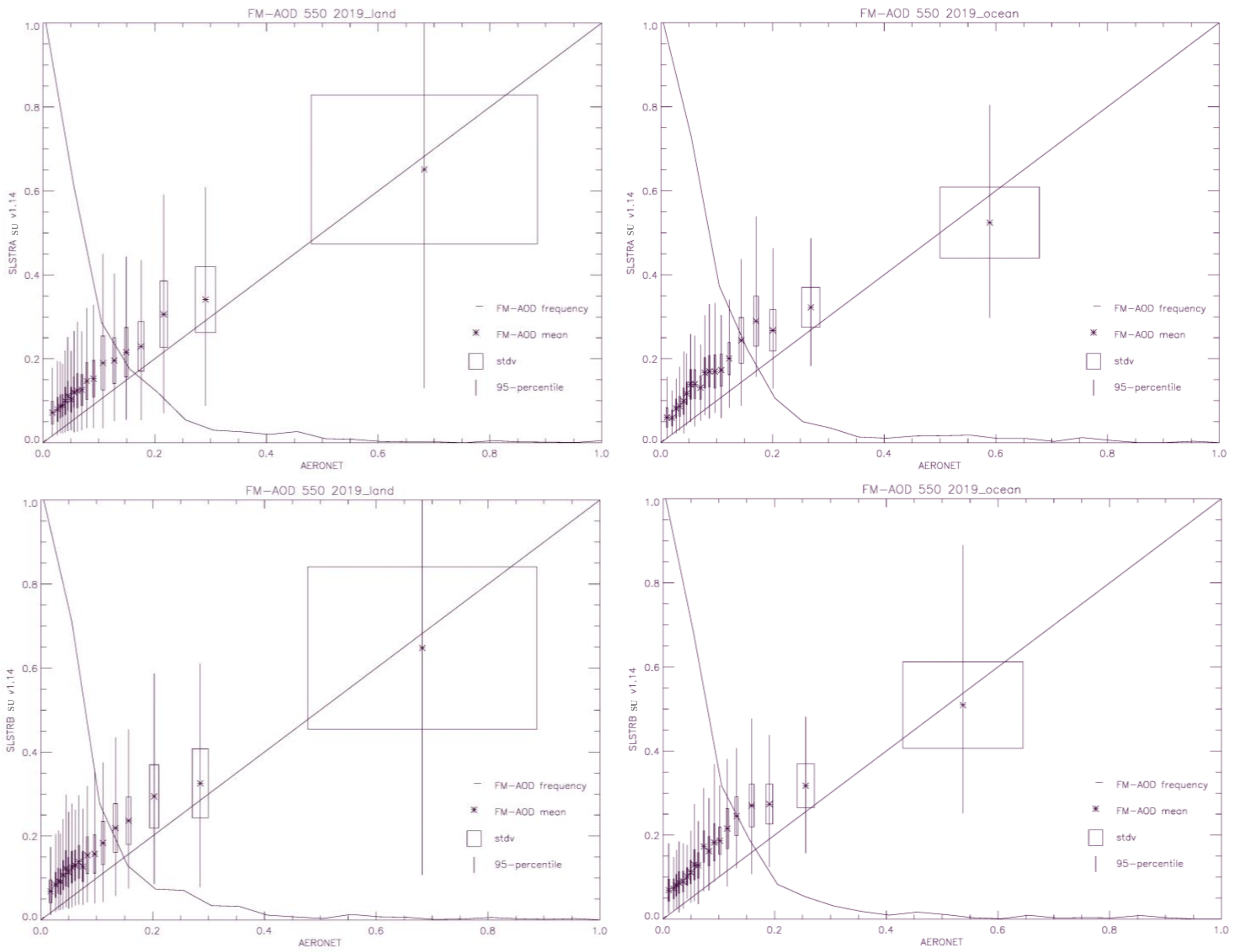

Figure 4.37 *Validation summary plots for FM-AOD of SLSTR/3A (top) and SLSTR/3B (bottom) over land (left) and ocean (right).*

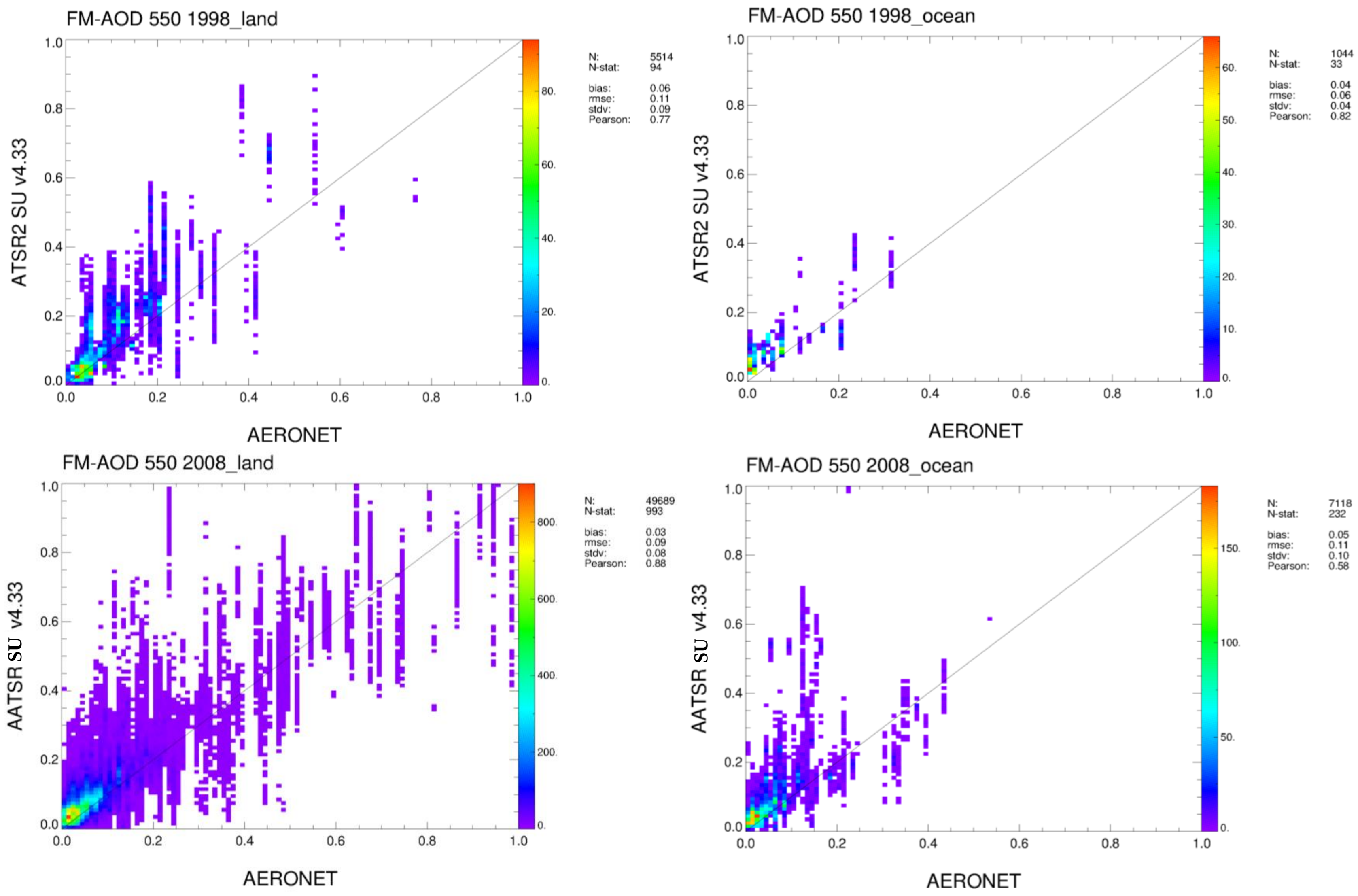

Figure 4.38 *Density scatter plots for FM-AOD of ATSR-2 (top) and AATSR (bottom) over land (left) and ocean (right).*

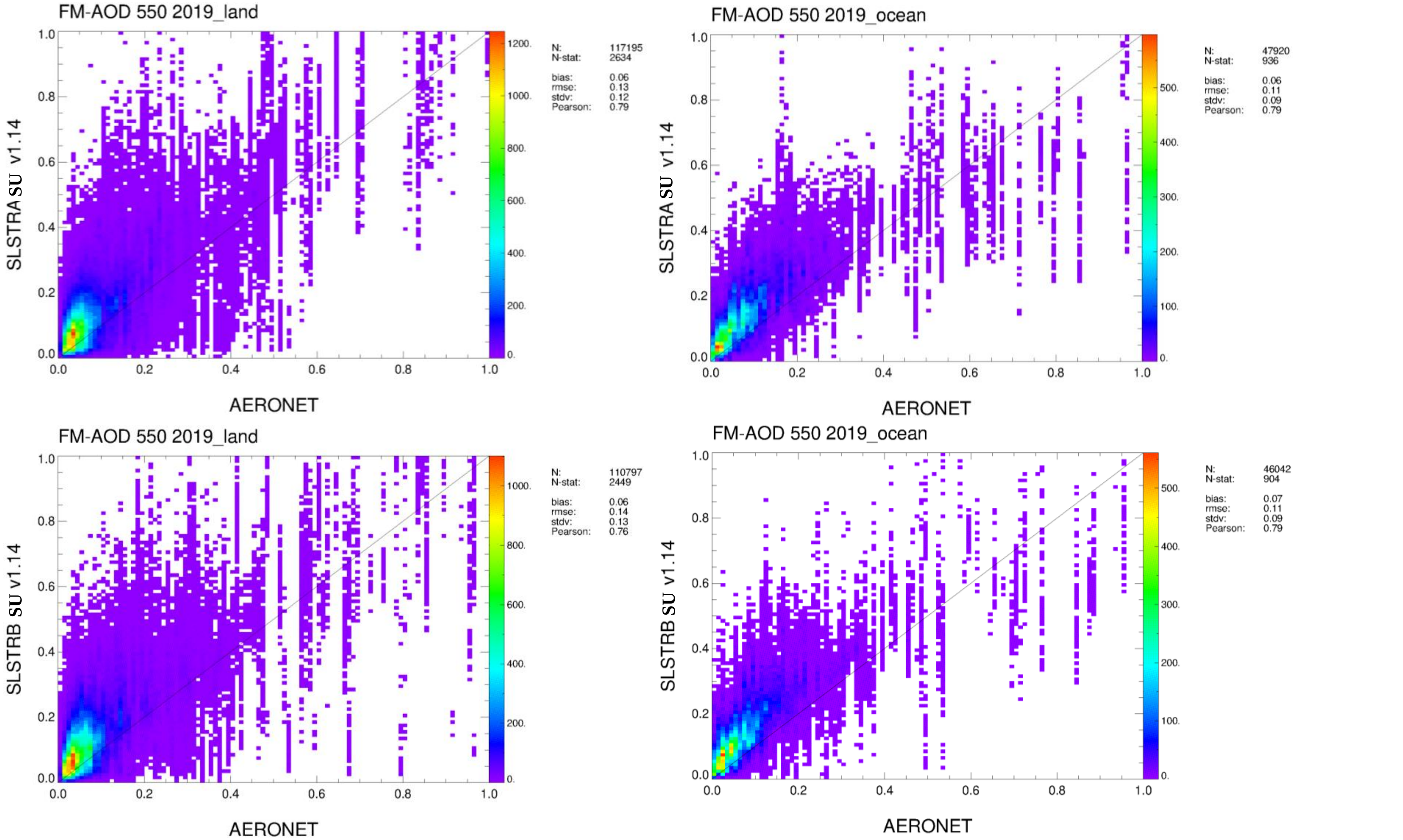

***Figure 4.39** Density scatter plots for FM-AOD of SLSTR/3A (top) and SLSTR/3B (bottom) over land (left) and ocean (right).*

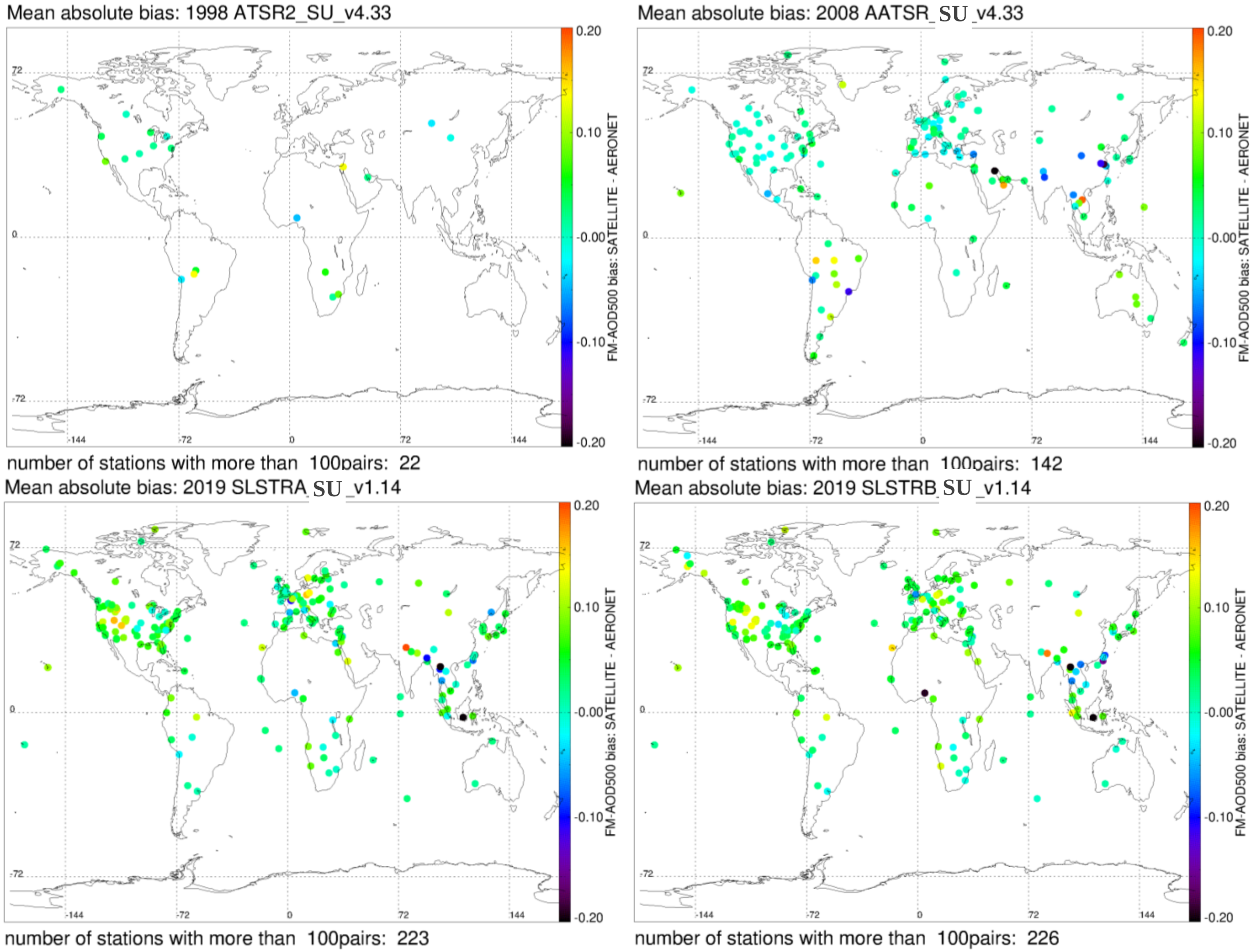

Figure 4.40 *Maps of significant station mean FM-AOD bias (Satellite – AERONET) for all 4 sensors.*

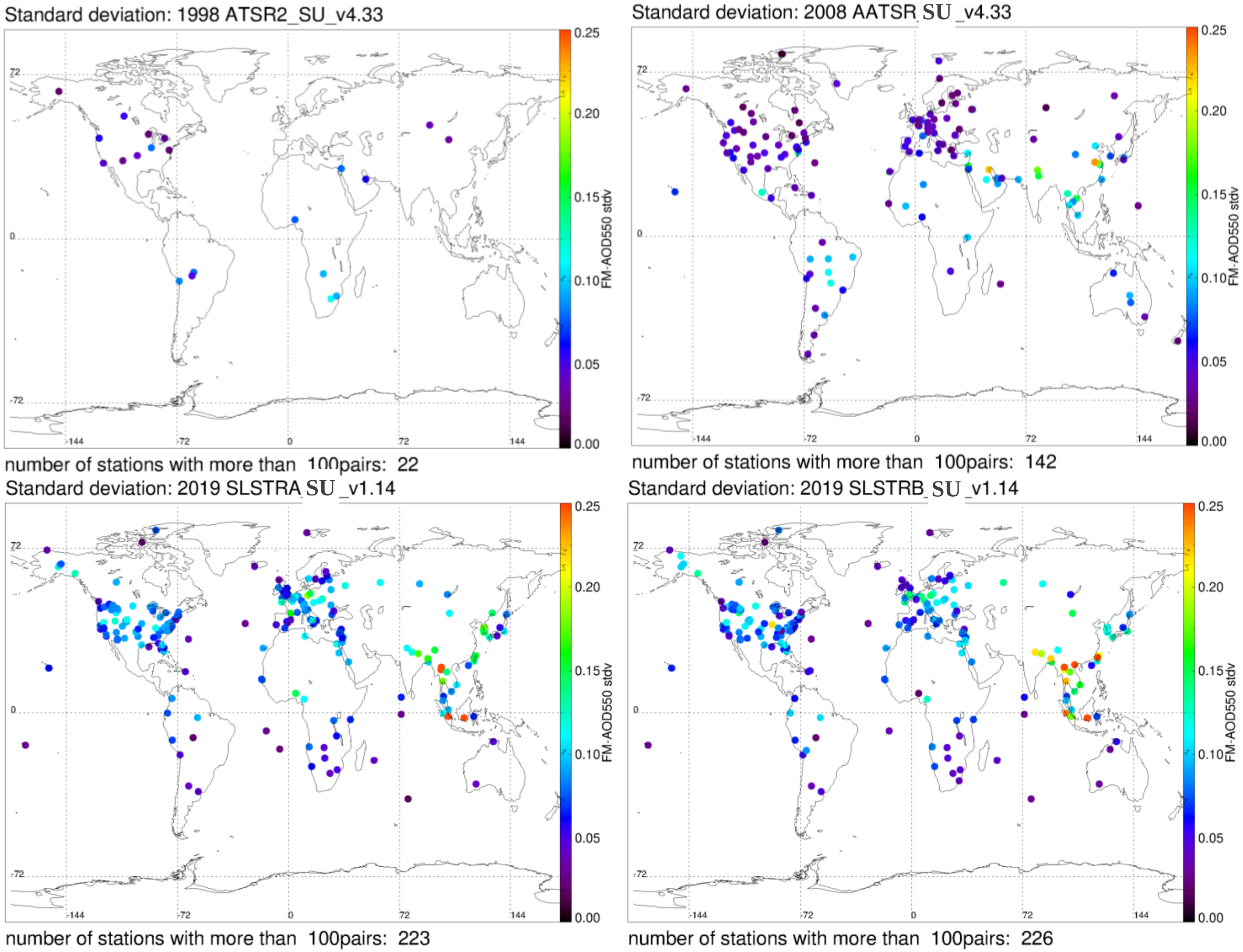

***Figure 4.41** Maps of significant station FM-AOD stdv of Satellite and AERONET for all 4 sensors.*

4.2.3 CRDP-3 SU v3 validation results

Table 4.10 (like Tab. 4.8 for SU v1) and Figures 4.42 – 4.45 (like Fig. 4.30 – 4.35 for SU v1) show the analysis of FM-AOD from SU v3 datasets against AERONET SDA station measurements. Overall, the FM-AOD charactersistics are mainly determined by the total AOD characteristics and show little change against v2.

Table 4.10 *Validation statistics for SU v3 FM-AOD* ***at 550nm***

year	sensor	alg_version	area	Number of sat pixel	number1 of stat obs	bias	rmse	stdv	Pearson corr
CRDP-2 SU v3 datasets									
1998	ATSR2	SU_v4.35	land	15173	303	0.04	0.12	0.11	0.72
1998	ATSR2	SU_v4.35	ocean	2476	84	0.05	0.09	0.07	0.84
2008	AATSR	SU_v4.35	land	155869	3225	0.03	0.10	0.09	0.82
2008	AATSR	SU_v4.35	ocean	23422	754	0.05	0.12	0.11	0.58
2020	SLSTRA	SU_v1.14	land	538236	12554	0.05	0.13	0.12	0.70
2020	SLSTRA	SU_v1.14	ocean	244603	4794	0.05	0.10	0.08	0.71
2020	SLSTRB	SU_v1.14	land	562057	12977	0.05	0.13	0.11	0.70
2020	SLSTRB	SU_v1.14	ocean	252847	4928	0.06	0.10	0.08	0.73

Summary for the validation of SU v3 FM-AOD

- Overall positive bias for all sensors over land and ocean remains
- Geographical patterns follow largely those of the AOD errors

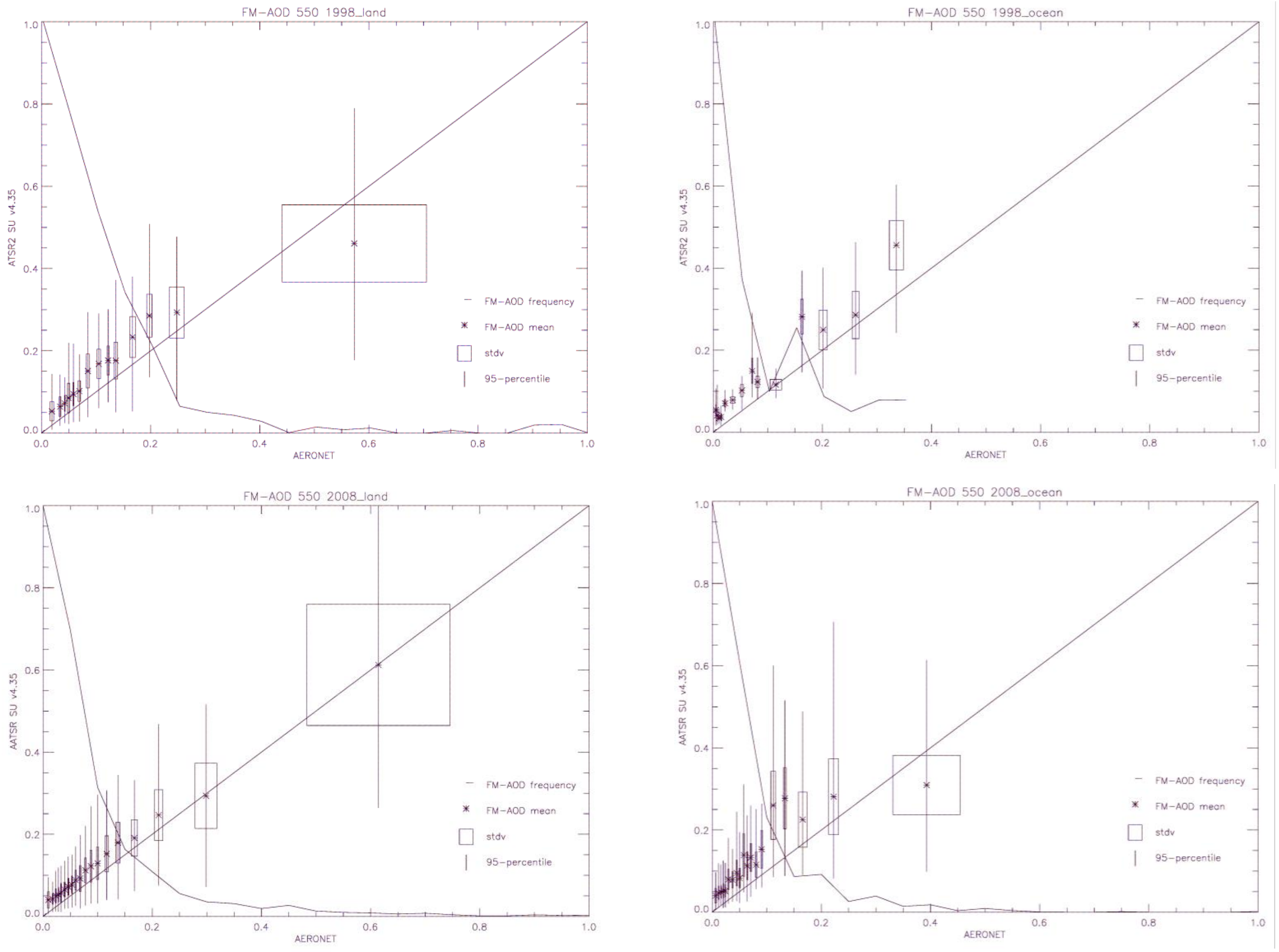

Figure 4.42 *Validation summary plots for FM-AOD of ATSR-2 (top) and AATSR (bottom) over land (left) and ocean (right).*

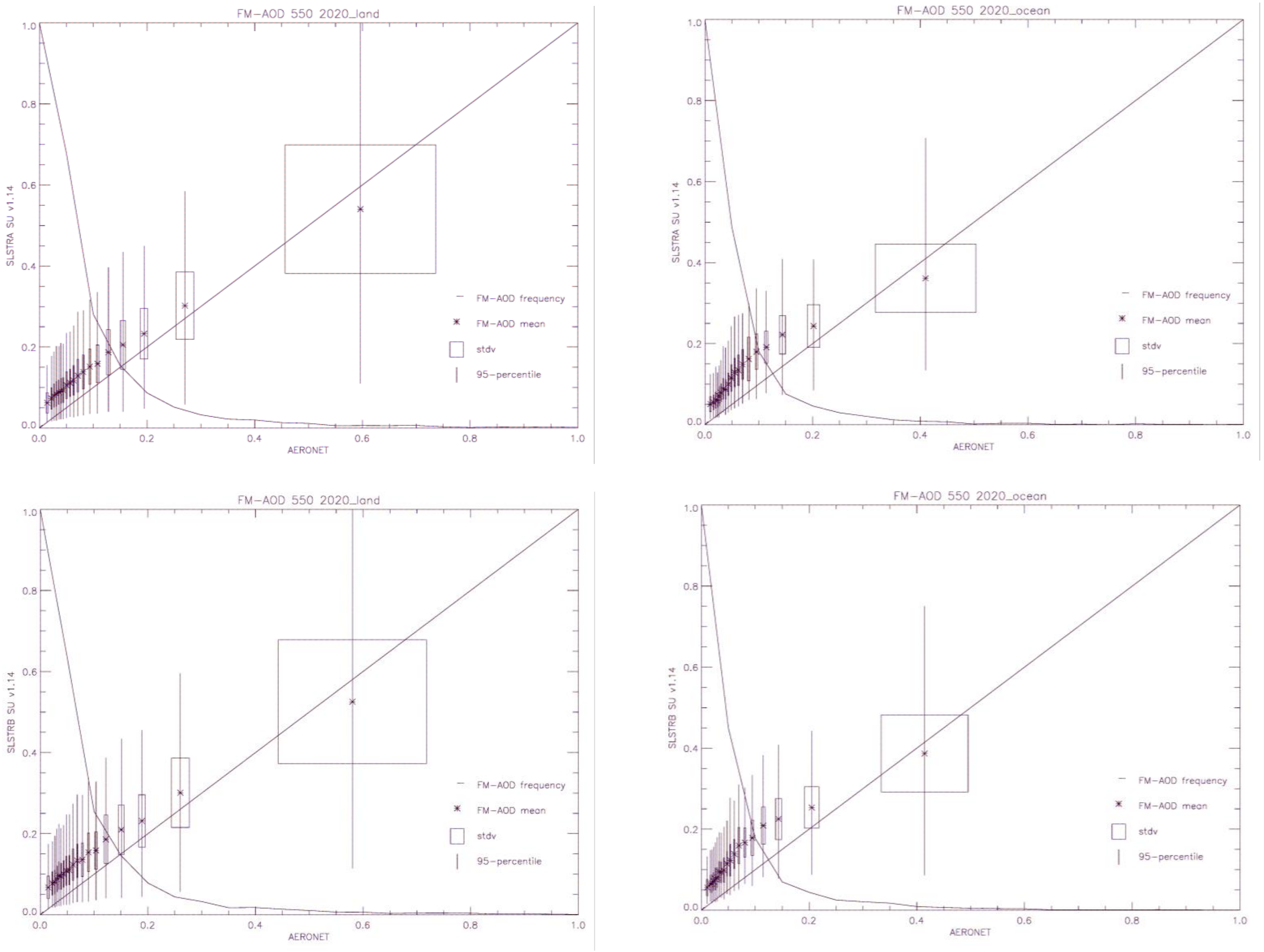

Figure 4.43 *Validation summary plots for FM-AOD of SLSTR/3A (top) and SLSTR/3B (bottom) over land (left) and ocean (right).*

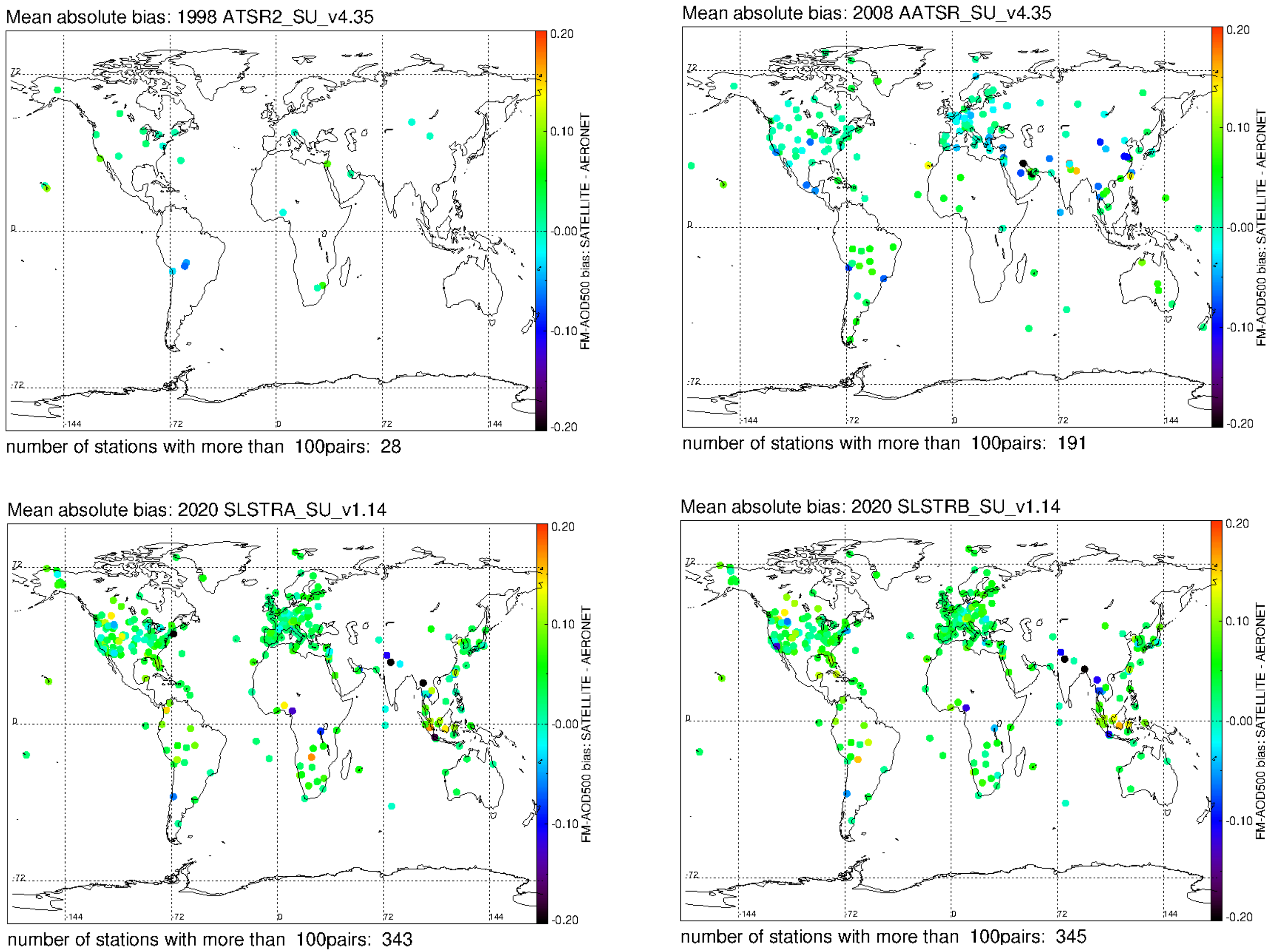

***Figure 4.44** Maps of significant station mean FM-AOD bias (Satellite – AERONET) for all 4 sensors.*

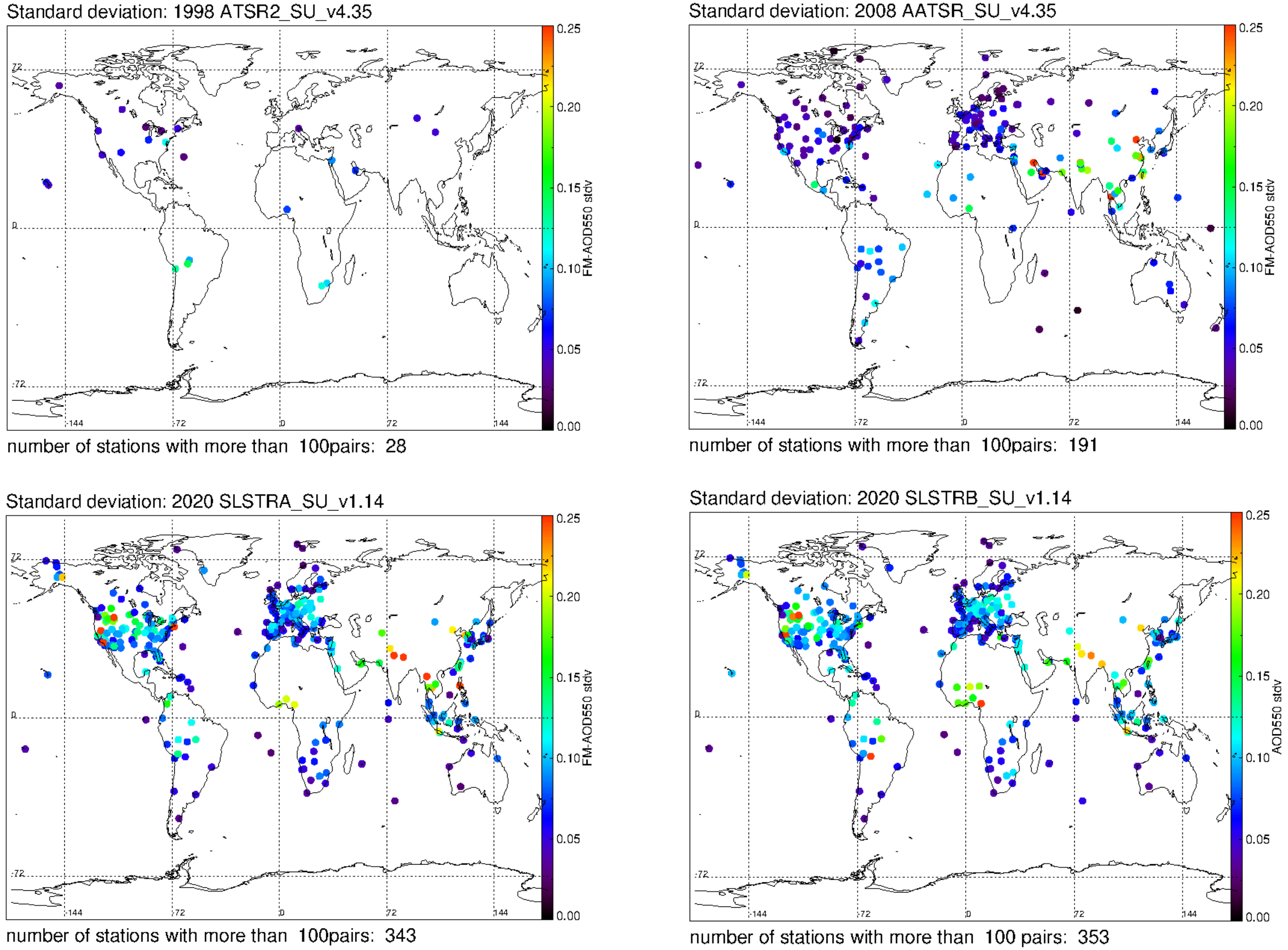

Figure 4.45 *Maps of significant station FM-AOD stdv of Satellite and AERONET for all 4 sensors.*

4.2.4 CRDP-2 RF v1 validation results

Table 4.7 (like Tab. 4.5 for SU v1) and Figures 4.33 – 4.35 (like Fig. 4.30 – 4.35 for SU v1) show the analysis of FM-AOD from CISAR v1 datasets against AERONET SDA station measurements. Overall, also for CISAR the FM-AOD charactersistics are mainly determined by the total AOD characteristics.

Table 4.11 *Validation statistics for FM-AOD* ***at 550nm***

year	sensor	alg_version	area	Number of sat pixel	number1 of stat obs	bias	rmse	stdv	Pearson corr
CRDP-2 RF v1 datasets									
2019	SLSTRA	RF_v2.0.0	land	168085	1046	0.03	0.32	0.43	0.23
2019	SLSTRA	RF_v2.0.0	ocean	83275	458	0.09	0.24	0.22	0.33

Summary for the validation of RF v1 FM-AOD

- Overall positive bias for for SLSTR/3A over land and ocean
- Geographical patterns follow largely those of the AOD errors

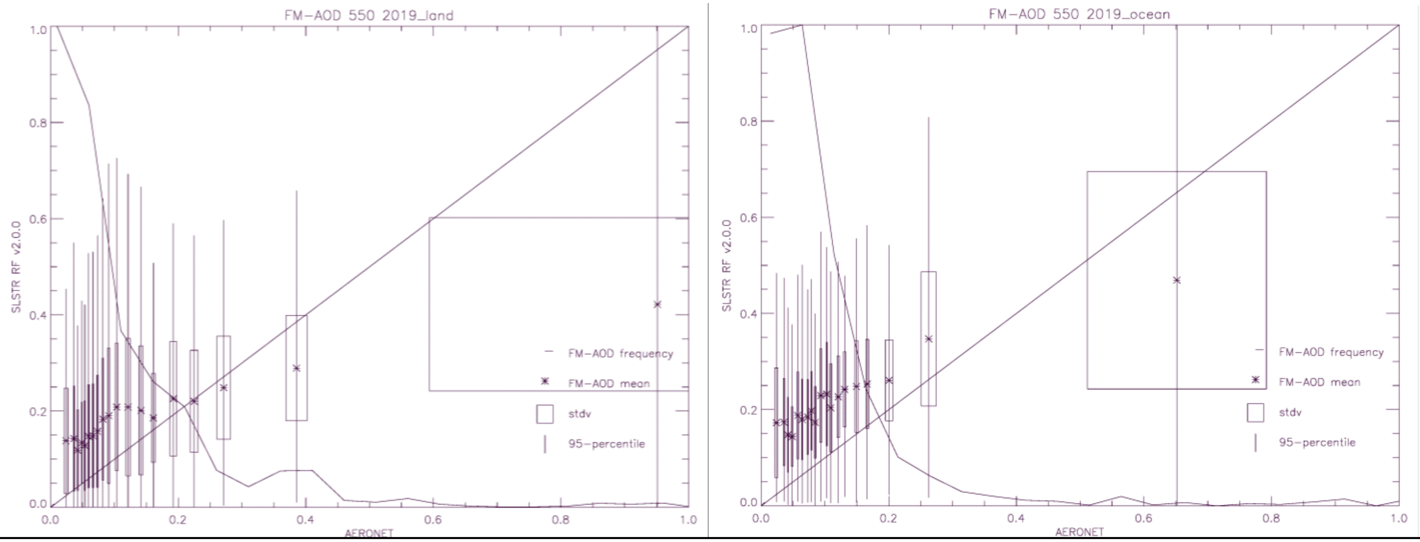

Figure 4.46 *Validation summary plots for FM-AOD of SLSTR/3A over land (left) and ocean (right).*

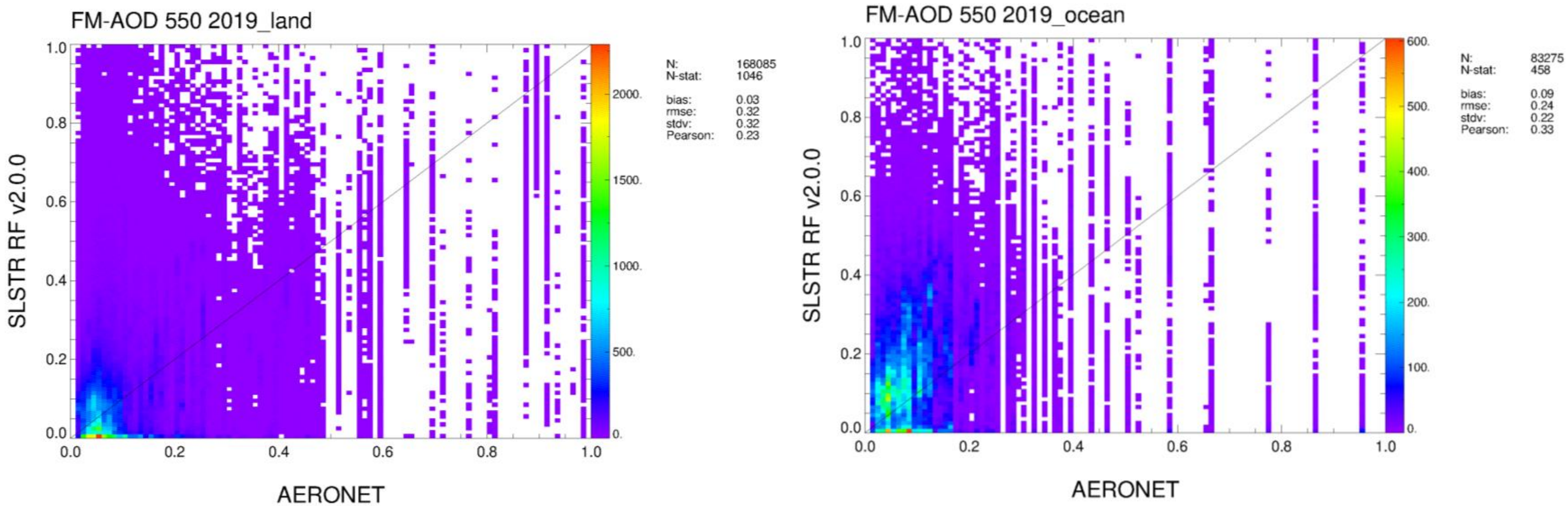

Figure 4.47 *Density scatter plots for FM-AOD of SLSTR/3A over land (left) and ocean (right).*

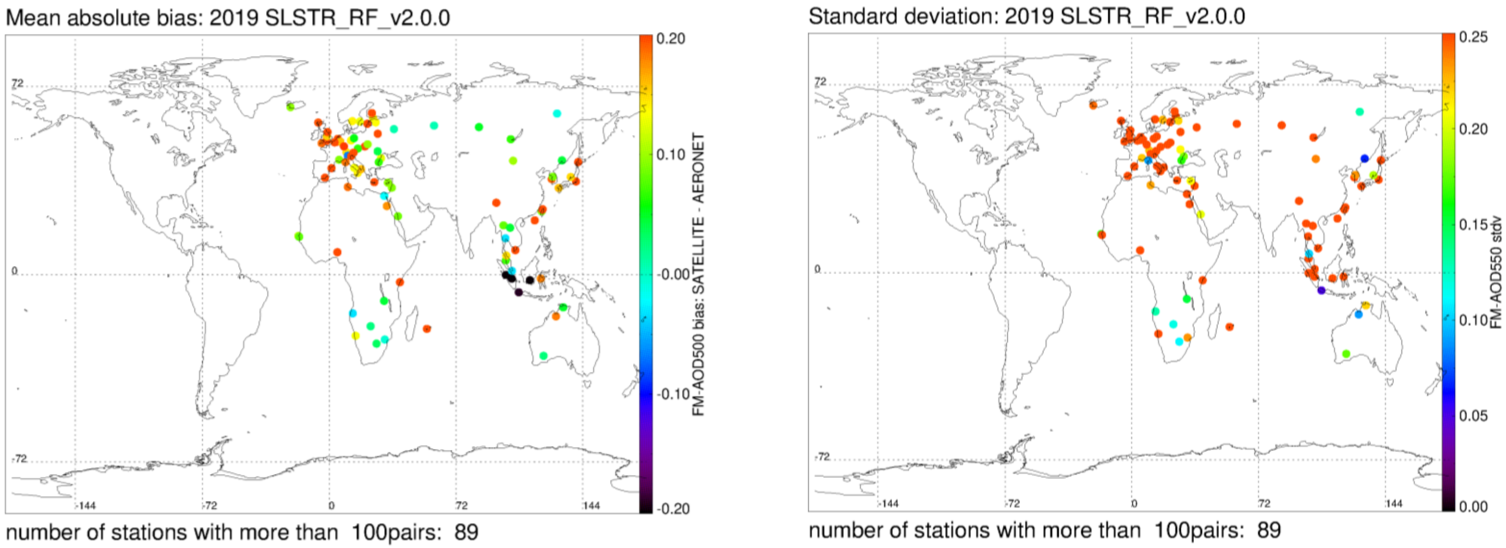

Figure 4.48 *Maps of significant station mean FM-AOD bias and stdv (Satellite – AERONET) for SLSTR/3A.*

4.2.5 CRDP-3 RF v2 validation results

Table 4.12 (like Tab. 4.8 for SU v1) and Figures 4.49 – 4.50 (like Fig. 4.30 – 4.35 for SU v1) show the analysis of FM-AOD from CISAR v2 datasets against AERONET SDA station measurements. Overall, also for CISAR the FM-AOD charactersistics are mainly determined by the total AOD characteristics.

Table 4.12 *Validation statistics for FM-AOD* ***at 550nm***

year	sensor	alg_version	area	Number of sat pixel	number1 of stat obs	bias	rmse	stdv	Pearson corr
CRDP-3 RF v2 datasets									
2020	SLSTRA	RF_V2.2.1	land	791357	19023	0.00	0.12	0.12	0.36
2020	SLSTRA	RF_ V2.2.1	ocean	155931	4730	0.03	0.10	0.09	0.60

Summary for the validation of RF v2 FM-AOD

- Overall clear reduction of bias and stdv as compared to v1
- Overall positive bias for for SLSTR/3A over land and ocean remains
- Geographical patterns follow largely those of the AOD errors

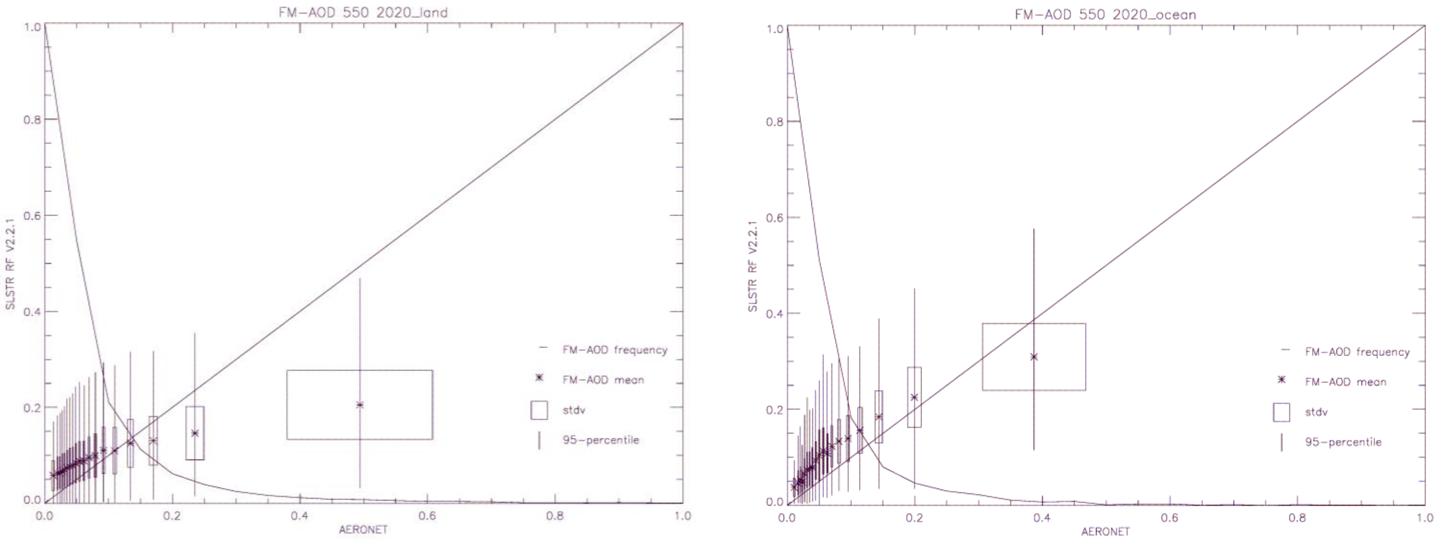

Figure 4.49 *Validation summary plots for FM-AOD of SLSTR/3A over land (left) and ocean (right).*

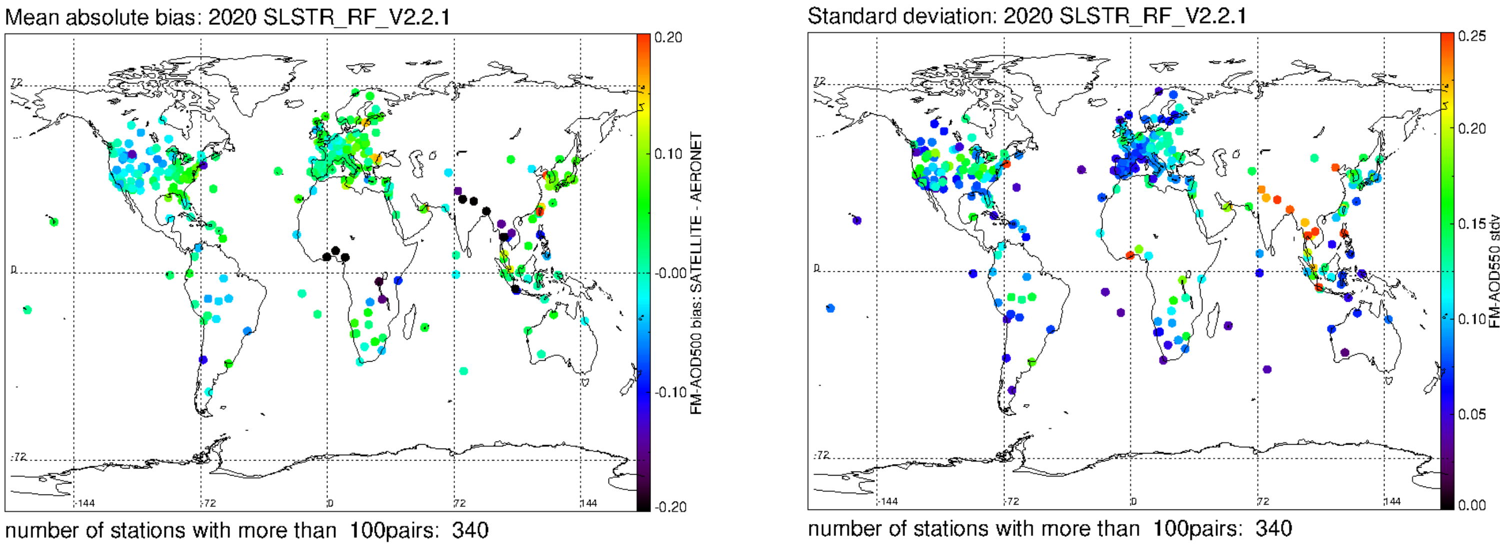

Figure 4.50 *Maps of significant station mean FM-AOD bias and stdv (Satellite – AERONET) for SLSTR/3A.*

4.3 Validation of background ocean AOD

The validation of AOD at 550 nm over clean background ocean is conducted against ship-bone MAN measurements and against selected Aeronet stations.

4.3.1 Validation against MAN measurements

We used the results of a matching analysis between MAN measurements and SLSTR data (done for 2020 and 2021 within the EUMETSAT LAW project and kindly provided to us through overlapping partnership, courtesy of FMI). Table 4.13 and Fig. 4.51 show the results of our analysis (only for 2020, for which our test datasets were processed) which yields a positive AOD bias of 0.02 (Swansea algorithm) and 0.04 (CISAR algorithm). No averaging of satellite pixels was made, but all retrieval pixels within a matching range for a MAN measurement were considered individually.

Table 4.13 *Validation statistics for AOD against MAN measurements*

year	sensor	alg_version	area	Number of sat pixel	number1 of stat obs	bias	rmse	stdv	Pearson corr
2020	SLSTRA	SU_v1.14	MAN	3171	38	0.02	0.07	0.07	0.84
2020	SLSTRB	SU_v1.14	MAN	5696	44	0.02	0.05	0.05	0.93
2020	SLSTRA	RF_V2.2.1	MAN	1804	30	0.04	0.10	0.09	0.49

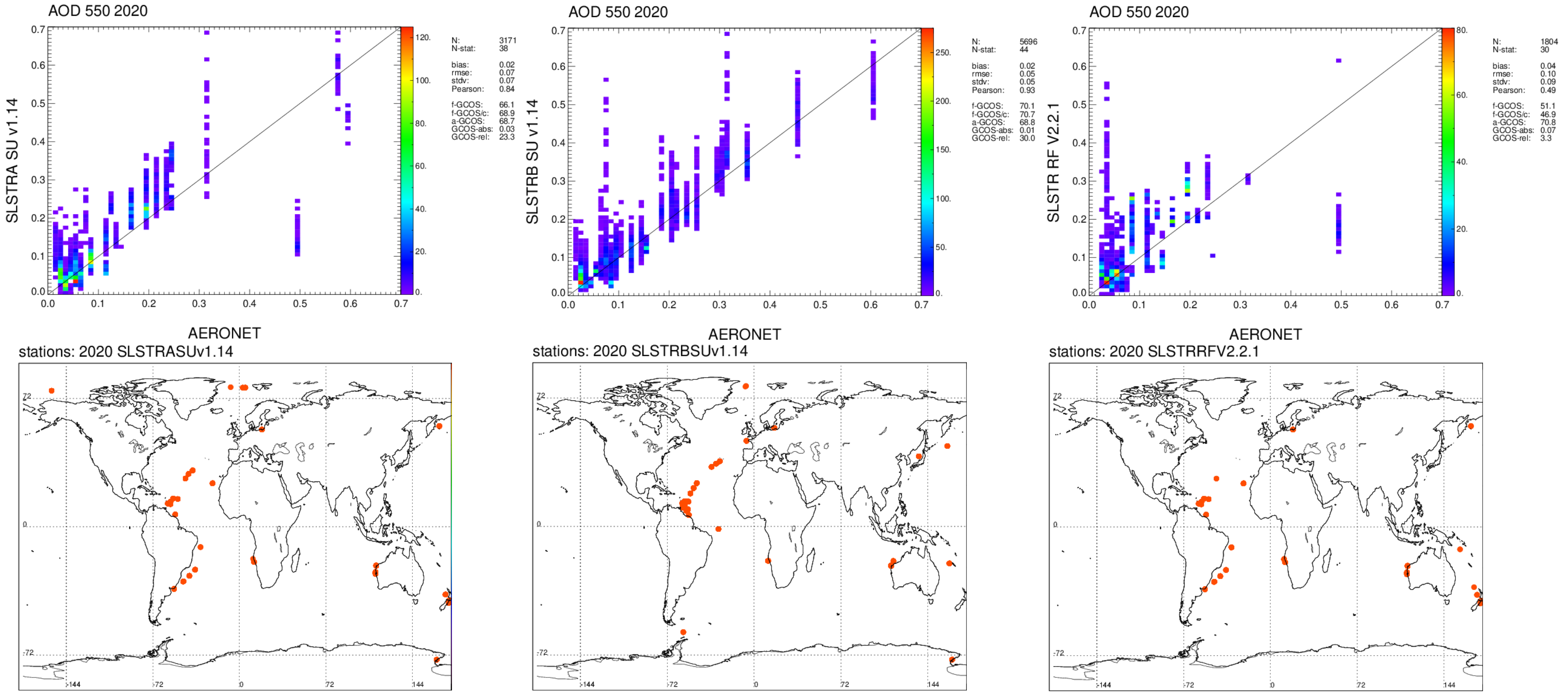

Figure 4.51 *Scatter plots and locations of AOD at 550nm against MAN measurements for SLSTR in 2020.*

4.3.2 Validation for selected clean background AERONET sites

For this analysis we used a climatological statistical analysis of Aeronet stations done by Stefan Kinne providing long term / multi-annual average distributions of AOD per station. We selected only those stations for which the 70% percentile of AOD remained below 0.1 to keep only stations with clean background aerosol content. In addition, we excluded all sites with altitude above 150m. This selection kept only 8 stations for which those criteria were valid throughout the year (not all of them operational for all years considered on our analysis). The analysis of the datasets for those stations is presented in Table 4.14 and Figure 4.52. It shows overall bias of 0.01 for SLSTR SU, -0.01 for SLSTR / RF and 0.05 for AATSR; for ATSR-2 the number of matching pairs is too small for a significant analysis. No averaging of satellite pixels was made, but all retrieval pixels within a matching range for a clean station measurement were considered individually.

Table 4.14 *Validation statistics for AOD against clean background Aeronet sites*

year	sensor	alg_version	area	Number of sat pixel	number1 of stat obs	bias	rmse	stdv	Pearson corr
2020	SLSTRA	SU_v1.14	clean	9831	177	0.01	0.04	0.03	0.77
2020	SLSTRB	SU_v1.14	clean	10816	196	0.01	0.04	0.04	0.76
2020	SLSTRA	RF_V2.2.1	clean	6695	179	-0.01	0.04	0.04	0.36
2008	AATSR	SU_v4.35	clean	3461	119	0.05	0.08	0.06	0.18

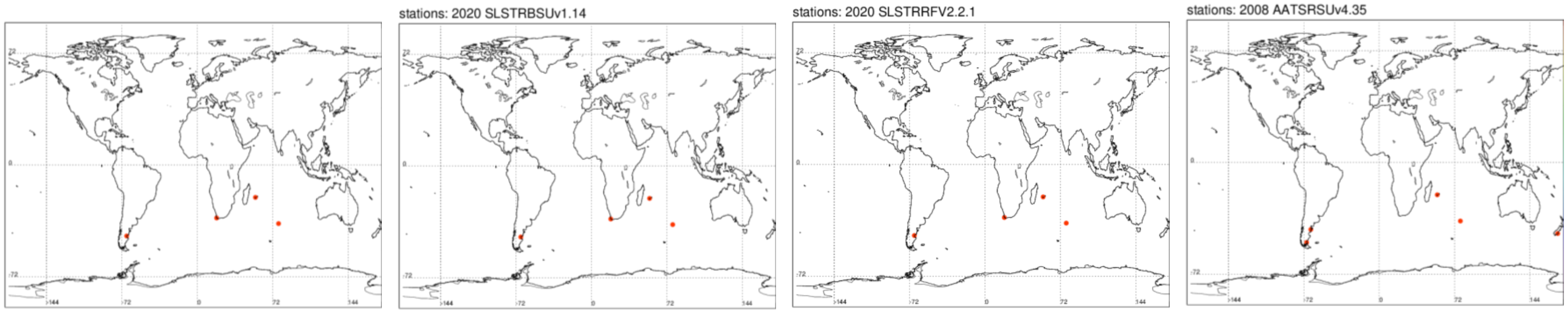

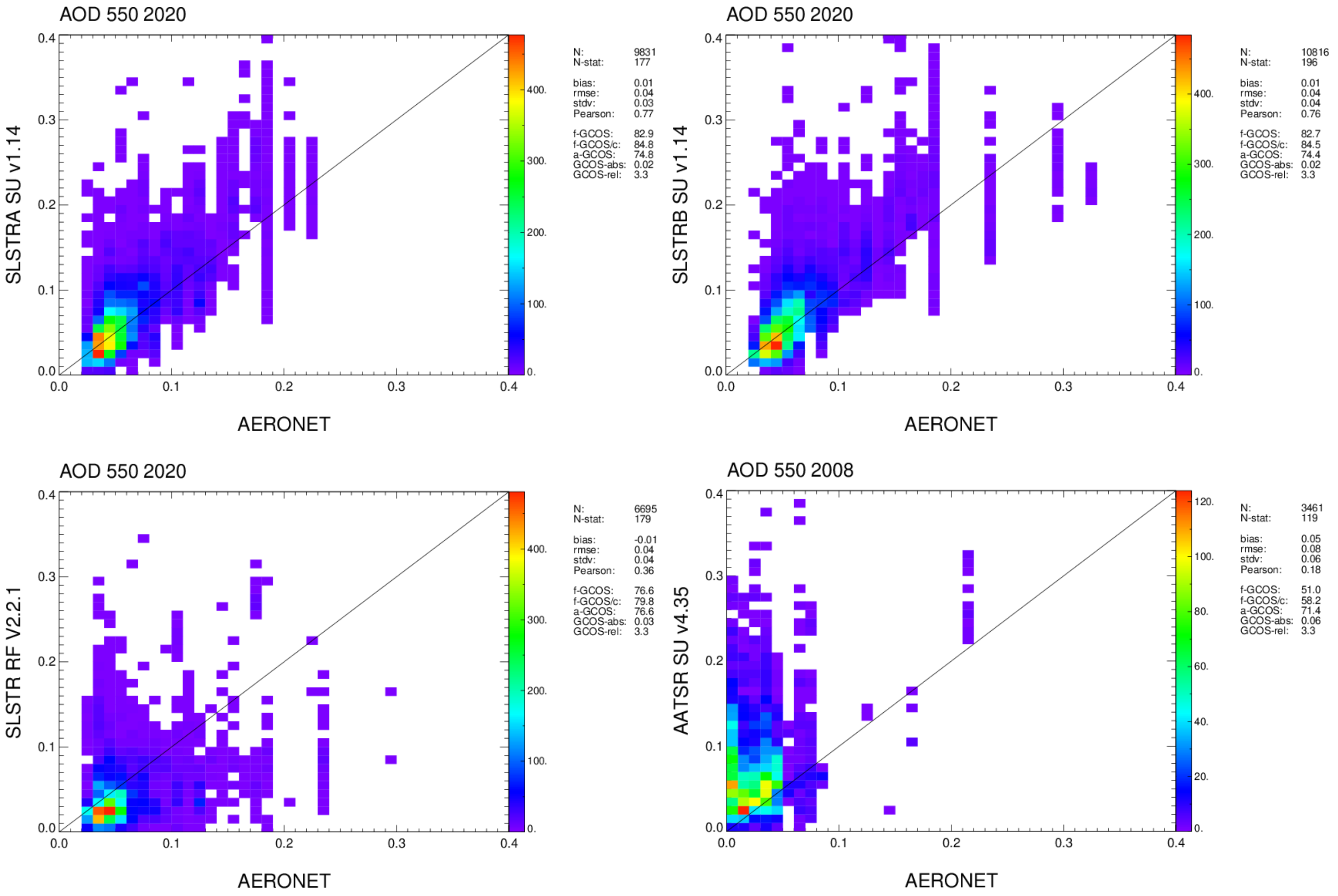

Figure 4.52 *Scatter plots and locations of AOD at 550nm over clean background Aeronet sites.*

8 EVALUATION OF LEVEL2 UNCERTAINTIES

5.1 Global validation of pixel-level uncertainties

Aerosol_cci products strive to contain prognostic pixel-level uncertainties calculated by error propagation (Popp, et al., 2016) according to the best practices developed during the first two phases of the CCI program (Merchant, et al., 2017). Therefore, the prognostic pixel-level uncertainties contained in the data files have been compared to estimated true errors (represented by the difference between satellite and AERONET AOD) to assess the quality of the uncertainties. Again this analysis is stratified per sensor / year and over land and ocean as well as for stations.

Pixel-level uncertainties must not be mixed up with errors, since the predicted uncertainties contained in the data files are "standard uncertainties" which means that they define the width of a Gaussian error distribution around the retrieval value, whereas an error is one random sample from such a distribution. Therefore, pixel-level uncertainties can only be compared to individual pixel errors by statistical means.

We use here the quantity "expected discrepancy" as defined by Sayer et al. 2020:

$$\varepsilon_T = \sqrt{[\varepsilon_{Sat}^2 + \varepsilon_{Aeronet}^2]}$$

ε_T allows to also consider other sources of errors in the validation, namely a small term due to the AERONET reference uncertainties (set to $\varepsilon_{Aeronet} = 0.01$) while we cannot quantify easily a third term due to sampling biases between the station point measurement and satellite pixel covered area; $\varepsilon_{Aeronet}$ matters only for small ε_{Sat}.

Furthermore, we also use the quantity "normalized error":

$$\Delta = (AOD_{Sat} - AOD_{Aeronet}) / \varepsilon_T.$$

If the uncertainty is a good representation of the expected discrepancy, Δ will be normally distributed so that a fraction $F_\Delta = 68.3\%$ of values should fall within the range [-1, +1], with zero mean $M_\Delta = 0.$ and unit standard deviation $S_\Delta = 1$. A non-zero mean ($M_\Delta \neq 0$) indicates the presence of residual systematic errors (an issue for algorithm development). A standard deviation less than one ($S_\Delta < 1.$) indicates uncertainties are overestimated ($f_\Delta > 68.3\%$), which could result from overestimation of individual sources of error, while a standard deviation greater than one ($S_\Delta > 1.$) indicates an underestimate ($f_\Delta < 68.3\%$), e.g. due to neglecting an important source of error .

Finally, we conduct a mean-bias correction for the error distributions in some of the subsequent analysis, since the concept of standard uncertainties requires bias-free error distributions (which can be interpreted as absence of remaining systematic and quantifiable biases).

5.1.1 CRDP-1 SU v1 validation results

In the following figures we show first (fig. 5.1 and fig. 5.2) the comparison of histograms of the estimated errors (red) and prognostic uncertainties (blue filled bars) to qualitatively illustrate per sensor / year and over land / ocean the distributions of prognostic uncertainties. It is obvious that while the error distributions are Gauss-like with partly some asymmetry and positive shift for SLSTR while all uncertainty distributions show a double peak, which is hardly visible over ocean, but very strong over land, in particular for both SLSTR instruments. The mean of uncertainties is larger over land than over ocean for all sensors and is significantly larger over land for SLSTR (0.15) than for the ATSR instruments (~0.09), while it is similar for all sensors over ocean (0.05 – 0.06); similarly the stdv of uncertainties is larger over land and for both SLSTR.

For a quantitative validation, we developed a new approach shown in fig. 5.3 and fig. 5.4, where we calculate a synthetic cumulative distribution of errors from prognostic uncertainties by adding up one Gaussian error distribution (normalized to a total integral of 1.) for each individual pixel-level uncertainty according to the definition of standard uncertainties. We compare then this synthetic error frequency distribution with the measured error distribution. Furthermore, we subtract the mean bias from the error distribution to make it more symmetric for direct comparison to the synthetic distribution (which by its definition is always symmetric). Finally, we calculate an average correction factor for the synthetic distribution (and thus the prognostic uncertainties) in relation to the mean-bias corrected error distributions as ratio of the standard deviations of both distributions. Those histograms and their width compared to the bias-corrected measured error histograms show that uncertainties are generally performing not too bad and in most cases are slightly too small with typical overall correction factors of ~1.15 for the ATSR instruments (1.28 for AATSR over ocean). For the SLSTR instruments over ocean a larger correction factor is needed (~1.4), while over land uncertainties need a slight decrease (correction factor of ~0.9). It should be noted that with a simple correction factor the bias-corrected measured error distribution and the synthetic error distribution calculated from the corrected uncertainties match reasonably well as shown in Fig. 5.3 and fig. 5.4, but do not match perfectly – this points to remaining unresolved issues for some of the pixels / retrieval conditions. It is also important to understand that this assessment of all uncertainties per senor in a bulk provides an average understanding and is dominated by the most numerous uncertainties as shown in fig. 5.1 and 5.2 (the smaller ones in general and to some extent the larger ones from the second peaks for SLSTR over land).

Following Sayer, et al., 2020 we analyse the potential of the prognostic uncertainties to discriminate between (“good” / “bad”) pixels with likely small / large errors in Fig. 5.5 and Fig. 5.6. We do this by plotting as function of binned uncertainties the absolute error below which are 38%, 68% and 95% of all pixels with this uncertainty. These percentages relate to 0.5 σ, 1 σ, and 2 σ (σ = standard width) for normal error distributions in each bin (along the vertical axis) – those theoretically expected values are shown as dashed lines in black, red and blue. In contrast to the average view of Fig. 5.3 and 5.4 the percentile plots allow a view as function of the amount of uncertainties.

The percentile plots show a reasonable agreement (within statistical noise) with the theoretical lines for the lower range of uncertainties (up to ~0.1 for all sensors or even 0.17 for ATSR-2 over land) while for higher uncertainties the error values are clearly below the expected lines, which means that errors are too small / uncertainties are too large. In summary, the uncertainties allow a reasonable split between "good" and "bad" pixels for the lower range with dominating numbers, but not any longer for the higher values. To indicate the statistical significance and to make the link to the average analysis of Fig. 5.3 and Fig. 5.4, the percentile plots also show the frequency distribution of uncertainties (dashed lines). It is obvious that (in particular for the ATSR instruments) the range of larger uncertainties has only few values and is therefore statistically weaker and contributes little to the average analysis, while for the SLSTR instruments there is a smaller but relevant contribution of larger uncertainties. Finally, it can be observed that the smallest uncertainties in the lowest bin have typically too large errors /are too small (in particular for SLSTR instruments).

Finally, we analyse the statistical distributions of Δ per sensor (fraction F_Δ of values within the range [-1, +1], mean M_Δ, standard deviation S_Δ) in Fig. 5.7 (station map of S_Δ values), Tab. 5.1 (summary statistics per sensor) and Fig. 5.8 (M_Δ and S_Δ per sensor). Maps per sensor of the stdv of distributions of normalized errors Δ in Fig. 5.7 show that at most stations average Δ values are larger than 1. but there is a wide spread of average Δ values. Tab. 5.1 lists and Fig. 5.8 shows the average values per sensor of mean M_Δ, standard deviation S_Δ (and fraction F_Δ). While mean M_Δ is close to 0. for all sensors, mean S_Δ is significantly larger than 1. for all sensors (in particular for SLSTR where $S_\Delta > 2.$) and all F_Δ are slightly below the Gaussian 68% (and even down to 50% for SLSTR over ocean). This means that on average uncertainties (dominating the statistics) are too small and need correction factors larger than 1. (as calculated from the histograms in Fig. 5.3 and 5.4); the need for correction is more significant for SLSTR (also consistent with Fig. 5.4 over ocean, but not over land).

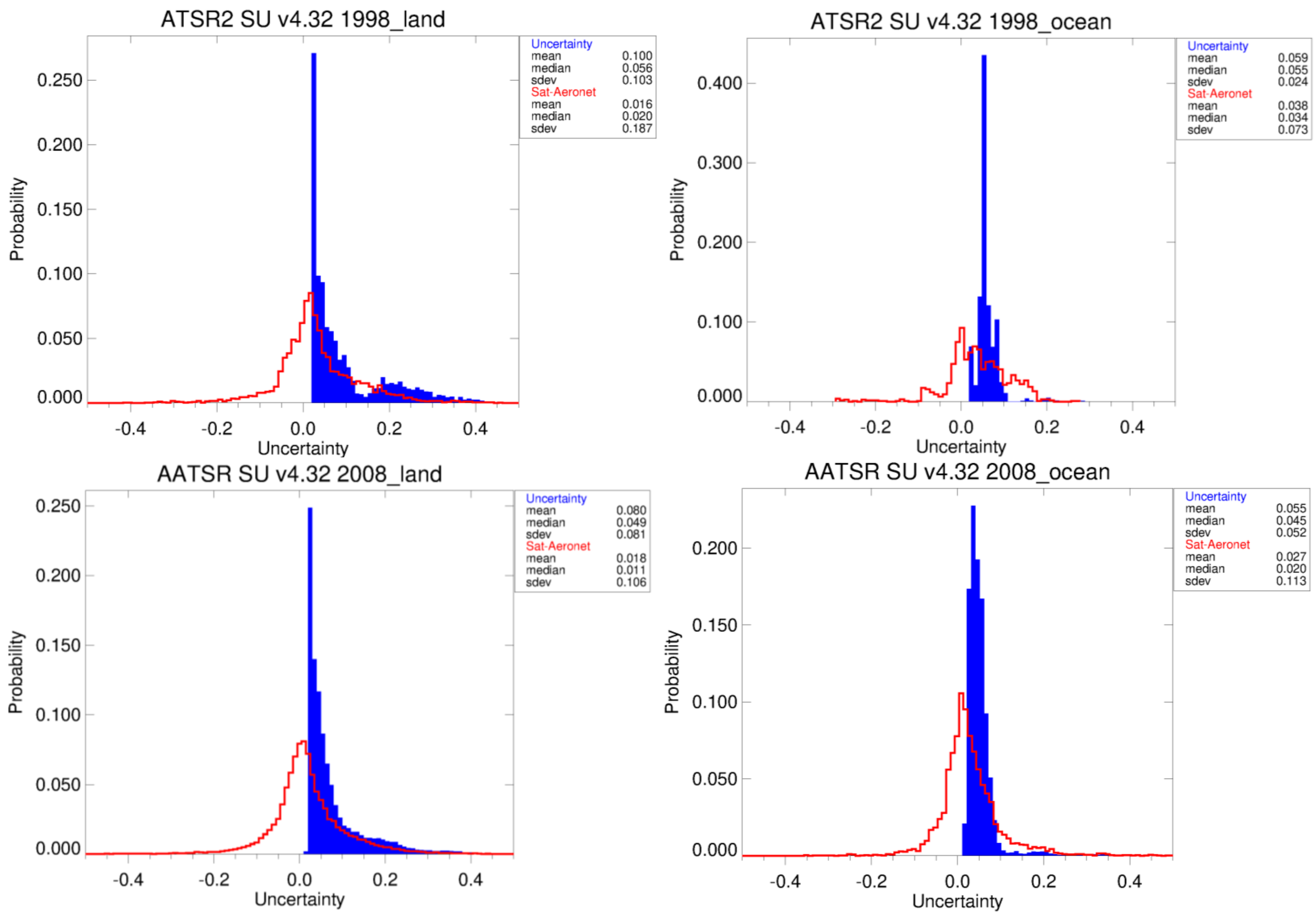

***Figure 5.1** Histograms of errors and uncertainties for ATSR-2 (top) and AATSR (bottom) over land (left) and ocean (right).*

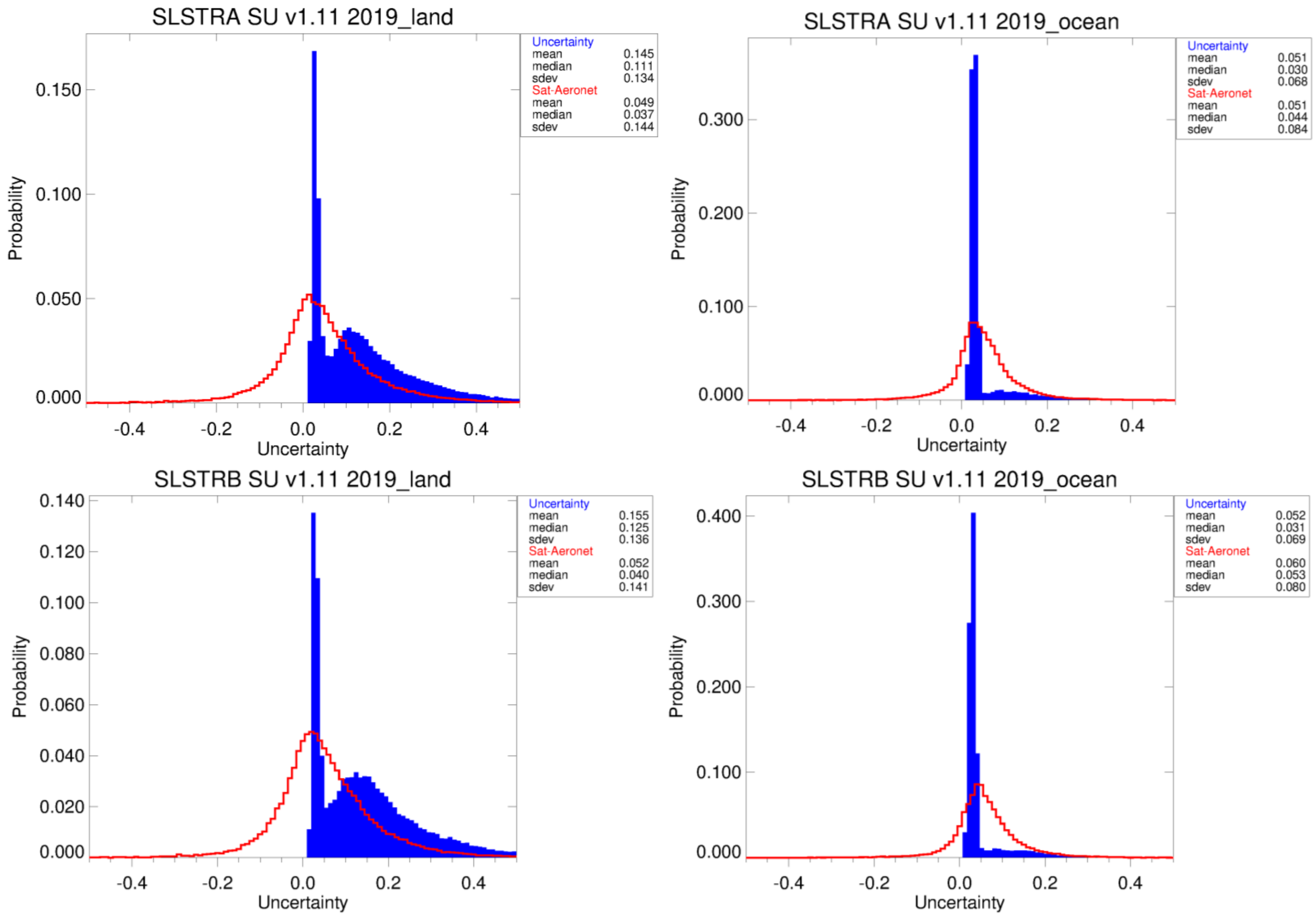

***Figure 5.2** Histograms of errors and uncertainties for SLSTR/3A (top) and SLSTR/3B (bottom) over land (left) and ocean (right).*

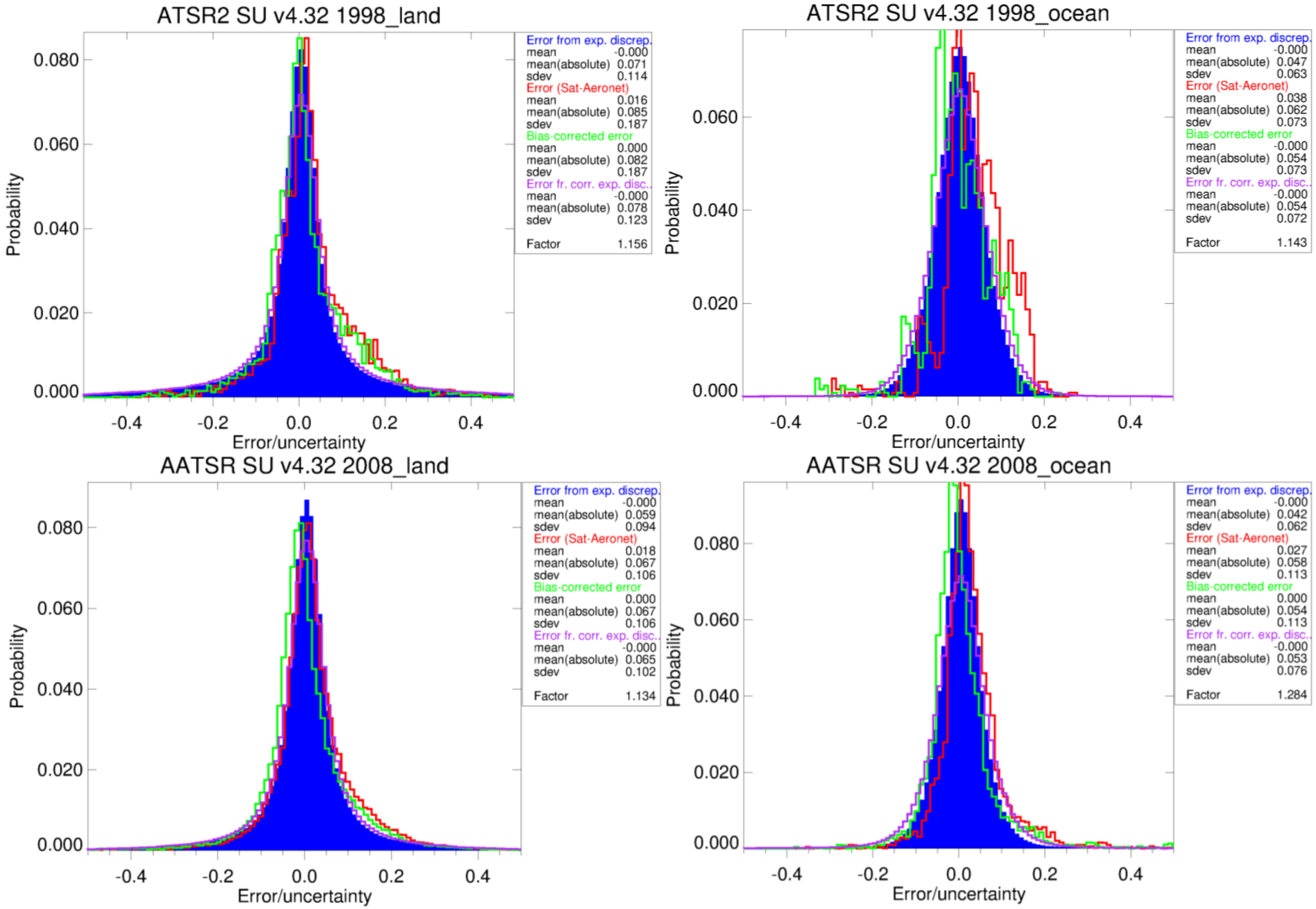

***Figure 5.3** Histograms of estimated errors (red; with bias correction: green) and errors calculated from uncertainties (blue; scaled to best fit the mean-bias corrected error distribution) for ATSR-2 (top) and AATSR (bottom) over land (left) and ocean (right).*

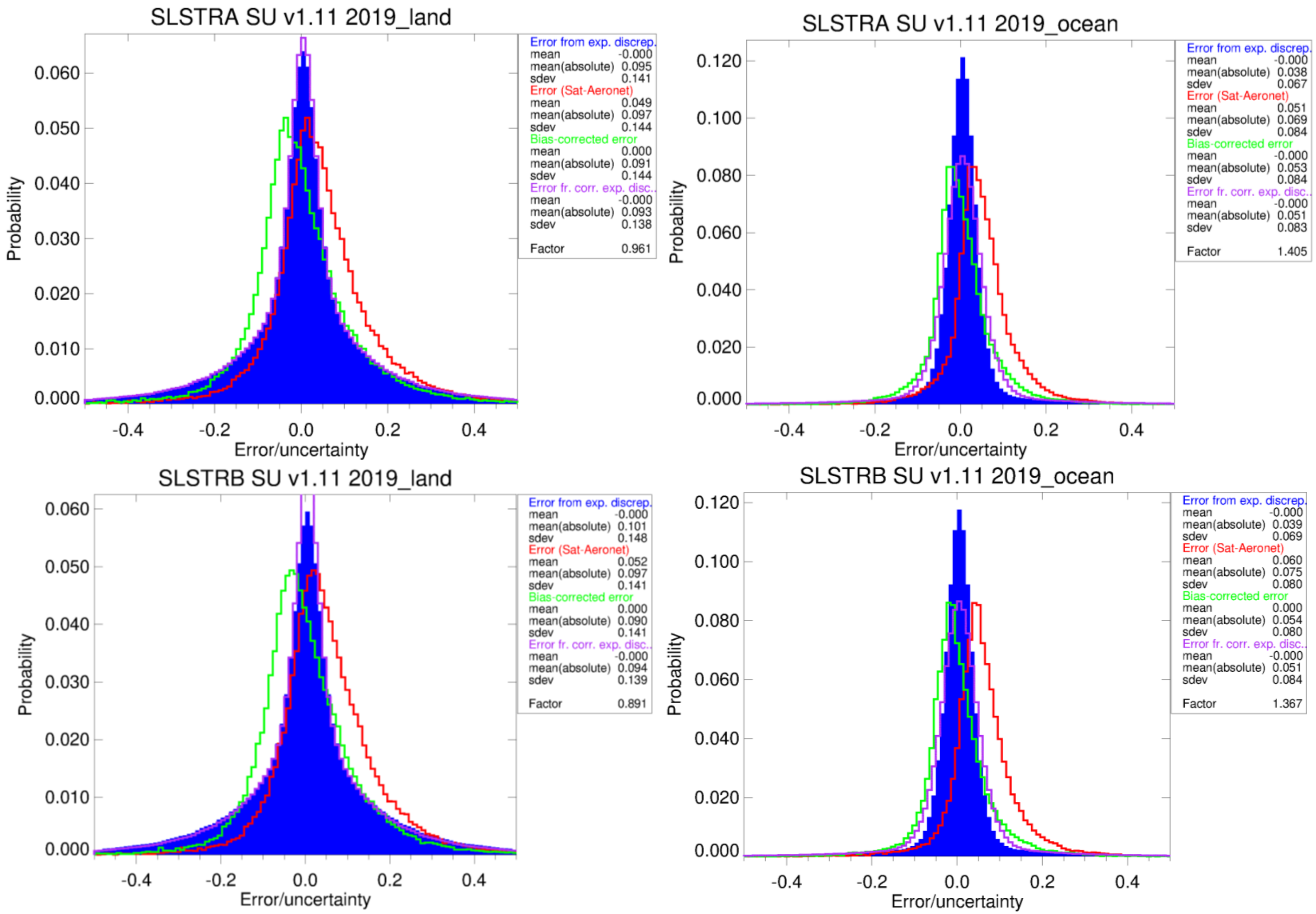

Figure 5.4 *Histograms of estimated errors (red; with bias correction: green) and errors calculated from uncertainties (blue; scaled to best fit the mean-bias corrected error distribution) for SLSTR/3A (top) and SLSTR/3B (bottom) over land (left) and ocean (right).*

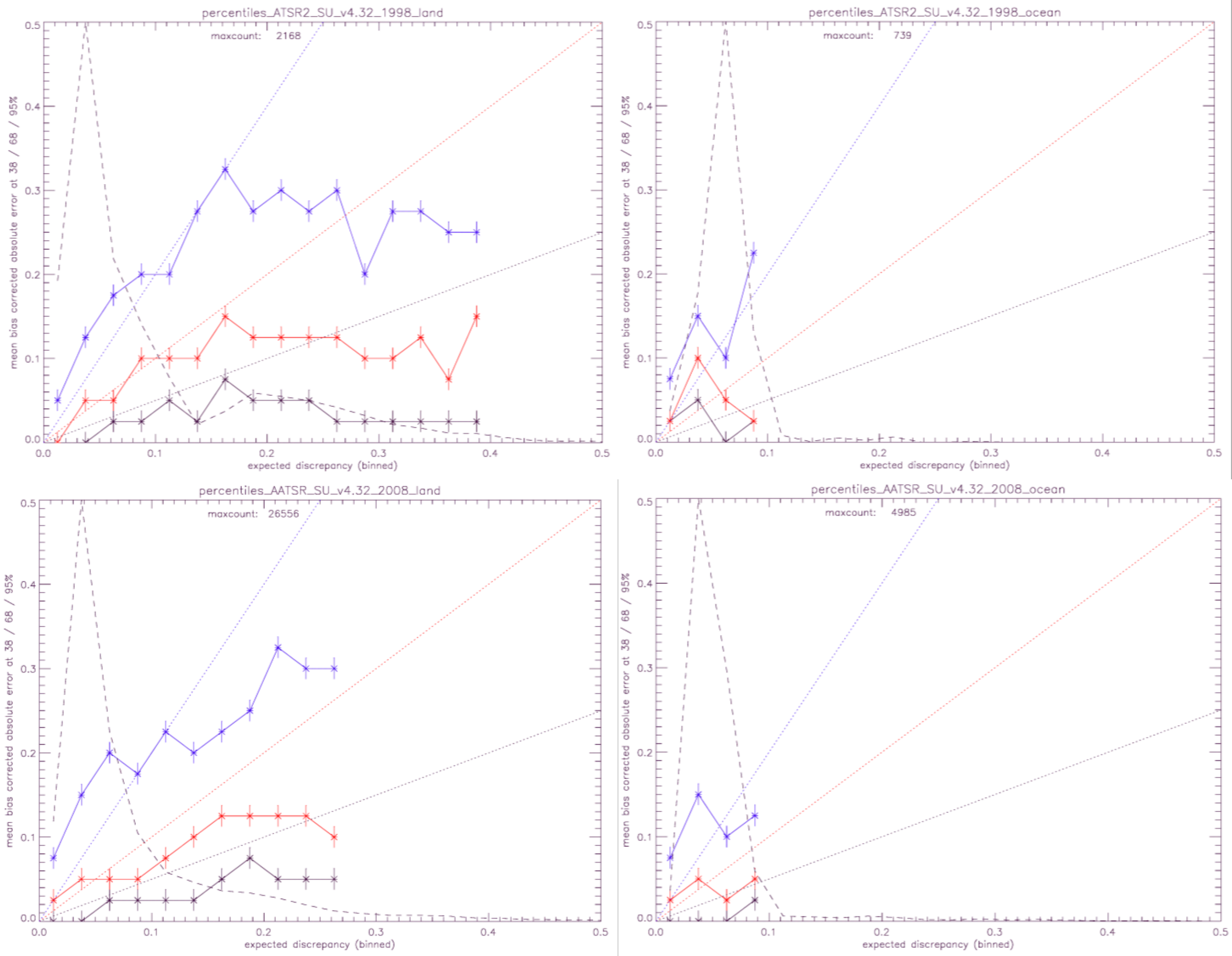

Figure 5.5 *Percentile plots of absolute errors at 38% (black), 68% (red) and 95% (blue) as function of binned expected discrepancy for ATSR-2 (top) and AATSR (bottom) over land (left) and ocean (right); dashed lines show the expected theoretical dependence.*

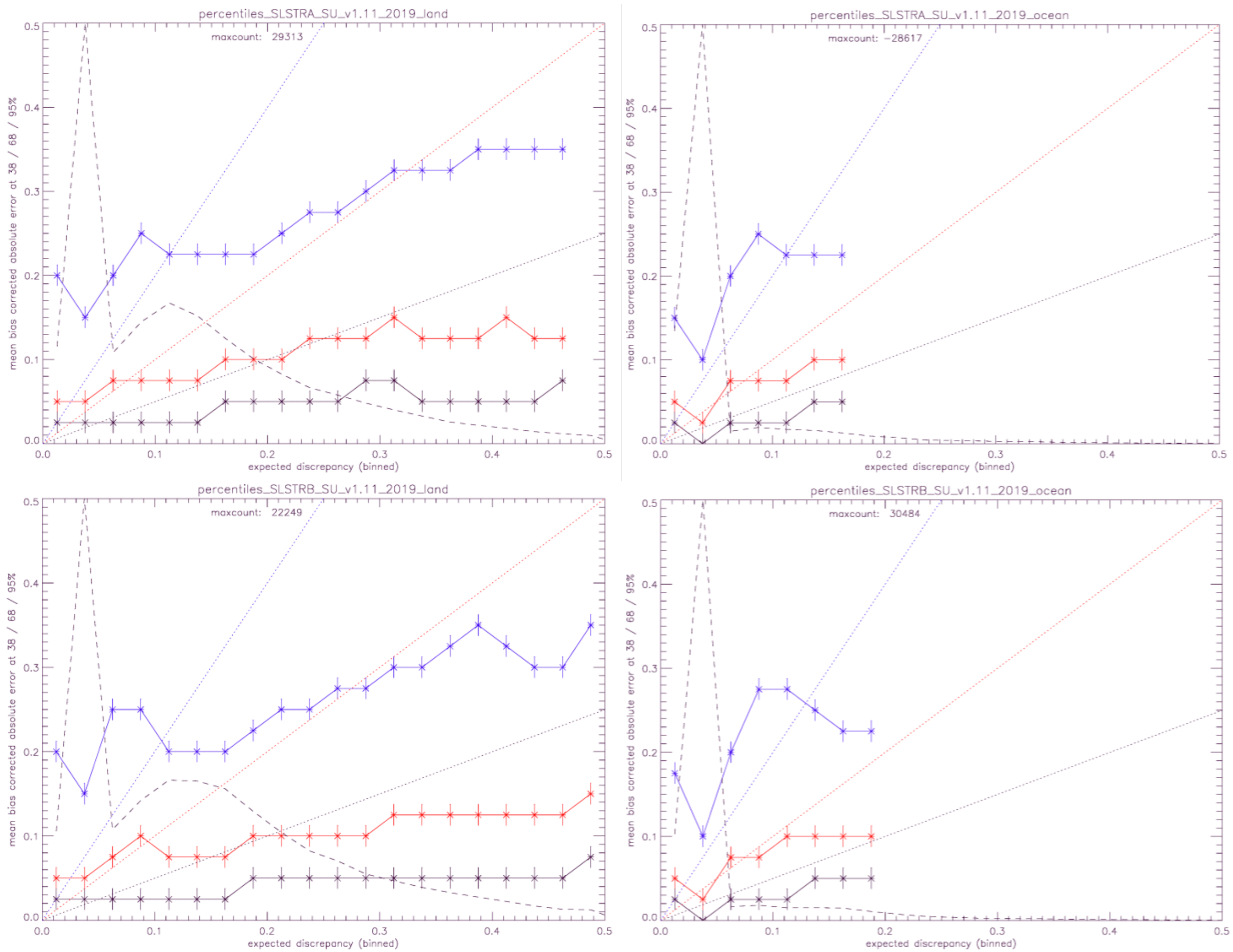

Figure 5.6 *Percentile plots of absolute errors at 38% (black), 68% (red) and 95% (blue) as function of binned expected discrepancy for SLSTR/3A (top) and SLSTR/3B (bottom) over land (left) and ocean (right); dashed lines show the expected theoretical dependence.*

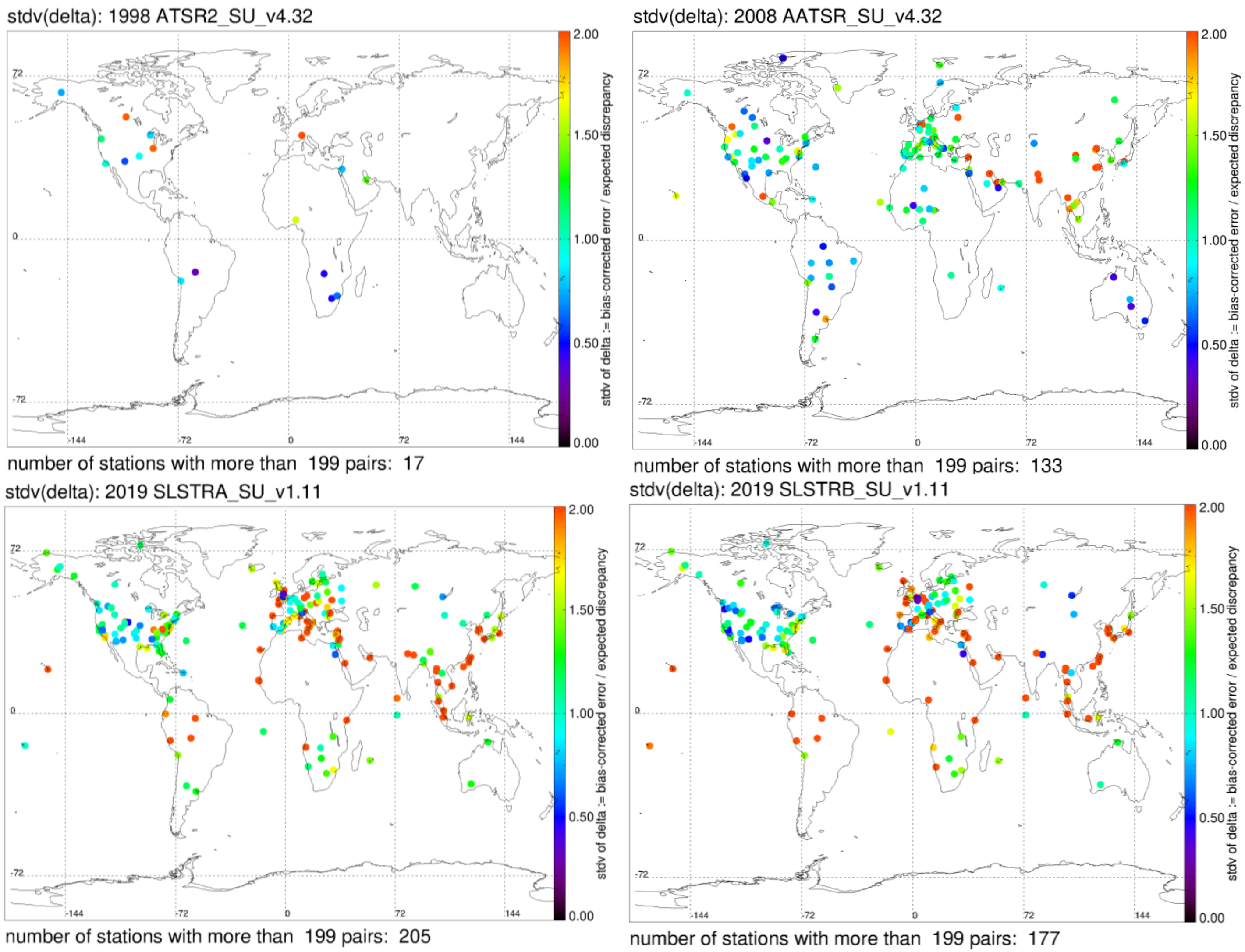

Figure 5.7 *Station maps of significant stdv of normalized errors Δ for the 4 sensors.*

Table 5.1 Statistical summary of validating SU v1 distributions of the normalized errors Δ for the 4 sensors

year	sensor	alg_version	area	mean-delta	stdv-delta	fraction-delta [%]
CRDP-1 SU v1 datasets						
Theoretical expectation				0.	1.	68.3
1998	ATSR2	SU_v4.32	land	0.02	2.57	64.8
1998	ATSR2	SU_v4.32	ocean	-0.03	1.49	62.9
2008	AATSR	SU_v4.32	land	-0.24	1.84	62.4
2008	AATSR	SU_v4.32	ocean	0.02	1.81	63.8
2019	SLSTRA	SU_v1.11	land	-0.04	2.45	65.6
2019	SLSTRA	SU_v1.11	ocean	0.06	2.41	49.8
2019	SLSTRB	SU_v1.11	land	0.03	2.48	68.4
2019	SLSTRB	SU_v1.11	ocean	0.12	2.44	51.0

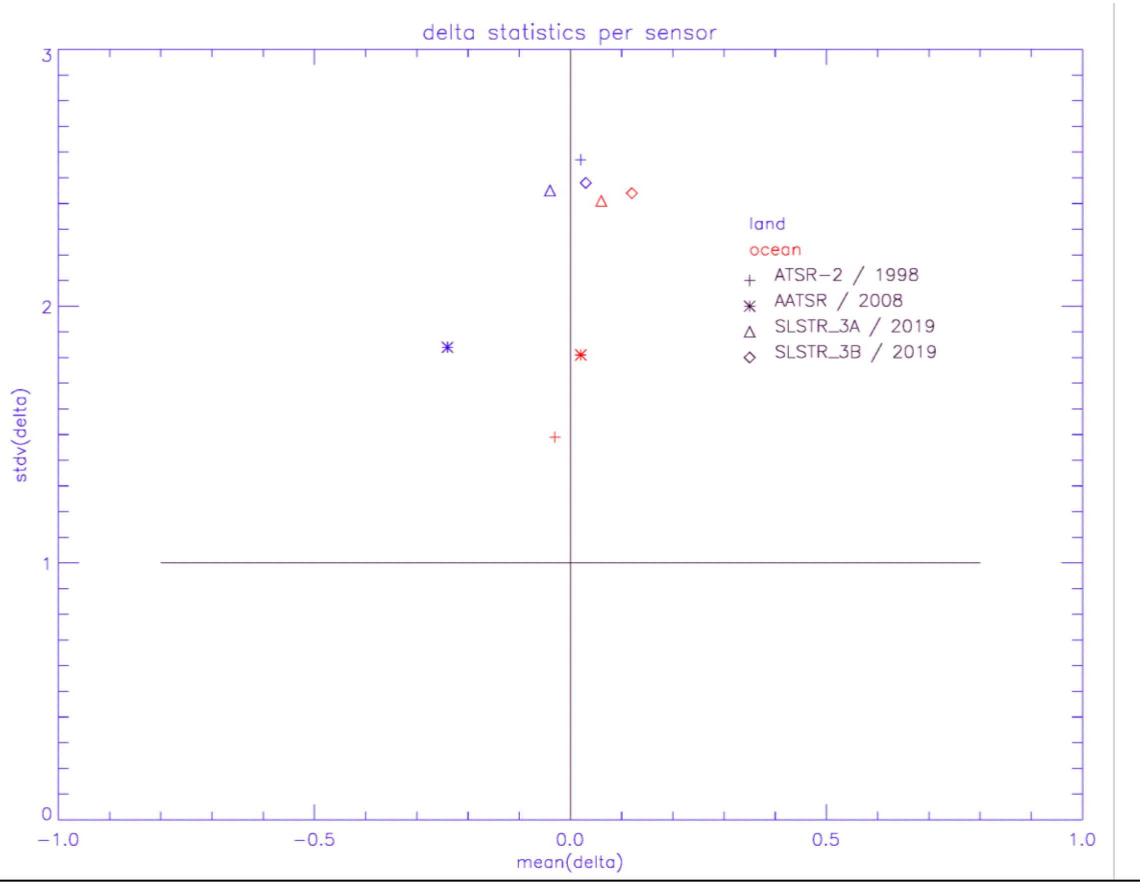

Figure 5.8 *Statistics of Δ (mean, stdv) per sensor over land and ocean.*

5.1.2 CRDP-2 SU v2 validation results

Table 5.2 and Figures 5.9 – 5.16 show the assessment of pixel-level uncertainties of the new SU v2 datasets with the same methods as for the SU v1 datasets (presented in Tab. 5.1 and Fig. 5.1 – 5.8). There is only minor change of the characteristics of the uncertainties between SU v1 and v2 datasets; for v2 the second peak of uncertainties is slightly reduced.

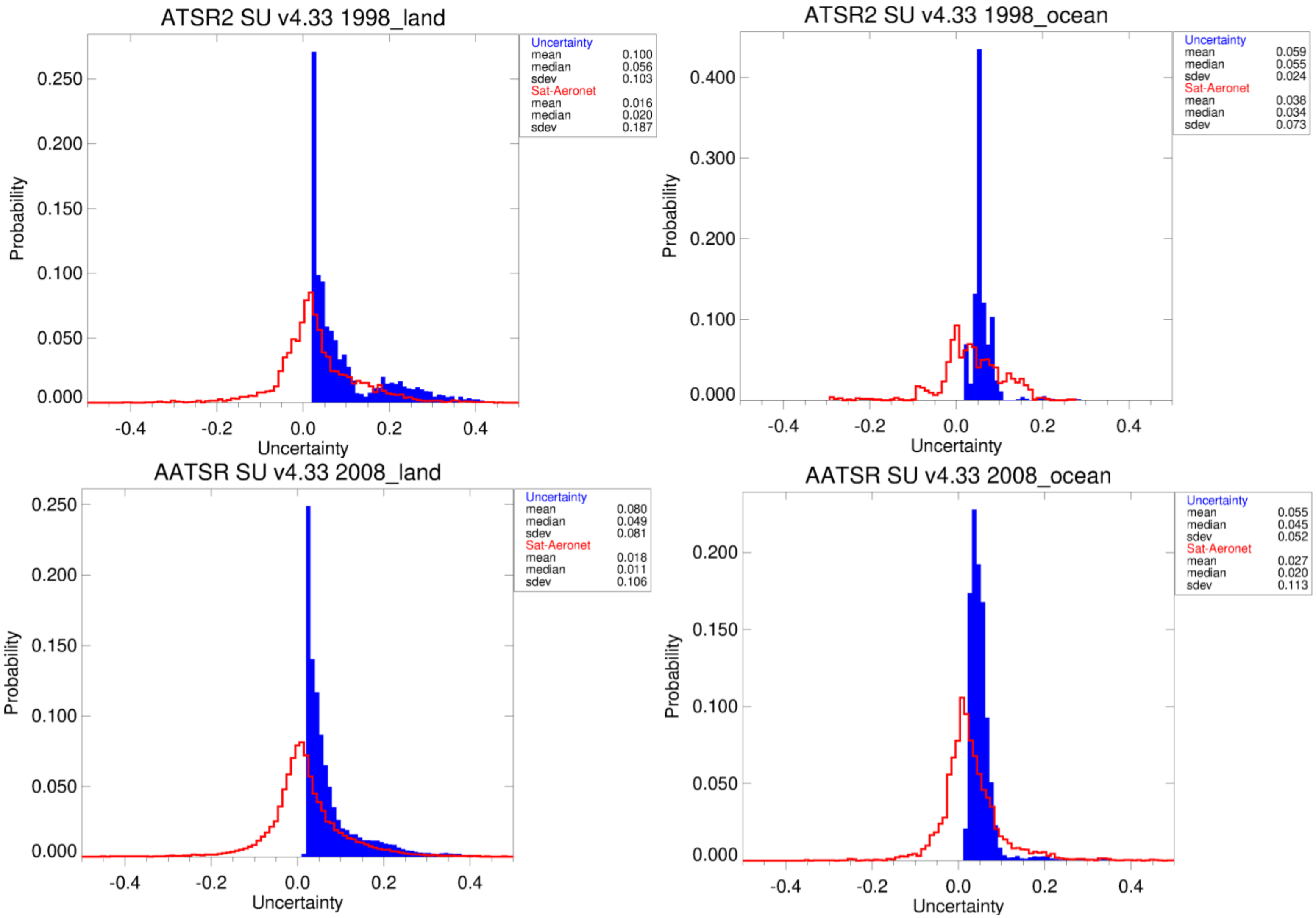

***Figure 5.9** Histograms of errors and uncertainties for ATSR-2 (top) and AATSR (bottom) over land (left) and ocean (right).*

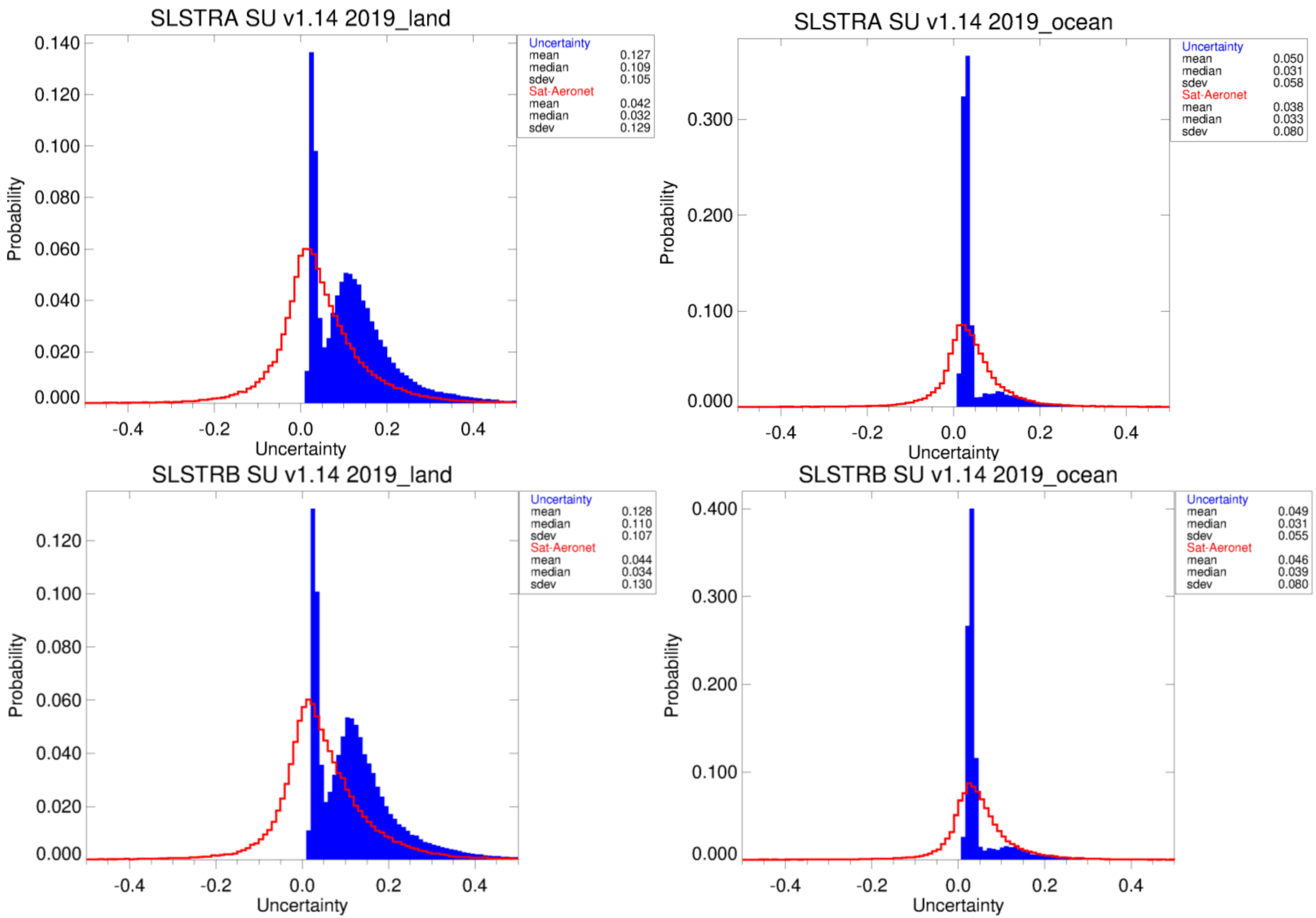

***Figure 5.10** Histograms of errors and uncertainties for SLSTR/3A (top) and SLSTR/3B (bottom) over land (left) and ocean (right).*

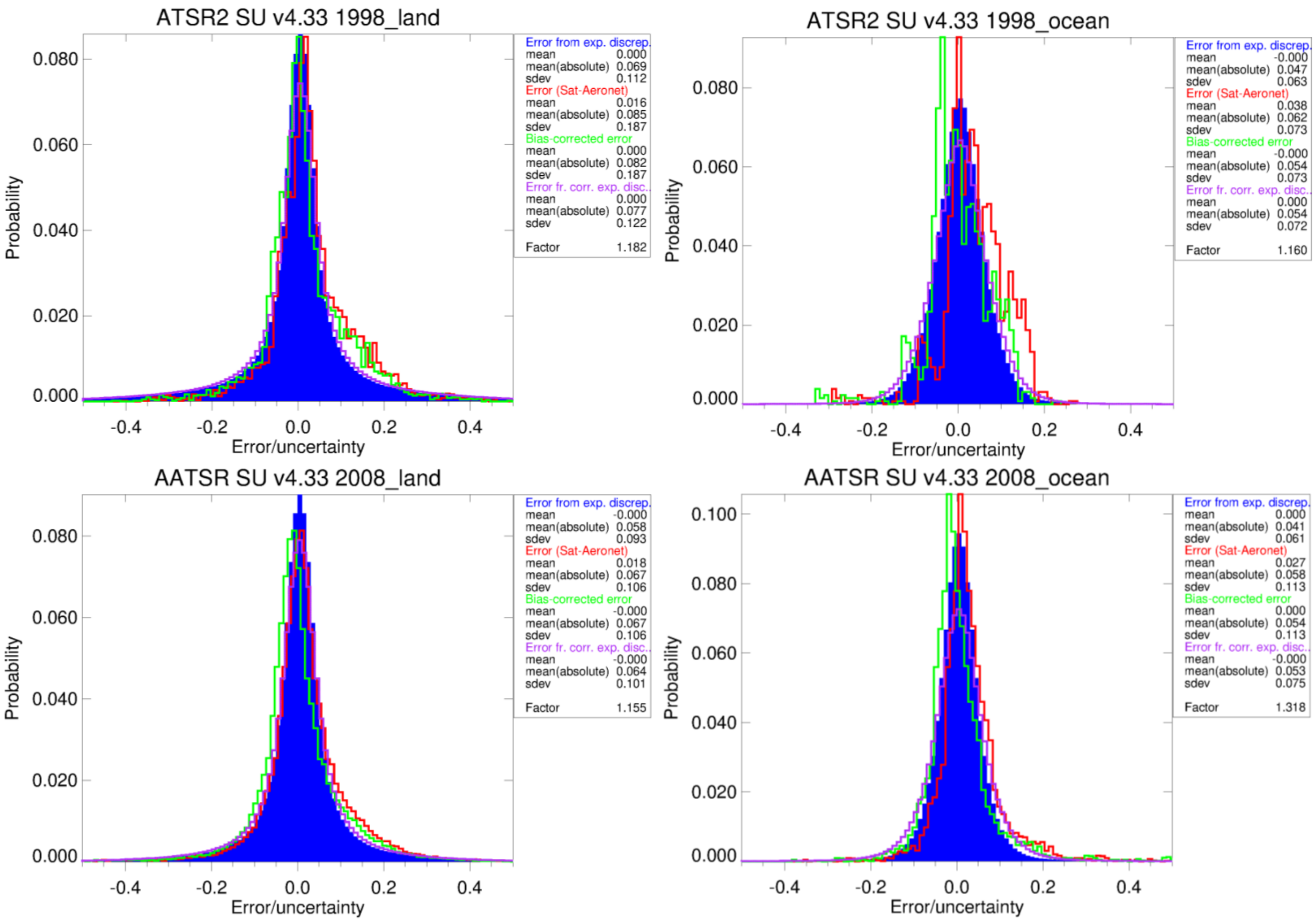

Figure 5.11 *Histograms of estimated errors (red; with bias correction: green) and errors calculated from uncertainties (blue; scaled to best fit the mean-bias corrected error distribution) for ATSR-2 (top) and AATSR (bottom) over land (left) and ocean (right).*

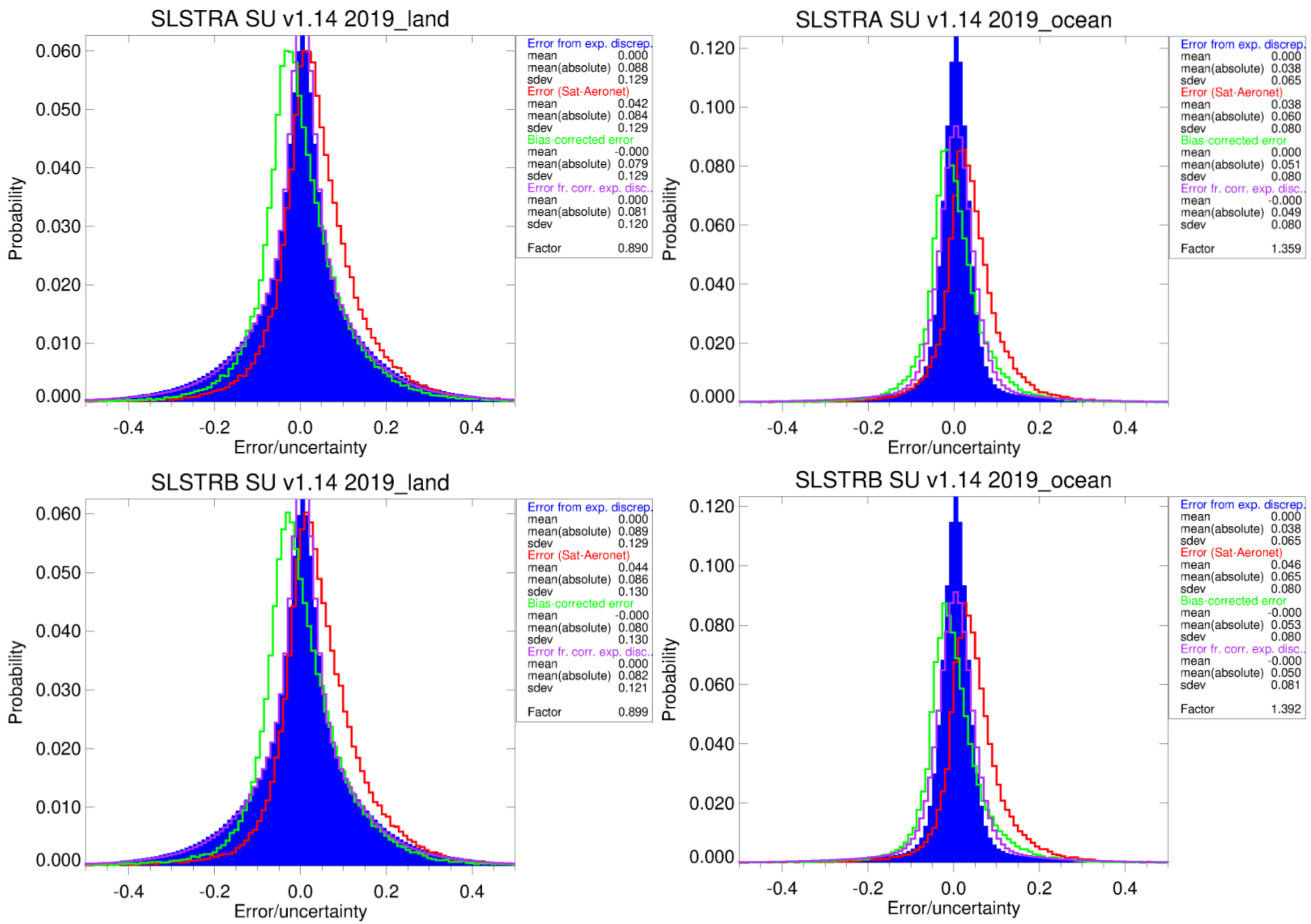

***Figure 5.12** Histograms of estimated errors (red; with bias correction: green) and errors calculated from uncertainties (blue; scaled to best fit the mean-bias corrected error distribution) for SLSTR/3A (top) and SLSTR/3B (bottom) over land (left) and ocean (right).*

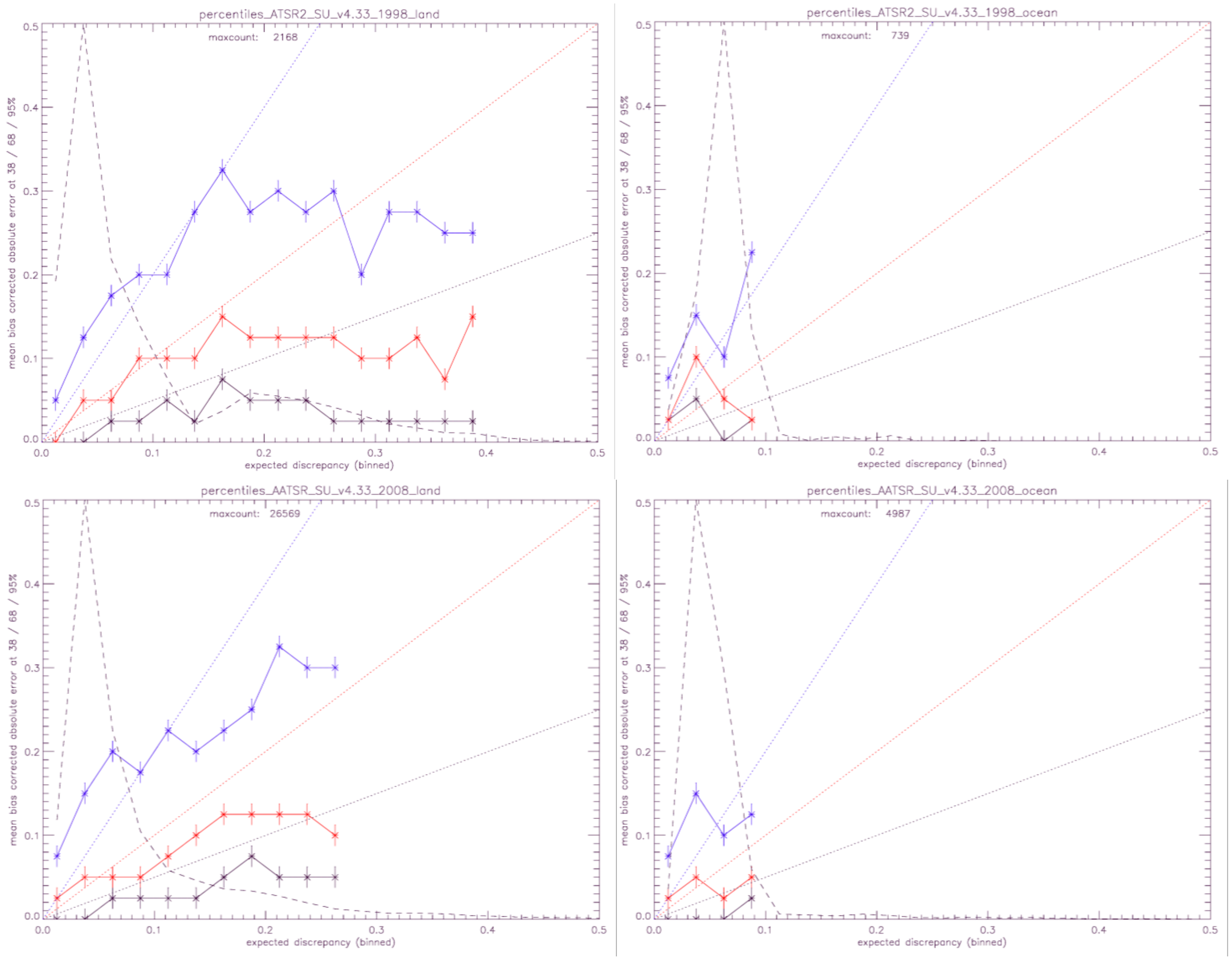

Figure 5.13 *Percentile plots of absolute errors at 38% (black), 68% (red) and 95% (blue) as function of binned expected discrepancy for ATSR-2 (top) and AATSR (bottom) over land (left) and ocean (right); dashed lines show the expected theoretical dependence.*

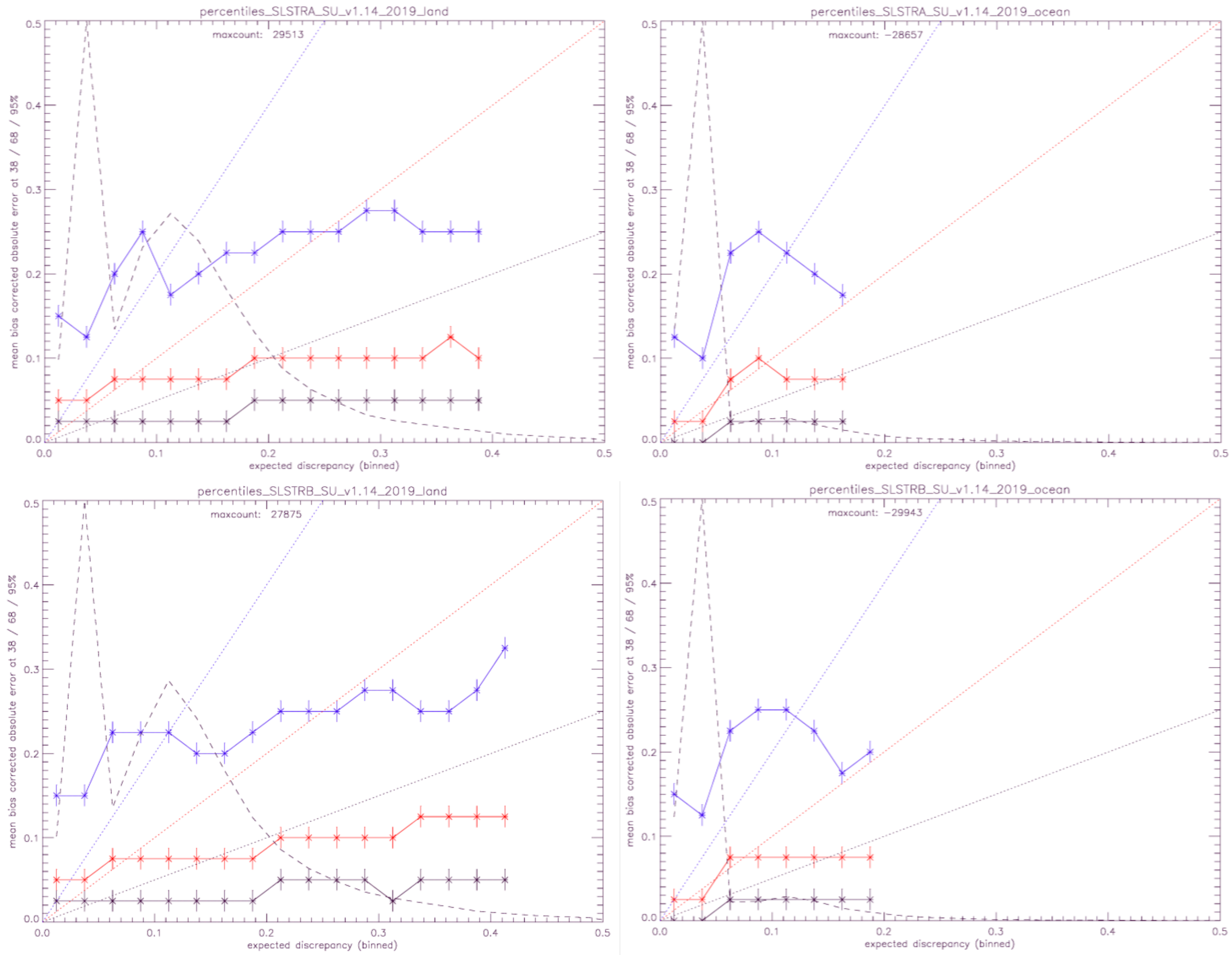

***Figure 5.14** Percentile plots of absolute errors at 38% (black), 68% (red) and 95% (blue) as function of binned expected discrepancy for SLSTR/3A (top) and SLSTR/3B (bottom) over land (left) and ocean (right); dashed lines show the expected theoretical dependence.*

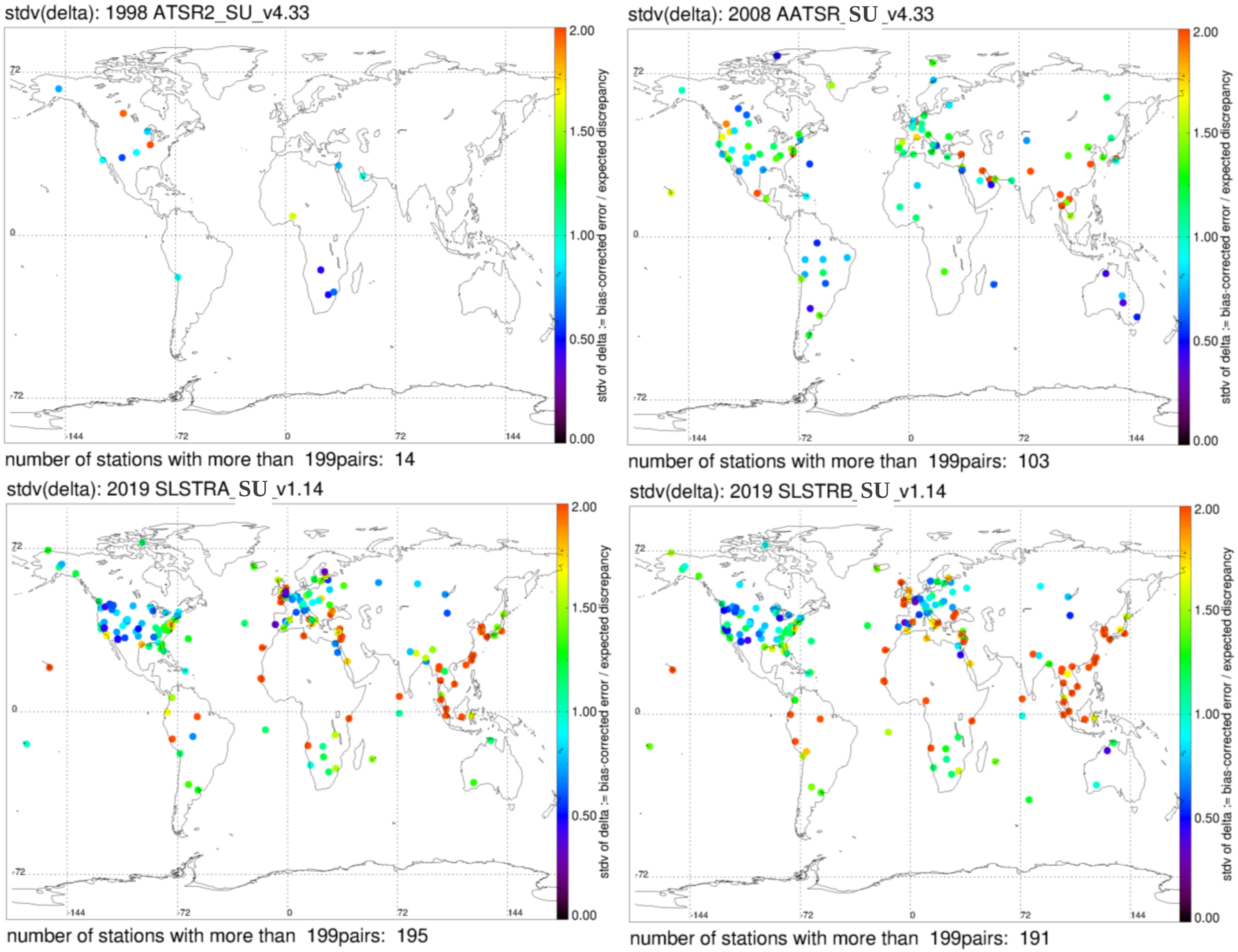

Figure 5.15 *Station maps of significant stdv of normalized errors Δ for the 4 sensors.*

Table 5.2 Statistical summary of validating SU v2 distributions of the normalized errors Δ for the 4 sensors

year	sensor	alg_version	area	mean-delta	stdv-delta	fraction-delta [%]
CRDP-2 SU v2 datasets						
Theoretical expectation				0.	1.	68.3
1998	ATSR2	SU_v4.33	land	0.02	2.57	64.8
1998	ATSR2	SU_v4.33	ocean	-0.03	1.49	62.9
2008	AATSR	SU_v4.33	land	-0.24	1.84	62.4
2008	AATSR	SU_v4.33	ocean	0.02	1.81	63.7
2019	SLSTRA	SU_v1.14	land	0.03	2.25	70.2
2019	SLSTRA	SU_v1.14	ocean	0.08	2.31	52.1
2019	SLSTRB	SU_v1.14	land	0.01	2.38	70.1
2019	SLSTRB	SU_v1.14	ocean	0.11	2.42	51.7

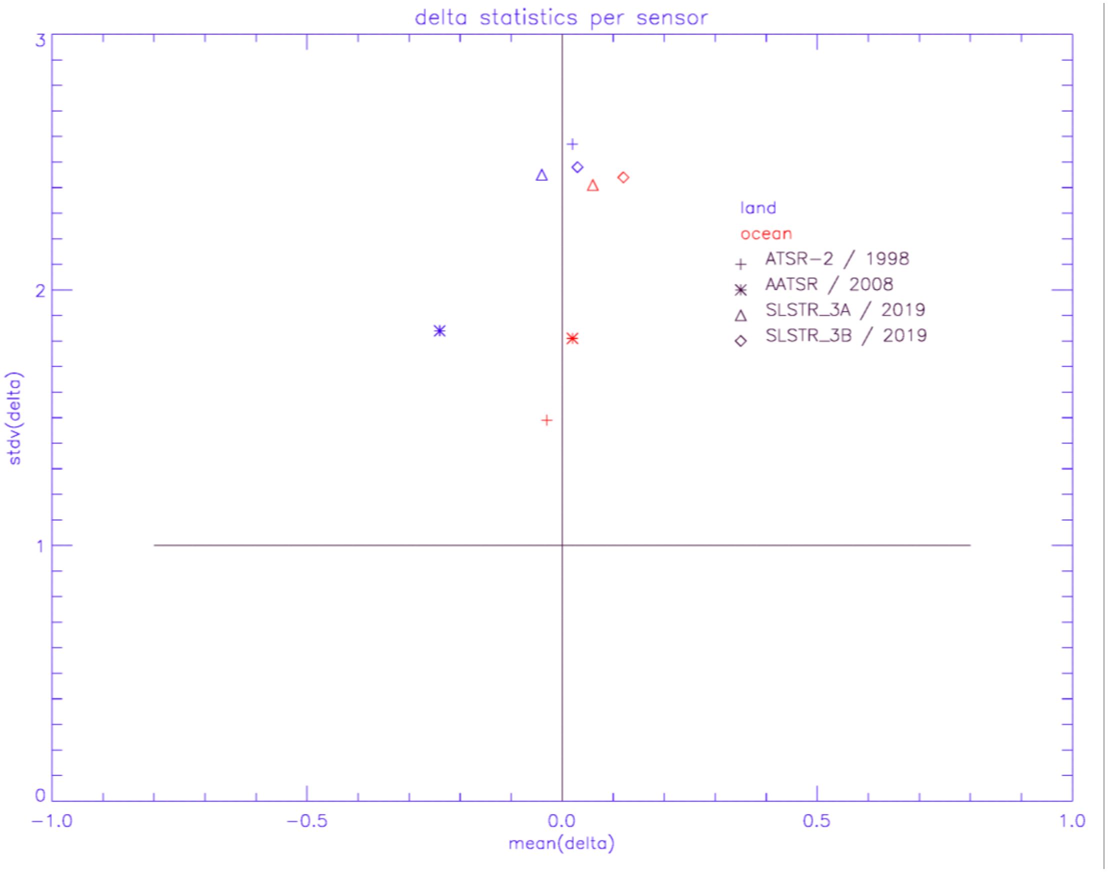

Figure 5.16 *Statistics of Δ (mean, stdv) per sensor over land and ocean.*

5.1.3 CRDP-3 SU v3 validation results

Table 5.3 and Figures 5.17 – 5.20 show the assessment of pixel-level uncertainties of the new SU v3 datasets with the same methods as for the SU v1 datasets (presented in Tab. 5.1 and Fig. 5.1 – 5.8). There is only minor change of the characteristics of the uncertainties between SU v1 and v3 datasets; for v3 uncertainties for the ATSR instruments are slightly reduced.

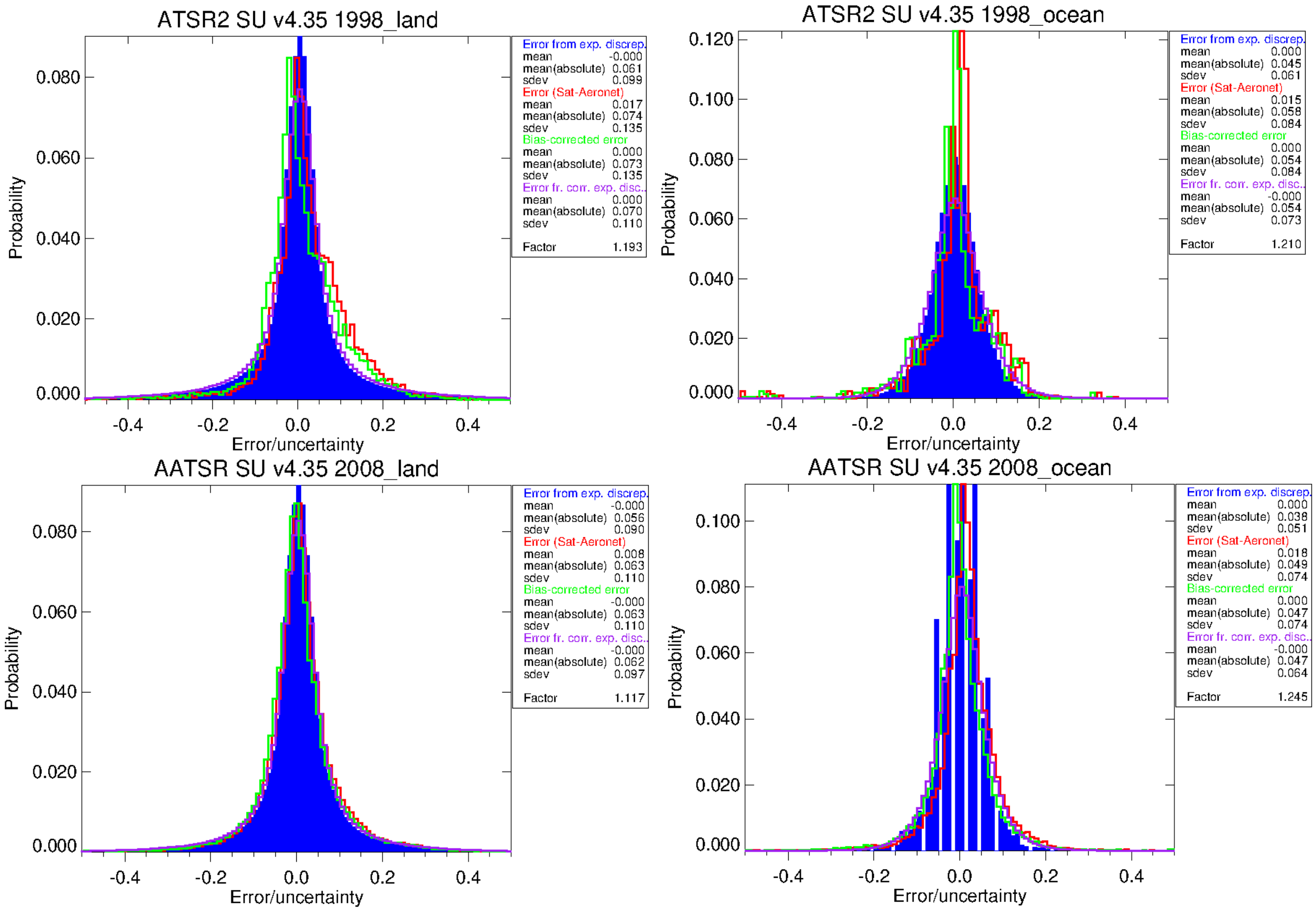

Figure 5.17 *Histograms of estimated errors (red; with bias correction: green) and errors calculated from uncertainties (blue; scaled to best fit the mean-bias corrected error distribution) for ATSR-2 (top) and AATSR (bottom) over land (left) and ocean (right).*

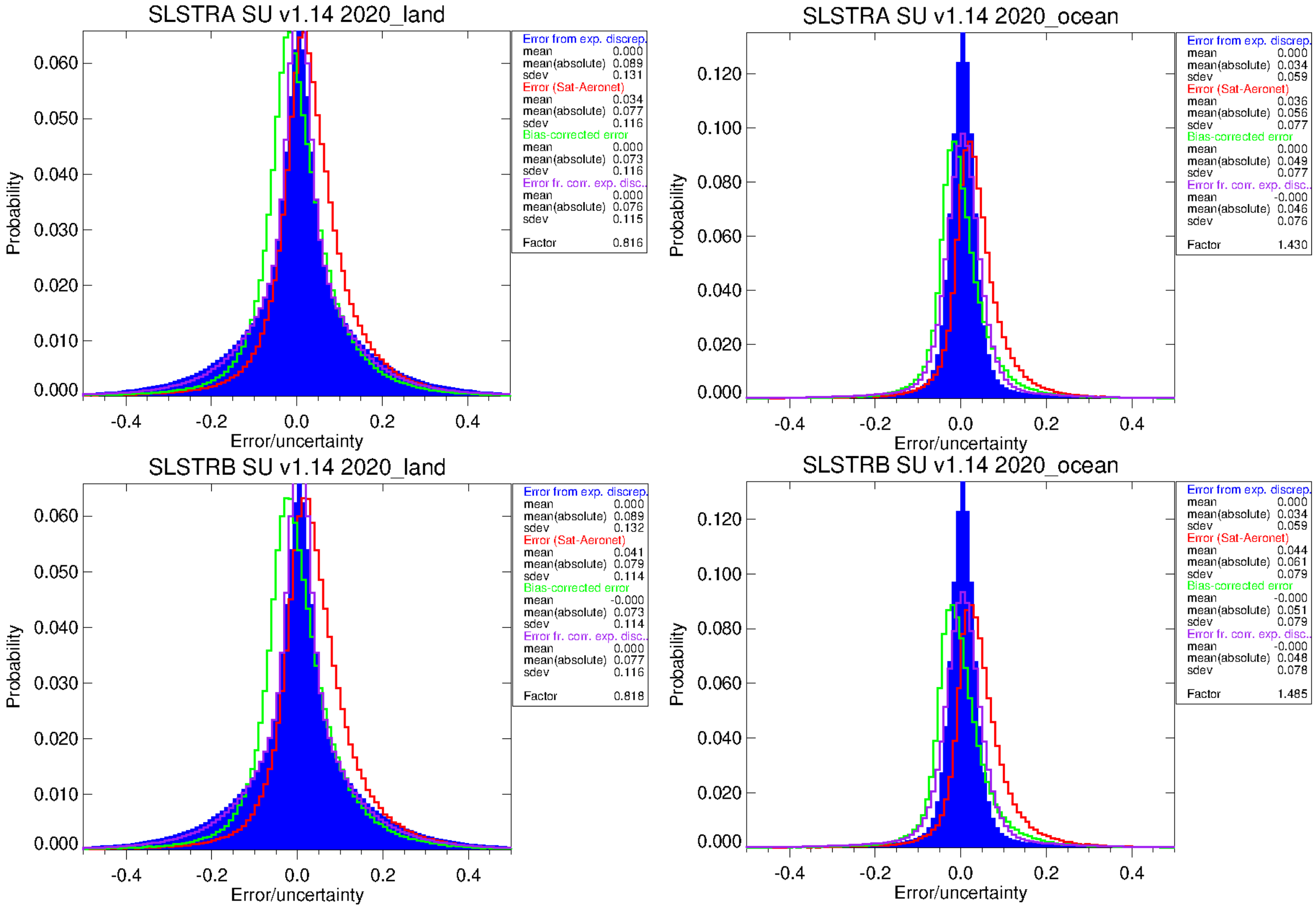

Figure 5.18 *Histograms of estimated errors (red; with bias correction: green) and errors calculated from uncertainties (blue; scaled to best fit the mean-bias corrected error distribution) for SLSTR/3A (top) and SLSTR/3B (bottom) over land (left) and ocean (right).*

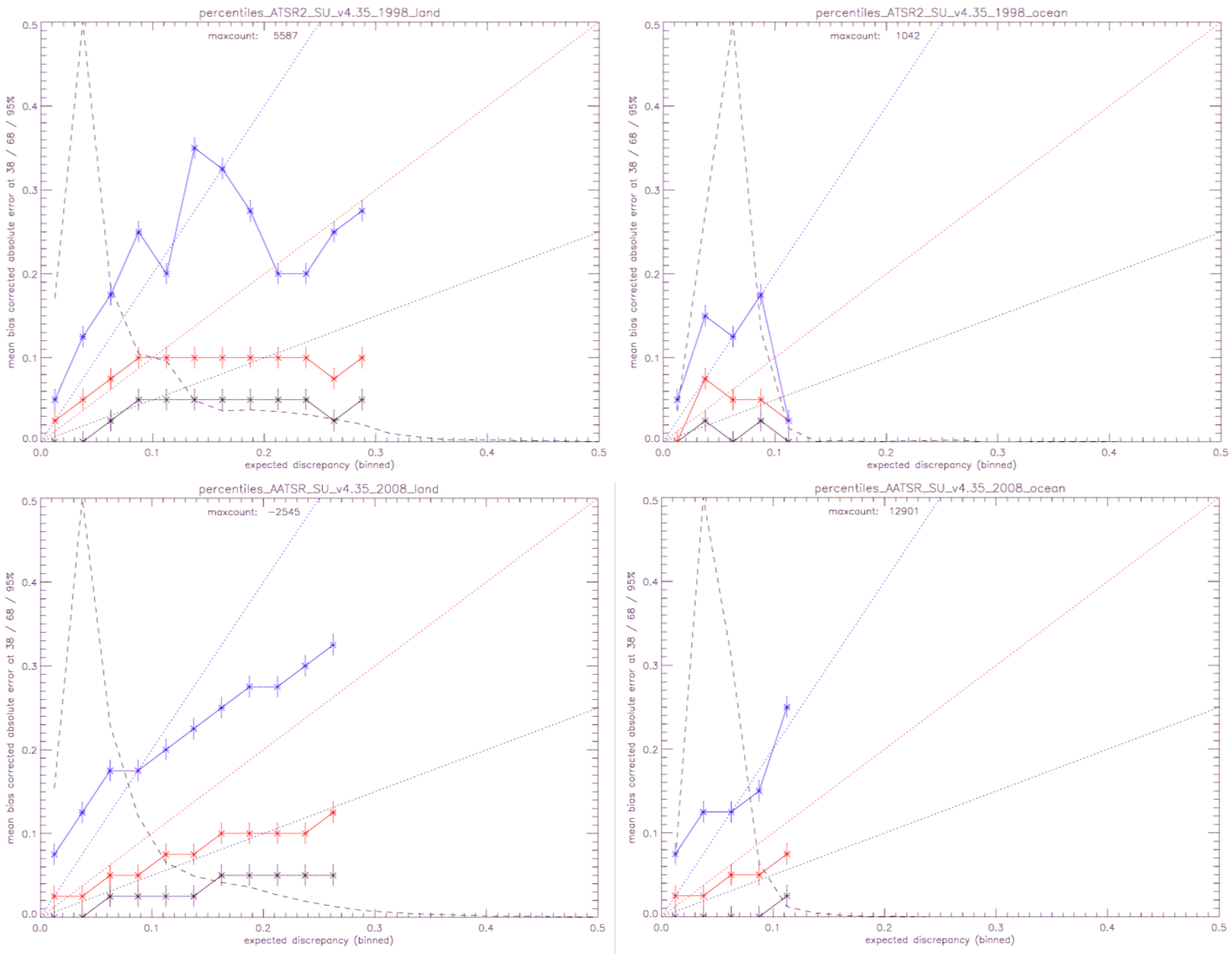

Figure 5.19 *Percentile plots of absolute errors at 38% (black), 68% (red) and 95% (blue) as function of binned expected discrepancy for ATSR-2 (top) and AATSR (bottom) over land (left) and ocean (right); dashed lines show the expected theoretical dependence.*

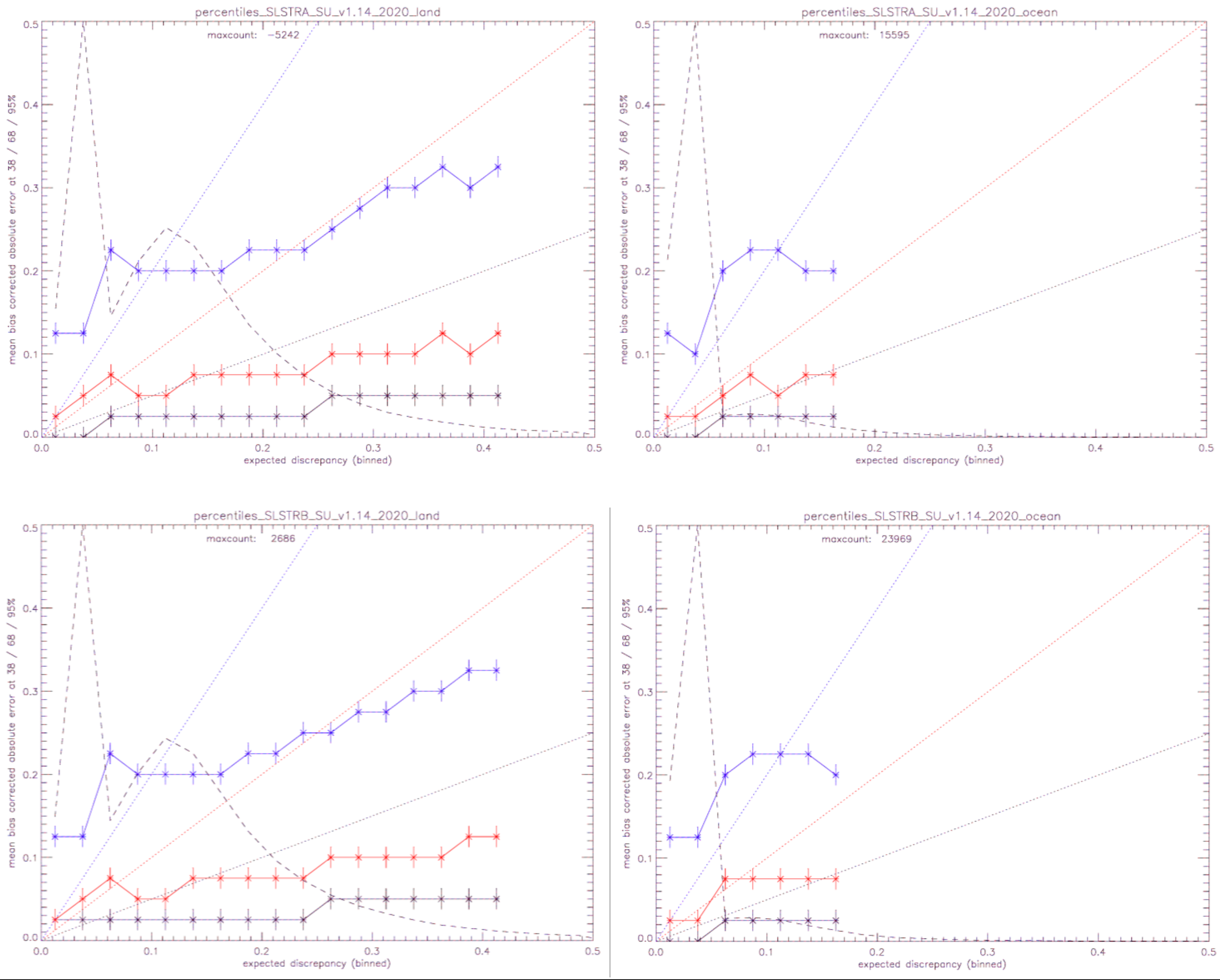

Figure 5.20 *Percentile plots of absolute errors at 38% (black), 68% (red) and 95% (blue) as function of binned expected discrepancy for SLSTR/3A (top) and SLSTR/3B (bottom) over land (left) and ocean (right); dashed lines show the expected theoretical dependence.*

Table 5.3 Statistical summary of validating SU v3 distributions of the normalized errors Δ for the 4 sensors

year	sensor	alg_version	area	mean-delta	stdv-delta	fraction-delta [%]
CRDP-3 SU v3 datasets						
Theoretical expectation				0.	1.	68.3
1998	ATSR2	SU_v4.35	land	-0.14	2.43	58.9
1998	ATSR2	SU_v4.35	ocean	-0.02	1.62	64.6
2008	AATSR	SU_v4.35	land	-0.11	1.89	64.9
2008	AATSR	SU_v4.35	ocean	-0.01	1.78	63.3
2020	SLSTRA	SU_v1.14	land	0.07	1.68	72.4
2020	SLSTRA	SU_v1.14	ocean	0.05	2.64	51.2
2020	SLSTRB	SU_v1.14	land	0.05	1.69	71.9
2020	SLSTRB	SU_v1.14	ocean	0.05	2.74	48.8

5.1.4 CRDP-2 RF v1 validation results

Table 5.4 and Figures 5.21 – 5.24 show the assessment of pixel-level uncertainties of the first CISAR RF v1 datasets with the same methods as for the SU v1 datasets (presented in Tab. 5.1 and Fig. 5.1 – 5.8). Overall, the CISAR uncertainties are smaller than those of the SU datasets, but they are too small in comparison to the true error estimates against AERONET.

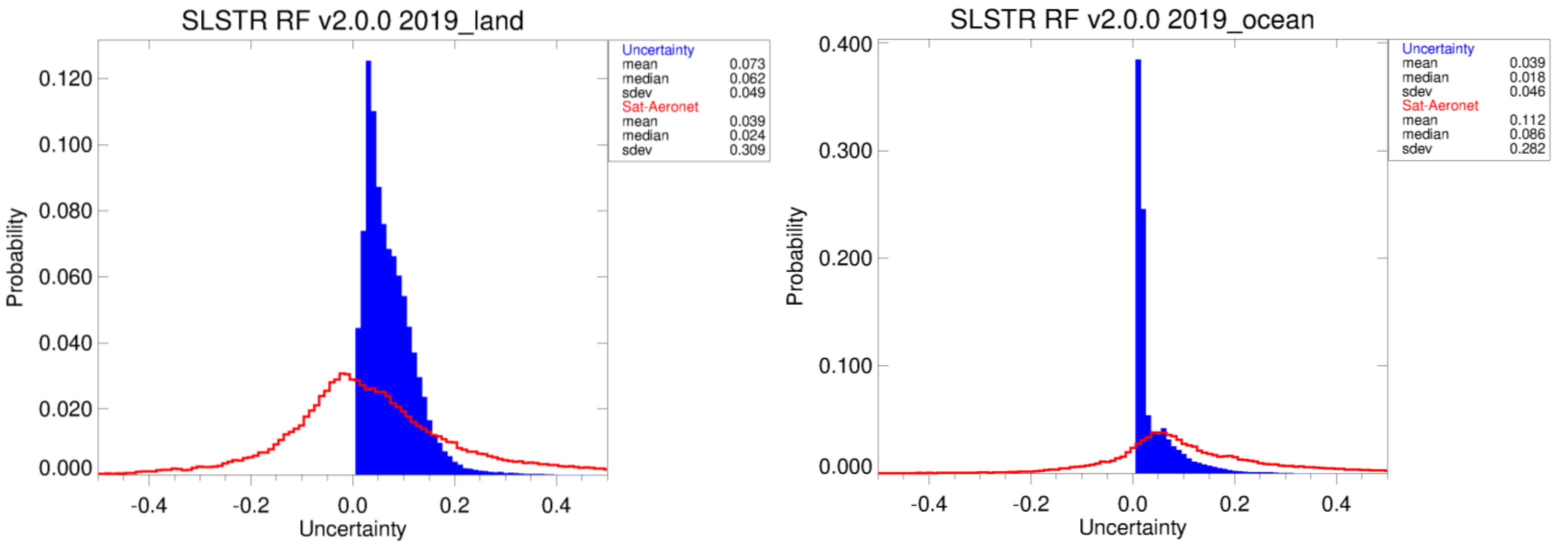

Figure 5.21 *Histograms of errors and uncertainties for SLSTR/3A over land (left) and ocean (right).*

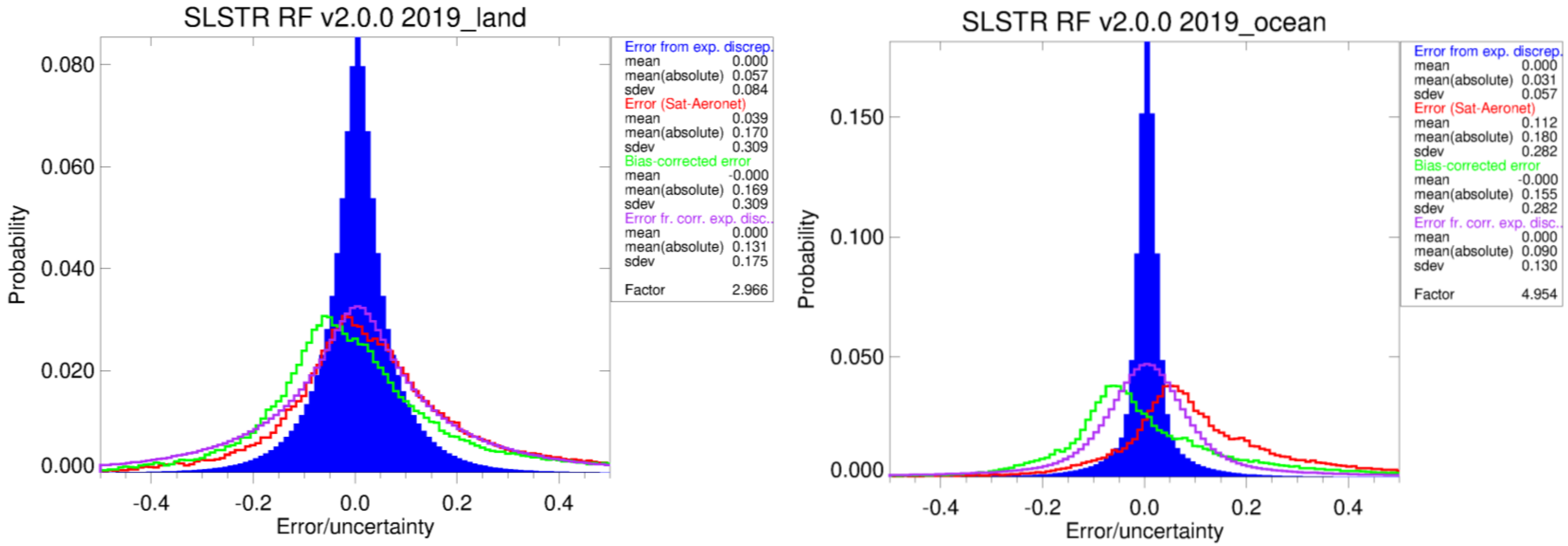

Figure 5.22 *Histograms of estimated errors (red; with bias correction: green) and errors calculated from uncertainties (blue; scaled to best fit the mean-bias corrected error distribution) for SLSTR/3A over land (left) and ocean (right).*

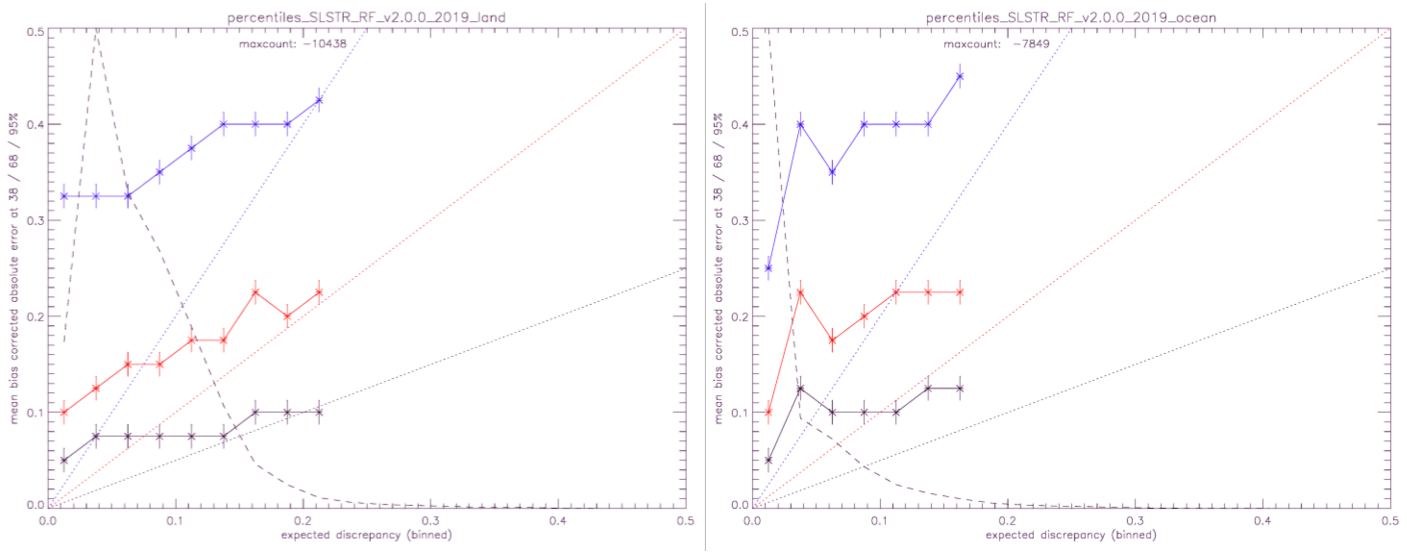

Figure 5.23 *Percentile plots of absolute errors at 38% (black), 68% (red) and 95% (blue) as function of binned expected discrepancy for SLSTR/3A over land (left) and ocean (right); dashed lines show the expected theoretical dependence.*

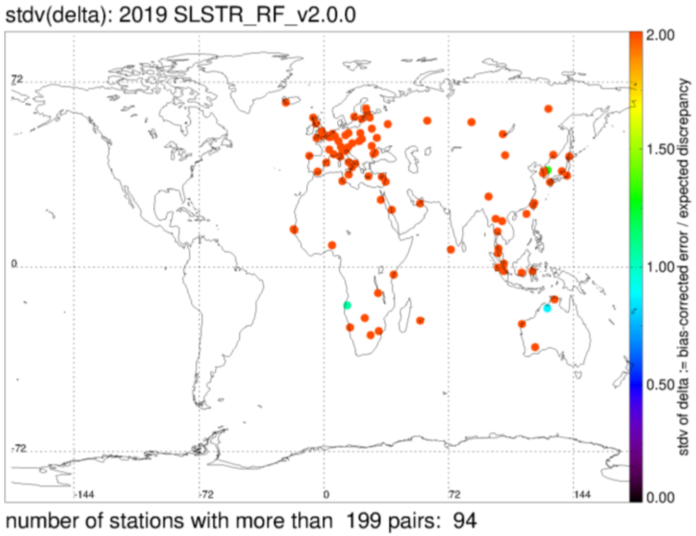

Figure 5.24 *Station maps of significant stdv of normalized errors Δ for SLSTR/3A.*

Table 5.4 Statistical summary of validating RF v1 distributions of the normalized errors Δ for SLSTR/3A

year	sensor	alg_version	area	mean-delta	stdv-delta	fraction-delta [%]
CRDP-2 RF v1 datasets						
Theoretical expectation				0.	1.	68.3
2019	SLSTRA	RF_v2.0.0	land	-0.08	5.96	27.2
2019	SLSTRA	RF_v2.0.0	ocean	- 0.93	8.69	12.4

5.1.5 CRDP-3 RF v2 validation results

Table 5.5 and Figures 5.25 – 5.26 show the assessment of pixel-level uncertainties of the first CISAR RF v2 datasets with the same methods as for the SU v1 datasets (presented in Tab. 5.1 and Fig. 5.1 – 5.8). Overall, the CISARv2 uncertainties match the true errors much better than in v1 (where they were much too small to represent the true error, while also the true error has decreased from v1 to v2). For v2, the uncertainties are now slightly too large.

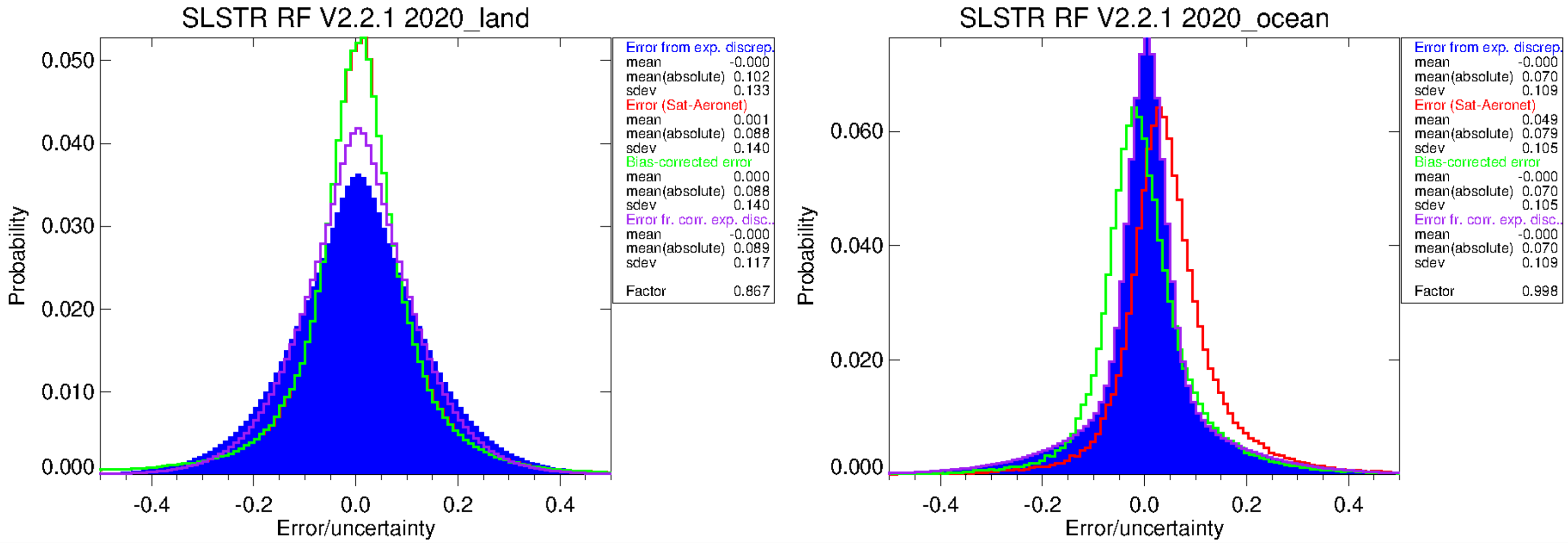

Figure 5.25 *Histograms of estimated errors (red; with bias correction: green) and errors calculated from uncertainties (blue; scaled to best fit the mean-bias corrected error distribution) for SLSTR/3A over land (left) and ocean (right).*

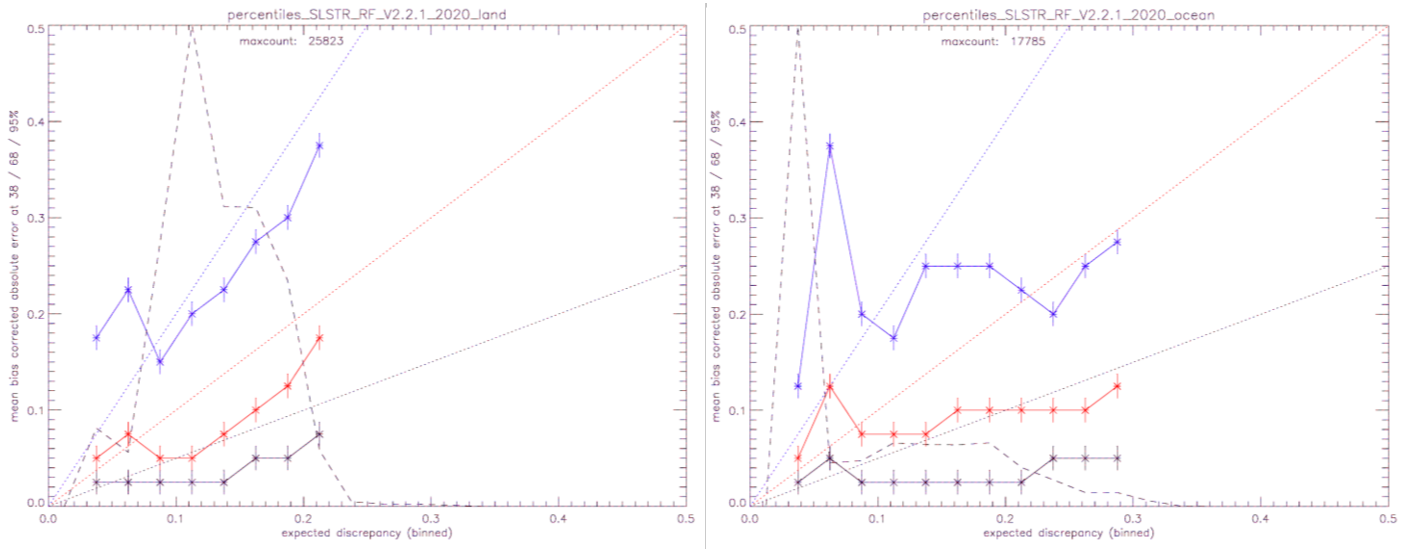

Figure 5.26 *Percentile plots of absolute errors at 38% (black), 68% (red) and 95% (blue) as function of binned expected discrepancy for SLSTR/3A over land (left) and ocean (right); dashed lines show the expected theoretical dependence.*

Table 5.5 Statistical summary of validating RF v2 distributions of the normalized errors Δ for SLSTR/3A

year	sensor	alg_version	area	mean-delta	stdv-delta	fraction-delta [%]
CRDP-2 RF v1 datasets						
Theoretical expectation				0.	1.	68.3
2020	SLSTRA	RF_V2.2.1	land	0.01	1.15	78.9
2020	SLSTRA	RF_ V2.2.1	ocean	0.09	1.67	62.3

5.2 Separate validation of pixel-level uncertainties for both hemispheres

The double peaks in histograms of the uncertainteis in Fig. 5.1 and Fig. 5.2 and theoretical understanding motivated the following additional analysis for SU v1 datasets where we split the assessment for stations in the Northern and Southern hemisphere. Prognositc uncertainteis are expected to increase with increasing AOD and increasing surface brightness, but also to strongly depend on the observation geometry where backscatter conditions also lead to increasing uncertainties. It is understood that dual view instrument observation geometry (mostly in the off-nadir view) differs significantly between the two hemispheres. In addition, the distribution of AERONET stations is largely uneven between the two hemispheres. Finally, the design of the two ATSR instruments has one major difference from the design of the two SLSTR instruments: Whereas ATSR has a forward view, SLSTR has a rearward view. As a consequnce of this opposite viewing directions, ATSR has more favourable retrieval conditions in the North where most Aeronet stations lie, while SLSTR has better conditions in the South with less Aeronet stations. Therefore, we expect that, on global average, SLSTR (with less stations in the best conditions of the South) will have larger errors and larger uncertainties than ATSR (with msot stations innthe more favourable North of the globe). To verify this hypothesis, the analysis conducted in section 5.1 was split into the two hemispheres for AATSR and SLSTR / S3A (ATSR-2 has too few stations to split the statitics and SLSTR / S3B is not shown but had similar results as for SLSTR / S3A; also analysis over ocena was made with equivalent results and is not shown here).

Fig 5.27 and Fig. 5.228 show that for both AATSR and SLSTR the favourable hemisphere (which is opposite to each other) has smaller uncertainties and the double peak is gone; those need some increase, while in the unfavourable hemisphere uncertainties are larger and need to be (significantly) decreased. Fig. 5.29 shows the percentile plots for AATSR and SLSTR/3A split into hemispheres, which proves a larger range of meaningful uncertainteis over the favourable hemisphere which are appropriate to discriminate “good” and “bad” pixels.

Table 5.6 shows also a tendency (but not in all metrics and cases) that for the ATSR instruments the pixel level uncertainties in the South are on average larger (more over land) and need to be decreased by a correction factor ~0.6 – 0.8 (over both land and ocean) to match the measured bias while in the North they need to be increased by ~1.1 – 1.3 (note lower number for the statistics of ATSR-2). For the SLSTR instruments both measured biases and pixel level uncertainties are smaller in the South, but they are too small and thus need to be increased by correction factors > 2. over land and ~1.2 over ocean.

Table 5.6 *Statistical summary of validating pixel level uncertainty distributions over the Southern / Northern hemisphere for the 4 sensors*

				Error from discrepancy		Mean-bias corrected error		Correction factor
year	**sensor**	**Algorithm / version**	**area**	**Mean(abs)**	**Stdv**	**Mean(abs)**	**Stdv**	
1998	ATSR2	SU_v4.32	land	0.07 0.05 0.15	0.11 0.07 0.19	0.08 0.08 0.09	0.19 0.20 0.12	1.16 1.71 0.62
1998	ATSR2	SU_v4.32	ocean	0.05 0.05 0.05	0.06 0.06 0.06	0.05 0.05 -	0.07 0.07 -	1.14 1.14 -
2008	AATSR	SU_v4.32	land	0.06 0.05 0.11	0.09 0.08 0.16	0.07 0.06 0.07	0.11 0.11 0.10	1.12 1.26 0.64
2008	AATSR	SU_v4.32	ocean	0.04 0.04 0.03	0.06 0.06 0.04	0.05 0.06 0.03	0.11 0.12 0.03	1.28 1.31 0.82
2019	SLSTRA	SU_v1.11	land	0.10 0.11 0.04	0.14 0.15 0.05	0.09 0.09 0.07	0.14 0.14 0.18	0.96 0.88 2.00
2019	SLSTRA	SU_v1.11	ocean	0.04 0.04 0.02	0.07 0.07 0.03	0.05 0.06 0.03	0.08 0.09 0.04	1.41 1.40 1.11
2019	SLSTRB	SU_v1.11	land	0.10 0.11 0.03	0.15 0.16 0.05	0.09 0.09 0.08	0.14 0.13 0.18	0.89 0.80 2.37
2019	SLSTRB	SU_v1.11	ocean	0.04 0.04 0.02	0.07 0.07 0.03	0.05 0.05 0.03	0.08 0.08 0.04	1.37 1.36 1.25

All North South"South validation is worse" "South validation is better"

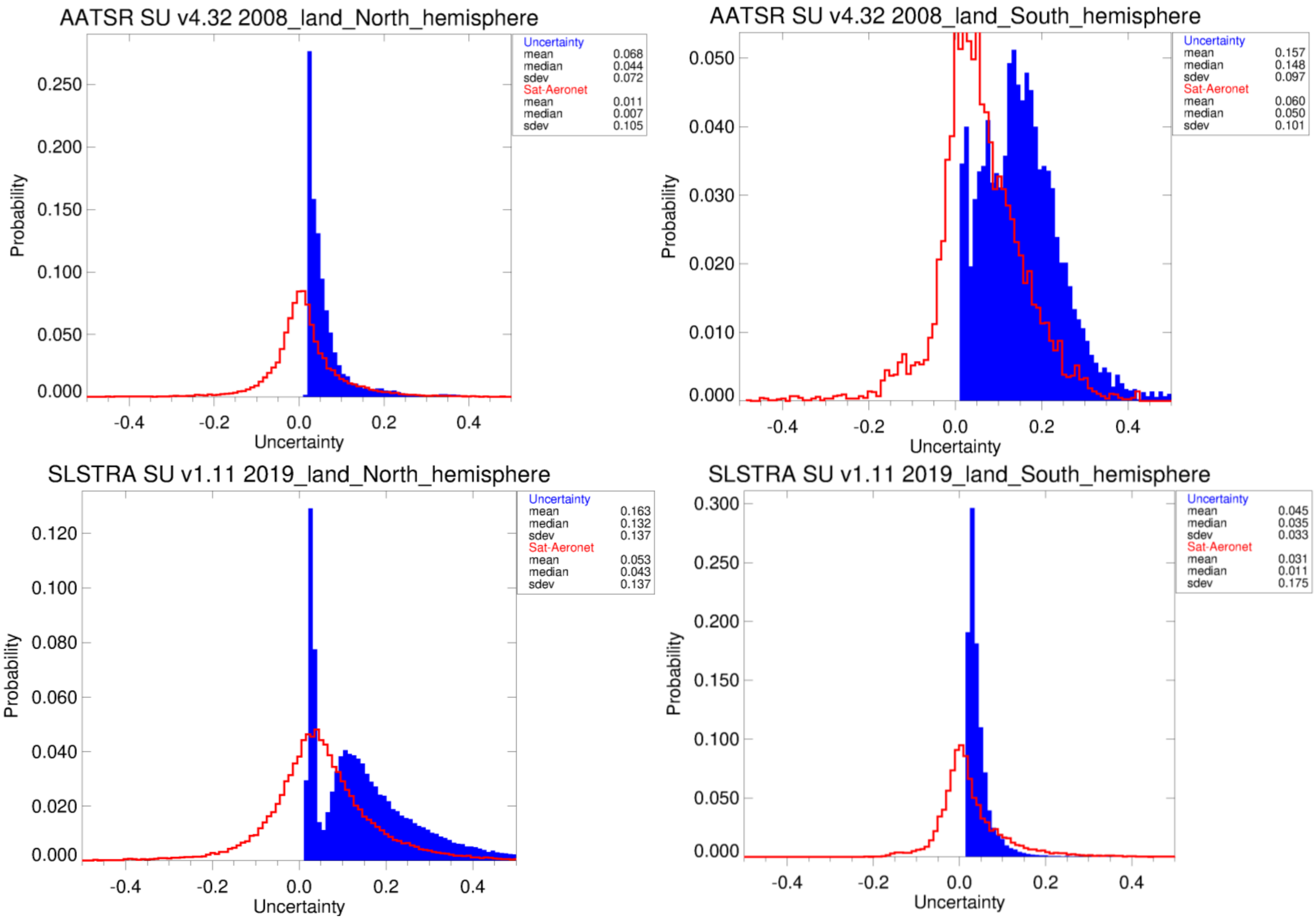

Figure 5.27 *Histograms of errors and uncertainties for AATSR (top) and SLSTR/3A (bottom) over the North (left) and South hemisphere (right).*

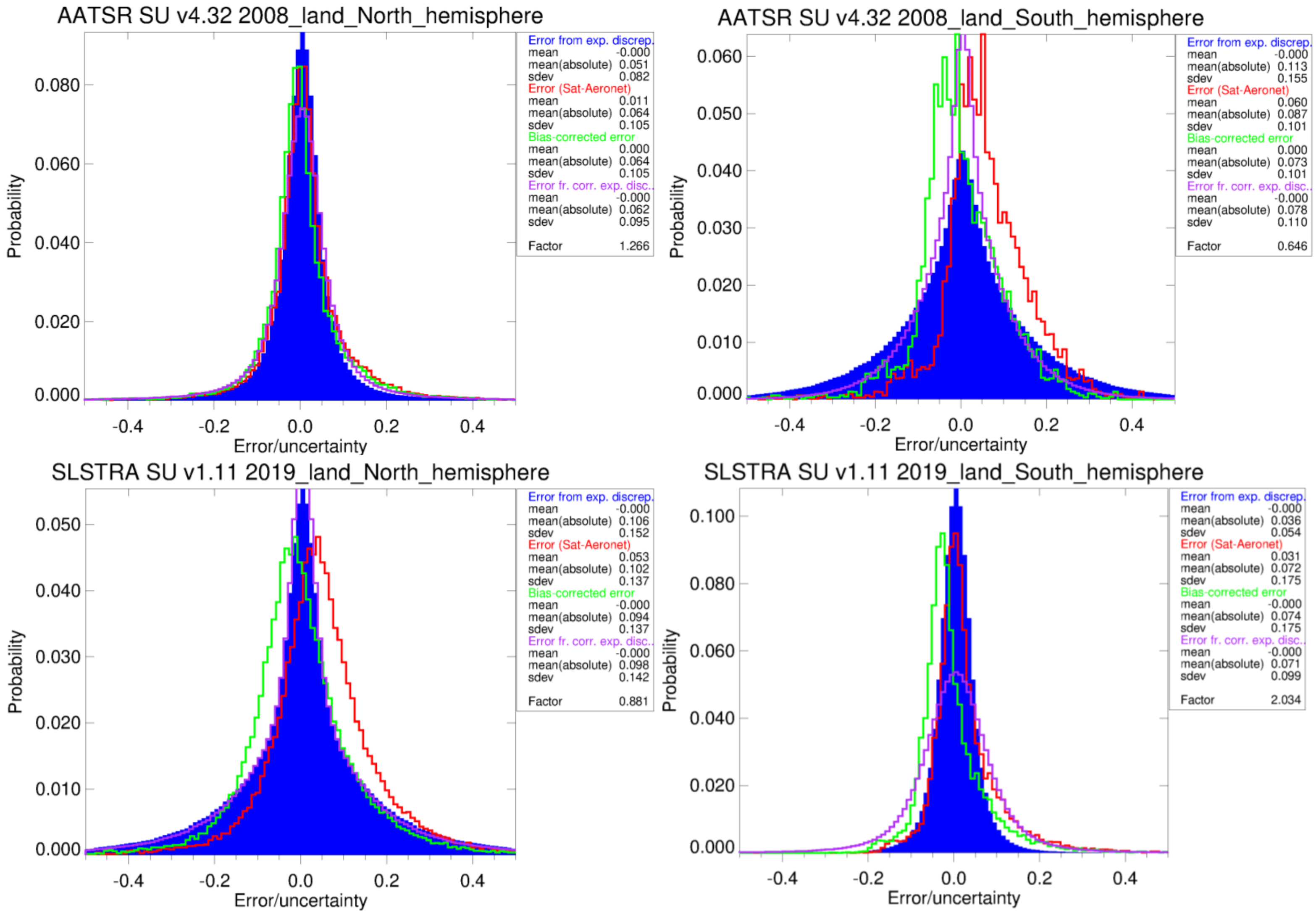

Figure 5.28 *Histograms of estimated errors (red; with bias correction: green) and errors calculated from uncertainties (blue; scaled to best fit the mean-bias corrected error distribution) for AATSR (top) and SLSTR/3A (bottom) over the North (left) and South (right) hemisphere.*

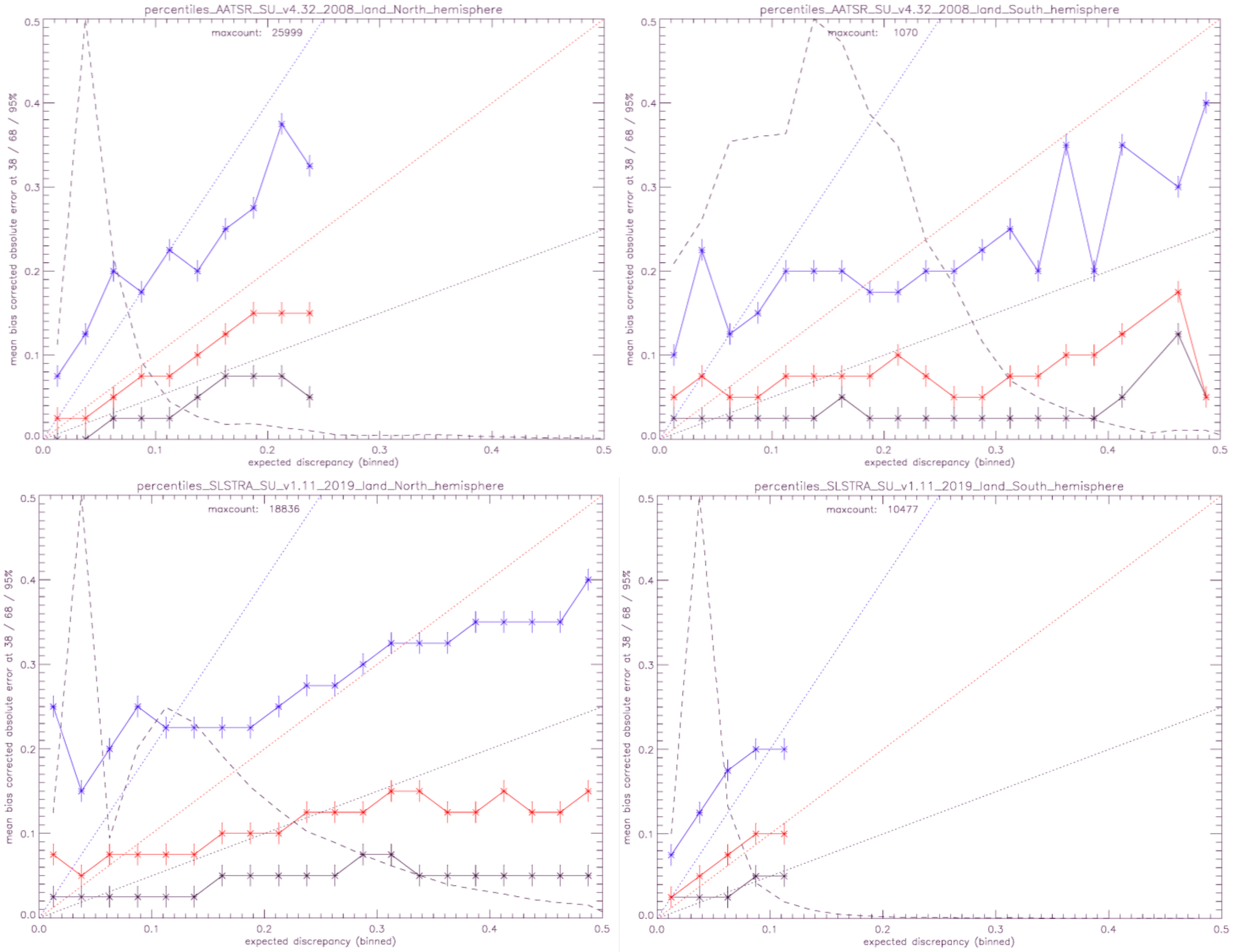

Figure 5.29 *Percentile plots of absolute errors at 38% (black), 68% (red) and 95% (blue) as function of binned expected discrepancy for AATSR (top) and SLSTR/3A (bottom) over the North (left) and South (right) hemisphere; dashed lines show the expected theoretical dependence.*

5.3 Comparison of the validation of uncertainties from 2 algorithms for entire 2020

In Figure 5.30 we compare the error histograms of true errors and errors derived from the expected discrepancies for SLSTR / 3a with the two algorithms Swansea and CISAR / RF. The analysis shows that for both algorithms uncertzainties are smaller over the Southern hemisphere over land and ocean. The CISAR / RF uncertainties provide a better representation of the true errors (as can be seen in the correction factors closer to 1.) than the Swansea uncertainties; also for CISAR / RF the consistency between land and ocean and is higher (similar correction factors).

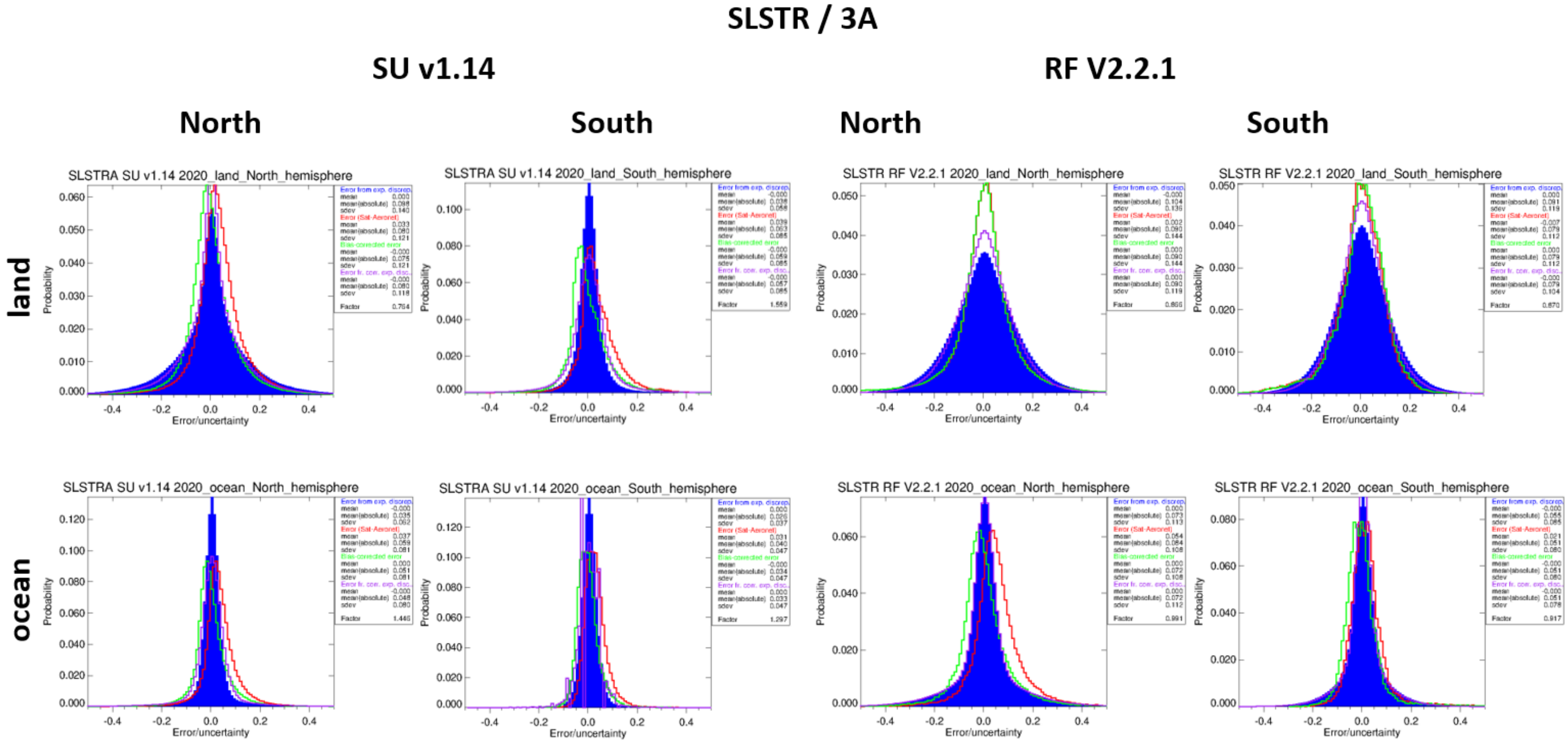

Figure 5.30 *Histograms of estimated errors (red; with bias correction: green) and errors calculated from uncertainties (blue; scaled to best fit the mean-bias corrected error distribution) for SLSTR/3A with 2 algorithms over the North (left) and South (right) hemisphere.*

Summary for the validation of AOD prognostic uncertainties

- all uncertainty distributions show a double peak (strong over land, in particular for both SLSTR instruments)
- mean of uncertainties is larger over land than over ocean for all sensors
- mean and stdv of uncertainties are significantly larger over land for SLSTR than for the ATSR instruments but similar for all sensors over ocean
- uncertainties are generally slightly too small; for the SLSTR instruments over ocean a larger correction factor is needed, while over land uncertainties need a slight decrease
- uncertainties allow a reasonable split between "good" and "bad" pixels for the lower range of prognostic uncertainties with dominating numbers, but not any longer for the higher values
- the smallest uncertainties in the lowest bin have typically too large errors /are too small (in particular for SLSTR instruments)
- statistical distributions of normalized errors per sensor show that on average uncertainties (dominating the statistics) are too small and need correction factors larger than 1. (in particular for SLSTR)
- separate analysis of the two hemispheres proves the favourable scattering angle conditions (avoiding backscatter) which have smaller uncertainties with less need for correction and more meaningful information to split "good" and "bad" pixels; those favourable conditions are in the Northern hemisphere for ATSR (with most AERONET stations dominating the validation statistics) , while they lie in the Southern hemisphere for SLSTR (with less AERONET stations). This is one reason for the weaker performance of AOD from SLSTR than ATSR, but also of the prognostic uncertainties.
- For the SU v2 datasets, larger uncertainties are slightly smaller, but overall there is not much change
- For the SU v3 datasets, ATSR uncertainties are slightly smaller, but overall there is not much change
- Uncertainties of the CISAR v1 algorithm are smaller than those of the SU algorithm, but they are too small compared to the true error estimates of AERONET
- Uncertainties of the CISAR v2 algorithm are much better matching the true errors, they are now a little too large compared to the true error estimates of AERONET

9 INTER-COMPARISON TO OTHER SATELLITE DATASETS

6.1 Level3 evaluation: inter-comparison of SU v1.11 AOD monthly products

6.1.1 Monthly global AOD

Evaluation of the L3 (1deg resolution) monthly (March, June, September and December) AOD products from the AATSR and Sentinel-3A, -3B (S3A, S3B) has been performed for years 2008 and 2019, respectively. AATSR monthly AOD product has been compared with MODIS, MISR and POLDER/GRASP AOD. S3A and S3B AOD products were inter-compared; both S3A and S3B AOD products were compared with MODIS and MISR AOD.

Total AOD monthly maps for AATSR, MODIS, MISR and POLDER for year 2008 are shown in Fig. 6.1. In March and December, AOD is not retrieved North of ~50-60°N (Northern Europe, Canada, central Russia and Siberia). The retrieval is limited over those areas by low solar zenith angle, which limits the radiative transfer calculations, and snow cover. Better coverage of MODIS instrument is clearly seen in more smoothed AOD maps.

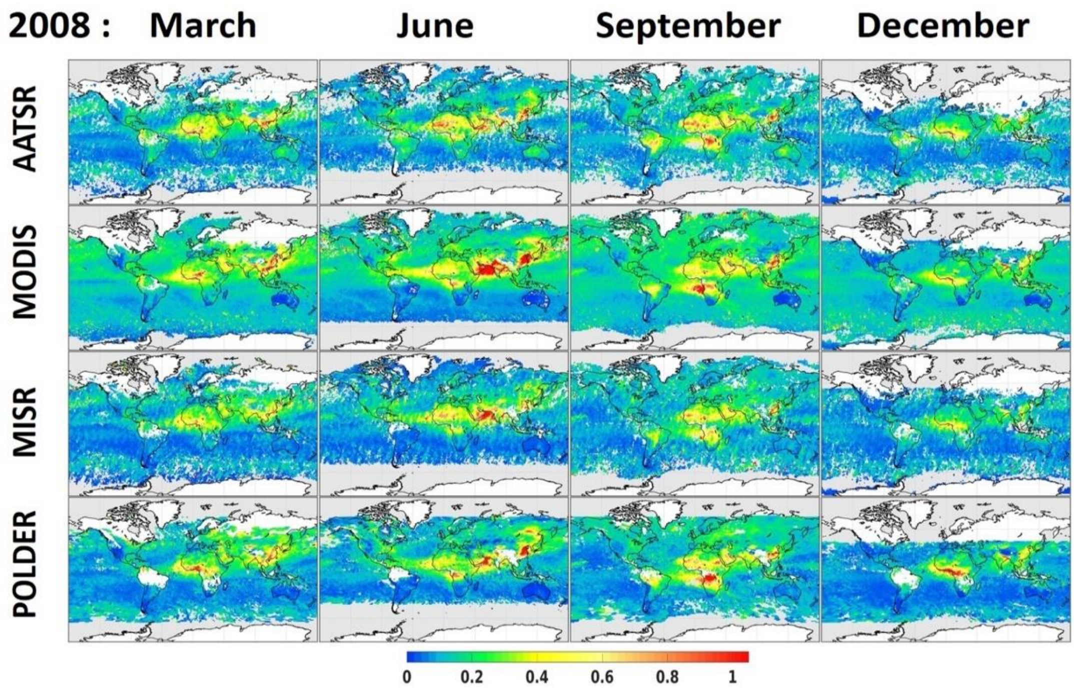

Figure 6.1 *AATSR, MODIS, MISR and POLDER total AOD for March, June, September and December 2008.*

Besides difference in coverage, difference in AOD is clear over the areas of potential high AOD loading (dust areas, biomass burning areas, areas of strong anthropogenic pollution). One of the main reasons for the difference in AOD is cloud screening. With more strict cloud screening, high AOD episodes cannot be retrieved, if high aerosol loading is recognised as cloud in the cloud screening module. Difference in AOD over ocean, where AOD loading is in general low (0.1-0.15) is also observed between products. Visual analysis of the maps gives an impression that AATSR, MISR and POLDER monthly AOD are close to each other, while MODIS provides higher AOD. Detailed analysis is provided in sections 6.1.2 and 6.1.3.

Total AOD monthly maps for S3A, S3B, MODIS and MISR for year 2019 are shown in Fig. 6.2. Sentinel-3 instruments have wider swath, as compared to AATSR, which results in better coverage. In 2019, S3A and S3B AOD monthly maps look as smooth as MODIS AOD maps.

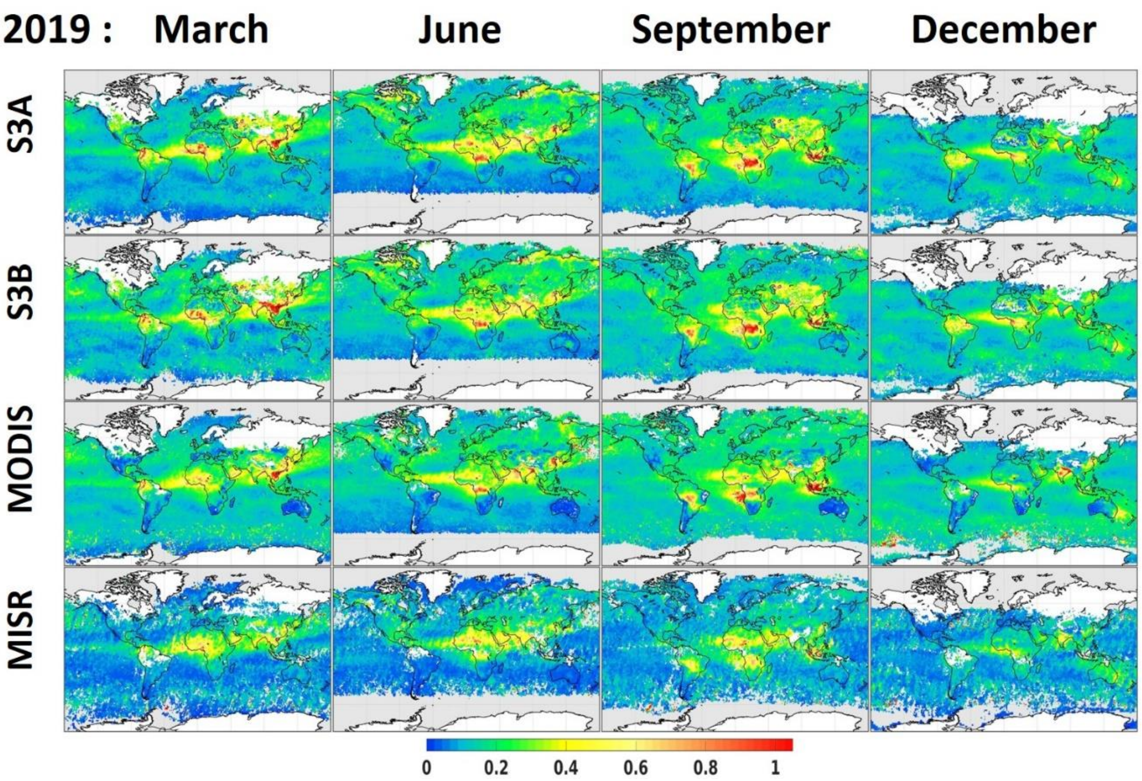

Figure 6.2 *Sentinel-3A (S3A), Sentinel-3B (S3B), MODIS and MISR total AOD for March, June, September and December 2019.*

6.1.2 Monthly regional AOD

In this study, we focus on different regions across the globe, as regional differences in AOD loading, types, seasonality and surface reflectance exist, which can affect the retrieval regional quality considerably. As such, applications drawn from the products will be analysed on a regional level.

To study regional differences over the globe, we chose 15 regions that seem likely to represent different aerosol / surface conditions (Fig. 1). There are 11 land regions: Europe (Eur), Boreal (Bor), Northern, Eastern and Western Asia (AsN, AsE and AsW, respectively), Australia (Aus), Northern and Southern Africa (AfN and AfS), Southern America (AmS), East and West of Northern America (NAE and NAW); Indian Ocean (InO), Pacific ocean (PO), two regions over Atlantic ocean: Saharan dust outbreak over the central Atlantic (AOd) and possible biomass burning outbreak over southern Atlantic (AOb), and one region, Indonesia (Ind), that includes both land and ocean. Furthermore, we studied AOD over all land, all ocean and globally, when observed. South-Eastern China (ChinaSE), which is part of the AsE region, was also considered separately as an area with considerable AOD changes during the last 25 years. Altogether, we consider the AOD in 17 regions, AOD over land, ocean and Global AOD.

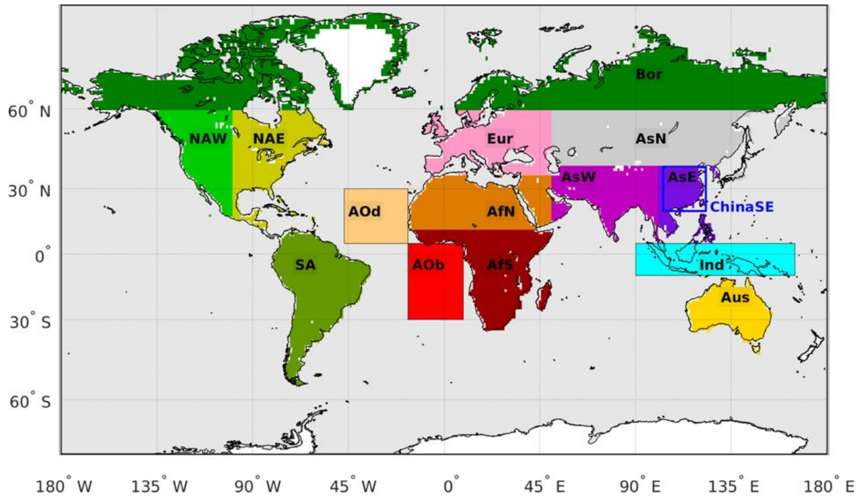

Figure 6.3 *17 Land and ocean regions defined in this study: Europe (Eur), Boreal (Bor), northern Asia (AsN), eastern Asia (AsE), western Asia (AsW), Australia (Aus), northern Africa (AfN), southern Africa (AfS), South America (SA), eastern North America (NAE), western North America (NAW), Indonesia (Ind), Atlantic Ocean dust outbreak (AOd), Atlantic Ocean biomass burning outbreak (AOb). In addition, Southeast China (ChinaSE), which is part of the AsE region, marked with a blue frame, is considered separately. Indian Ocean (InO) and Pacific Ocean (PO) regions are not shown. Land, ocean and global AOD were also considered.*

Monthly regional AOD for AATSR, MODIS, MISR and POLDER (2008) and for S3A, S3B, MODIS and MISR (2019) are shown in Fig. 6.4.

In both years, all products have similar tendency of high AOD over Asia (AsW, AsE and ChinaSE), Africa (AfN, AfS), the area of the Saharan dust transport (AOd) and over the Atlantic Ocean, influenced by the transport of biomass burning aerosols (AOb).

In 2008 in Asia, MODIS and POLDER AOD are higher than those from the AATSR and MISR products in March and June, while in September and December the difference between AATSR and MODIS and POLDER is smaller. Global AOD is similar for AATSR, MISR and POLDER, while MODIS global AOD is higher. For details, see Table 6.1, Table 6.4 and discussion below.

In the year 2019, the difference between S3A and S3B AOD is small in all regions, except for AsE and ChinaSE, where S3B is slightly higher (for details, see Table 6.2, Table 6.5 and discussion below). S3A and S3B total AOD is close to the MODIS product for Europe, Asia, Indonesia, dust and biomass burning areas, while in South Africa, South and North America S3A and S3B AOD is higher than MODIS and the MODIS AOD product is close to MISR.

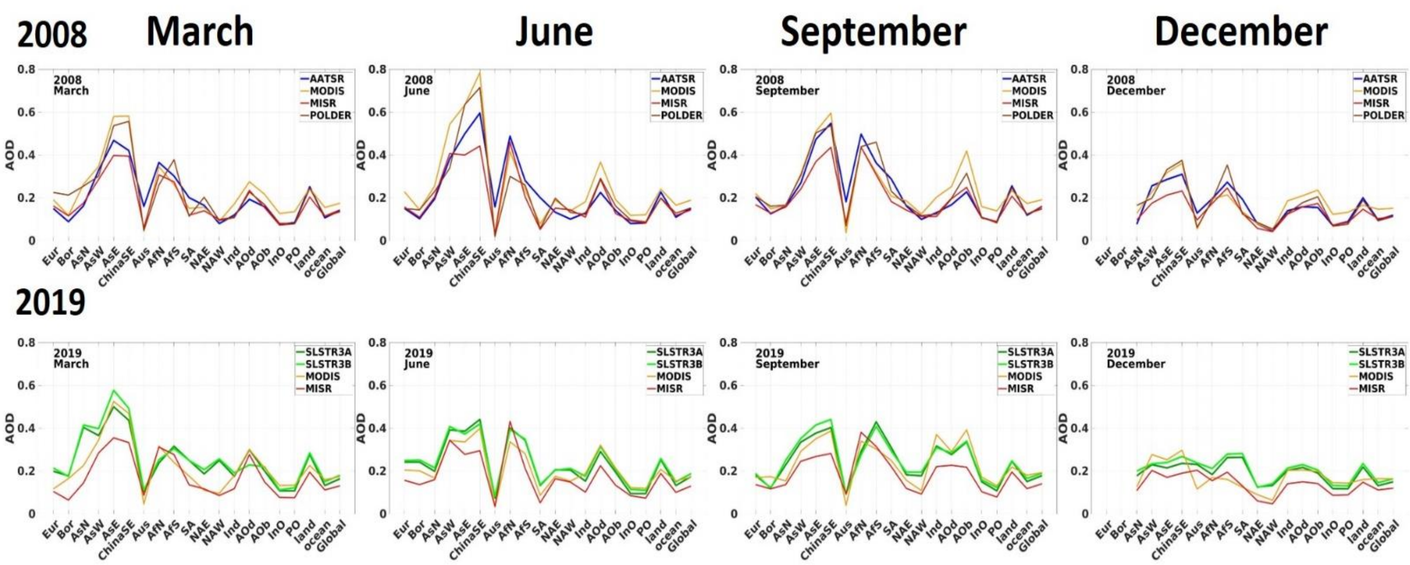

Figure 6.4 Monthly AOD for AATSR, MODIS, MISR and POLDER (2008, upper panel) and for S3A, S3B, MODIS and MISR (2019, lower panel) for different regions, as in Fig. 6.3

6.1.3 Regional and global difference in monthly AOD

Maps of the difference in monthly AOD between AATSR and MODIS, AATSR and MISR (middle panel), AATSR and POLDER (lower panel) total AOD monthly products are shown in Fig. 6.5. Maps of the difference in monthly AOD between S3A and S3B, S3A and MODIS, S3B and MODIS, S3A and MISR, S3B and MISR total AOD monthly products are shown in Fig.6.6.

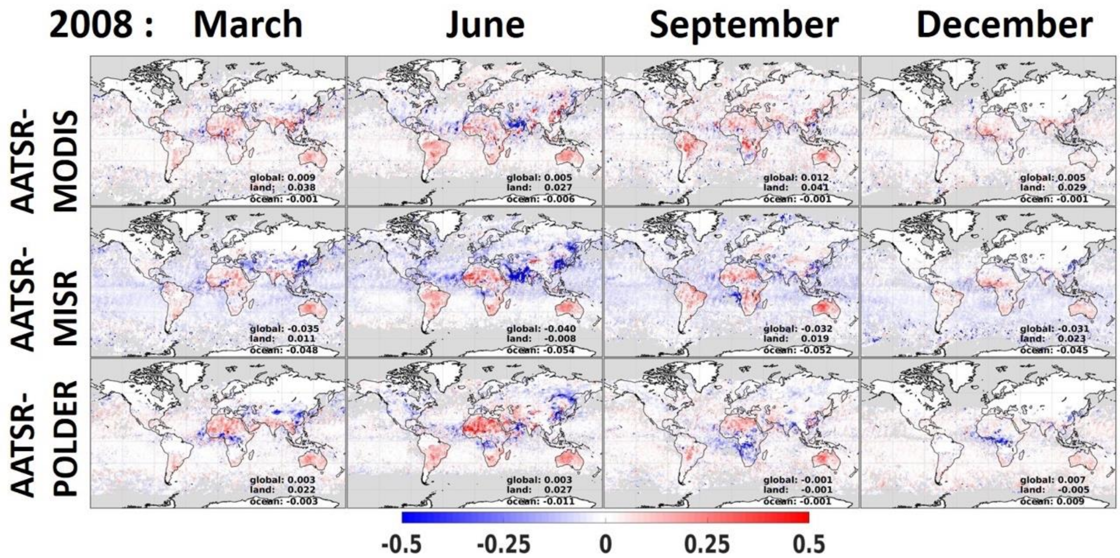

Figure 6.5 *Difference between AATSR and MODIS (upper panel), AATSR and MISR (middle panel), AATSR and POLDER (lower panel) total AOD monthly products, for year 2008.*

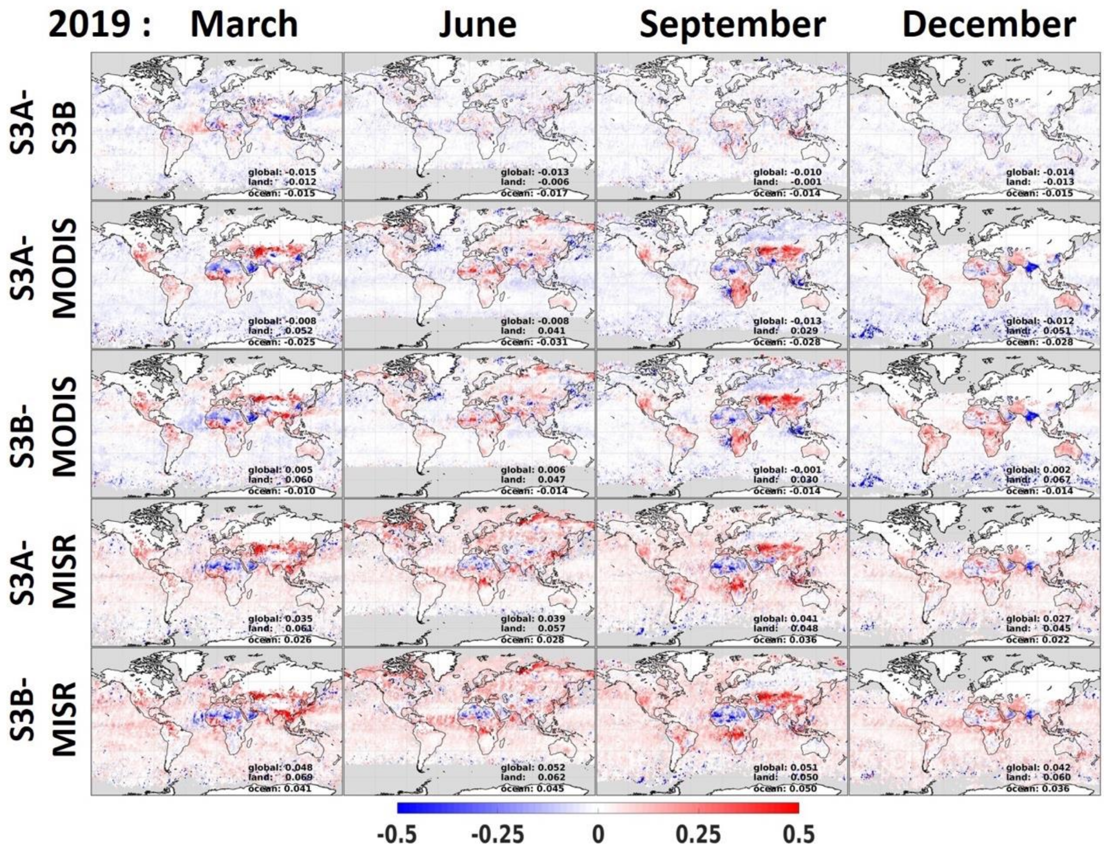

Figure 6.6 *Difference between S3A and S3B (upper panel), S3A and MODIS, S3B and MODIS, S3A and MISR, S3B and MISR total AOD monthly products, for year 2019.*

Absolute differences in AOD monthly means between satellite products over selected regions are summarised in Table 6.1 (for year 2008) and Table 6.2 (for year 2019).

Table 6.1 *Offset between AATSR and MODIS, MISR and POLDER monthly AOD for regions defined as in Figure 6.3*

regions	**Eur**	**Bor**	**AsN**	**AsW**	**AsE**	**ChinaSE**	**Aus**	**AfN**	**AfS**	**SA**
March										
AATSR-MODIS	-0.041	-0.029	-0.101	-0.018	-0.112	-0.161	0.115	0.020	0.040	0.050
AATSR-MISR	-0.012	-0.027	-0.013	0.043	0.070	0.026	0.099	0.058	0.027	0.082
AATSR-POLDER	-0.075	-0.124	-0.092	0.028	-0.069	-0.136	0.112	0.105	-0.076	0.087
June										
AATSR-MODIS	-0.077	-0.042	-0.060	-0.161	-0.134	-0.189	0.133	0.072	0.043	0.122
AATSR-MISR	-0.006	-0.007	-0.009	-0.025	0.099	0.154	0.123	0.028	0.076	0.148
AATSR-POLDER	0.001	-0.041	-0.035	0.043	-0.136	-0.119	0.138	0.188	0.021	0.143
September										
AATSR-MODIS	-0.016	-0.023	-0.003	-0.042	-0.037	-0.048	0.145	0.061	0.045	0.080
AATSR-MISR	0.036	-0.003	0.004	0.028	0.104	0.112	0.098	0.061	0.055	0.105
AATSR-POLDER	-0.002	-0.035	-0.005	-0.035	-0.030	0.011	0.113	0.058	-0.097	0.057
December										
AATSR-MODIS	-0.043	NaN	-0.051	0.028	-0.032	-0.051	0.074	0.000	0.059	0.058
AATSR-MISR	-0.013	NaN	-0.020	0.081	0.073	0.078	0.032	0.022	0.027	0.065
AATSR-POLDER	-0.031	NaN	-0.088	0.058	-0.046	-0.065	0.067	0.008	-0.080	0.069

Table 6.1 *continued*

regions	NAE	NAW	Ind	AOd	AOb	InO	PO	Land	Ocean	Globe
March										
AATSR-MODIS	0.009	-0.010	-0.052	-0.082	-0.058	-0.051	-0.052	0.007	-0.048	-0.034
AATSR-MISR	0.025	-0.019	0.010	-0.042	0.004	0.003	0.005	0.048	-0.007	0.006
AATSR-POLDER	-0.038	-0.015	0.012	-0.034	-0.010	-0.005	0.005	0.007	-0.008	-0.003
June										
AATSR-MODIS	-0.056	-0.038	-0.053	-0.142	-0.051	-0.038	-0.038	-0.013	-0.056	-0.037
AATSR-MISR	-0.019	-0.043	0.019	-0.061	0.014	-0.013	0.001	0.029	-0.008	0.008
AATSR-POLDER	-0.065	-0.031	0.006	-0.066	-0.021	-0.017	-0.005	0.027	-0.019	-0.001
September										
AATSR-MODIS	-0.024	-0.025	-0.072	-0.085	-0.191	-0.051	-0.051	0.022	-0.055	-0.031
AATSR-MISR	0.019	-0.013	0.018	-0.028	-0.021	0.002	-0.002	0.048	-0.006	0.011
AATSR-POLDER	-0.004	-0.017	0.007	-0.031	-0.087	-0.002	0.005	0.008	-0.004	0.001
December										
AATSR-MODIS	0.000	-0.004	-0.046	-0.052	-0.081	-0.052	-0.044	0.034	-0.050	-0.032
AATSR-MISR	0.021	0.004	0.016	0.000	-0.019	-0.002	0.004	0.053	-0.006	0.006
AATSR-POLDER	-0.006	-0.009	0.012	-0.020	-0.050	0.003	0.012	0.011	0.004	0.006

***Table 6.2** Offset between S3A and S3B, S3A and MODIS, S3B and MODIS, S3A and MISR, S3B and MISR monthly AOD for regions defined as in Figure 6.3*

(table cont. ->)

regions	Eur	Bor	AsN	AsW	AsE	ChinaSE	Aus	AfN	AfS	SA
March										
S3A-S3B	-0.015	0.003	-0.011	-0.032	-0.077	-0.056	-0.006	-0.015	0.011	0.000
S3A-MODIS	0.082	0.013	0.178	0.021	-0.025	-0.032	0.059	-0.079	0.076	0.073
S3A-MISR	0.094	0.113	0.259	0.081	0.145	0.104	0.018	-0.074	0.039	0.114
S3B-MODIS	0.097	0.010	0.189	0.053	0.052	0.024	0.065	-0.064	0.065	0.073
S3B-MISR	0.109	0.110	0.270	0.113	0.222	0.160	0.024	-0.059	0.028	0.114
June										
S3A-S3B	-0.007	-0.010	-0.016	-0.016	0.013	0.021	-0.008	0.008	-0.005	-0.004
S3A-MODIS	0.037	0.041	0.031	0.049	0.050	0.042	0.042	0.064	0.063	0.046
S3A-MISR	0.085	0.105	0.039	0.048	0.108	0.146	0.038	-0.031	0.131	0.081
S3B-MODIS	0.044	0.051	0.047	0.065	0.037	0.021	0.050	0.056	0.068	0.050
S3B-MISR	0.092	0.115	0.055	0.064	0.095	0.125	0.046	-0.039	0.136	0.085
September										
S3A-S3B	-0.009	0.003	-0.021	-0.017	-0.038	-0.038	0.003	0.016	0.021	0.016
S3A-MODIS	0.010	-0.052	0.075	0.043	0.026	0.016	0.055	-0.048	0.127	0.060
S3A-MISR	0.043	0.005	0.092	0.089	0.109	0.121	0.003	-0.089	0.115	0.089
S3B-MODIS	0.019	-0.055	0.096	0.060	0.064	0.054	0.052	-0.064	0.106	0.044
S3B-MISR	0.052	0.002	0.113	0.106	0.147	0.159	0.000	-0.105	0.094	0.073
December										
S3A-S3B	-0.003	NaN	-0.022	-0.004	-0.025	-0.032	-0.007	-0.028	-0.016	-0.018
S3A-MODIS	-0.013	NaN	0.052	-0.047	-0.038	-0.061	0.115	0.014	0.102	0.139
S3A-MISR	0.031	NaN	0.069	0.027	0.044	0.046	0.027	0.029	0.068	0.133
S3B-MODIS	-0.010	NaN	0.074	-0.043	-0.013	-0.029	0.122	0.042	0.118	0.157
S3B-MISR	0.034	NaN	0.091	0.031	0.069	0.078	0.034	0.057	0.084	0.151

Table 6.2 *continued*

regions	NAE	NAW	Ind	AOd	AOb	InO	PO	Land	Ocean	Globe
March										
S3A-S3B	-0.020	-0.007	-0.016	0.071	-0.019	-0.004	-0.014	-0.008	-0.018	-0.016
S3A-MODIS	0.077	0.154	-0.004	-0.001	-0.015	-0.025	-0.026	0.051	-0.027	-0.010
S3A-MISR	0.070	0.164	0.058	0.023	0.051	0.031	0.032	0.082	0.021	0.033
S3B-MODIS	0.097	0.161	0.012	-0.072	0.004	-0.021	-0.012	0.059	-0.009	0.006
S3B-MISR	0.090	0.171	0.074	-0.048	0.070	0.035	0.046	0.090	0.039	0.049
June										
S3A-S3B	0.002	-0.007	-0.023	-0.024	-0.013	-0.020	-0.015	-0.006	-0.017	-0.014
S3A-MODIS	0.030	0.052	-0.035	-0.030	-0.019	-0.028	-0.024	0.045	-0.021	0.002
S3A-MISR	0.042	0.056	0.051	0.066	0.061	0.010	0.021	0.064	0.032	0.044
S3B-MODIS	0.028	0.059	-0.012	-0.006	-0.006	-0.008	-0.009	0.051	-0.004	0.016
S3B-MISR	0.040	0.063	0.074	0.090	0.074	0.030	0.036	0.070	0.049	0.058
September										
S3A-S3B	-0.012	-0.017	0.008	-0.008	-0.004	-0.009	-0.015	-0.002	-0.015	-0.011
S3A-MODIS	0.026	0.069	-0.054	-0.014	-0.057	-0.022	-0.024	0.027	-0.030	-0.014
S3A-MISR	0.064	0.085	0.096	0.050	0.118	0.046	0.029	0.050	0.033	0.038
S3B-MODIS	0.038	0.086	-0.062	-0.006	-0.053	-0.013	-0.009	0.029	-0.015	-0.003
S3B-MISR	0.076	0.102	0.088	0.058	0.122	0.055	0.044	0.052	0.048	0.049
December										
S3A-S3B	0.002	-0.008	-0.011	-0.013	-0.014	-0.015	-0.014	-0.016	-0.014	-0.014
S3A-MODIS	0.036	0.069	0.000	0.012	-0.007	-0.028	-0.027	0.059	-0.033	-0.014
S3A-MISR	0.065	0.086	0.062	0.067	0.049	0.031	0.028	0.071	0.020	0.030
S3B-MODIS	0.034	0.077	0.011	0.025	0.007	-0.013	-0.013	0.075	-0.019	0.000
S3B-MISR	0.063	0.094	0.073	0.080	0.063	0.046	0.042	0.087	0.034	0.044

To estimate the maximum value (limit) for the difference in AOD between two products, which allows to conclude if products are close to each other (difference between products is below that limit) or significant difference between products exists (difference between products is above that limit), we introduce the concept of an accepted difference (AD).The root sum squared method, which assumes that the normal distribution describes the variation of dimensions, has been applied to calculate an accepted difference (AD) as in:

$$AD = \sqrt{ae_1^2 + ae_2^2},$$

where ae_1 and ae_2 are accepted errors for the inter-compared AOD products 1 (AOD_1, product for evaluation) and 2 (AOD_2, reference product), respectively.

Accepted errors were defined based on the GCOS requirements for AOD (003; 10%) applied to the monthly AOD averaged over each region of interest. For AOD<=0.3, *ae*=0.03; for AOD>0.3, *ae*=AOD*0.1 (10% of AOD).

Relative difference (RD) has been calculated as in

$$RD = \frac{AOD_1 - AOD_2}{AD},$$

|RD|<1 shows that the difference between two products is within the AD.

RD results showing the difference between products above the accepted difference (|RD|>1) were classified according to the *sign of difference* (negative difference, **N**, when AOD from the evaluated product is lower than that from the reference product ($AOD_1<AOD_2$)), or positive difference, **P**, opposite case when $AOD_1>AOD_2$) and *value of difference* (RD increases from group 1 (**g1**) to group 3 (**g3**)), as summarized in Table 6.3.

Table 9.3 *Classification of the groups considered in the analysis of the relative difference between the products, based on the RD sign and range.*

RD	<-2.0	<-1.5	<-1.0		>1.0	>1.5	>2.0
Group	Ng3	Ng2	Ng1		Pg1	Pg2	Pg3

Relative differences between evaluating (AATSR, S3A, S3B) and reference (MODIS, MISR, PARASOL) products, and between S3A and S3B, are presented in Table 6.4. Cases where RD accedes the AD are coloured (blue for negative, red for positive); intensity of the colour increases with the RD increase, according to the group classification.

Over land, ocean and globe, the difference between AATSR and GRASP is within the accepted difference. AATSR AOD is higher than MISR AOD (Pg1) over land and lower than MODIS AOD (Ng1) over ocean. Differences between AATSR and MISR over ocean and AATSR and MODIS over lands are within AD.

Regional analysis shows a considerable difference between the products. In March, June and September, AATSR AOD over Australia is much higher (Pg3) than AOD from MODIS, MISR and POLDER. Similar differences (Pg2, Pg3) are often observed over South America. Over China SE, AATSR AOD is lower than MODIS but often higher than MISR. AATSR AOD is often lower over the Atlantic, both over dust transport (Ng3 with MODIS in March, June and September) and biomass burning transport (Ng3 with MODIS and POLDER in September) areas. Over Eur, AATSR retrieves lower AOD than POLDER in March and June (both are in Ng2), while difference with MODIS and MISR AOD is within accepted value. AATSR product shows negligible of negative AOD difference with MODIS and MISR over Bor, AsN, NAW, NAE, Ind, AOd, AOb, InO and PO.

Table 9.4 *Relative AOD difference between AATSR and MODIS, MISR and POLDER monthly AOD for regions defined as in Figure 6.3, for year 2008. Cases with RD>1 (AOD difference is outside the accepted difference) are coloured; legend below the table.*

regions	Eur	Bor	AsN	AsW	AsE	ChinaSE	Aus	AfN	AfS	SA	NAW	NAE	Ind	AOd	AOb	InO	PO	Land	Ocean	Globe
March																				
AATSR-MODIS	-0.97	-0.68	-2.38	-0.38	-1.50	-2.24	2.71	0.40	0.94	1.18	0.21	-0.24	-1.23	-1.93	-1.37	-1.20	-1.23	0.16	-1.13	-0.80
AATSR-MISR	-0.28	-0.64	-0.31	0.97	1.14	0.45	2.33	1.22	0.63	1.93	0.59	-0.45	0.24	-0.99	0.09	0.07	0.12	1.13	-0.16	0.14
AATSR-POLDER	-1.77	-2.92	-2.17	0.63	-0.97	-1.95	2.64	2.22	-1.57	2.05	-0.90	-0.35	0.28	-0.80	-0.24	-0.12	0.12	0.16	-0.19	-0.07
June																				
AATSR-MODIS	-1.81	-0.99	-1.41	-2.43	-1.66	-1.92	3.13	1.12	1.01	2.88	-1.32	-0.90	-1.25	-3.00	-1.20	-0.90	-0.90	-0.31	-1.32	-0.87
AATSR-MISR	-0.14	-0.16	-0.21	-0.45	1.55	2.08	2.90	0.42	1.79	3.49	-0.45	-1.01	0.45	-1.44	0.33	-0.31	0.02	0.68	-0.19	0.19
AATSR-POLDER	0.02	-0.97	-0.82	0.84	-1.68	-1.28	3.25	3.28	0.49	3.37	-1.53	-0.73	0.14	-1.56	-0.49	-0.40	-0.12	0.64	-0.45	-0.02
September																				
AATSR-MODIS	-0.38	-0.54	-0.07	-0.97	-0.53	-0.59	3.42	0.92	0.93	1.89	-0.57	-0.59	-1.70	-2.00	-3.71	-1.20	-1.20	0.52	-1.30	-0.73
AATSR-MISR	0.85	-0.07	0.09	0.66	1.73	1.60	2.31	0.92	1.16	2.47	0.45	-0.31	0.42	-0.66	-0.49	0.05	-0.05	1.13	-0.14	0.26
AATSR-POLDER	-0.05	-0.82	-0.12	-0.82	-0.43	0.14	2.66	0.87	-1.66	1.34	-0.09	-0.40	0.16	-0.73	-2.00	-0.05	0.12	0.19	-0.09	0.02
December																				
AATSR-MODIS	-1.01	NaN	-1.20	0.66	-0.73	-1.07	1.74	0.00	1.39	1.37	0.00	-0.09	-1.08	-1.23	-1.91	-1.23	-1.04	0.80	-1.18	-0.75
AATSR-MISR	-0.31	NaN	-0.47	1.91	1.72	1.81	0.75	0.52	0.64	1.53	0.49	0.09	0.38	0.00	-0.45	-0.05	0.09	1.25	-0.14	0.14
AATSR-POLDER	-0.73	NaN	-2.07	1.37	-1.03	-1.34	1.58	0.19	-1.73	1.63	-0.14	-0.21	0.28	-0.47	-1.18	0.07	0.28	0.26	0.09	0.14

RD	<-2.0	<-1.5	<-1.0		>1.0	>1.5	>2.0
Group	Ng3	Ng2	Ng1		Pg1	Pg2	Pg3

Similar analysis has been performed to evaluate a difference between S3A, S3B, MODIS and MISR satellite monthly AOD products. The results of the analysis are shown in Table 6.5.

Differences between S3A and S3B AOD are, with few exceptions (AOd region, March), within the accepted value. Being close to each other in AOD retrieved, S3A and S3B products show similar global and regional differences with MODIS and MISR, respectively. Because of that, difference between S3 products and MODIS and MISR AOD products will be discussed below.

Positive offsets between S3 and MODIS and MISR are observed over land. In both NH and SH, difference between S3 AOD and MISR AOD is high (Pg2, Pg3). AOD difference with MODIS is, in general, within AD in the NH, while in the SH difference with MODIS often as high as for Pg2-Pg3.

AfN is the only region, where S3 AOD is lower than MODIS and MISR AOD in March and September. In June and December difference with MISR is within the AD, difference with MODIS is slightly above the AD (Pg1) in June and within the AD in December.

Over ocean, difference between S3 and MODIS and MISR is, with only few exceptions, within the AD. However, S3 AOD is higher (Pg1-Pg3) than MISR AOD in dust and biomass burning transport areas (AOd, AOb). AOd region in March is the only region, where the difference between S3A and S3B AOD fits to the group Pg2. Over Indian and Pacific oceans difference between S3 and MODIS (all cases) and MISR (except for few cases from Pg1) is within AD.

Globally, differences between S3A and MODIS and MISR are within AD. Difference between S3B and MODIS is within AD, while difference with MISR is a bit higher (Pg1).

Table 9.5 *Relative AOD difference between S3A, S3B, MODIS and MISR monthly AOD for regions defined as in Figure 6.3, for year 2019. Cases with RD>1(AOD difference is outside the accepted difference) and regions from the Northern and Southern hemispheres (NH and SH, respectively) are coloured; legend below the Table.*

regions	Eur	Bor	AsN	AsW	AsE	ChinaSE	Aus	AfN	AfS	SA	NAW	NAE	Ind	AOd	AOb	InO	PO	Land	Ocean	Globe
March																				
S3A-S3B	-0.35	0.07	-0.19	-0.59	-1.01	-0.85	-0.14	-0.35	0.25	0.00	-0.47	-0.16	-0.38	1.67	-0.45	-0.09	-0.33	-0.19	-0.42	-0.38
S3A-MODIS	1.93	0.31	3.54	0.42	-0.34	-0.50	1.39	-1.81	1.74	1.72	1.81	3.63	-0.09	-0.02	-0.35	-0.59	-0.61	1.20	-0.64	-0.24
S3A-MISR	2.22	2.66	5.15	1.71	2.36	1.89	0.42	-1.71	0.90	2.69	1.65	3.87	1.37	0.54	1.20	0.73	0.75	1.93	0.49	0.78
S3B-MODIS	2.29	0.24	3.69	1.01	0.67	0.35	1.53	-1.47	1.52	1.72	2.29	3.79	0.28	-1.69	0.09	-0.49	-0.28	1.39	-0.21	0.14
S3B-MISR	2.57	2.59	5.27	2.27	3.28	2.69	0.57	-1.36	0.65	2.69	2.12	4.03	1.74	-1.13	1.65	0.82	1.08	2.12	0.92	1.15
June																				
S3A-S3B	-0.16	-0.24	-0.38	-0.28	0.24	0.34	-0.19	0.14	-0.10	-0.09	0.05	-0.16	-0.54	-0.55	-0.31	-0.47	-0.35	-0.14	-0.40	-0.33
S3A-MODIS	0.87	0.97	0.73	0.94	0.98	0.71	0.99	1.22	1.38	1.08	0.71	1.23	-0.82	-0.68	-0.45	-0.66	-0.57	1.06	-0.49	0.05
S3A-MISR	2.00	2.47	0.92	0.92	2.21	2.74	0.90	-0.53	2.87	1.91	0.99	1.32	1.20	1.56	1.44	0.24	0.49	1.51	0.75	1.04
S3B-MODIS	1.04	1.20	1.11	1.22	0.74	0.36	1.18	1.08	1.48	1.18	0.66	1.39	-0.28	-0.13	-0.14	-0.19	-0.21	1.20	-0.09	0.38
S3B-MISR	2.17	2.71	1.30	1.20	1.98	2.42	1.08	-0.67	2.96	2.00	0.94	1.48	1.74	2.07	1.74	0.71	0.85	1.65	1.15	1.37
September																				
S3A-S3B	-0.21	0.07	-0.49	-0.35	-0.68	-0.64	0.07	0.38	0.35	0.37	-0.28	-0.40	0.18	-0.19	-0.08	-0.21	-0.35	-0.05	-0.35	-0.26
S3A-MODIS	0.24	-1.23	1.77	0.96	0.50	0.29	1.30	-1.06	2.41	1.39	0.61	1.63	-1.11	-0.33	-1.10	-0.52	-0.57	0.64	-0.71	-0.33
S3A-MISR	1.01	0.12	2.17	1.98	2.26	2.41	0.07	-1.84	2.16	2.06	1.51	2.00	2.20	1.18	2.62	1.08	0.68	1.18	0.78	0.90
S3B-MODIS	0.45	-1.30	2.26	1.30	1.18	0.92	1.23	-1.41	2.08	1.04	0.90	2.03	-1.28	-0.14	-1.02	-0.31	-0.21	0.68	-0.35	-0.07
S3B-MISR	1.23	0.05	2.66	2.29	2.87	2.98	0.00	-2.17	1.82	1.72	1.79	2.40	2.04	1.37	2.69	1.30	1.04	1.23	1.13	1.15
December																				
S3A-S3B	-0.07	NaN	-0.52	-0.09	-0.59	-0.75	-0.16	-0.66	-0.38	-0.42	0.05	-0.19	-0.26	-0.31	-0.33	-0.35	-0.33	-0.38	-0.33	-0.33
S3A-MODIS	-0.31	NaN	1.23	-1.11	-0.90	-1.44	2.71	0.33	2.40	3.28	0.85	1.63	0.00	0.28	-0.16	-0.66	-0.64	1.39	-0.78	-0.33
S3A-MISR	0.73	NaN	1.63	0.64	1.04	1.08	0.64	0.68	1.60	3.13	1.53	2.03	1.46	1.58	1.15	0.73	0.66	1.67	0.47	0.71
S3B-MODIS	-0.24	NaN	1.74	-1.01	-0.31	-0.68	2.88	0.99	2.78	3.70	0.80	1.81	0.26	0.59	0.16	-0.31	-0.31	1.77	-0.45	0.00
S3B-MISR	0.80	NaN	2.14	0.73	1.63	1.84	0.80	1.34	1.98	3.56	1.48	2.22	1.72	1.89	1.48	1.08	0.99	2.05	0.80	1.04

	NH	SH			RD	<-2.0	<-1.5	<-1.0		>1.0	>1.5	>2.0
					Group	Ng3	Ng2	Ng1		Pg1	Pg2	Pg3

Summary for the inter-comparison to other satellite AOD products (SU v1.11)

- Over land, ocean and globally, the difference between AATSR and GRASP is within the accepted difference estimated with the root sum squared method considering the GCOS requirements for AOD. AATSR AOD is higher than MISR AOD over land and lower than MODIS AOD over ocean; both differenced are slightly above the accepted difference. Differences between AATSR and MISR over ocean and AATSR and MODIS over lands are within AD. Regional analysis shows a considerable difference between the products.
- Differences between S3A and S3B AOD are, with one exception for AOd region in March, within the accepted value.
- Positive offsets between S3 (S3A and S3B) and MODIS/MISR AOD products are observed over land. Over ocean, difference between S3 and MODIS and MISR is, with only few exceptions, within the AD. Globally, differences between S3A and MODIS and MISR are within AD. Difference between S3B and MODIS is within AD, while difference with MISR is slightly higher. Regional analysis shows a considerable difference between the products.

6.2 Inter-comparison of (A)ATSR/SLSTR SU AOD product versions

6.2.1 ATSR2 and AATSR SU AOD v4.33 vs v4.32: coverage, global and regional AOD distribution

ATSR2 SU monthly AOD products retrieved with two different versions, v4.33 and v.4.32, and the difference in monthly AOD between two products (v.4.33 – v.4.32) are shown in Fig.6.7 for March, June, September and December 1998. For the ***AATSR***, similar data are shown in Fig.6.9 for year 2008. Difference between products will be discussed regarding (i) coverage, (ii) AOD spatial global/land/ocean distribution and (iii) regional AOD differences.

Difference in coverage in ***ATSR2*** SU AOD product retrieved with algorithm v4.33 and v4.32, especially over ocean, is clearly seen in Fig.6.7; difference in ***AATSR*** SU AOD is not easily recognised with visual inspection of the AOD maps, Fig.6.9.

In Table 6.6 we show changes in the coverage (in %) in SU v4.33 AOD monthly product with respect to the coverage in v4.32 for ATSR2 and AATSR over the globe, land and ocean. For ***ATSR2***, the global coverage has been increased by 58% in March with the main contribution from the increased coverage over ocean (by 75% with respect to v4.32). Second high increase in coverage (41.1% globally, 57.6% over ocean) has been observed in September. The smallest changes in coverage (4.4% and 5.2% globally and over ocean, respectively) are observed in December. Statistical analysis of the changes in coverage in the ***AATSR*** products confirm our conclusions made by the visual inspection. For all months, difference in coverage between v.4.33 and v.4.32 is less than 1%.

Table 9.6 *Changes in coverage (in %) in SU v4.33 AOD monthly product with respect to the coverage in v4.32 for ATSR2 (1998) and AATSR (2008) over the globe, land and ocean, for March, June, September and December.*

product	**ATSR2 (1998)**			**AATSR (2008)**		
month	**globe**	**land**	**ocean**	**globe**	**land**	**ocean**
March	58.0	22.6	75.1	0.1	0.0	0.1
June	26.3	16.8	34.2	0.1	0.0	0.1
September	41.1	16.8	57.6	0.1	0.0	0.1
December	4.4	2.0	5.2	0.8	0.4	0.8

When a difference in coverage between products exists, the direct comparison of the global/land/ocean AOD means does not necessarily show the difference related to the processors applied. To reveal the contribution of the application of different processors to the global/land/ocean means, pixel-by-pixel difference in AOD should be studied over an area of interest.

Spatial differences in monthly AOD between v.4.33 and v4.32 (v.4.33-v.4.32) for collocated pixels (pixels retrieved in both v.4.33 and v.4.32 products) are shown in Fig.6.7 and Fig.6.9 (right panels) for ***ATSR2 and AATSR***, respectively. For ATSR2, differences in AOD for collocated pixels over ocean are, with a few exceptions, around 0, which resulted with less than -0.002 AOD difference over ocean globally. Over land, highest differences in AOD (up to ±0.03 AOD) are observed over the Saharan desert in March and June and over biomass burning areas in central/south Africa and Amazon in September, which is a month from a typical biomass burning season. In December an offset between two products is small (about -0.001 over land, 0.000 over ocean and globally).

Monthly scatter density plots for the collocated monthly AOD ***ATSR2*** pixels retrieved over land and over ocean with processor versions v.4.32 and v4.33 are shown in Fig.6.8. Fit of the density plot is shown as AOD averaged over selected bins (of 0.1 AOD); for each bin, AOD standard deviation is shown as error bar. A common tendency for all four months has been observed in AOD over land, where for AOD >1 (as retrieved with v4.32) v.4.33 AOD has a negative offset (is lower compared to v.4.32). However, the contribution of the offset between pixels with AOD>1 to the global offset is small because the number of AOD>1 pixels is considerably lower than the number of AOD<1 pixels. Over ocean, no clear tendency in the offset between v4.33 and v.4.32 have been revealed.

No clear differences between ***AATSR*** SU AOD monthly products retrieved with v.4.33 and v.4.32 processors (Fig.6.9, Fig.6.10, Table 6.6) have been revealed.

Regional differences in AOD retrieved with processors 4.33 and 4.32 are shown in Fig.11 for March, June, September, December for ATSR2 (year 1998) and AATSR (2008). Regions are defined and in Fig.6.3.

ATSR2 v4.33 AOD is a bit higher in March in Asia (up to 0.13 in ChinaSE), SA and AOd. In June, difference is smaller over Asia and close to 0 for other selected regions. In September, AOD v4.33 is ca. 0.02 higher over Africa and South America and ca. 0.35 higher over AOd. In December, regional differences between ATSR2 v4.33 and v.4.32 AOD are negligible (close to 0).

Regional differences between AATSR v4.33 and v.4.32 AOD are negligible (close to 0).

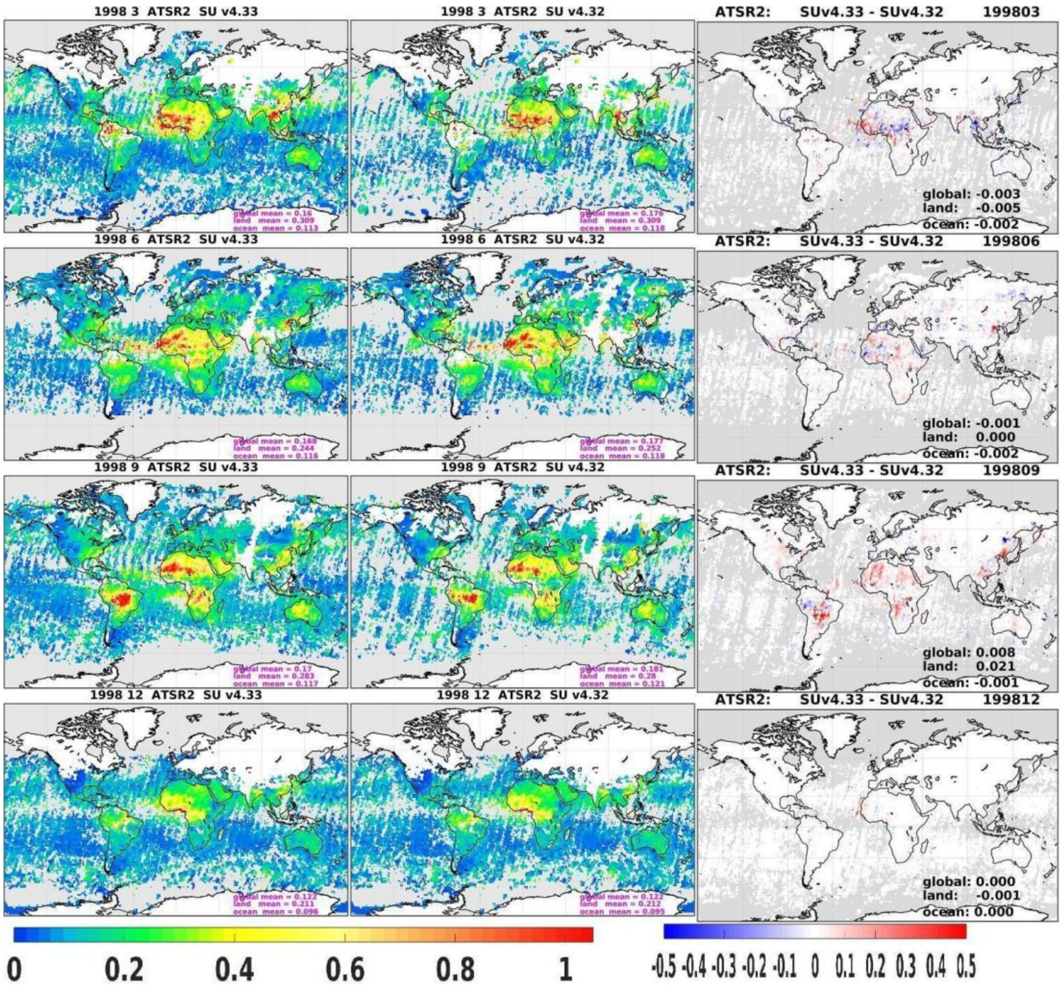

Figure 6.7 *ATSR2 SU monthly AOD v.4.33 (left column), v4.32 (middle column) and difference between versions 4.33 and 4.32 (right column), for year 1998, March, June, September, December (horizontal panels starting from the top).*

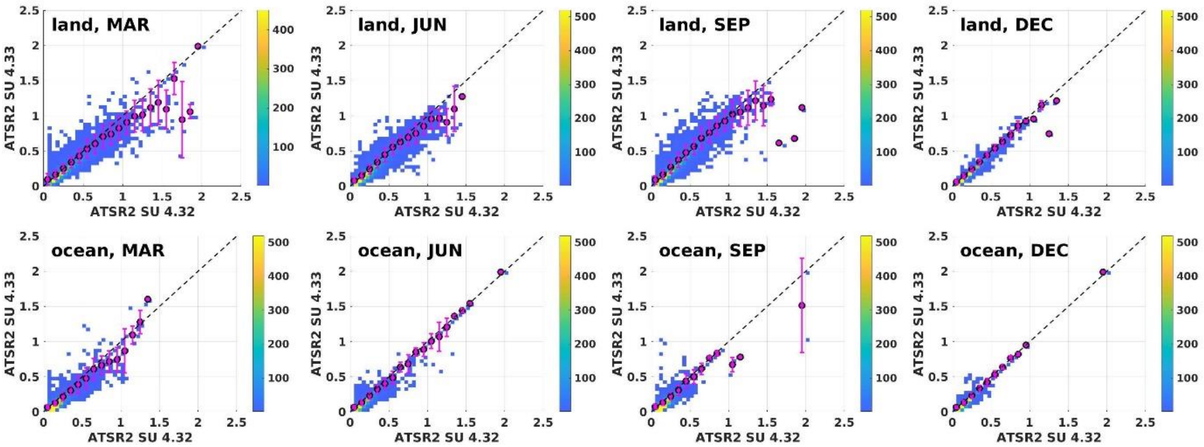

Figure 6.8 *Scatter density plots and AOD averaged over bins (magenta dots for mean, AOD std as error bars) for ATSR2 SU v.4.33 and v4.32 collocated monthly AOD, for year 1998, March, June, September, December (vertical panels), land and ocean (horizontal panels)*

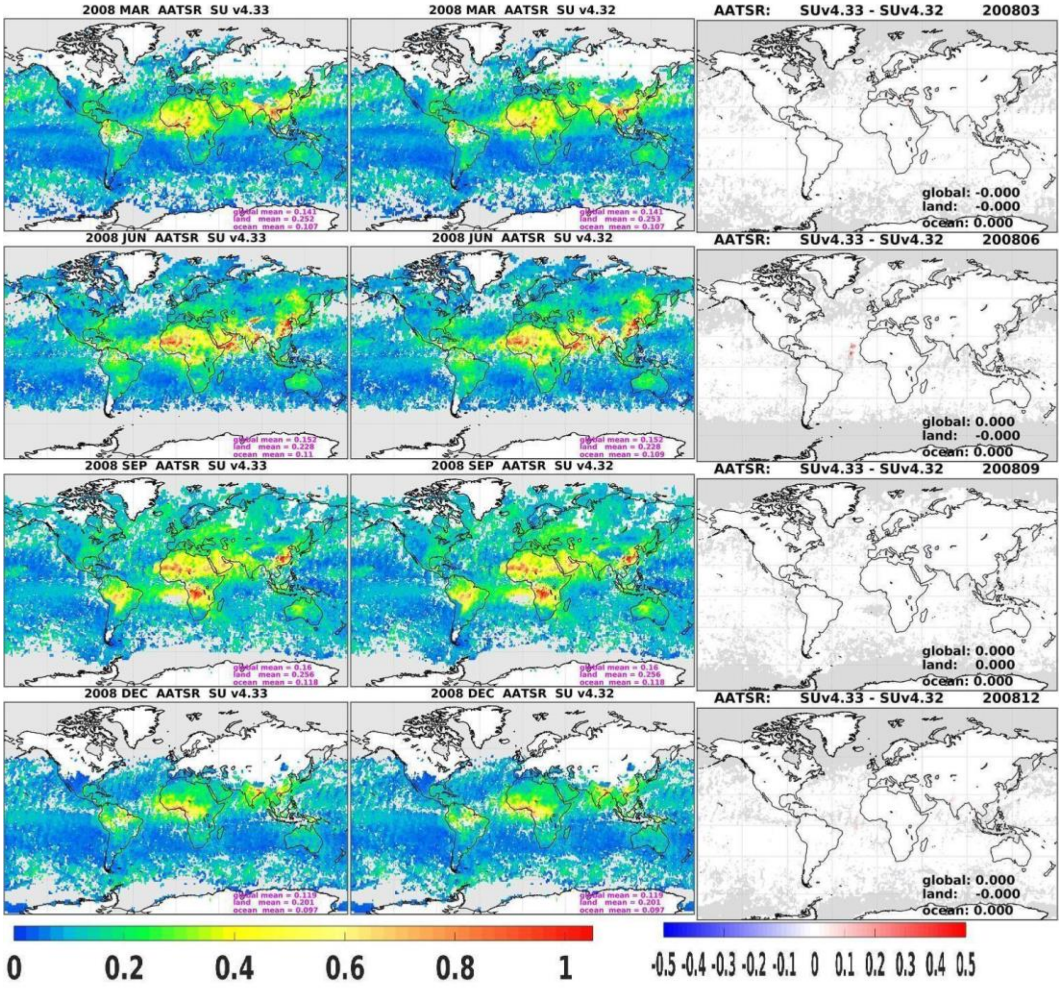

Figure 6.9 *AATSR2 SU monthly AOD as in Fig.6.7 for year 2008.*

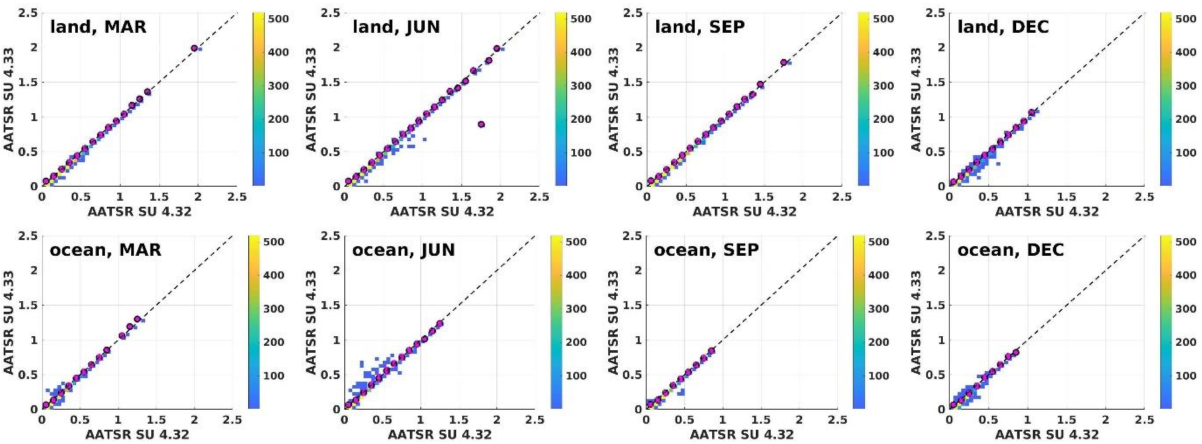

Figure 6.10 *for ATSR2 SU v.4.33 and v4.32 collocated monthly AOD, as Fig.6.8*

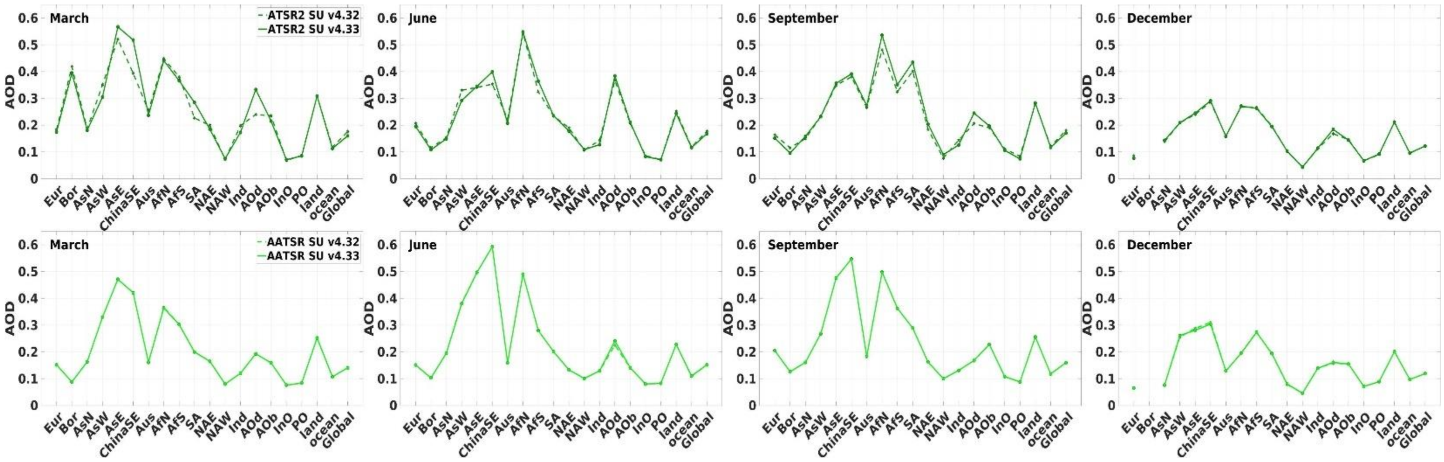

Figure 6.11 *Regional differences in AOD retrieved with processors 4.33 (solid line) and 4.32 (dashed line) for March, June, September, December (horizontal panels, top down) for ATSR2, year 1998, and AATSR, year 2008 (top down, respectively). Note, a dashed line is not visible if solid and dashed line are overlapping in case a difference between products is close to zero.*

6.2.2 S3A and S3B SU AOD v1.14 vs v1.11: coverage, global and regional AOD distribution

Similar (as in Sect.6.2.1.1, for ATSR2/AATSR SU AOD products) analysis has been performed to reveal differences in monthly AOD products retrieved with versions v1.14 and v1.11 applied to S3A and S3B instruments. Results are shown for both S3A (Fig.6.12 and Fig.6.13) and S3B (Fig.6.14 and Fig.6.15). However, since the difference between S3A and S3B AOD is small, we discuss the difference in AOD products v1.14 and v1.11 for S3A only.

In March, lower AOD has been retrieved with v.1.14 over the belt ca 30°N-50°N. The difference was as high as -0.5 AOD over plateau/desert areas east from the Caspian Sea. Positive offset between v1.14 and v1.11 is observed over bright surface areas: Sahara, Arabian Peninsula, Plateau of Iran. Positive and negative offsets cancelled partially each other, which resulted in lower (by 0.015) AOD in March over land.

In June, the belt of negative AOD offset in the NH has moved further to the North, reaching ca 70°N-75°N. Monthly AOD is lower over central Africa and south-east of Australia (west of New South Wales). Positive bias in June is located over the same areas as in March, as well as north-east from Aral Sea and over Plateau of Tibet.

In September, the 30°N-50°N belt of negative offset is observed only over Eurasia. AOD in v.1.14 is also a bit lower in the biomass burning areas in central Africa and South America. As in March and June, AOD in ver.1.14 if higher over bright surface areas: Sahara, Arabian Peninsula, Plateau of Iran. AOD is slightly higher in v1.14 also over the boreal area in the NH. September is the only month (out of four months chose for inter-comparison) when overall AOD v1.14 over land is higher than AOD v1.14.

In December, both positive and negative offsets up to ±0.02 are observed over Sahara. For the rest of the land, the offset is lower.

Difference in AOD between v1.14 and v1.11 over ocean is low, ca -0.007 for all four months; no spots of considerably higher differences have been observed.

Pixel-by-pixel AOD inter-comparison (Fig 6.13) shows that offset up to 0.6 may exist between two products. However, averaged over bins AOD closely follow 1:1 line, with some small (within ± 0.01) deviation for AOD>1.

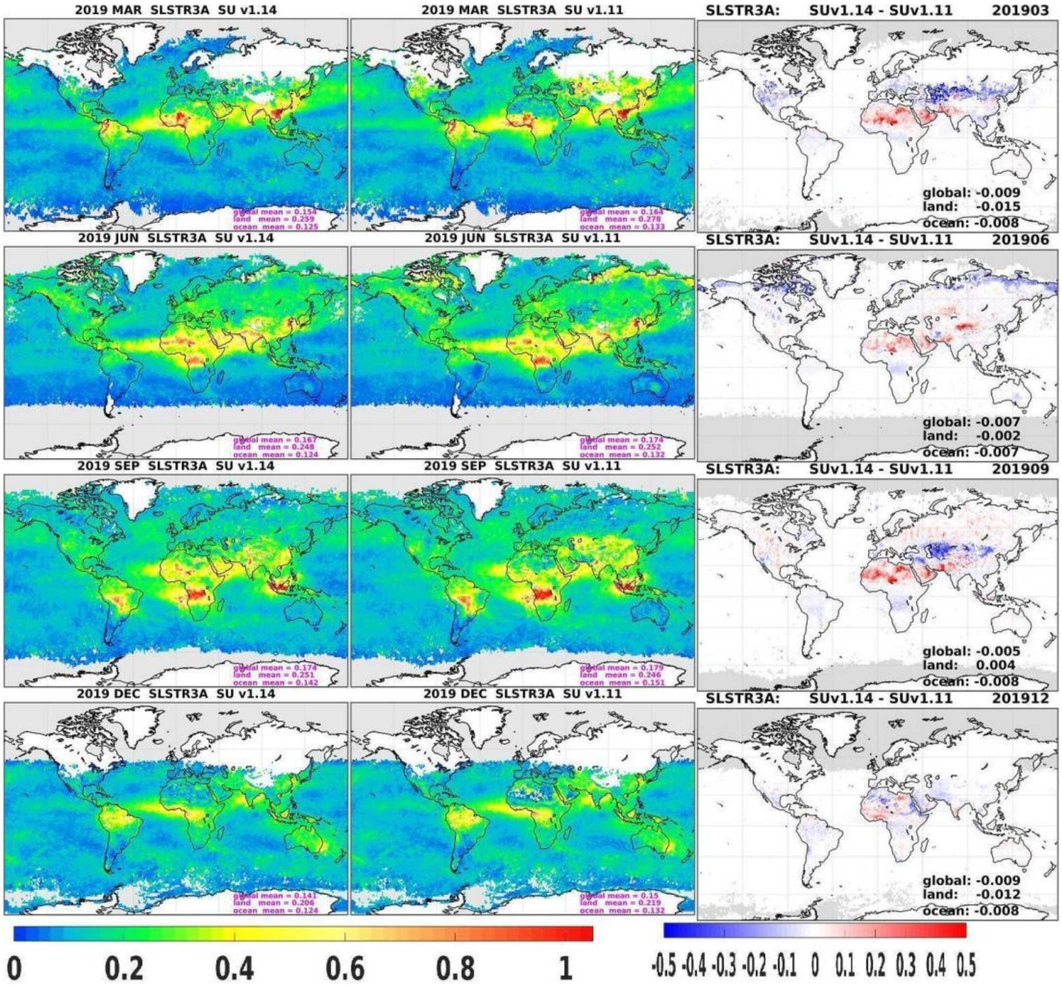

Figure 6.12 *S3A SU monthly AOD v.1.14 (left column), v1.11 (middle column) and difference between versions 1.14 and 1.11 (right column), for year 2019, March, June, September, December (horizontal panels starting from the top).*

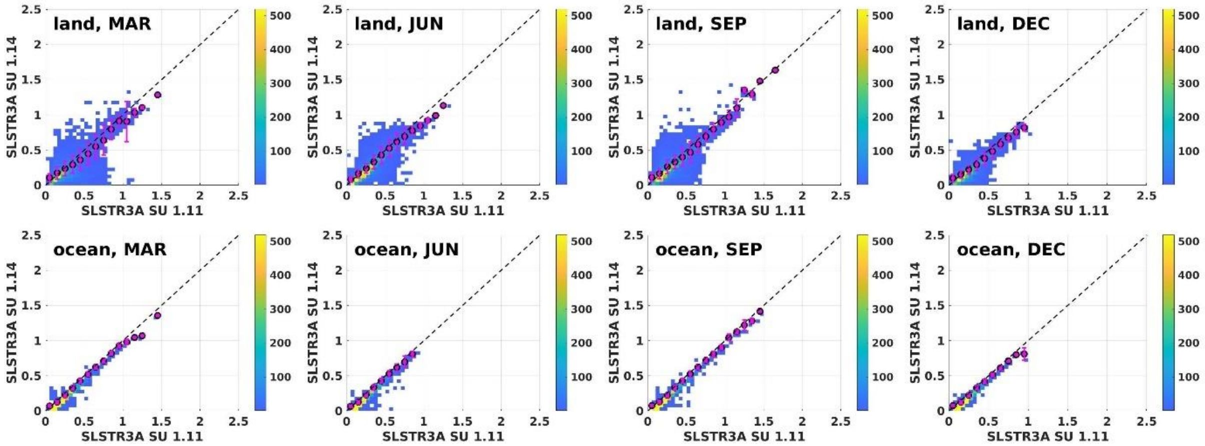

Figure 6.13 *Scatter density plots and AOD averaged over bins (magenta dots for mean, AOD std as error bars) for S3A SU v.1.14 and v1.11 collocated monthly AOD, for year 2019, March, June, September, December (vertical panels), land and ocean (horizontal panels)*

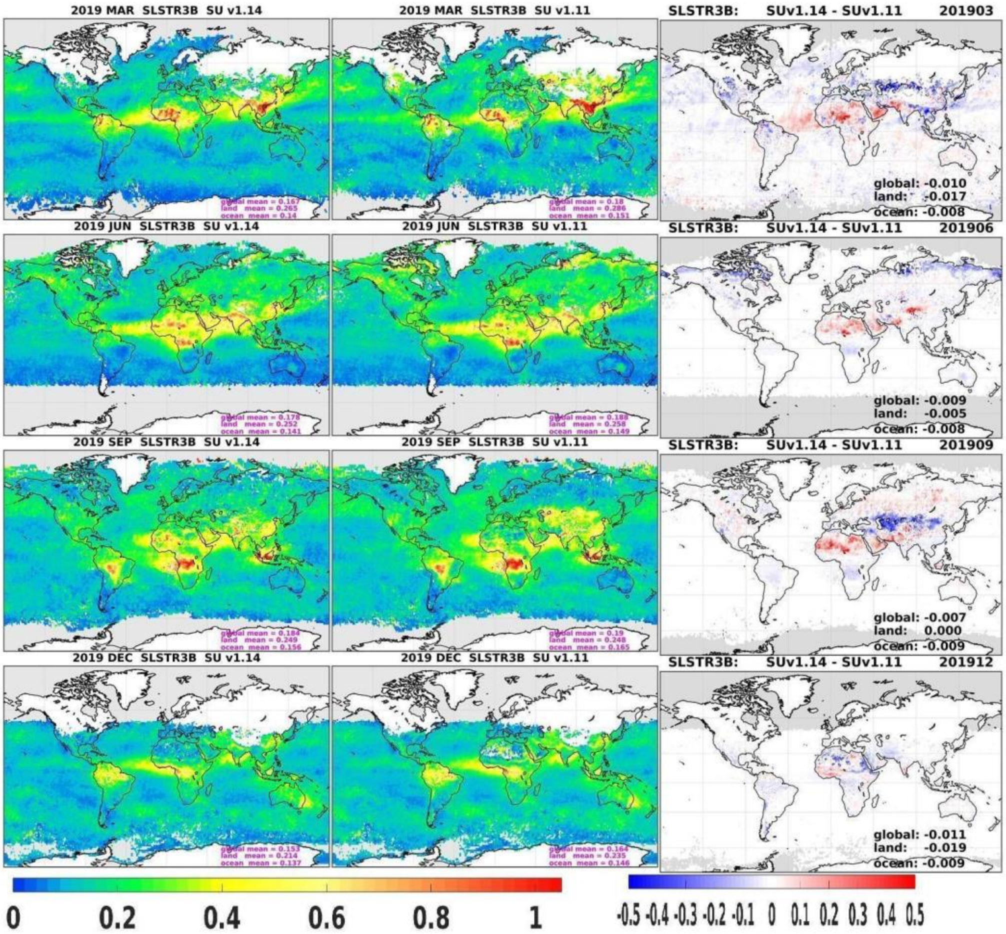

Figure 6.14 *S3B, same as Fig.6.12*

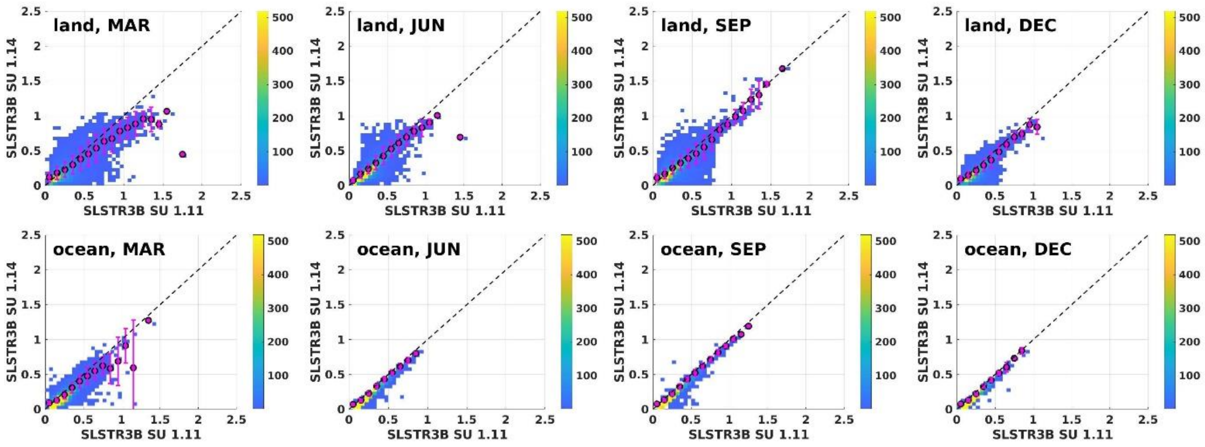

Figure 6.15 *S3B, same as Fig.6.12*

Results from the regional AOD inter-comparison (Fig.6.16) show that in March lower (by 0.1-0.2) AOD is retrieved over Eur, Bor, AsE, ChinaSE, NAW; AOD is higher over AfN and AOd. IN June, AOD is lower over Bor and higher over AfN. In September AOD is higher over AfN. For other months/regions, the difference between AOD v1.14 and AOD v1.11 is low.

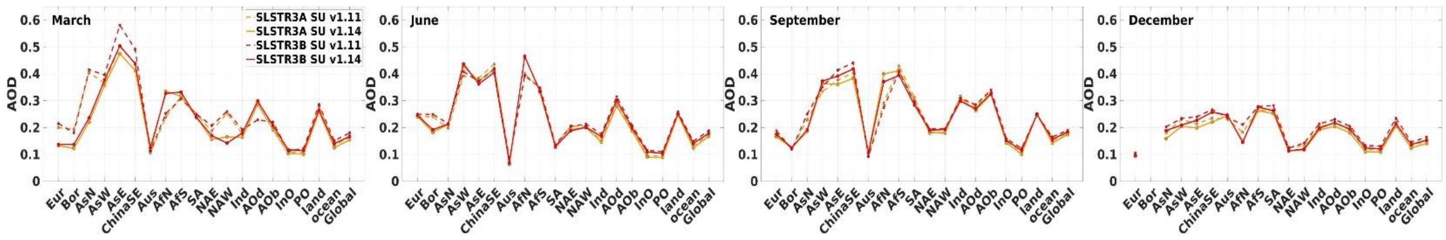

Figure 6.16 *S3A and S3B regional differences in AOD retrieved with processors 1.14 (solid line) and 1.11 (dashed line) for March, June, September, December (horizontal panels, top down), year 2019. Note, a dashed line is not visible if solid and dashed line are overlapping in case a difference between products is close to zero.*

6.3 Level3, SU (A)ATSR AOD (v4.33) and SU S3A and S3B AOD (v1.14) products evaluation: inter-comparison of monthly AOD products with other satellite monthly AOD products

In Sect 6.1 an analysis has been performed for evaluation of the AATSR SU v4.32 AOD and S3A/S3B SU v1.11 monthly AOD products with other satellite products. Inter-comparison with MODIS, MISR, POLDER has been performed for AATSR AOD evaluation; S3A and S3B SU AO>D products have been inter-compared and evaluated with MODIS and MISR. In this section, similar analysis has been applied for evaluation of the AATSR SU v4.33 AOD and S3A/S3B SU v1.14 monthly AOD products with other satellite products.

Additional analysis includes evaluation of ATSR2 SU AOD product with ATSR2 SDV v2.31 AOD. S3A RF v2.0.0 AOD available for months September and December for selected areas is inter-compared with SU v1.14 AOD.

Results from the analysis are introduced in slightly different way as in Sect. 6.1: results from evaluation of the ATSR2 AOD and AATSR AOD are combined in Sect.6.3.1 and Sect.6.3.2, respectively. Results from evaluation of S3A and S3B products are combined in Sect.6.3.3.

6.3.1 ATSR2 SU v4.33 monthly total AOD product evaluation

For year 1998, AOD products from other satellites which can be used for the evaluation of the ATSR2 SU monthly AOD product do not exist. For ATSR2 SU AOD product evaluation we use the AOD monthly product from the same satellite, ATSR2, retrieved with different algorithm, ADVv2.31 (https://climate.esa.int/sites/default/files/Aerosol_cci2_PVIR_v3.41.pdf), as a reference. In ADV, AOD is not retrieved over bright surfaces (e.g., deserts), thus inter-comparison between two AOD products is not possible over those areas.

In Fig. 6.17 we show a global AOD distribution of two monthly AOD products, SU v.4.33 and ADV v2.31, for March, June, September and December, as well as a spatial distribution of the difference between those products.

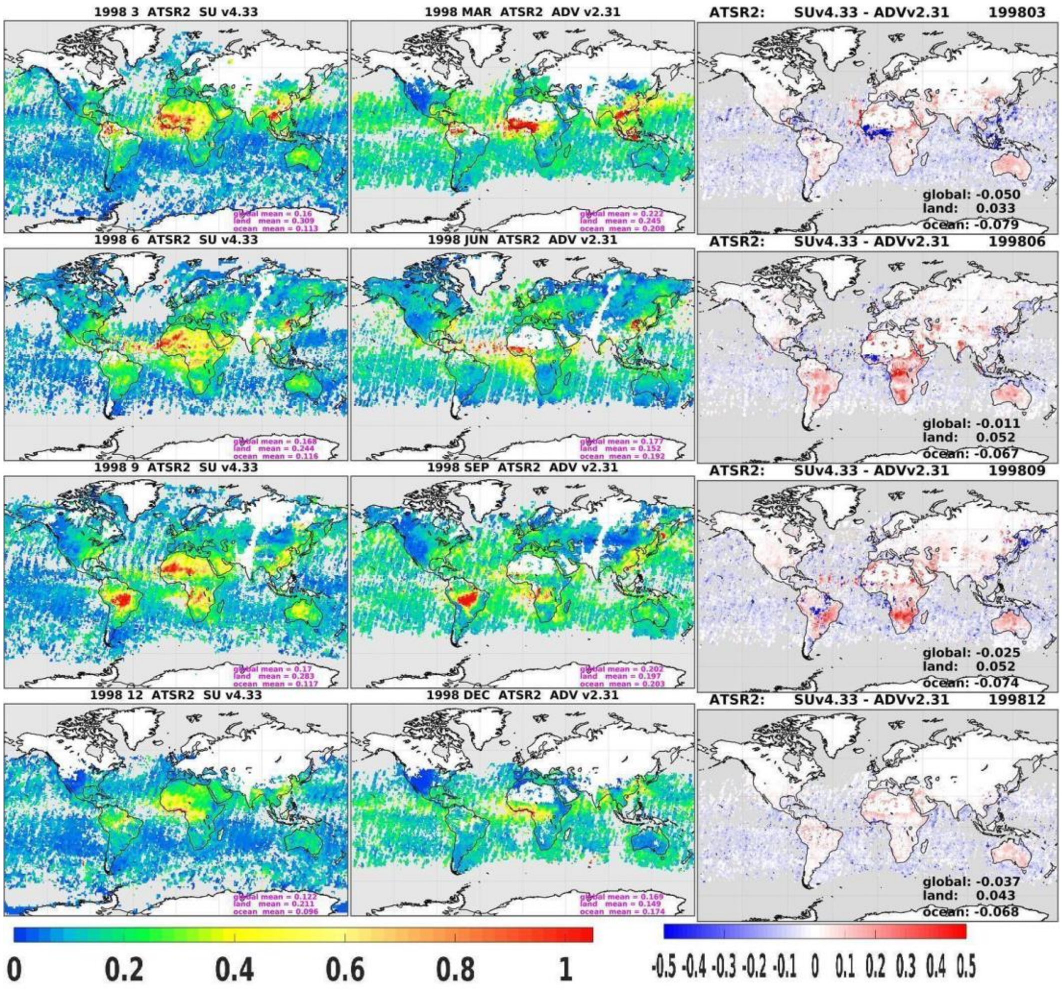

Fig. 6.17 *Monthly AOD for SU v.4.33 and ADV v2.31 products (left and middle panels, respectively) and the difference between two products (right panel) for March, June, September and December 1998 (horizontal panels top down).*

For SU AOD, better coverage in the SH in March and December, lower AOD over ocean are clearly recognized. Difference (SU-ADV) between global means calculated from *all pixels retrieved* for March/June/September/December is -0.04/-0.01/-0.07/-0.05. For land and ocean, the difference is 0.06/0.09/0.09/0.05 and -0.09/-0.08/-0.07/-0.08, respectively. Thus, SU AOD is higher over land by 0.05-0.09, lower over ocean by ca. 0.08 and globally (by 0.01-0.07) based on four months analysis. Difference calculated for *pixels retrieved in both products* is a bit lower, as in Fig.6.17, left vertical panel.

Over land, SU AOD is higher all around the globe, except for the Atlantic coast south from Sahara. Positive offset between SU and ADV AOD is higher over Africa, Australia and South. America. Negative offset over ocean is a bit higher in the equatorial zone (30°S-30°N) and lower in the directions to the poles. Regional differences between SU v4.33 and ADV v2.31 AOD monthly products are shown in Fig.6.18

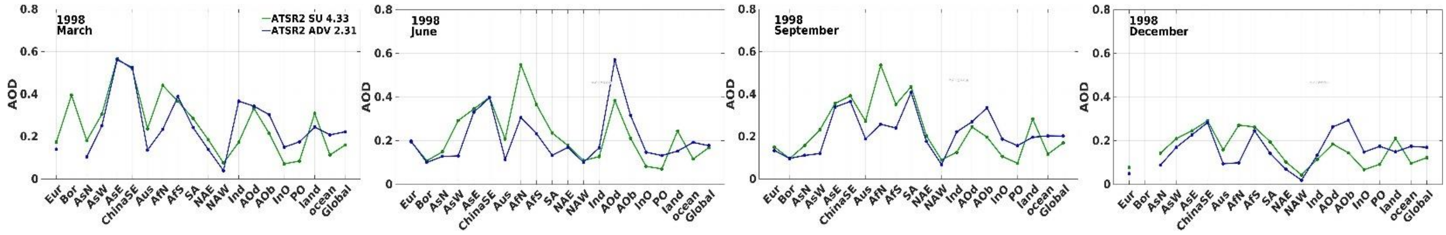

Figure 6.18 *ATSR2 SU v4.33 and ADV v2.31 monthly AOD for four months in year 1998 for different regions defined as in Fig. 6.3.*

6.3.2 AATSR SU v4.33 monthly total AOD product evaluation

Since no considerable changes in monthly AOD have been revealed between SU AOD v4.33 and v4.32 products (Sect.6.2.1), we expect that the main results for evaluation of SU v4.33 monthly AOD product with MODIS, MISR and POLDER will be similar to the SU v4.32 monthly AOD product evaluation (Sect. 6.1).

Total AOD monthly maps for AATSR SU v4.33, MODIS, MISR and POLDER for year 2008 are shown in Fig. 6.19. Visual analysis of the maps gives an impression that AATSR, MISR and POLDER monthly AOD are close to each other, while MODIS provides higher AOD.

Two main reasons for a difference between AOD products (Fig.6.19 and Fig.6.20) are: (i) difference in satellite coverage and (ii) difference in cloud screening. Second is determined mainly by the characteristics of the satellite instruments (spectral coverage), as well as differences in cloud screening approaches. To avoid cloud contamination in the AOD products, which results in unrealistically high AOD, cloud screening should be quite strict. However, if cloud screening is too strict, high aerosol loading areas are recognised as clouds; for those episodes AOD is not retrieved and monthly AOD is underestimated. Thus, the main differences between the AOD products are expected in the areas with potentially high AOD loading (e.g., dust, biomass burning, highly polluted areas), as it is clearly seen in Fig.6.20.

Globally, the difference is lower between SU AOD and POLDER AOD. In March and June, difference over land is lower between SU and MODIS; in September and December difference over land is lower between SU and POLDER. Over ocean, difference between SU and MISR and SU and POLDER is equally small (<0.01) and negative for all months, except for POLDER in December. SU AOD is lower than MODIS AOD over ocean by ca 0.05.

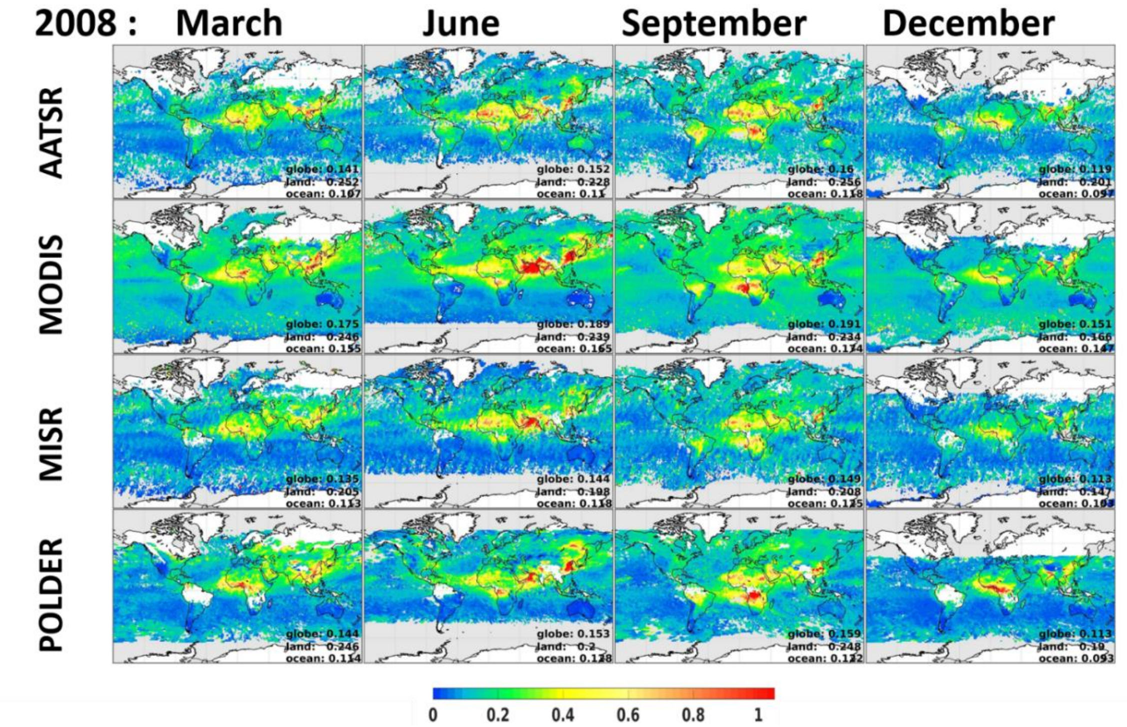

Figure 6.19 *AATSR SU v4.33, MODIS, MISR and POLDER total AOD for March, June, September and December 2008.*

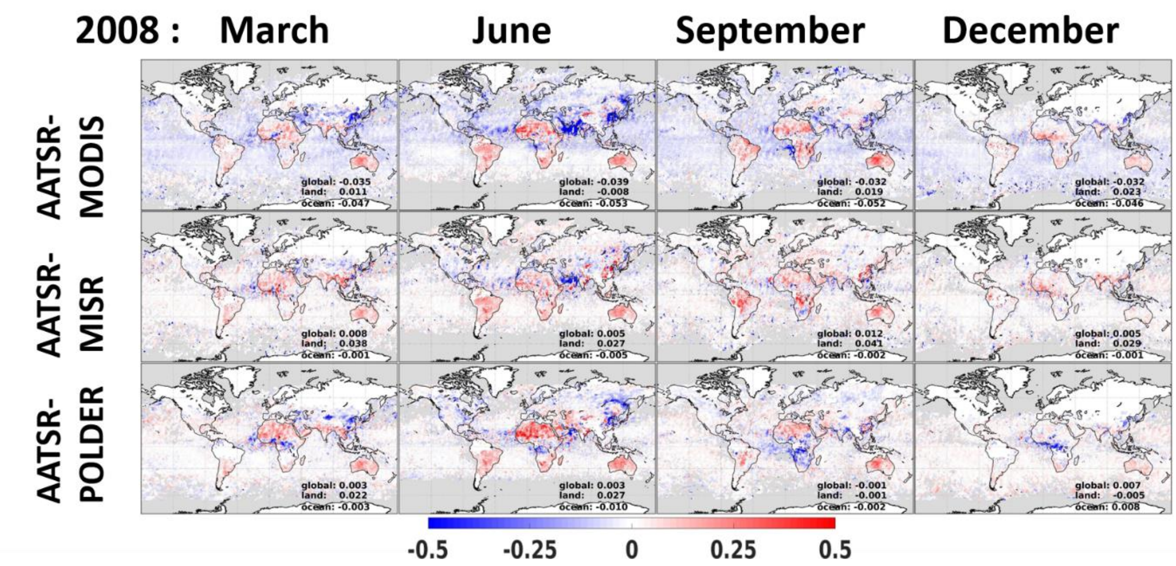

Figure 6.20 *Difference between AATSR SU v4.33 and MODIS (upper panel), AATSR SU v4.33 and MISR (middle panel), AATSR SU v4.33 and POLDER (lower panel) total monthly products, for year 2008.*

As expected, an offset between monthly AOD products (Fig.6.21) is higher in the regions with high AOD loading – Asia, Africa, areas in the Atlantic Ocean which undergo dust and biomass burning aerosol transport. In Asia, MODIS and POLDER AOD are higher than those from the AATSR and MISR products in March and June, while in September and December the difference between AATSR and MODIS and POLDER is smaller. SU AOD is highest in AfN (Sahara) and lowest in AOd region, which is somehow contradictory. Global AOD is similar for AATSR, MISR and POLDER, while MODIS global AOD is higher.

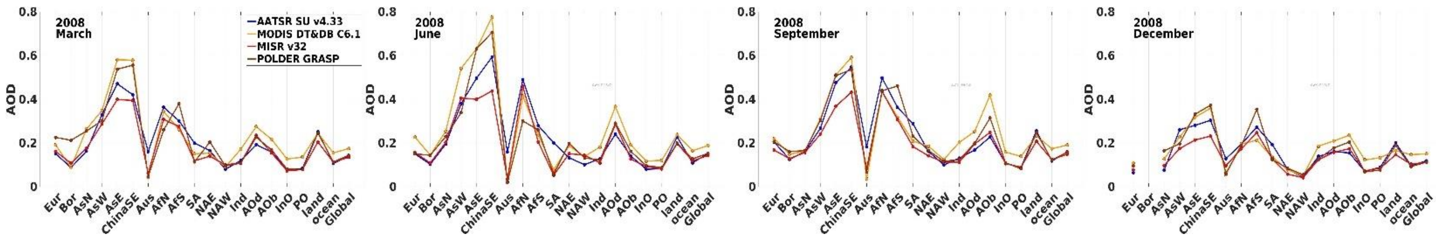

Figure 6.21 AATSR SU v4.33, MODIS , MISR and POLDER GRASP monthly AOD for four months in year 2008 for different regions defined as in Fig. 6.3.

To estimate the maximum value (limit) for the difference in AOD between two products, which allows to conclude if products are close to each other (difference between products is below that limit) or significant difference between products exists (difference between products is above that limit), we introduce the concept of an accepted difference (AD).The root sum squared method, which assumes that the normal distribution describes the variation of dimensions, has been applied to calculate an accepted difference (AD) as explained in Sect.6.1.3

Over land, ocean and globe, the difference between AATSR and POLDER is within the accepted difference. AATSR AOD is higher than MISR AOD (Pg1) over land and lower than MODIS AOD (Ng1) over ocean. Differences between AATSR and MISR over ocean and AATSR and MODIS over lands are within the AD.

Regional analysis shows a considerable difference between the products. In March, June and September, AATSR AOD over Australia is much higher (Pg3) than AOD from MODIS, MISR and POLDER. Similar differences (Pg2, Pg3) are often observed over South America. Over China SE, AATSR AOD is lower than MODIS but often higher than MISR. AATSR AOD is often lower over the Atlantic, both over dust transport (Ng3 with MODIS in March, June and September) and biomass burning transport (Ng3 with MODIS and POLDER in September) areas. Over Eur, AATSR retrieves lower AOD than POLDER in March and June (both are in Ng2), while difference with MODIS and MISR AOD is within accepted value. AATSR product shows negligible of negative AOD difference with MODIS and MISR over Bor, AsN, NAW, NAE, Ind, AOd, AOb, InO and PO.

Table 9.7 *Relative AOD difference between AATSR SU v1.14 and MODIS, MISR and POLDER monthly AOD for regions defined as in Figure 6.3, for year 2008. Cases with RD>1 (AOD difference is outside the accepted difference) are coloured; legend below the table.*

regions	Eur	Bor	AsN	AsW	AsE	ChinaSE	Aus	AfN	AfS	SA	NAW	NAE	Ind	Aod	Aob	InO	PO	Land	Ocean	Globe
March																				
AATSR-MODIS	-0,94	0,00	-2,38	-0,38	-1,47	-2,21	2,76	0,38	0,94	1,15	0,26	-0,24	-1,23	-1,93	-1,37	-1,20	-1,23	0,14	-1,13	-0,80
AATSR-MISR	-0,24	-0,47	-0,31	0,96	1,17	0,45	2,33	1,17	0,61	1,91	0,59	-0,47	0,24	-0,99	0,09	0,07	0,12	1,11	-0,14	0,14
AATSR-POLDER	-1,74	-2,95	-2,17	0,63	-0,94	-1,94	2,69	2,20	-1,61	2,03	-0,94	-0,38	0,28	-0,80	-0,24	-0,12	0,12	0,14	-0,16	-0,07
June																				
AATSR-MODIS	-1,81	-0,99	-1,39	-2,45	-1,67	-1,87	3,18	1,17	0,99	2,90	-1,27	-0,90	-1,25	-2,66	-1,20	-0,90	-0,90	-0,26	-1,30	-0,87
AATSR-MISR	-0,14	-0,14	-0,19	-0,47	1,52	2,10	2,92	0,45	1,77	3,49	-0,45	-1,01	0,45	-1,06	0,33	-0,31	0,02	0,71	-0,19	0,19
AATSR-POLDER	0,00	-0,97	-0,82	0,81	-1,67	-1,23	3,28	3,29	0,47	3,37	-1,53	-0,73	0,14	-1,18	-0,49	-0,40	-0,12	0,66	-0,42	-0,02
September																				
AATSR-MODIS	-0,35	-0,54	-0,05	-0,97	-0,50	-0,55	3,44	0,95	0,93	1,89	-0,57	-0,59	-1,70	-2,00	-3,71	-1,20	-1,20	0,52	-1,32	-0,73
AATSR-MISR	0,87	-0,07	0,09	0,64	1,80	1,65	2,33	0,94	1,16	2,47	0,47	-0,31	0,42	-0,66	-0,49	0,05	-0,05	1,13	-0,16	0,26
AATSR-POLDER	-0,02	-0,82	-0,12	-0,84	-0,46	0,14	2,71	0,89	-1,67	1,34	-0,09	-0,40	0,16	-0,73	-2,00	-0,05	0,12	0,19	-0,09	0,02
December																				
AATSR-MODIS	-1,01	NaN	-1,20	0,78	-0,85	-1,17	1,74	-0,02	1,41	1,34	0,05	-0,09	-1,11	-1,15	-1,91	-1,23	-1,04	0,82	-1,18	-0,75
AATSR-MISR	-0,28	NaN	-0,49	2,03	1,58	1,69	0,75	0,49	0,61	1,56	0,52	0,09	0,35	0,07	-0,45	-0,05	0,09	1,27	-0,14	0,14
AATSR-POLDER	-0,73	NaN	-2,10	1,51	-1,14	-1,43	1,58	0,16	-1,75	1,63	-0,12	-0,21	0,26	-0,40	-1,18	0,07	0,28	0,26	0,09	0,14
						RD	<-2.0	<-1.5	<-1.0		>1.0	>1.5	>2.0							
						Group	Ng3	Ng2	Ng1		Pg1	Pg2	Pg3							

6.3.3 S3A and S3B SU v1.14 monthly total AOD product evaluation

Total AOD monthly maps for S3A and S3B SU v1.14, MODIS, MISR, S3A RF v2.0.0 for year 2019 are shown in Fig. 6.2. Sentinel-3 instruments have wider swath, as compared to AATSR, which results in better coverage. This, a better agreement between S3A/S3A and MODIS related to close coverage is expected. In 2019, S3A and S3B AOD monthly maps look as smooth as MODIS AOD maps.

Global MODIS AOD is higher than S3A and S3B AOD for all month (except for June). MISR global AOD is lowest. Since S3A RF AOD has not been retrieved globally, global statistics for that product are not calculated.

Maps of the difference in monthly AOD between S3A and S3B SU, S3A/S3B SU and MODIS, S3A/S3B SU and MISR, S3A RF and S3A SU total AOD monthly products are shown in Fig.6.6.

Globally for all months and over land (except September), S3A SU AOD is ca. 0.01 lower than S3B AOD. Over ocean S3A AOD is ca 0.05 lower.

MODIS AOD is ca 0.01-0.02 higher than S3A/S3B SU AOD globally and over ocean. No clear offset has been revealed between MODIS and S3A/S3B SU over land. MISR AOD is lower than that from the other products.

S3A RF AOD clearly differs from the other AOD products with unrealistically high AOD e.g., over Eurasia in September (0.3-0.5 over Europe, 0.5-0.8 over Finland) and over potentially clean areas over ocean (0.3-0.5). One of the reasons for high AOD values in S3A RF AOD product can be cloud contamination, which may be a consequence from the absence of cloud masking module in the aerosol retrieval in RF (CISAR) algorithm.

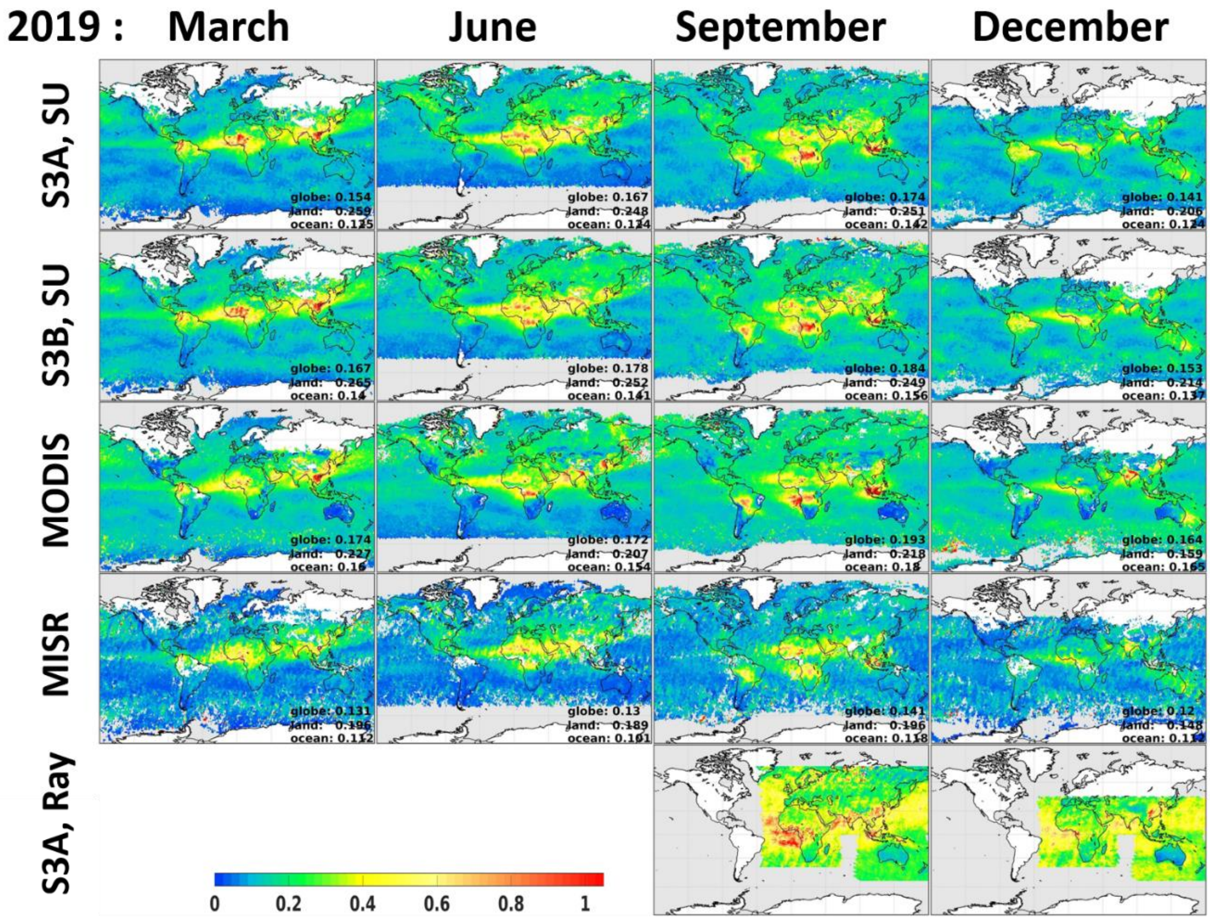

Figure 6.22 *Sentinel-3A (S3A), Sentinel-3B (S3B) SU v1.14, MODIS and MISR total AOD for March, June, September and December 2019. S3A RF v2.0.0 AOD is available for certain regions in September and December*

Differences between SU v1.14 S3A and S3B, S3A/S3B and MODIS, S3A/S3B and MISR total AOD monthly products are shown in Fig.6.23. Compared with SU v1.11, difference between S3A and S3B AOD has not changed much globally, over land and ocean. However, global/land/ocean differences with MODIS have changed (in most cases increased) in absolute values and in sign (e.g., difference in global AOD between S3B SU and MODIS). Some of the areas with positive/negative offsets have changed in size and/or moved. S3A/S3B SU global/land/ocean differences with MISR have decreased by 0.01-0.02 AOD.

S3A RF AOD over ocean is 0.2-0.45 higher compared with other AOD products (Fig.6.24). Over land, S3A RF AOD is lower by 0.3-0.4 over Saharan desert, biomass burning areas in South Africa and Indonesia in September and over some areas in Australia in December.

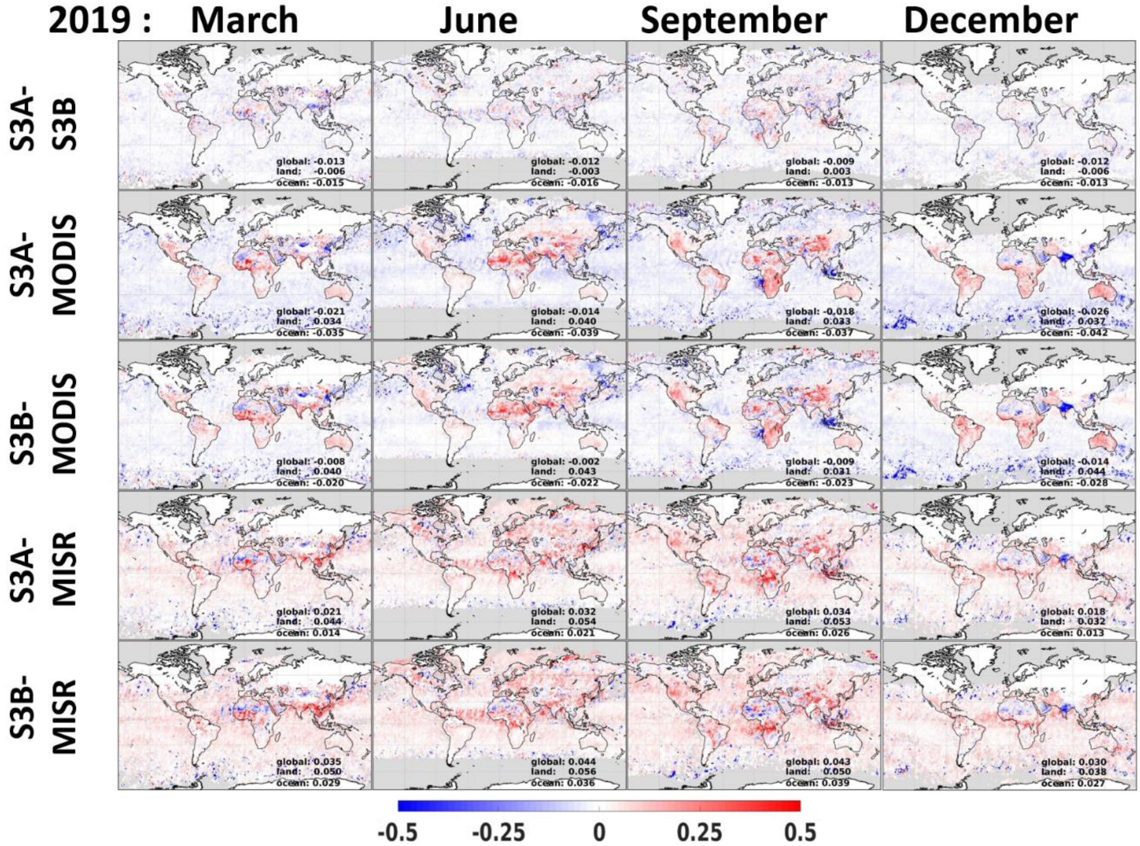

Figure 6.23 *Differences between SU v1.14 S3A and S3B, S3A/S3B and MODIS, S3A/S3B and MISR total AOD monthly products, for March, June, September and December 2019.*

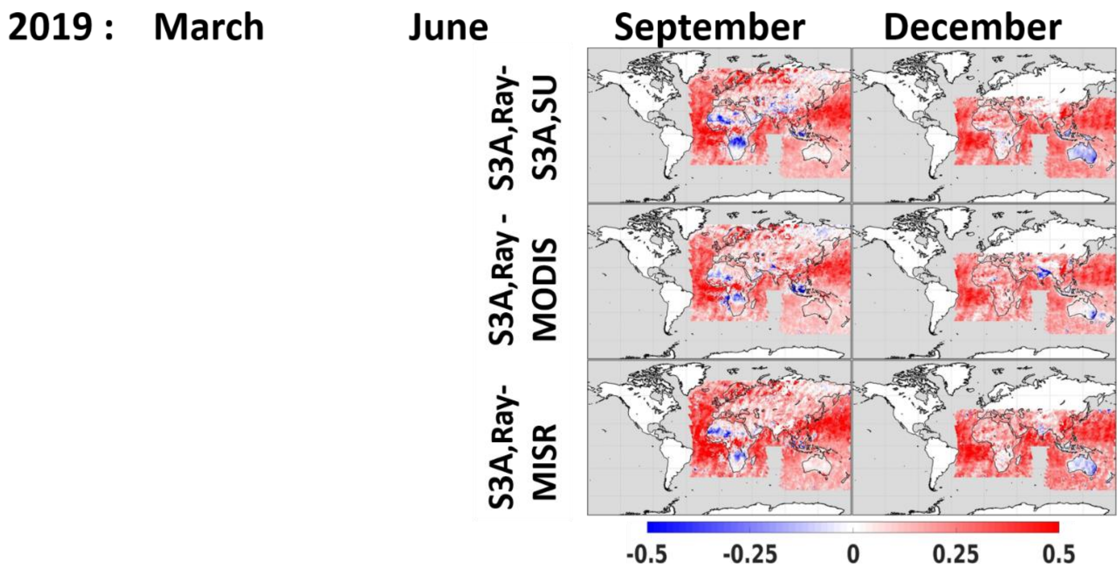

Figure 6.24 *Difference between S3A RF v2.0.0 and S3A SU v1.14 (upper panel), MODIS (middle panel) and MISR (lower panel) total AOD monthly products, for September and December 2019.*

Difference between S3A and S3B SU v1.14 AOD is close to 0 in all regions defined in Fig.3, except for AsE and ChinaSE, where S3B is slightly higher (Fig.6.25). S3A/S3B total AOD is close to the MODIS product for Europe, Asia, Indonesia, dust and biomass burning areas. In South Africa, South and North America S3A/S3B SU AOD is higher than MODIS and MISR, which are close to each other.

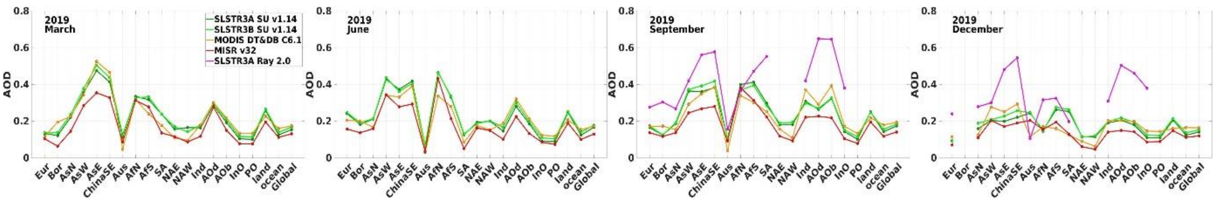

Figure 6.25 S3A/S3B SU v1.14, MODIS, MISR, S3A RF v2.0.0 monthly AOD for four months in year 2019 for different regions defined as in Fig. 6.3.

S3A RF v2.0.0 monthly AOD regional means for September and December 2019 are shown in Fig.6.25 for the regions which are covered in the product. All regions for which the mean AOD values are shown, except AOd, are fully covered in the RF product, thus S3A RF regional AOD values are directly comparable with S3A/S3B SU, MODIS and MISR monthly AOD products. In September, RF AOD is up to 0.1-0.3 higher in all regions (Eur, Bor, AsN, AsE, ChinaSE, Aus, AfS, SA, Ind, AOd, AOb, InO) except for AfN. In AfN, AOD is lower over Sahara and higher for other areas in the region. In December, RF AOD is higher over all regions except Aus, where RF AOD is as low as MODIS, and SA, where S3A RF AOD is higher than MODIS and MISR but lower than S3A/S3B SU AOD.

AD analysis (see Sect.6.1.3 for details) has been performed to evaluate a difference between S3A/S3B SU v.1.14, MODIS and MISR satellite monthly total AOD products. The results of the analysis are shown in Table 6.8.

In March differences between S3A and S3B SU v1.14 AOD calculated for chosen regions have increased compared with v1.11, where difference between two products, with few exceptions (AOd region, March) was within the accepted value. For Eur, AsN and NAE, RD between S3A and S3B in SU v1.14 AOD product is negative and 2-4 time higher than the AD. Over AfN, S3A AOD is higher than S3B AOD with the RD almost twice higher than accepted difference. In June, September and December, difference between S3A and S3B products is withing the AD for most of the regions. In general, S3A and S3B SU AOD products show similar regional differences with MODIS and MISR.

Because of that, the discussion bellow will be about the difference between S3 (S3A and S3B together) v1.14 AOD product and MODIS and MISR AOD products. General conclusions will be drawn, which may include few exceptions over certain month or certain area.

For all months except December, RD difference between S3 and MODIS is within the AD over land. However, significant discrepancies in AOD have been revealed in several regions. In Aus, AfS, SA and NaW, the difference between S3 and MODIS AOD can be classifies as Pg2-Pg3, while negative difference is observed in Bor region in March and September and in Asia in December.

Difference between S3 and MISR AOD products is within AD in Eur (except for June), Aus and AfN. Positive offsets between S3 are MISR, classified as Pg2-Pg3, are observed over other land regions, which resulted in positive RD above AD over the whole land region.

Table 9.8 *Relative AOD difference between S3A and S3B SU v1.14, MODIS and MISR monthly AOD for regions defined as in Figure 6.3, for year 2019. Cases with RD>1(AOD difference is outside the accepted difference) and regions from the Northern and Southern hemispheres (NH and SH, respectively) are coloured; legend below the Table.*

regions	Eur	Bor	AsN	AsW	AsE	ChinaSE	Aus	AfN	AfS	SA	NAW	NAE	Ind	Aod	Aob	InO	PO	Land	Ocean	Globe
March																				
S3A-S3B	-1,93	-1,37	-3,79	-0,73	-1,41	-1,23	0,05	1,85	0,23	-0,26	-1,20	-2,24	-0,66	1,37	-0,66	-0,19	-0,49	-0,64	-0,61	-0,61
S3A-MODIS	0,38	-1,72	-0,12	0,26	-0,71	-0,85	1,58	0,37	1,76	1,46	1,11	1,63	-0,38	-0,33	-0,57	-0,68	-0,78	0,75	-0,82	-0,47
S3A-MISR	0,68	1,37	1,79	1,57	2,04	1,61	0,61	0,48	0,89	2,43	0,94	1,84	1,08	0,24	0,99	0,64	0,59	1,48	0,31	0,54
S3B-MODIS	0,47	-1,37	0,24	0,65	-0,29	-0,44	1,86	0,20	2,06	1,44	1,44	1,08	0,00	-0,07	-0,21	-0,38	-0,45	0,90	-0,47	-0,16
S3B-MISR	0,78	1,72	2,14	1,93	2,44	2,01	0,90	0,31	1,21	2,40	1,27	1,30	1,46	0,49	1,34	0,94	0,92	1,63	0,66	0,85
June																				
S3A-S3B	-0,19	-1,58	-0,07	0,34	0,02	0,00	-0,45	1,20	-0,37	-0,24	-0,26	-0,31	-0,71	-0,80	-0,47	-0,59	-0,49	-0,24	-0,59	-0,49
S3A-MODIS	0,85	-0,45	1,06	1,57	0,84	0,49	0,75	2,24	1,14	0,94	0,40	1,11	-0,99	-0,93	-0,61	-0,78	-0,71	0,97	-0,71	-0,12
S3A-MISR	1,98	1,06	1,25	1,53	1,98	2,43	0,64	0,52	2,64	1,77	0,71	1,20	1,04	1,30	1,27	0,12	0,35	1,39	0,54	0,87
S3B-MODIS	0,97	-0,21	1,08	1,71	0,63	0,27	0,87	2,21	1,22	1,04	0,28	1,13	-0,49	-0,43	-0,35	-0,33	-0,35	1,06	-0,31	0,14
S3B-MISR	2,10	1,30	1,27	1,67	1,79	2,22	0,75	0,49	2,71	1,86	0,59	1,23	1,53	1,81	1,53	0,57	0,71	1,48	0,94	1,13
September																				
S3A-S3B	-0,54	0,14	-1,51	0,26	-0,96	-0,99	0,38	2,50	0,07	0,07	-0,35	-0,31	-0,02	-0,49	-0,34	-0,38	-0,52	0,07	-0,54	-0,38
S3A-MODIS	-0,12	-1,13	0,75	1,53	0,22	-0,04	1,60	1,15	2,15	1,08	0,54	1,74	-1,31	-0,64	-1,35	-0,68	-0,73	0,78	-0,90	-0,45
S3A-MISR	0,66	0,19	1,15	2,52	1,98	2,12	0,38	0,31	1,89	1,77	1,44	2,10	2,02	0,87	2,40	0,92	0,52	1,30	0,57	0,78
S3B-MODIS	0,09	-1,13	0,87	1,69	0,80	0,58	1,53	0,62	1,85	0,75	0,78	2,00	-1,53	-0,49	-1,31	-0,47	-0,40	0,73	-0,57	-0,21
S3B-MISR	0,87	0,19	1,27	2,67	2,51	2,68	0,31	-0,23	1,59	1,44	1,67	2,36	1,81	1,01	2,44	1,13	0,85	1,25	0,90	1,01
December																				
S3A-S3B	-0,28	NaN	-1,04	-0,71	-0,97	-1,08	0,16	-1,44	-0,35	-0,71	-0,21	-0,61	-0,54	-0,59	-0,59	-0,54	-0,52	-0,68	-0,52	-0,54
S3A-MODIS	-0,52	NaN	0,80	-1,72	-1,23	-1,70	3,04	-0,47	2,43	2,99	0,59	1,25	-0,28	0,00	-0,42	-0,85	-0,82	1,11	-0,97	-0,54
S3A-MISR	0,52	NaN	1,15	0,02	0,66	0,73	0,94	-0,12	1,60	2,88	1,27	1,63	1,18	1,30	0,90	0,54	0,47	1,37	0,28	0,49
S3B-MODIS	-0,45	NaN	1,51	-1,60	-0,57	-0,85	3,09	-0,59	2,73	3,25	0,54	1,34	-0,12	0,31	-0,09	-0,52	-0,54	1,30	-0,66	-0,26
S3B-MISR	0,59	NaN	1,86	0,14	1,32	1,58	0,99	-0,24	1,91	3,13	1,23	1,72	1,34	1,60	1,23	0,87	0,75	1,56	0,59	0,78
						RD	<-2.0	<-1.5	<-1.0		>1.0	>1.5	>2.0							
						Group	Ng3	Ng2	Ng1		Pg1	Pg2	Pg3							

Over ocean, difference between S3 and MODIS and MISR is, with only few exceptions, within the AD. However, S3 AOD is higher (Pg1-Pg3) than MISR AOD in dust and biomass burning transport areas (AOd, AOb) and lower than MODIS over Ind and Aod in September. Over Indian and Pacific oceans difference between S3 and MODIS (all cases) and MISR (except for few cases from Pg1) is within AD.

Globally, differences between S3 and MODIS and MISR are within the AD for all months and regions, except for S3B-MISR in June and September (Pg1).

6.4 Monthly AOD: evaluation results for year 2020

Evaluation of S3A_SU, S3B_SU (both v1.14) and S3A_Rayference (v2.2.1) monthly AOD products was performed for four months (March, June, September and December) in year 2020. Listed products were inter-compared with MODIS Terra DTDB C6.1 and MISR v32 monthly AOD products. S3A_SU and S3B_SU AOD products were also inter-compared.

Total AOD monthly maps for listed above products are shown in Fig. 6.26. For all months, S3B_SU AOD over ocean is ca 0.01-0.02 higher than S3A_SU; similar difference is observed between S3B and S3A global AOD. MODIS Terra AOD is 0.01-0.03 higher than S3B_SU AOD; Absolute difference between S3B and Terra and S3B and MISR is similar, but MISR AOD is lower than SU AOD. S3A_Rayference AOD is 2-3 times lower than AOD from S3A_SU, S3B_SU, Terra and MISR.

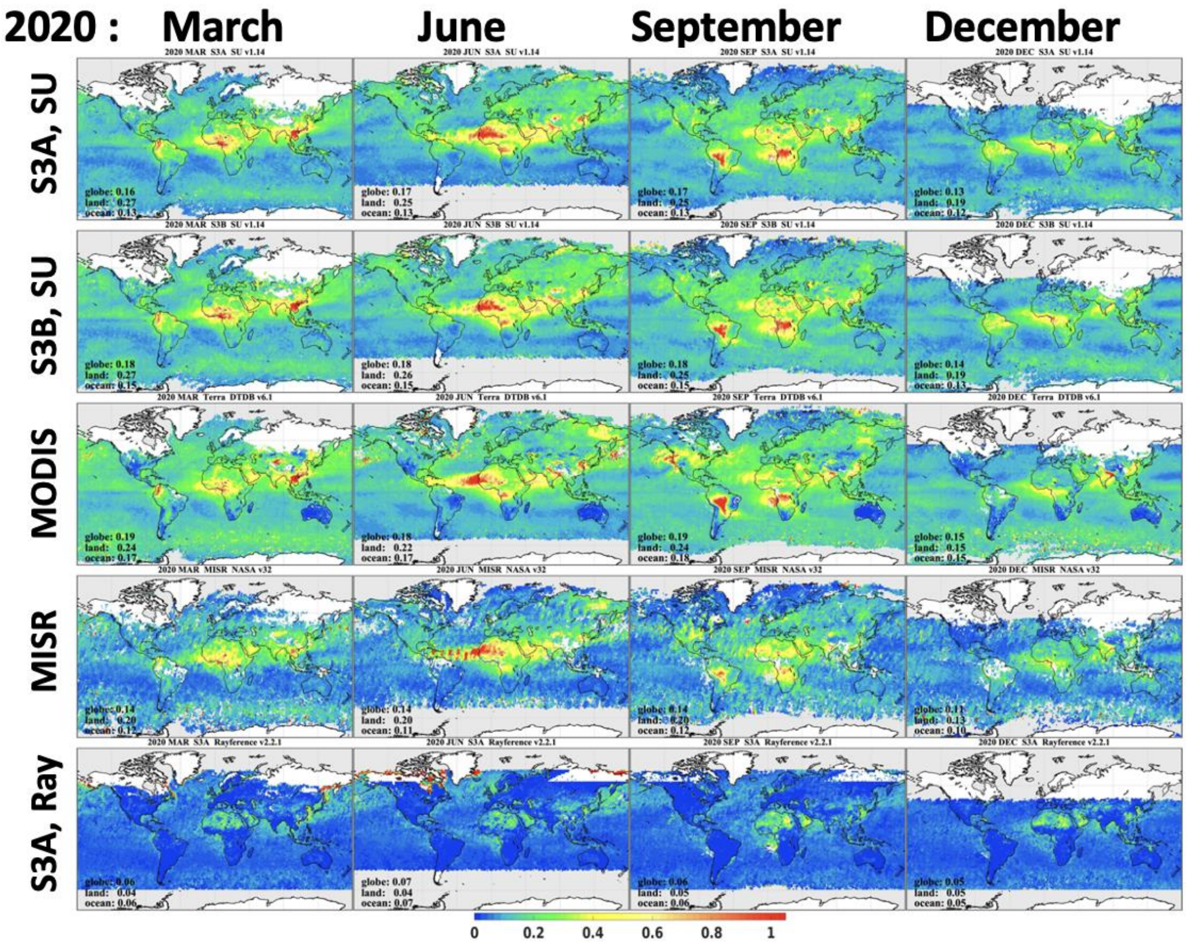

Figure 6.26 *S3A_SU, S3B_SU (both v1.14), Terra DTDB (C6.1), MISR (v32) and S3A_Rayference (v2.2.1) total AOD for March, June, September and December 2020.*

Evaluation of S3A_SU, S3B_SU (both v1.14), Terra DTDB (C6.1), MISR (v32) and S3A_Rayference (v2.2.1) monthly AOD products was performed against AERONET AOD monthly product. Note, that monthly aggregates which were subjects for evaluation and monthly reference AERONET AOD were created from all retrieved over month pixels; thus, evaluation results show, first of all, how well satellite products reproduce “climate” AOD value. One should keep in mind that in this type of evaluation difference in coverage over month may influence the results. Evaluation results are shown as scatter density plots (Fig.6.27); coefficients for linear regression, as well as correlation coefficient (r), standard deviation (σ), root mean square error (rms), fraction of points which fall into MODIS Error Envelope (EE, defined as ±0.05±0.2*AOD) and satisfy GCOS requirements (GCOS, 0.03 or 10% of AOD) are provided.

Difference in validation results for S3A_SU and S3B_SU is small. R is high (~0.8 for both products), rms is low (~0.1), fraction of matchups with AERONET which fit into EE is 60-64%, 24-29% of matchups fit to GCOS requirements. MISR shows slightly worse correlation (0.77), but higher EE and GCOS; Terra shows highest among all products correlation with AERONET (0.86); EE and GCOS are higher than S3A_SU and S3B_SU but lower than MISR. For all four products AOD above 0.7 is underestimated; underestimation is slightly higher for MISR.

Considerable underestimation of monthly AOD is observed in the S3A Rayference product.

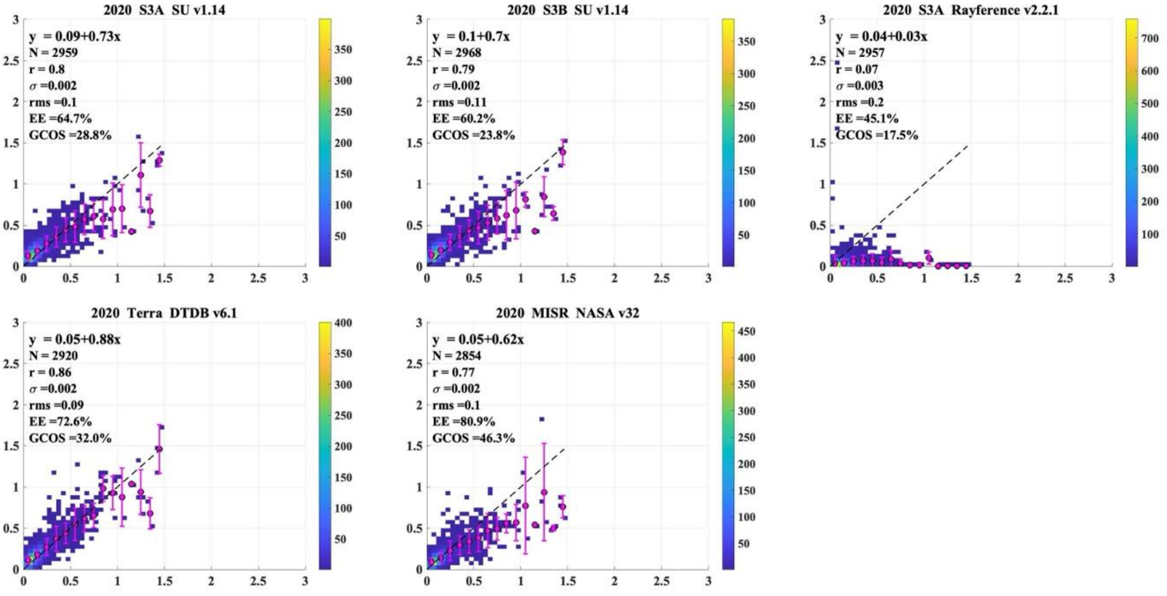

Figure 6.27 *S3A_SU, S3B_SU (both v1.14), S3A_Rayference (v2.2.1), Terra DTDB (C6.1) and MISR (v32) monthly AOD evaluation with AERONET, for year 2020.*

Spatial distribution of differences between S3A_SU and S3B_SU monthly total AOD is shown in Fig. 6.28. In general, the difference between S3A_SU and S3B_SU monthly total AOD is small (below 0.01). However, regional, and seasonal variations of differences exist. The highest difference is observed in June over the Atlantic Ocean regions which can be exposed to the Saharan dust transport. Vertical (along longitude) patches of the difference of opposite signs (over- and underestimation) may be a consequence of lower S3B coverage (not studied further). No areas were recognised, where one product provides constantly higher or lower AOD.

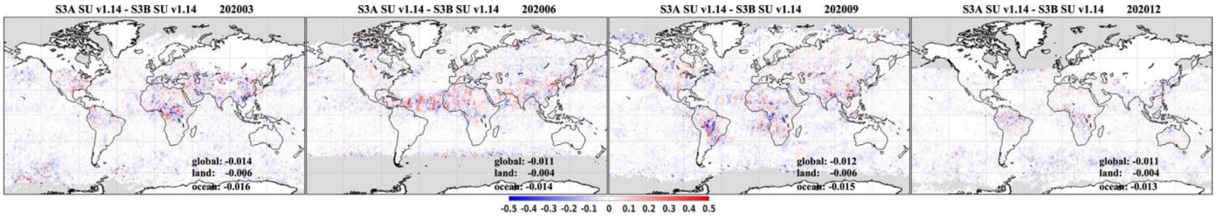

Figure 6.28 *Differences between SU v1.14 S3A and S3B total AOD monthly products, for March, June, September and December 2020.*

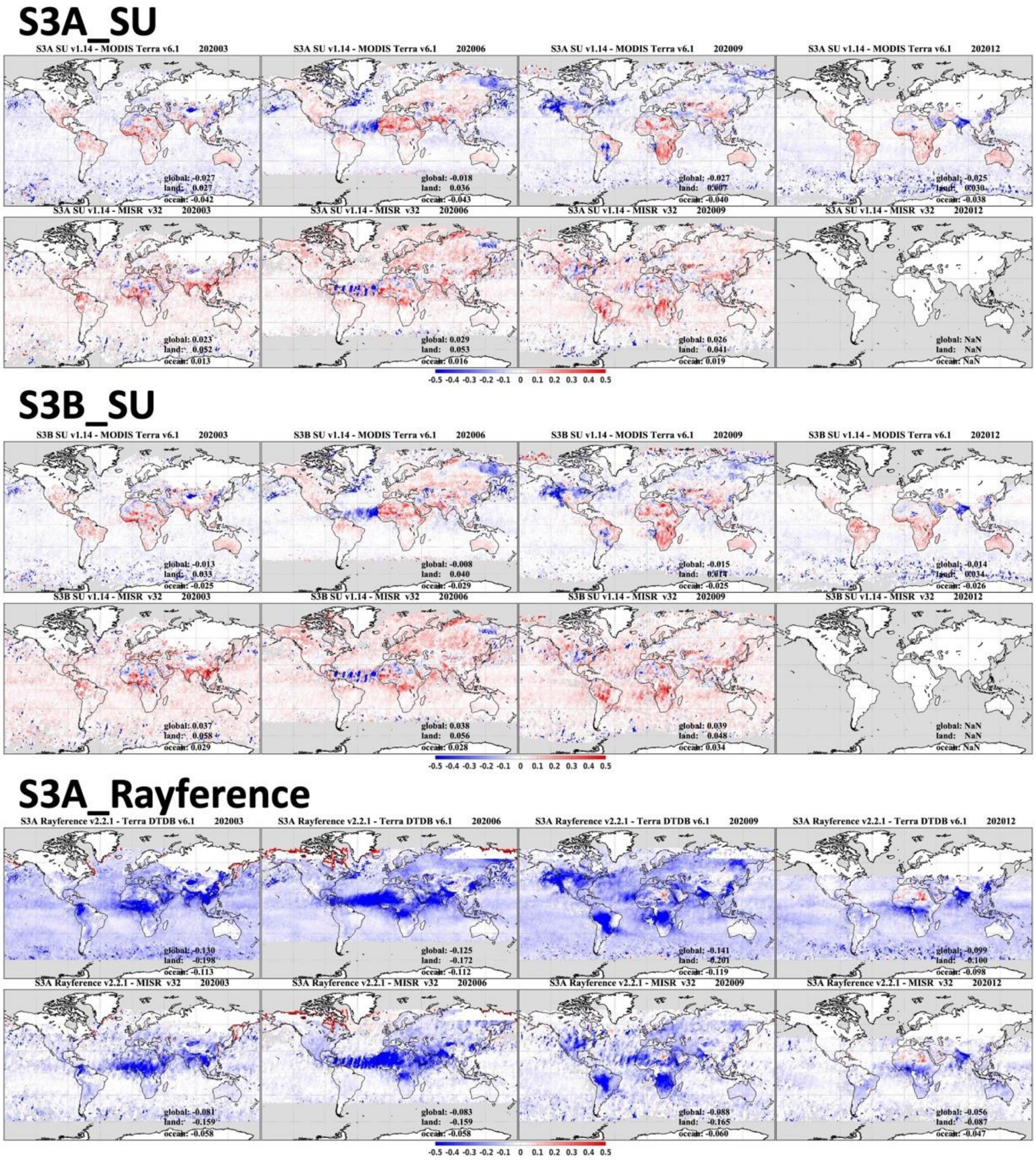

Figure 6.29 *For SU v1.14 S3A and S3B, Rayference v2.2.1 S3A (double panels top down), difference with MODIS (upper sub-panel) and MISR (lower sub-panel) total AOD monthly products, for March, June, September and December 2020.*

For SU v1.14 S3A and S3B and Rayference v2.2.1 S3A, spatial differences with MODIS and MISR total AOD monthly products, for March, June, September and December 2020, are shown in Fig.6.29. Over ocean, AOD from SU products is similar or slightly smaller than MODIS AOD and a bit higher than MISR total monthly AOD. Over land, regional differences are more pronounced. Rayference AOD is considerably lower than MODIS and MISR AOD around the globe except for close to poles regions, where Rayference AOD is much higher (possibly, retrieval over ice).

Regional differences (Fig. 6.30) between SU and MODIS AOD are more pronounced for the regions with possible high AOD loading (biomass burning) – Afs, SA, NAW, NAE. As biomass burning episodes are seasonal, the amplitude of difference is also seasonal with peaks during the biomass burning seasons. As mentioned above, difference in monthly AOD, besides differences in retrieval approaches and cloud screening, can be explained by the difference in coverage, when some biomass burning episodes are missed in the products from a satellite with lower spatial coverage. Difference between SU and MISR total AOD products is high also in possibly polluted regions in Asia.

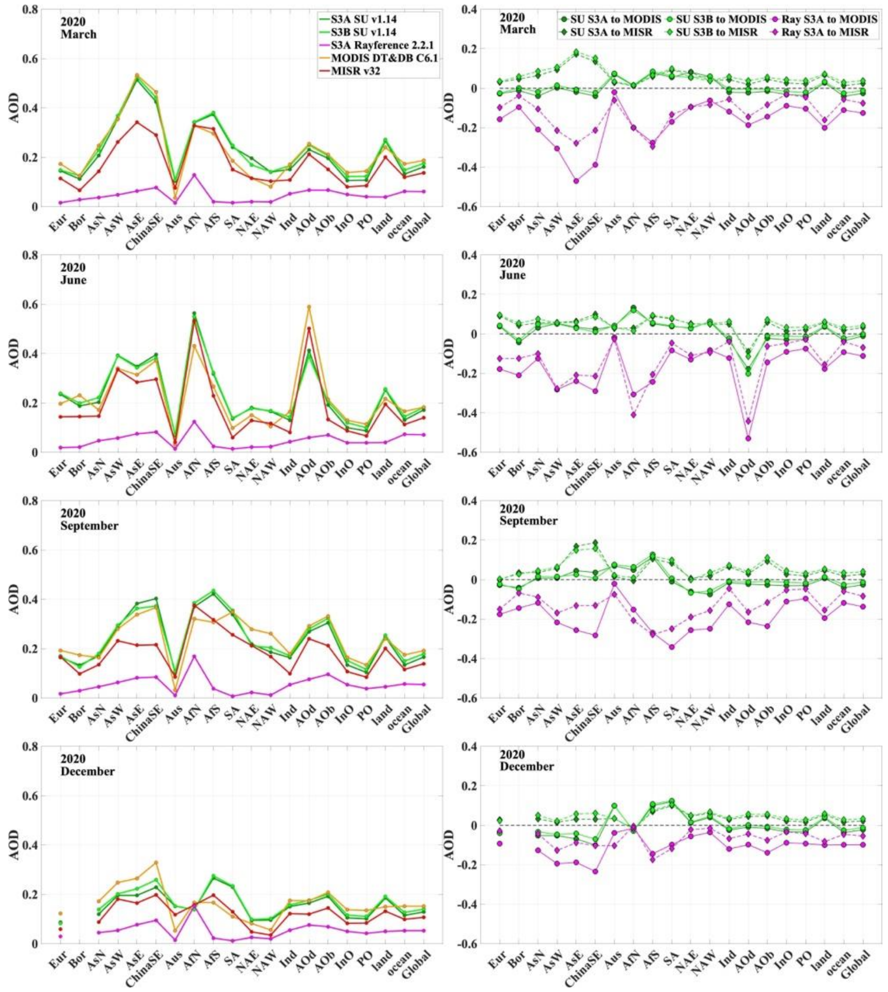

Figure 6.30 S3A/S3B SU v1.14, S3A Rayference v2.2.1, MODIS, MISR, monthly AOD for four months in year 2020 (left panel) and regional differences (right panel) for regions defined as in Fig. 6.3.

In Fig.6.31 we show regional evaluation results of the S3A SU total monthly AOD with AERONET. Correlation coefficient is high 0.8- 0.94 in Asia, AOd, AOb, and Africa regions. Over boreal regions (Bor, NAE, NAW) correlation coefficient is lower (0.5-0.55); AOD >0.5 is often underestimated. The lowest correlation coefficient is obtained for Europe, where monthly AOD is low (<0.4).

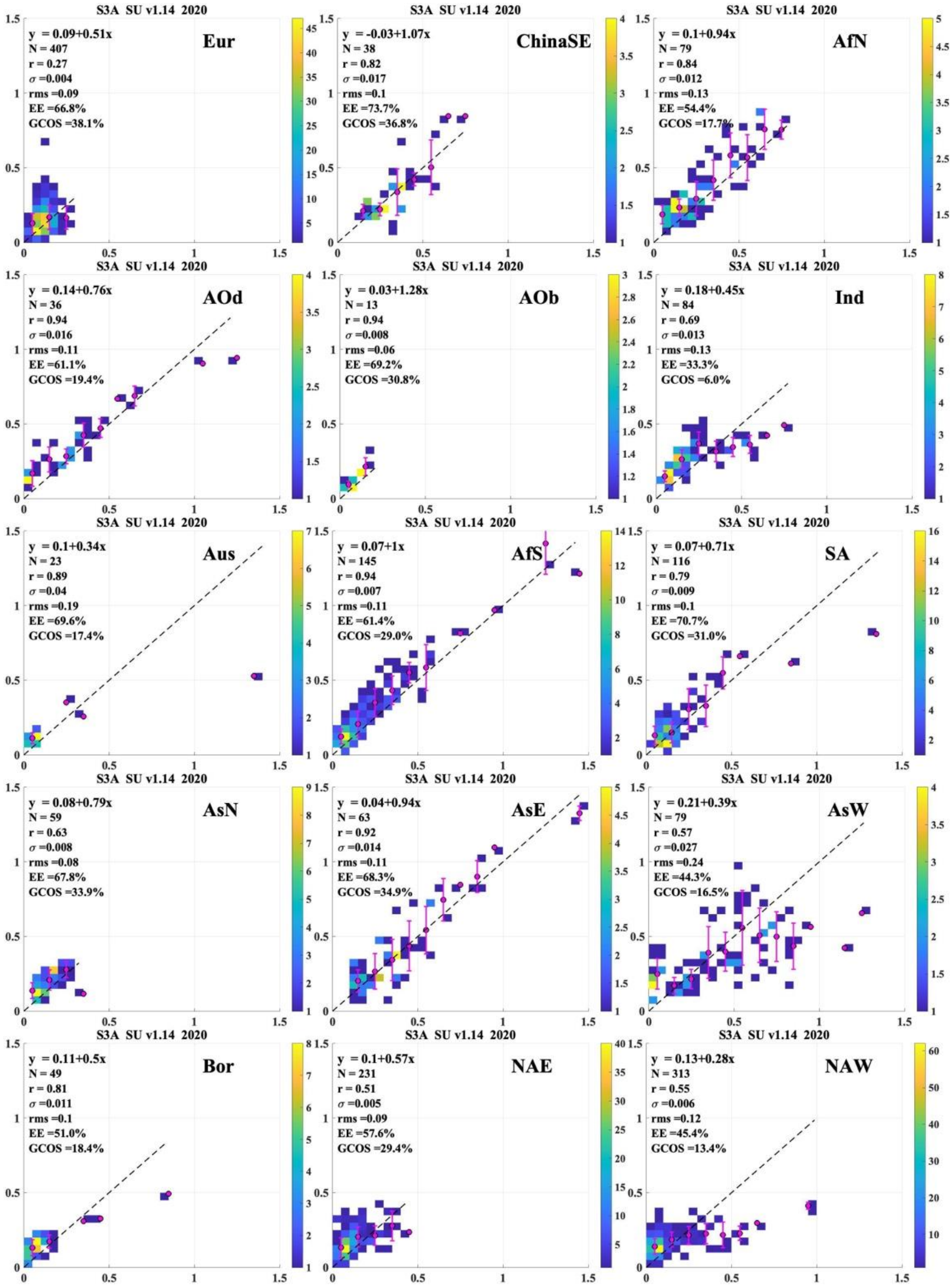

Figure 6.31 *SU S3A v1.14 regional evaluation results with AERONET for year 2020*

In Fig.6.32 we show SU S3A and S3B, MODIS and MISR evaluation with AERONET for four areas, Afs, SA, NAW, NAE, where the difference between total monthly AOD from different products is higher. For AfS, correlation coefficient is slightly better for S3A. Terra and MISR show underestimation of high AOD, though fraction of pixels with satisfy GCOS requitements is slightly higher for Terra and MISR. For SA, validation statistics are slightly better for MODIS. For NAE and NAW validation statistics are better for MODIS and MISR; AOD >0.3 are underestimated for S3A, S3B and MISR.

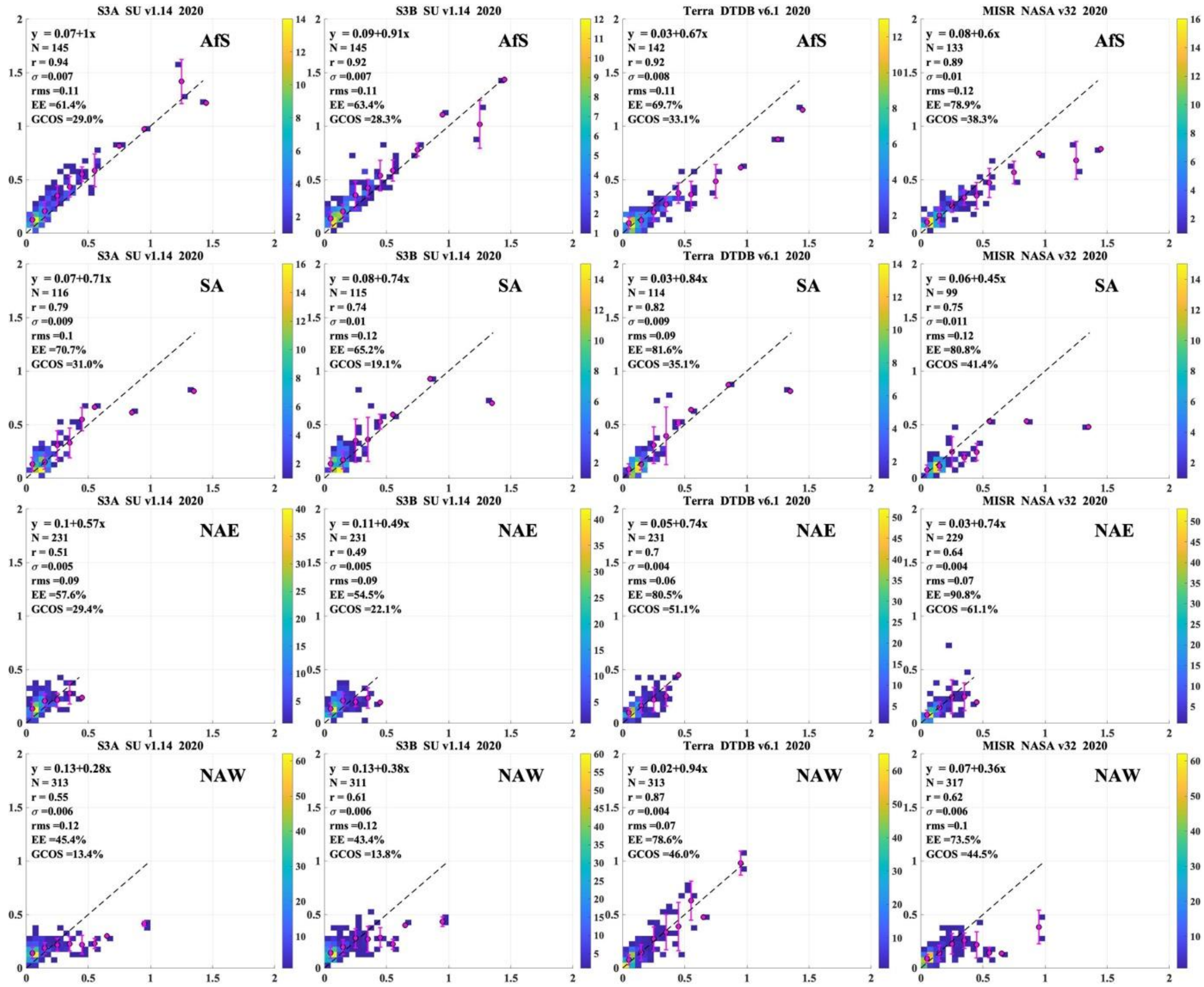

Figure 6.32 *SU S3A and S3B (both v1.14), MODIS and MISR (columns left to right) total monthly AOD evaluation results with AERONET for year 2020.*

6.5 Evaluation of SU ATSR2 and AATSR v4.35 monthly total AOD

6.5.1 V4.35 vs v4.33: Monthly total AOD spatial distribution

ATSR2 SU monthly AOD products retrieved with two different versions, v4.33 and v.4.35, and the difference in monthly AOD between two products (v.4.35 – v.4.33) are shown in Fig.6.33 for March, June, September and December 1998. For the ***AATSR***, similar data are shown in Fig.6.34 for year 2008.

For both ATSR2 and AATSR products, monthly total AOD over ocean remains the same in v4.33 and v4.35. In v4.35, AOD over land lowered by ca 0.02 in March and September and a bit more, by 0.04, in June. In December, AOD decrease over land was low (0.007). AOD decrease over land was mainly due to AOD changes over bright surface (Sahara, Arabian Peninsula) and in the Amazon area. To the south from the Saharan area, insignificant AOD increase has been observed.

Some changes in AOD were observed also in the South Africa in June (AOD decrease on the north of the area and increase in the south). Consequently, global AOD has lowered by ca. 0.005 in March and September and a bit more, by 0.013, in June.

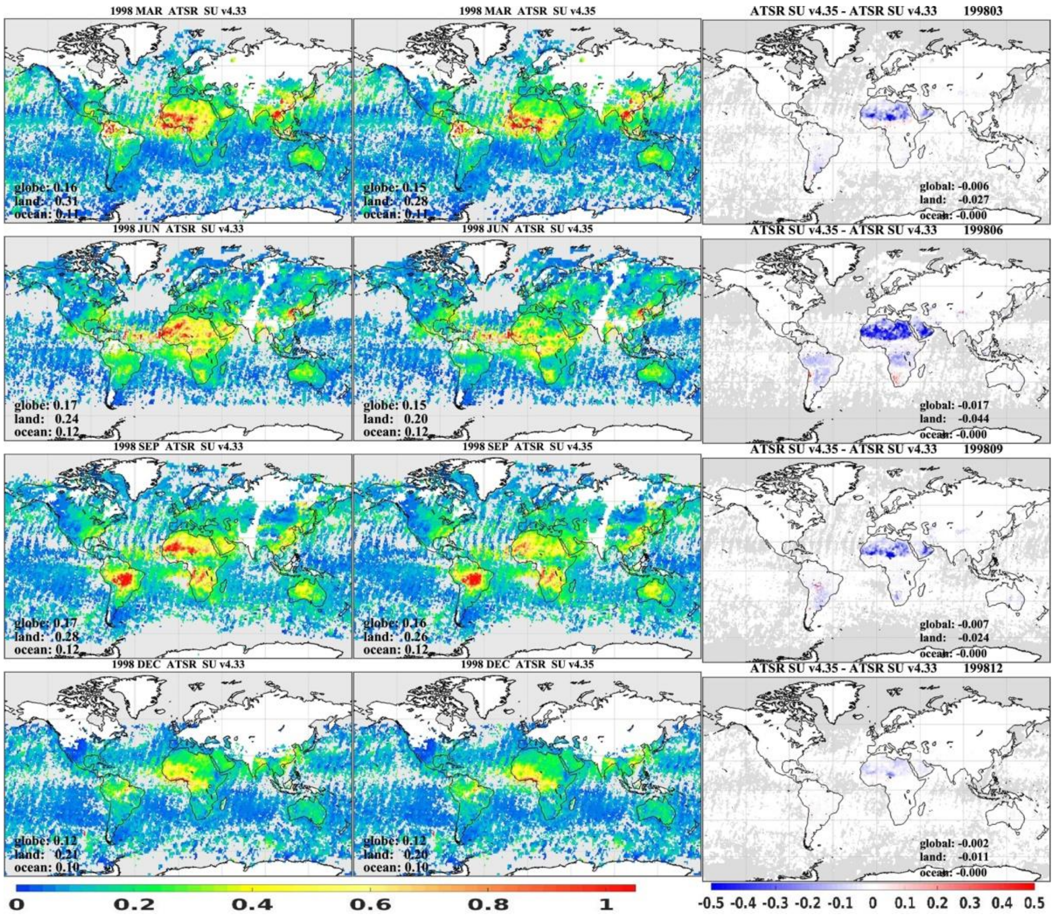

Figure 6.33 *SU ATSR2 v4.33 (left), v4.35 (middle) and difference between v4.35 and v4.33 (right) monthly total AOD for March, June, September and December (top down) 1998.*

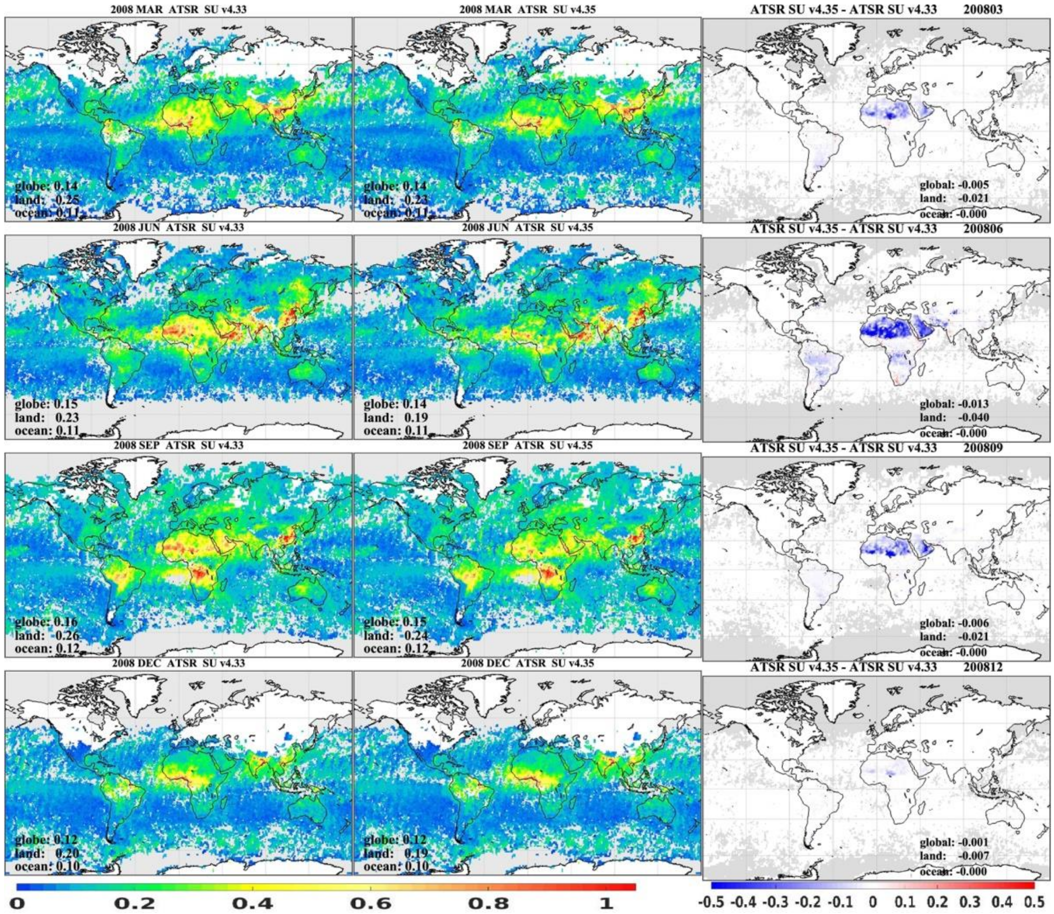

***Figure 6.34** SU AATSR v4.33 (left), v4.53 (middle) and difference between v4.35 and v4.33 (right) monthly total AOD for March, June, September and December (top down) 2008.*

6.5.2 SU v4.35 vs v4.33: Monthly total AOD evaluation with AERONET

Evaluation of SU v4.33 and v4.35 monthly AOD with AERONET was performed for selected years (1998 for the ATSR2 and 2008 for the AATSR) and for regions defined as in Fig.6.3. Below we show evaluation results for three areas, where differences in AOD between two versions of the products were more clear: the Northern Africa (AfN, which includes Saharan desert), the Southern Africa (AfS, which includes biomass burning areas) and South America (SA). Global validation results over land are also shown.

Evaluation results for **ATSR2** are shown in Fig.6.35. For the AfN region, more points fit to the EE and satisfy GCOS requirements in the new v4.35 (54% and 17% against 345 and 8% as in v4.33), rms lowered from 0.19 to 0.14, bias lowered from 0.16 to 0.13, though correlation coefficient has also lowered (0.62 against 0.71). Slope for the linear regression may be biased by single AOD point with underestimated AOD. Changes in validation statistics in AfS are smaller; based on the fraction of points in EE, rms and bias, small improvements were observed, while correlation coefficient and fraction of points which satisfy GCOS requirements lowered insignificantly (from 0.66 to 0.63 and from 23% to 20%, respectively). In SA no significant changes in the agreement between ATSR2 and AERONET monthly AOD have been revealed; number of validation points was low to make solid conclusions of the product development in this region. Globally over land, validation statistics improved insignificantly.

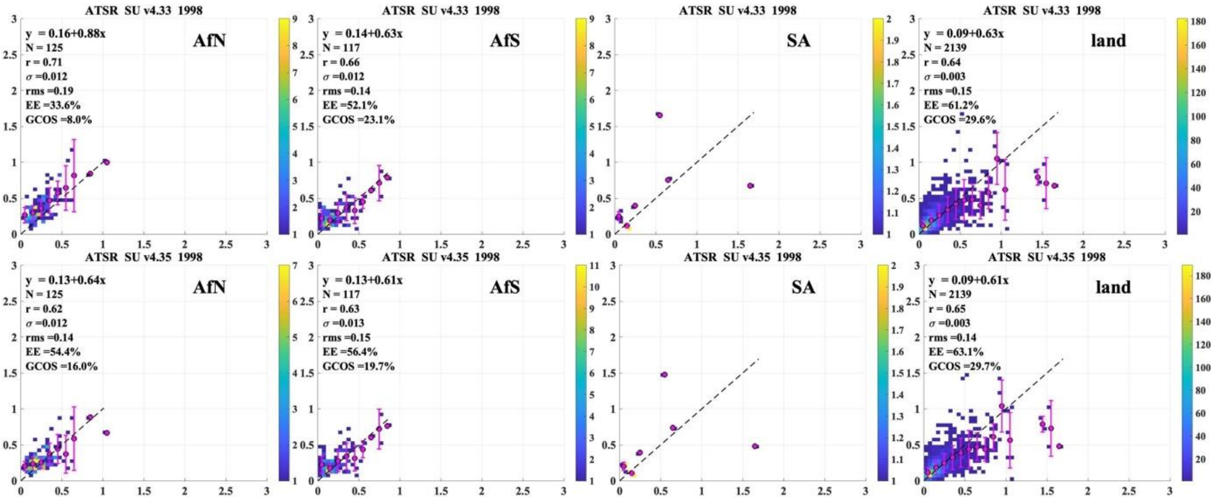

Figure 6.35 *SU ATSR2 v4.33 (upper panel) and v4.35 (lower panel) monthly total AOD scatter density plots and evaluation statistics with AERONET for three regions, AfN, AfS and SA, and globally over land (left to right) for year 1998. Statistics for SA are not show due to limited number of collocations (12).*

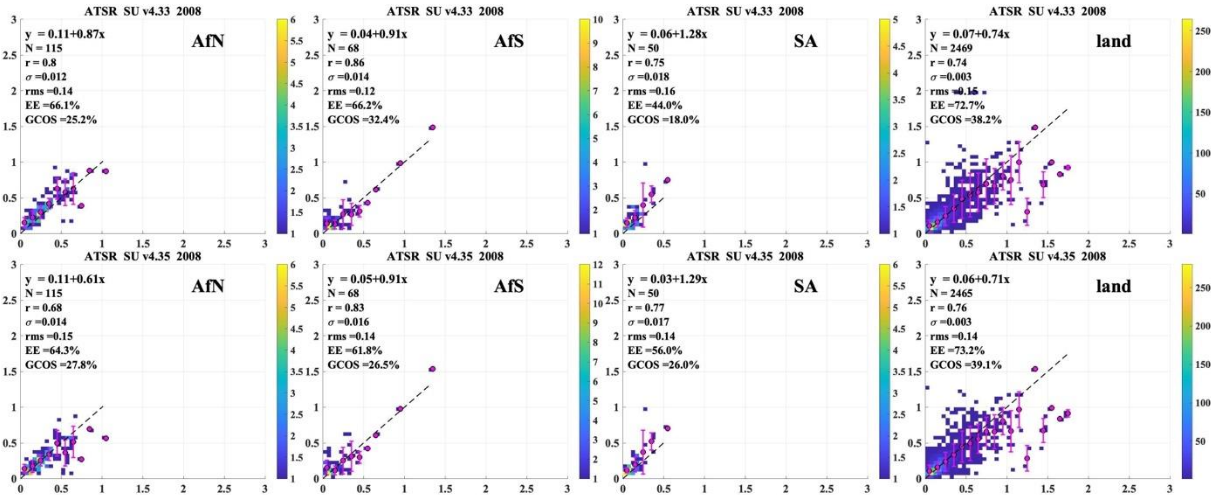

Figure 6.36 *SU AATSR v4.33 (upper panel) and v4.35 (lower panel) monthly total AOD scatter density plots and evaluation statistics with AERONET for three regions, AfN, AfS and SA, and globally over land (left to right) for year 2008.*

Similar conclusions can be done on the development of the **AATSR** product. As for the SA region, fraction of points which satisfy GCOS requirements and fraction of points in EE have increased, while correlation coefficient has lowered. Over land, correlation coefficient, GCOS fraction and fraction of points in EE is higher for the AATSR product compared to the ATSR2 product.

6.5.3 SU AATSR V4.35: Monthly total AOD spatial difference to other satellite products

As for SU AATSR v4.33 (Fig. 6.20), maps of the difference in monthly AOD between AATSR and MODIS, AATSR and MISR (middle panel), AATSR and POLDER (lower panel) total AOD monthly products are shown in Fig.6.37. Since the biggest changes in SU AOD have been revealed over land in June, differences between SU AOD and other AOD products have changed more in June compared to other months. In this month, difference over land with MODIS has increased from -0.008 to -0.048; difference with MISR and GRASP has changed from positive (0.027) to negative (-0.014 and -0.018 for MISR and GRASP, respectively).

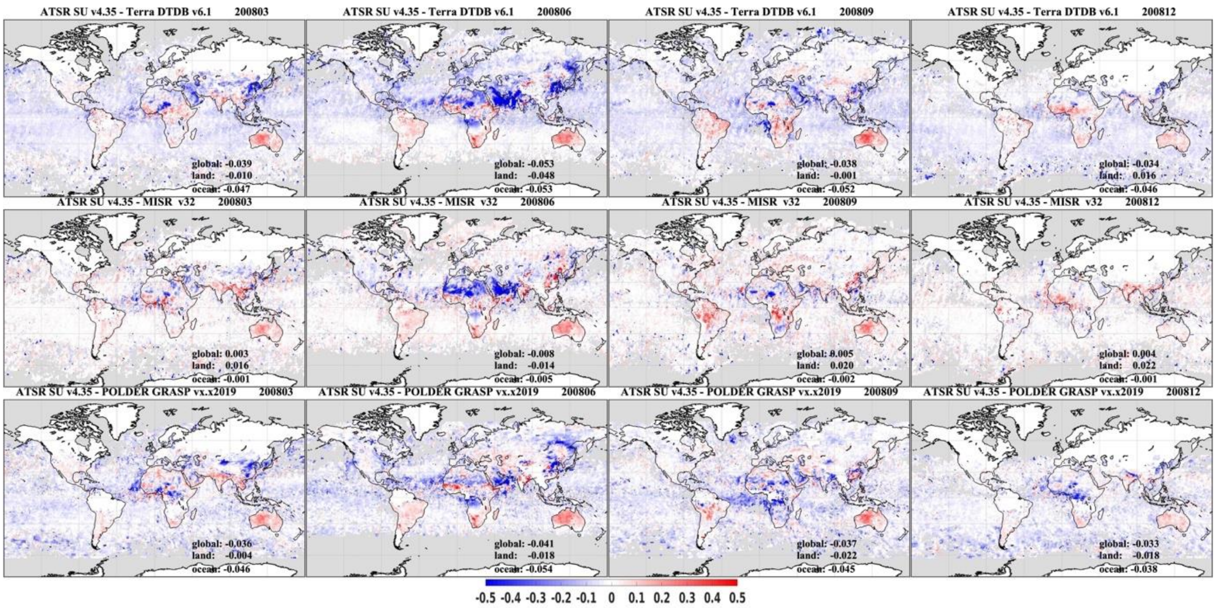

Figure 6.37 *Difference between AATSR SU v4.35 and MODIS (upper panel), AATSR and MISR (middle panel), AATSR and POLDER (lower panel) total AOD monthly products for for March, June, September and December (left to right) 2008.*

Regional AOD for SU AATSR v4.35 and v4.33, as well as for MODIS Terra, MISR and GRASP, are shown in Fig. 6.38. Compared to SU v4.33, existing differences with regional MODIS, MISR and POLDER GRASP have changed in AfN and SA, where SU AOD was lowered. Changes are more pronounced in June.

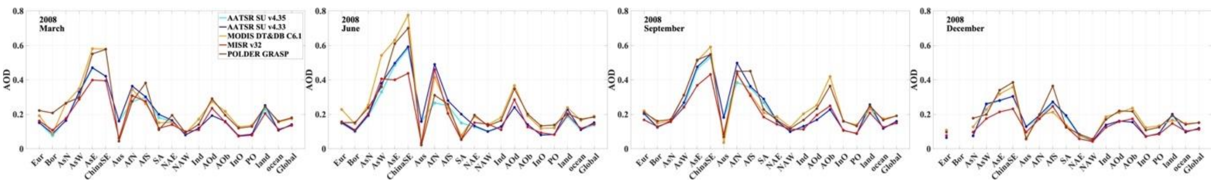

Figure 6.38 *AATSR SU v4.33, AATSR SU v4.35, MODIS, MISR and POLDER GRASP monthly AOD for four months in year 2008 for different regions defined as in Fig. 6.3.*

6.5.4 Regional evaluation of monthly AOD from different satellite products

Regional evaluation of monthly AOD from different products, SU v4.35, MODIS, MISR and GRASP has been performed. Evaluation results are shown for five chosen regions, where the absolute difference in AOD between different satellite products is highest: AfN, AfS, ChinaSE, AOd and Aus (Fig.6.39).

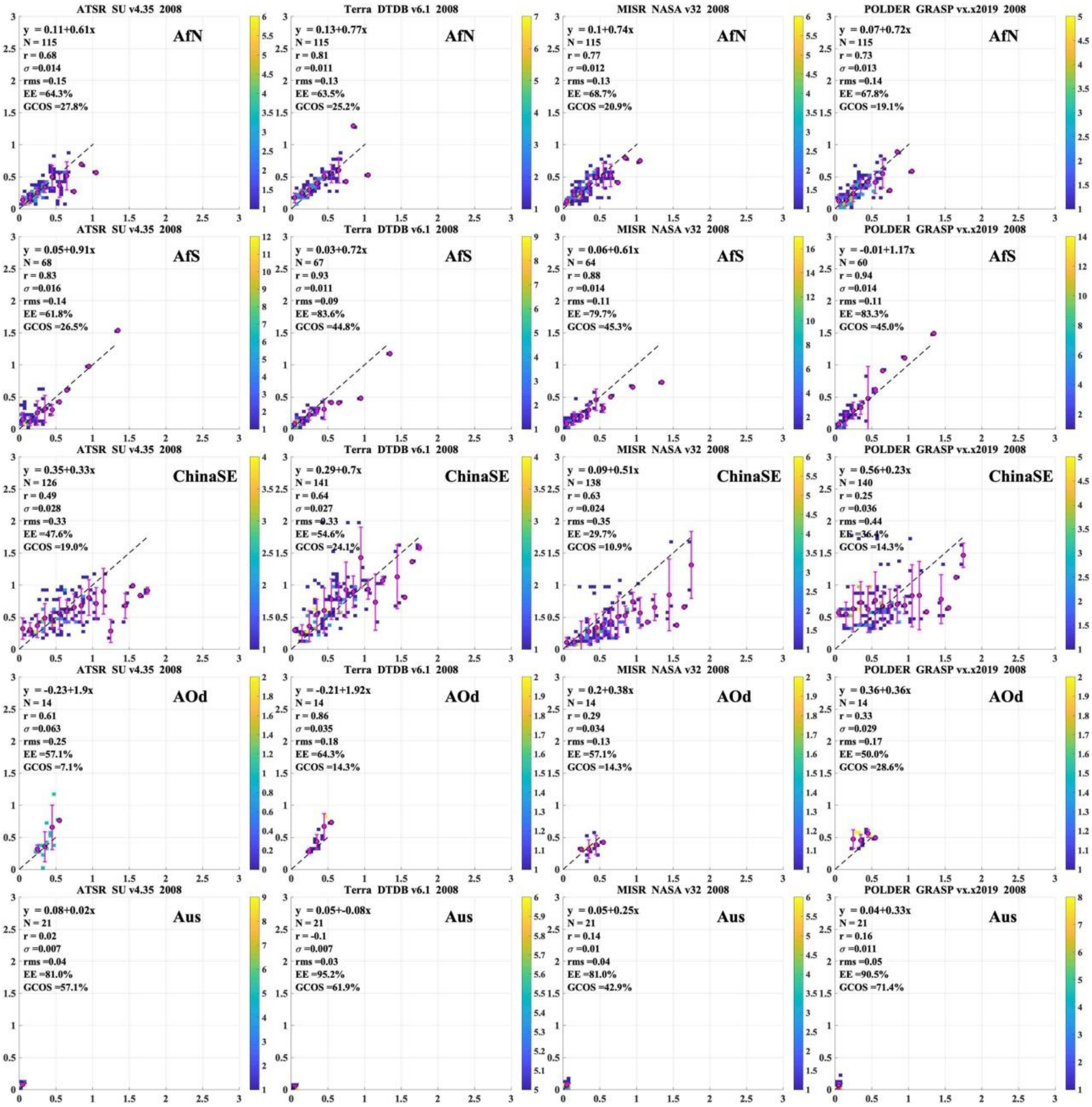

Figure 6.39 *For AfN, AfS, ChinaSE, AOd and Aus (top down; regions defined as in Fig. 6.3.), regional evaluation of AATSR SU v4.33, MODIS, MISR and POLDER GRASP monthly AOD (left to right) for year 2008.*

In the AfN region, AOD>0.5 in SU product is slightly underestimated. GCOS fraction is slightly higher, EE fraction is similar to MODIS but slightly lower than for MISR and GRASP. Rms is slightly higher, correlation coefficient is slightly lower for SU AOD compared to other products in both AfN and AfS regions. In ChinaSE, SU AOD<0.4 is overestimated; AOD>0.8 is underestimated.

In AOd and Aus regions the low number of validation points (14 and 21, respectively) does not allow making solid conclusions. However, high deviation of the SU and AERONET AOD matchups from the 1:1 line and corresponding high rms in AOd region show that the performance of SU algorithm is unstable in this region. In Aus, agreement for low (<0.2) AOD is quite good for all products; AOD>0.2 is not presented among available matchups. Cloud screening may be the reason for rejecting high AOD in the satellite products in this area (however, the availability of high AERONET AOD in Aus region has not been checked in the current study).

7 SUMMARY

Summary for the validation of total AOD

- High positive bias and larger scatter for SLSTR
- decreasing for bias for SLSTR with increasing AOD over land
- constant bias for SLSTR over the whole AOD range over ocean
- SLSTR uncertainties over land significantly larger
- Indication of hemispheric differences in data quality (with less stations in the South), swapped for ATSR and SLSTR
- The SU v2 datasets show better coverage for ATSR-2 and reduced bias / scatter for SLSTR in some regions
- The SU v3 datasets show slightly reduced bias for the ATSR instruments
- The validation of the RF v1 total AOD reveals a high positive bias and larger scatter for SLSTR / 3A (mostly over ocean for AOD < 0.4, but also over land for AOD < 0.2)
- The validation of the RF v2 total AOD shows a significant improvement (reduced bias and noise, but small positive bias for low AOD remaining) while there is now a new under-estimation for AOD>0.2 over land
- FR v2 monthly mean datasets show significant negative bias which is under further investigation.

Summary for the validation of FM-AOD

- Overall positive bias for all sensors over land and ocean
- Bias and stdv over land larger for SLSTR than for the ATSR instruments with ~0.045)
- Over ocean bias appears to increase with increasing AOD for SLSTR
- Geographical patterns follow largely those of the AOD errors
- For the SU v2 and v3 dataset there is not much change of the FM-AOD characteristics
- Also the new RF v1 FM-AOD dataset shows overall positive bias for for SLSTR/3A over land and ocean
- The RF v2 FM-AOD also shows significant improvement with remaining positive bias

Summary for the validation of AOD prognostic uncertainties

- all uncertainty distributions show a double peak (strong over land, in particular for both SLSTR instruments)
- mean of uncertainties is larger over land than over ocean for all sensors
- mean and stdv of uncertainties are significantly larger over land for SLSTR than for the ATSR instruments but similar for all sensors over ocean
- uncertainties are generally slightly too small; for the SLSTR instruments over ocean a larger correction factor is needed, while over land uncertainties need a slight decrease
- uncertainties allow a reasonable split between “good” and “bad” pixels for the lower

range with dominating numbers, but not any longer for the higher values

- the smallest uncertainties in the lowest bin have typically too large errors /are too small (in particular for SLSTR instruments)
- statistical distributions of normalized errors per sensor show that on average uncertainties (dominating the statistics) are too small and need correction factors larger than 1. (in particular for SLSTR)
- separate analysis of the two hemispheres proves the favourable scattering angle conditions (avoiding backscatter) which have smaller uncertainties with less need for correction and more meaningful information to split "good" and "bad" pixels; those favourable conditions are in the Northern hemisphere for ATSR (with most AERONET stations dominating the validation statistics), while they lie in the Southern hemisphere for SLSTR (with less AERONET stations). This is one reason for the weaker performance of AOD from SLSTR than ATSR, but also of the prognostic uncertainties.
- For the SU v2 and v3 datasets, larger uncertainties are slightly smaller, but overall there is not much change (v3 small reduction for ATSR instruments)
- Uncertainties of the CISAR algorithm are smaller than those of the SU algorithm, but they are too small compared to the true error estimates of AERONET
- The CISAR v2 uncertainties are significantly improved and provide a good representation of the true errors, also consistently between North and South hemispheres and land and ocean

<u>Summary for the inter-comparison to other satellite AOD products (AATSR SU v4.32, S3A/S3B SU v1.11)</u>

- Over land, ocean and globally, the difference between AATSR and GRASP is within the accepted difference estimated with the root sum squared method considering the GCOS requirements for AOD. AATSR AOD is higher than MISR AOD over land and lower than MODIS AOD over ocean; both differenced are slightly above the accepted difference. Differences between AATSR and MISR over ocean and AATSR and MODIS over lands are within AD. Regional analysis shows a considerable difference between the products.
- Differences between S3A and S3B AOD are, with one exception for AOd region in March, within the accepted value.
- Positive offsets between S3 (S3A and S3B) and MODIS/MISR AOD products are observed over land. Over ocean, difference between S3 and MODIS and MISR is, with only few exceptions, within the AD. Globally, differences between S3A and MODIS and MISR are within AD. Difference between S3B and MODIS is within AD, while difference with MISR is slightly higher. Regional analysis shows a considerable difference between the products.

Summary for the inter-comparison between ATSR2/AATSR SU v4.33 and v4.32 AOD products

- ATSR2 AOD global coverage in SU v4.33 product has been increased by 58%-26%-41% in March, June and September, respectively. For those months, coverage over land has been increased by ca 20%, and over ocean by 75%-34%-58%, with respect to the coverage in v.4.32. In December, changes in coverage are low (<5%)
- A common tendency for all four months has been observed in AOD over land, where for AOD >1 (as retrieved with v4.32) v.4.33 AOD has a negative offset compared with v.4.32
- ATSR2 v4.33 AOD is a bit higher in March in Asia, SA and AOd. In June, difference over Asia is smaller and close to 0 for other selected regions. In September, AOD v4.33 is ca. 0.02 higher over Africa and South America and ca. 0.35 higher over AOd. In December, regional differences between ATSR2 v4.33 and v.4.32 AOD are negligible (close to 0).
- No clear differences between *AATSR* SU AOD monthly products retrieved with v.4.33 and v.4.32 processors have been revealed

Summary for the inter-comparison between ATSR2/AATSR SU v4.35 and v4.33 AOD products

- ATSR2 and AATSR AOD over ocean has not changed in v4.35 compared to v4.33
- ATSR2 and AATSR AOD over land has lowered over Sahara / Arabian peninsula and South America. The difference between v4.35 and v4.33 over Sahara is higher in June (up to 0.5), lower in March and September and negligible in December
- For ATSR2, more points fit to the EE and satisfy GCOS requirements in the new v4.35 (54% and 17% against 34.5 and 8% as in v4.33), rms lowered from 0.19 to 0.14, bias lowered from 0.16 to 0.13, though correlation coefficient has also lowered (0.62 against 0.71) in the AfN region. Similar conclusions can be done on the development of the AATSR product.
- Over land, correlation coefficient, GCOS fraction and fraction of points in EE is higher for the AATSR product compared to the ATSR2 product.

Summary for the inter-comparison between S3A/S3B SU v1.14 and v1.11 AOD products

- Coverage of the S3A/S3B products has not changed in v1.14
- A belt of negative AOD offset has been observed in March between ca 30°N-50°N. In June, the belt of negative AOD offset has moved further to the North, reaching ca 70°N-75°N. In September the belt has moved back 30°N-50°N and narrowed to Eurasia.
- Over bright surfaces, AOD in ver.1.14 is slightly higher; AOD over biomass burning areas is slightly lower
- Difference in AOD between v1.14 and v1.11 over ocean is low, ca -0.007 for all four months; no spots of considerably higher differences have been observed.
- Pixel-by-pixel AOD products v1.14 and v1.11 inter-comparison shows that offset up to 0.6 may exist between two products. However, averaged over bins AOD closely follow 1:1 line, with some small (within ± 0.01) deviation for AOD>1.

Summary for the inter-comparison of ATSR2 and AATSR SU v4.32 monthly total AOD products to other satellite AOD products

- ATSR2 SU AOD product has a better coverage in the SH in March and December compared with ATSR2 ADV product.
- ATSR2 SU AOD is higher over land by 0.05-0.09, lower over ocean by ca. 0.08 and globally (by 0.01-0.07)
- No considerable changes in monthly AOD have been revealed between AATSR SU AOD v4.33 and v4.32 products; the main results from the evaluation of SU v4.33 monthly AOD product with MODIS, MISR and POLDER have not changed much, as compared with evaluation results of SU v4.32 monthly AOD product evaluation.
- Over land, ocean and globally, the difference between AATSR and GRASP is within the accepted difference estimated with the root sum squared method considering the GCOS requirements for AOD. AATSR AOD is higher than MISR AOD over land and lower than MODIS AOD over ocean; both differenced are slightly above the accepted difference. Differences between AATSR and MISR over ocean and AATSR and MODIS over lands are within AD. Regional analysis shows a considerable difference between the products.
- An offset between AATSR monthly AOD products is higher in the regions with high AOD loading – Asia, Africa, areas in the Atlantic Ocean which undergo dust and biomass burning aerosol transport.

Summary for the inter-comparison of S3A and S3B SU v1.14 and S3A RF v2.0.0 monthly total AOD products to other satellite AOD products for year 2019

- Compared with SU v1.11, difference between S3A and S3B AOD has not changed much globally, over land and ocean. However, reginal differences have changed considerably in March.
- In March, relative difference between S3A and S3B in SU v1.14 AOD product in Eur, AsN and NAE is negative and 2-4 time higher than the absolute difference. Over AfN, S3A AOD is higher than S3B AOD with the RD almost twice higher than AD.
- In June, September and December, regional differences between S3A and S3B products are withing the AD for most of the regions. In general, S3A and S3B SU AOD products show similar regional differences with MODIS and MISR.
- For all months except December, RD difference between S3 SU and MODIS is within the AD over land. However, significant discrepancies in AOD have been revealed in several regions (positive in Aus, AfS, SA and NaW, negative in Bor region in March and September and in Asia in December).
- Over land, difference between S3 SU and MISR AOD products is within AD in Eur (except for June), Aus and AfN. Positive offsets between S3 are MISR are observed over other land regions, which resulted in positive RD above AD over the whole land region.
- Over ocean, difference between S3 and MODIS and MISR is, with only few exceptions, within the AD.

- Globally, differences between S3 and MODIS and MISR are within the AD for all months and regions, except for S3B-MISR in June and September
- S3A RF AOD clearly differs from the other AOD products with unrealistically high AOD e.g., over Eurasia in September (0.3-0.5 over Europe, 0.5-0.8 over Finland) and over potentially clean areas over ocean (0.3-0.5). One of the reasons for high AOD values in S3A RF AOD product can be cloud contamination, which may be a consequence from the absence of cloud masking module in the aerosol retrieval in RF (CISAR) algorithm.

<u>Summary for the inter-comparison of S3A and S3B SU v1.14 and S3A Rayference v2.2.1 monthly total AOD products to other satellite AOD products for year 2020</u>

- SU S3A and S3B total monthly AOD spatial distribution and difference from MODIS Terra and MISR AOD is similar to one from year 2019
- Validation results of the total AOD monthly products for year 2020 confirm a good performance of SU S3A and S3B v1.14 products. Correlation with AERONET is high (0.8- 0.94) in Asia, AOd, AOb, and Africa regions. Over boreal regions (Bor, NAE, NAW) correlation coefficient is lower (0.5-0.55); AOD >0.5 is often underestimated. The lowest correlation coefficient is obtained for Europe, where monthly AOD is low (<0.4).
- Regional differences of SU and MODIS and MISR products are more pronounced in the areas where high AOD loading episodes occur (e.g., biomass burning in AfS, SA)
- Rayference v2.2.1 total monthly AOD is strongly underestimated.

8 REFERENCES

Eck, T. F., Holben, B. N., Reid, J. S., Smirnov, A., O'Neill, N. T., Slutsker, I., and Kinne, S.: Wavelength dependence of the optical depth of 5 biomass burning, urban, and desert dust aerosols, J. Geophysical Research, 104, 31 333–31 349, 1999.

Thomas Popp, Gerrit de Leeuw, Christine Bingen, Christoph Brühl, Virginie Capelle, Alain Chedin, Lieven Clarisse, Oleg Dubovik, Roy Grainger, Jan Griesfeller, Andreas Heckel, Stefan Kinne, Lars Klüser, Miriam Kosmale, Pekka Kolmonen, Luca Lelli, Pavel Litvinov, Linlu Mei, Peter North, Simon Pinnock, Adam Povey, Charles Robert, Michael Schulz, Larisa Sogacheva, Kerstin Stebel, Deborah Stein Zweers, Gareth Thomas, Lieuwe Gijsbert Tilstra, Sophie Vandenbussche, Pepijn Veefkind, Marco Vountas and Yong Xue, Development, Production and Evaluation of Aerosol Climate Data Records from European Satellite Observations (Aerosol_cci), Remote Sensing, 8, 421; doi:10.3390/rs8050421, 2016

Christopher J. Merchant, Frank Paul, Thomas Popp, Michael Ablain, Sophie Bontemps, Pierre Defourny, Rainer Hollmann, Thomas Lavergne, Alexandra Laeng, Gerrit de Leeuw, Jonathan Mittaz, Caroline Poulsen, Adam C. Povey, Max Reuter, Shubha Sathyendranath, Stein Sandven, Viktoria F. Sofieva and Wolfgang Wagner, Uncertainty information in climate data records from Earth observation, Earth System Science Data, 9, 511–527, https://doi.org/10.5194/essd-9-511-2017, 2017

Sayer, A. M., Govaerts, Y., Kolmonen, P., Lipponen, A., Luffarelli, M., Mielonen, T., Patadia, F., Popp, T., Povey, A. C., Stebel, K., and Witek, M. L.: A review and framework for the evaluation of pixel-level uncertainty estimates in satellite aerosol remote sensing, Atmospheric Measurements and Techniques, 13, 373–404, https://doi.org/10.5194/amt-13-373-2020, 2020.

O'Neill, N. T.,T. F., Eck, A. Smirnov, B. N.Holben, S. Thulasiraman, Spectral discrimination of coarse and fine mode optical depth, J. Geophys. Res., Vol.. 108, No. D17, 4559-4573, 10.1029/2002JD002975, 2003.

9 ANNEX:

A1 Inter-comparison between (A)ATSR SU v.4.33 and ADV v.2.31 AOD550

Comparison of SU AOD product to SDV/ADV and ORAC is not contractually committed. However, since other satellite products are not available for the evaluation of ATSR2 SU AOD product, ATSR2 SU v4.33 product has been inter-compared with ATSR ADV v2.31 product (Sect. 6.2.1).

Inter-comparison between AATSR SU v4.33 and ADV v2.31 and between S3A SU v1.14, SDV v2.2, ORAC v1.0 and MODIS has been performed on voluntary basis. Results are presented in Fig. A1.1-4.

Monthly AOD for AATSR SU v.4.33 and ADV v2.31 products and the difference between two products for March, June, September and December 2008 are shown in Fig. A1.1.

Regionally averaged monthly total AOD for AATSR SU v4.33 and ADV v2.31 are shown in Fig.A1.2 for March, June, September and December 2008.

S3A SU v.1.14 monthly AOD and difference between S3A SU v.1.14 and SDV v2.2, ORAC v1.0 and MODIS AOD monthly products for March, June, September and December 2019 are shown in Fig. A1.3

Regional AOD for S3A AOD products (SU v1.14, SDV v2.2, ORAC v1.0) are combined in Fig. A1.4, left panel; regional AOD for S3B AOD products (SU v1.14, SDV v2.2) are combined in Fig. A1.4, right panel. Regional monthly AOD for MODIS and MISR are shown on each sub-plot.

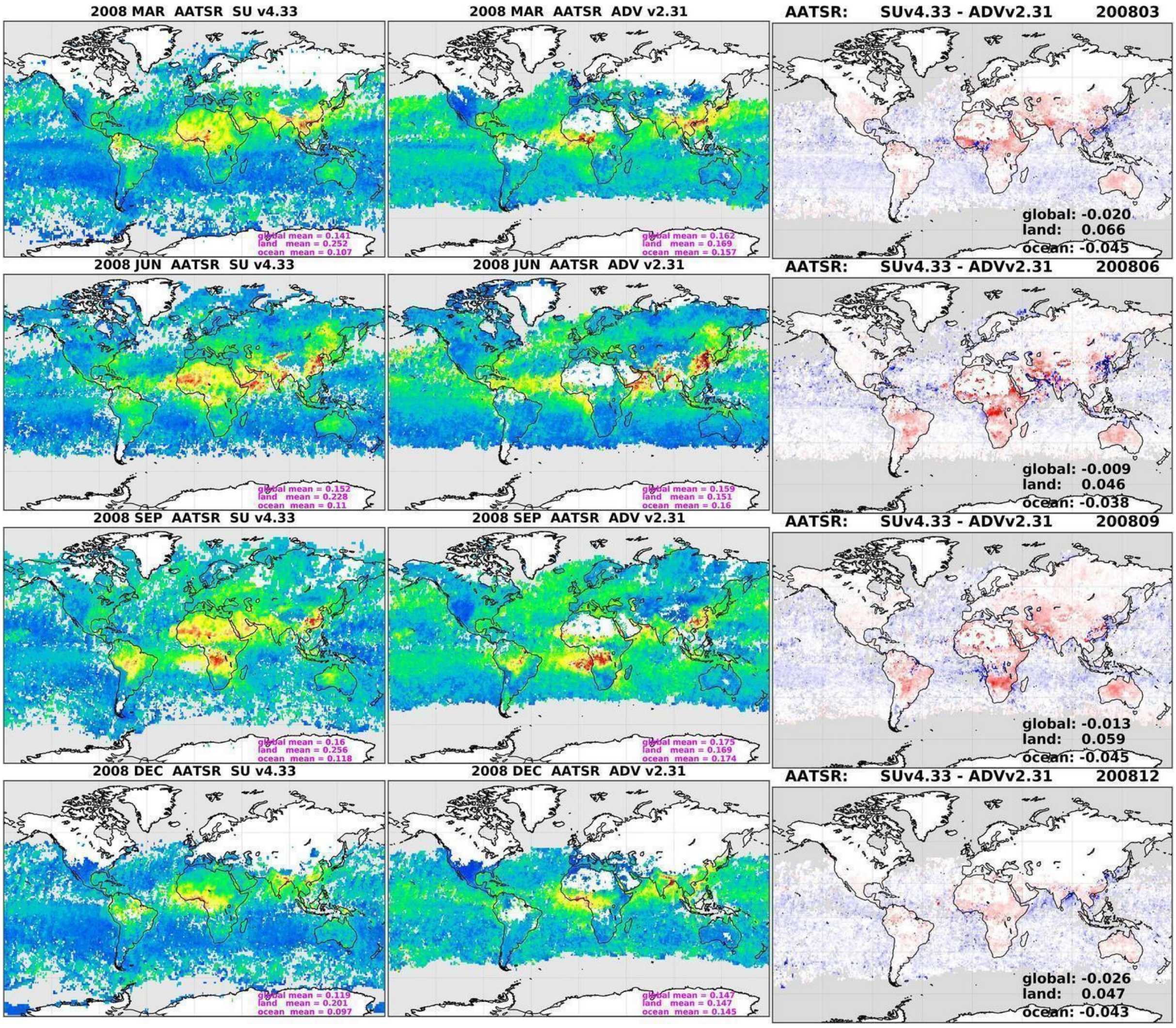

***Fig. A1.1** Monthly AOD for AATSR SU v.4.33 and ADV v2.31 products (left and middle panels, respectively) and the difference between two products (right panel) for March, June, September and December 2008 (horizontal panels top down).*

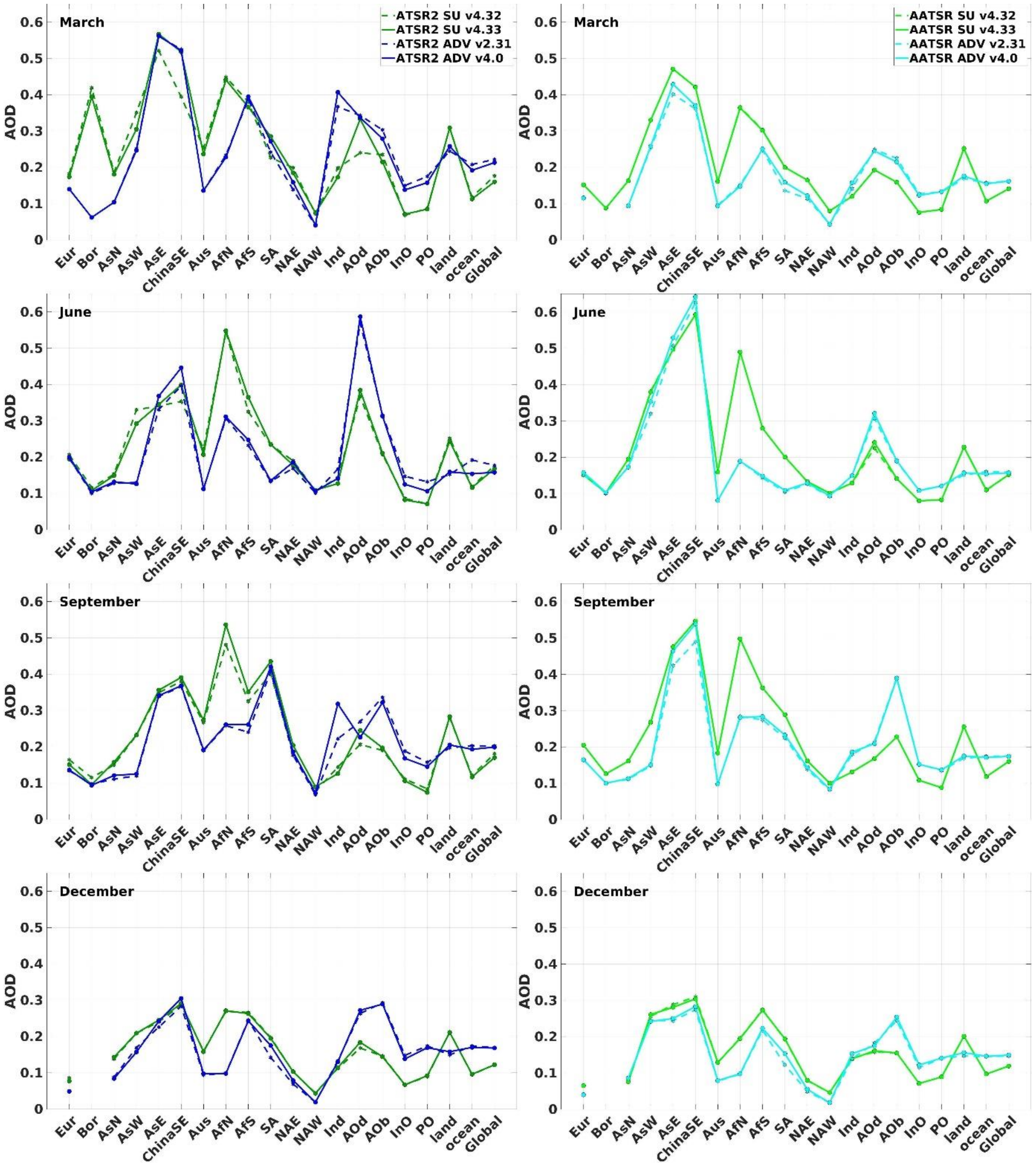

Figure A1.2 *AATSR SU v4.33 and ADV v2.31 monthly AOD for four months in year 2008 for different regions defined as in Fig. 6.3.*

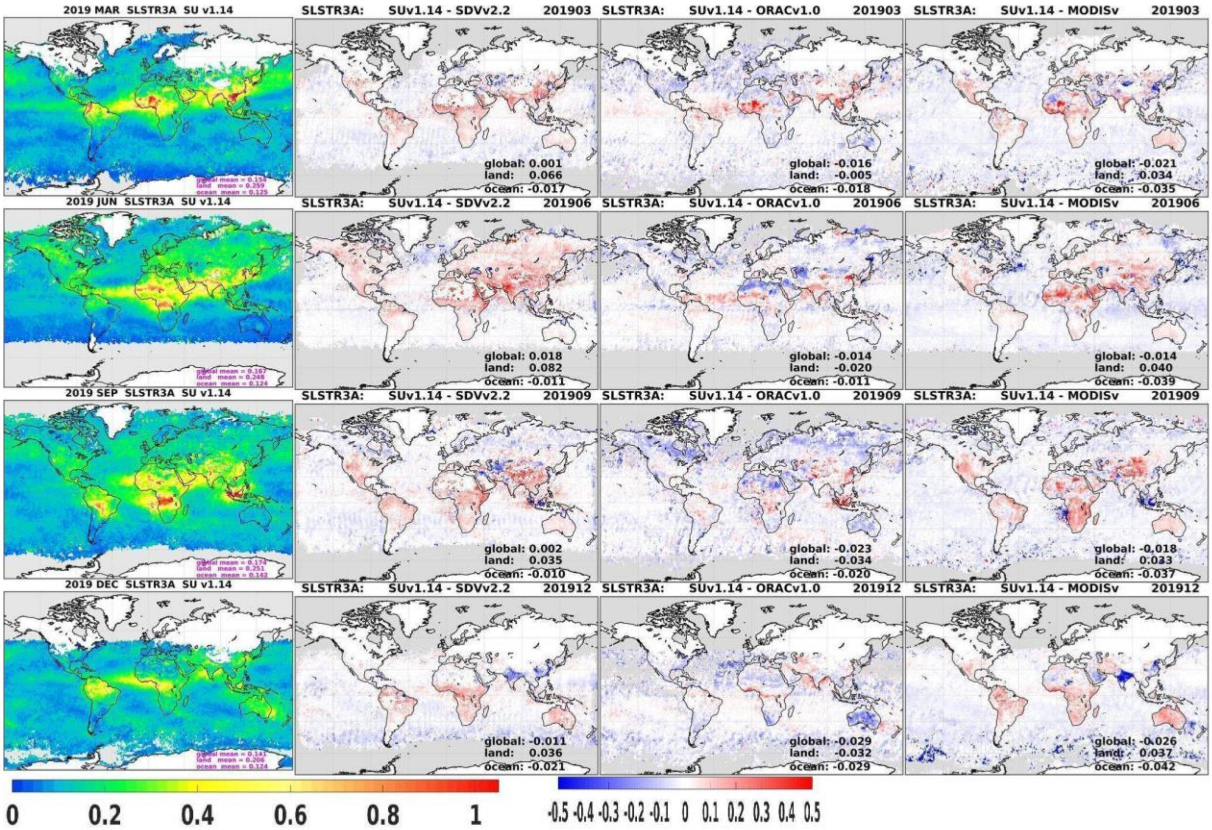

Fig. A1.3 *Monthly AOD for S3A SU v.1.14 and difference between S3A SU v.1.14 AOD product and SDV v2.2, ORAC v1.0 and MODIS products (vertical panels from left to right) for March, June, September and December 2019 (horizontal panels top down).*

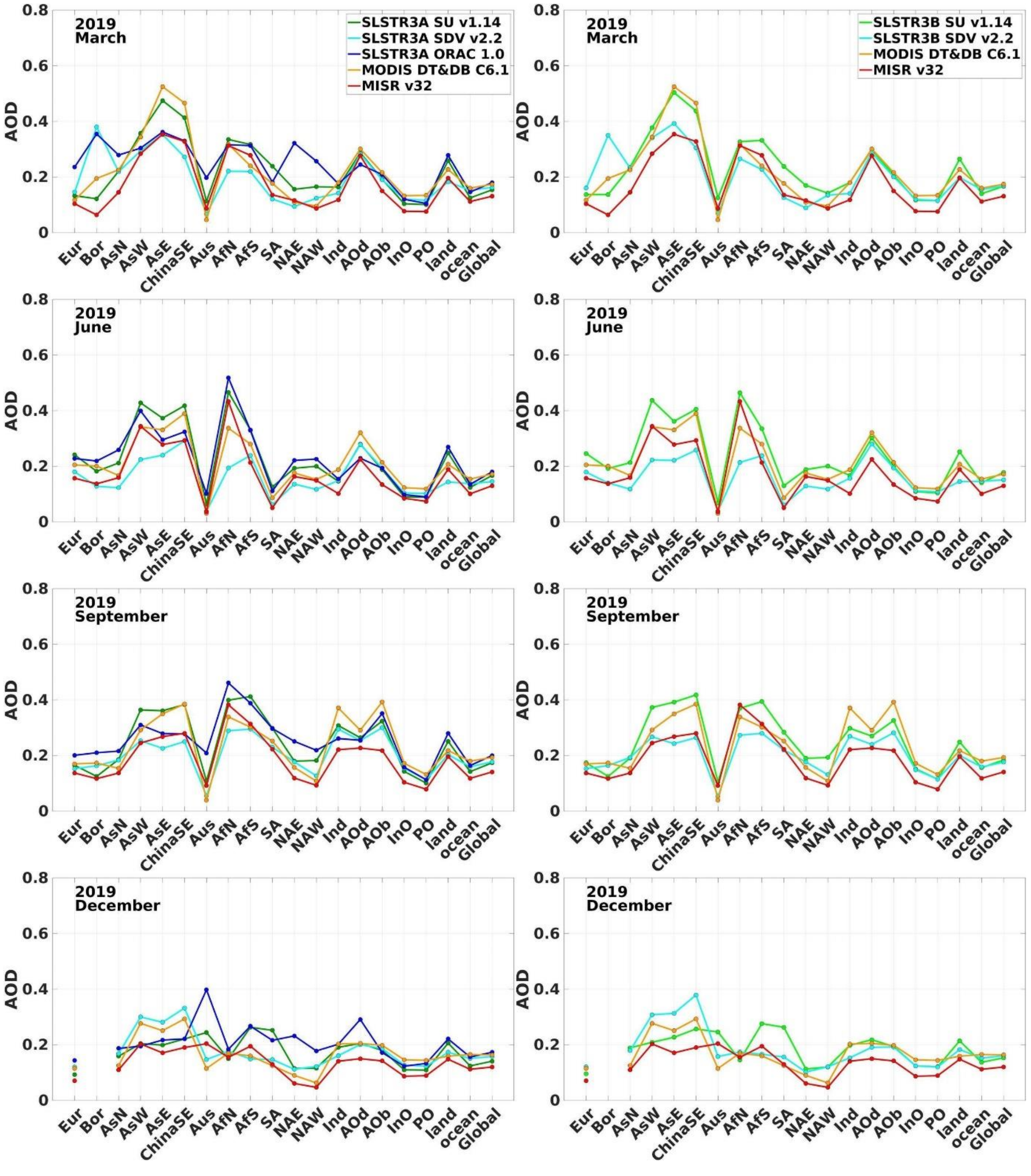

Fig. A1.4 *Left panel: S3A SU v1.14, SDV v2.2, ORAC v1.0, MODIS and MISR monthly total AOD. Right panel: S3B SU v1.14, SDV v2.2, MODIS and MISR monthly total AOD. Both for regions defined in Fig6.3*

End of the document